Swansea University
Prifysgol Abertawe

Cronfa
Setting Research Free

Swansea University E-Theses

Characterisation of osteopontin and CD44 in endometrium of infertile women.

De Mello, Natalie Victoria

How to cite:

De Mello, Natalie Victoria (2013) *Characterisation of osteopontin and CD44 in endometrium of infertile women..* thesis, Swansea University.
http://cronfa.swan.ac.uk/Record/cronfa42761

Use policy:

This item is brought to you by Swansea University. Any person downloading material is agreeing to abide by the terms of the repository licence: copies of full text items may be used or reproduced in any format or medium, without prior permission for personal research or study, educational or non-commercial purposes only. The copyright for any work remains with the original author unless otherwise specified. The full-text must not be sold in any format or medium without the formal permission of the copyright holder. Permission for multiple reproductions should be obtained from the original author.

Authors are personally responsible for adhering to copyright and publisher restrictions when uploading content to the repository.

Please link to the metadata record in the Swansea University repository, Cronfa (link given in the citation reference above.)

http://www.swansea.ac.uk/library/researchsupport/ris-support/

Characterisation of Osteopontin and CD44 in endometrium of infertile women

Natalie Victoria De Mello

Submitted to Swansea University in fulfilment of the requirements for the degree of Doctor of Philosophy

Swansea University

College of Medicine

2013

SWANSEA LIBRARY UNIVERSITY

ProQuest Number: 10807530

All rights reserved

INFORMATION TO ALL USERS
The quality of this reproduction is dependent upon the quality of the copy submitted.

In the unlikely event that the author did not send a complete manuscript
and there are missing pages, these will be noted. Also, if material had to be removed,
a note will indicate the deletion.

ProQuest 10807530

Published by ProQuest LLC (2018). Copyright of the Dissertation is held by the Author.

All rights reserved.
This work is protected against unauthorized copying under Title 17, United States Code
Microform Edition © ProQuest LLC.

ProQuest LLC.
789 East Eisenhower Parkway
P.O. Box 1346
Ann Arbor, MI 48106 – 1346

Summary

Cell adhesion proteins osteopontin, CD44 and integrin αVβ3 interact to form an adhesion complex between the embryo and endometrial surface forming an attachment that can lead to implantation. Whilst receptivity has been investigated extensively, the expression of this adhesion complex has yet to be studied simultaneously in the endometrium. This thesis establishes the expression of the adhesion complex in fertile and infertile endometrium. In addition the regulation of the adhesion complex components by distinct signalling pathways and the key regulators estrogen receptor, nuclear factor kappa B and signal transducer and activator of transcription 1 have been investigated in endometrial cell lines.

Objectives:

To establish the expression profile of adhesion complex components in samples obtained from fertile and infertile women. To model *in vitro* hormonal regulation of adhesion complex components to mimic estrogen and progesterone stimulus in the menstrual cycle. To determine if adverse environments common to poly cystic ovarian syndrome and endometriosis affect uterine expression of the adhesion complex via high glucose and pro-inflammatory cytokines. To investigate the direct regulation of *Osteopontin* and *CD44* by estrogen and cytokine signalling through estrogen receptor α, nuclear factor kappa B and signal transducer and activator of transcription 1.

Methodology:

Investigation of human biopsies and cell line models by immunohistochemistry, quantitative polymerase chain reaction, chromatin immunoprecipitation and enzyme linked immunosorbent assay.

Conclusions:

Adverse uterine environments including high glucose and pro-inflammatory cytokines may regulate the expression of the adhesion complex, and contribute to a lack of endometrial receptivity in endometriosis and poly cystic ovarian patients. CD44, ITGAV and ITGB3 levels may be used as markers for loss of receptivity in unexplained infertility.

DECLARATION

This work has not previously been accepted in substance for any degree and is not being concurrently submitted in candidature for any degree.

Signed .. .. (candidate)

Date ....22/8/2014.....

STATEMENT 1

This thesis is the result of my own investigations, except where otherwise stated. Where correction services have been used, the extent and nature of the correction is clearly marked in a footnote(s).

Other sources are acknowledged by footnotes giving explicit references. A bibliography is appended.

Signed ... . (candidate)

Date .....22/8/2014.....

STATEMENT 2

I hereby give consent for my thesis, if accepted, to be available for photocopying and for inter-library loan, and for the title and summary to be made available to outside organisations.

Signed .... (candidate)

Date .....22/8/2014.....

Contents page

Acknowlegdements

Over the course of my studies I have been fortunate to receive the encouragement and support of a number of people.

Firstly, I would like to thank my supervisors Professor Steven Conlan, Professor John White, Dr. Deya Gonzales and Dr. Lewis Francis. Collectively they have provided invaluable guidance and support, and I am thankful for their dedication and enthusiasm. The welsh government for funding this research project and allowing me to develop my skills as a scientist. Thanks are also offered to the clinical staff at the ABMU Health Board, specifically Dr Lavina Margarit, Sarika Nandanan, and the consultants in the gynaecological department and pathology department, who have offered assistance and participated in exciting collaborative work. Importantly, the patients who have kindly donated samples to be part of this research are also gratefully acknowledged, as without them this study would not have been possible. My colleagues in the Centre for NanoHealth, who are too numerous to list individually, are thanked for their friendship, stimulating discussions, support, and of course good nights out!

Finally, I wish to acknowledge the continued support of my family and close friends. In particular Stephen Evans and James Plant who's dedicated friendship helped me through some very challenging times.

My family are owed the greatest thanks of all, for keeping me grounded, their constant love, and their understanding of my devotion to my studies. In particular, I would like to thank my partner Daniel Roberts who has been my best friend and my rock throughout my time at university. Here's to getting 'real' jobs and starting our life together!

List of Figures

List of Tables

Abbreviations

3β-HSD	3-beta-Hydroxysteriod Dehydrogenase
α	
αVβ3	Integrin alpha V beta 3 (protein)
A	
ABMU HB	Abertawe Bro Morgannwg University Health Board
AKT	Serine/Threonine Protein Kinase
AnPCOS	Anovulatory PCOS
AP-1	Activator Protein 1
AREG	Amphiregulin
ART	Assisted Reproductive Techniques
ATCC	American Type Culture Collection
B	
BMI	Body Mass Index
BSA	Bovine Serum Albumin
C	
CC1	Cell Concentration 1
CD44v3	CD44 receptor variant 3
CD44v6	CD44 receptor variant 6
CD44v7	CD44 receptor variant 7
CD44v8	CD44 receptor variant 8
cDNA	complementary DNA
ChIP	Chromatin Immunoprecipitation
Cq	Quantification cycle
CUM	Cumulative
D	
DBD	DNA Binding Domain
dH2O	Distilled water
DMEM/F-12	Dulbecco's Modified Eagle's Medium: Nutrient Mixture F-12
DNA	Deoxyribonucleic Acid
DPX	Dinbutyl Pthalate Xylene
E	
E_1	Estrone
E_2	17β-Estradiol
E_3	Estriol
ECACC	European Collection of Cell Cultures
ECM	Extracellular Matrix
ELISA	Enzyme Linked Immunosorbent Assay
EMSA	Electrophoretic Mobility Shift Assay
Endo	Endometriosis
ER	Estrogen Receptor
ERE	Estrogen Response Element

ERα	Estrogen Receptor alpha
ERβ	Estrogen Receptor beta
Eta-1	Early T-lymphocyte Activation-1
F	
FBS	Foetal Bovine Serum
FC	Fertile Control group
FSH	Follicle Stimulating Hormone
G	
GAPDH	Glyceraldehyde 3-phosphate Dehydrogenase
GLUT4	Glucose transporter type 4
GREB1	Growth regulation in estrogen in breast cancer 1
H	
HA	Hyaluronic Acid
H&E	Haematoxylin and Eosin
HEC-1	Human Endometrial Adenocarcinoma Cells
HRP	Horseradish Peroxidase
I	
IFGR	Interferon Gamma Receptor
IFNγ	Interferon-gamma
IgG	Immunoglobulin G
IHC	Immunohistochemistry
IKBα/β	Inhibitor of Kappa B alpha/beta
IKK	Inhibitor of Kappa B Kinase
IL-1β	Interleukin 1-beta
IL-4	Interleukin 4
IL-6	Interleukin 6
IL-8	Interleukin 8
IL-10	Interleukin 10
IL-12	Interleukin 12
IL-18	Interleukin 18
IL-1RacP	IL-1 receptor accessory protein
iNOS	Inducible Nitric Oxide
iOPN	Intracellular OPN
IP	Immunoprecipitation
IRAK	Interleukin-1 Receptor-Associated Kinase
IRF-1	Interferon Regulatory Factor 1
IRF-2	Interferon Regulatory Factor 2
ISCI	Intracytoplasmic Sperm Injection
ITGAV	Integrin, alpha V
ITGB3	Integrin, beta 3 (platelet glycoprotein IIIa, antigen CD61)
IVF	In Vitro Fertilisation
J	
JAK2	Janus Kinase2
JAK-STAT	Janus Kinase - Signal Transducer and Activator of Transcription

	pathway
K	
K-W	Kruskal-Wallace
L	
LH	Lutenising Hormone
M	
MCP-1	Monocyte chemmoattractant protein-1
MMP	Matrix Metalloproteinase
MMP-9	Matrix Metalloproteinase 9
mRNA	Messenger Ribonucleic Acid
Muc-1	Mucin-1
M-WU	Mann-Whitney U
MyD88	Myeloid Differentiation primary response gene 88
N	
NaCl	Sodium Chloride
NaHCO3	Sodium bicarbonate
NF-KappaB1	Nuclear factor kappa B1
NFκB	Nuclear factor kappa B
NIK	NFκB Inducing Kinase
O	
OPN	Osteopontin
OvPCOS	Ovulatory PCOS
P	
P_4	Progesterone
PBS	Phosphate Buffered Saline
PCOS	Poly Cystic Ovarian Syndrome
PIC	Proteinase Inhibitor cocktail
POL II	Polymerase II
PR	Progesterone Receptor
Q	
Qc	Quantitative Cycle threshold
QPCR	Quantitative real time Polymerase Chain Reaction
R	
RANTES	Regulated on Activation Normal T Cell Expressed and Secreted
RFU	Relative Fluorescence Units
RGD	Arginine-Glycine-Aspartic acid
RIP	Receptor Interacting Protein
RNA	Ribonucleic acid
RPL-19	60s Ribosomal Protein L-19
S	
SD	Standard Deviation
SDS	Sodium Dodecyl Sulphate
SP-1	Specificity Protein 1
SPP-1	Secreted Phosphoprotein 1

STAT1	Signal Transducer and Activator of Transcription 1
T	
TAB1	Tumour growth factor-beta activated kinase binding protein 1
TGF-β	Transforming Growth Factor beta
TNFR2	TNF Receptor 2
TNFα	Tumour Necrosis Factor-alpha
TOLLIP	Toll Interacting Protein
TRADD	Tumour necrosis factor receptor type 1-Associated Death Domain protein
TRAF	TNF Receptor Associated Factor
TRAF6	TNF Receptor Associated Factor 6
U	
UIF	Unexplained Infertility
X	
XBP1	X-box Binding Protein 1

Chapter 1

Introduction

1.1 Female infertility and reproductive disorders

Infertility is defined by the National Institute for Health and Care Excellence (NICE) as "the failure of a couple to conceive after 1 year of unprotected intercourse in the absence of a known reproductive pathology" (NICE, 2012). It is estimated that infertility affects one in every six heterosexual couples in the UK (2012), 30% of infertility cases are attributed to male factors whilst in infertile women 25% are caused by ovulatory disorders, 10% are caused by uterine or peritoneal disorders and 25% are classified as 'unexplained'. Standard investigations include semen analysis, ovulation assessment, tubal patency, uterine abnormalities and ruling out infections i.e. *Chlamydia trachomatis* (NICE, 2012). Following the results of the above tests there are three main treatment options; firstly medical treatment to restore ovulation through the use of drugs; secondly surgery to remove any abnormalities and; thirdly assisted reproduction techniques (ART). For patients that undergo *in vitro* fertilisation (IVF) or intracytoplasmic sperm injection (ISCI), poor embryo quality or failures of the embryo to implant maybe detected in these patients. However infertility problems may still persist after conventional treatment or diagnostics. Endometrial receptivity and implantation are not currently used as a measure of infertile status.

1.1.1 Polycystic Ovarian Syndrome (PCOS)

Polycystic ovarian syndrome (PCOS) was originally named Stein-Leventhal syndrome after it was first described by Irving F. Stein and Michael L. Leventhal in 1935 (Stein and Leventhal 1935). It was later named after the physical characteristics of the disease which occur in some women where the follicles in the ovary appear cystic on investigation by ultrasound. Cystic ovaries are caused when the follicles become arrested in development. Immature follicles can contribute to infertility due to lack of ovulation of mature ovums. PCOS is currently diagnosed by the Rotterdam criteria where it is recognised as a syndrome and the presence of cystic ovaries may not occur. The syndrome is diagnosed if two of the following three criteria are met; (1) oligoovulation (infrequent or irregular ovulation) or anovulation (absence of

ovulation for >3 months), (2) clinical or biochemical signs of hyperandrogenism or (3) polycystic ovaries, all in the absence of other diseases (The Rotterdam ESHRE/ASRM-sponsored PCOS consensus workshop group 2004; Legro et al. 2013). Visual manifestations of hyperandrogenism such as hirsutism and acne can be used as indicators, and biochemical analysis of circulating androgens is also considered in this assessment. Polycystic ovaries are defined as 12 or more follicles in each ovary measuring 2-9 mm in diameter and/or increased ovarian volume (>10ml). Common conditions associated with PCOS include obesity, high body mass index, metabolic syndrome, insulin resistance and diabetes (Tan et al. 2010; Ciampelli et al. 1999). Common features of metabolic syndrome include insulin resistance, obesity and dyslipidemia which are often present in women with PCOS. Insulin resistance can lead to high levels of circulating glucose, and insulin sensitising treatments for this form of diabetes (type 2) may have positive effects on fertility (Sharpless 2003; Essah et al. 2007; Steiner et al. 2007; Froment and Touraine 2006). Women identified with PCOS are further sub divided into anovulatory and ovulatory PCOS based on their ovulation status. Women who fail to ovulate for more than three months are characterised as anovulatory. Women who are diagnosed with PCOS but ovulate infrequently or have menstrual cycles that are irregular or longer (more than 50 days) are classed as ovulatory PCOS. It is estimated that 5-10% of women in the UK are diagnosed with PCOS (Treasure et al. 2013; Kelly et al. 2001).

1.1.2 Endometriosis

An infertility associated disorder first described in 1860 by Carl Von Rokitansky (Rokitansky 1855; Batt 2011), endometriosis is where endometrial gland and stroma cells are found outside of the uterine cavity. A theory developed by Sampson describes the endometrial cells detaching from the endometrial layer. It is possible that as blood during a menstrual cycle can flow through the fallopian tubes and reside in the pelvic cavity detached cells may then be deposited there (Sampson 1927). These cells are still influenced by steroid hormones and continue to proliferate, differentiate and break down every month in response to sex steroid

hormones of the menstrual cycle. This is what is thought to cause an exacerbation in symptoms including the pelvic pain that is commonly associated with endometriosis. Endometriosis affects between 6-10% of the general UK population and this increases to 25-50% within infertile women (Bulletti et al. 2010). Endometriosis is diagnosed by the presence of abnormalities in the pelvic region such as cysts or endometriomas on the outer wall of the reproductive organs, the presence of which can be confirmed by ultra sound. Current treatment methods are effective at pain management and include the administration of progestin, estrogen plus progestins, gonadotropin-releasing hormone agonist and antagonists, danazol and aromatase inhibitors. However these treatments render the patient infertile as they inhibit ovulation. Surgical options including laparoscopy can be conducted to confirm and ascertain the extent of endometriosis. Laparoscopic ablation of endometrial implants may serve to reduce pain and have shown to increase fertility (Grzechocinska and Wielgos 2012). Research investigating the role of inflammation in endometriosis and the possible impact on infertility has been conducted (Weiss et al. 2009; Kyama et al. 2003; Lebovic et al. 2001) with studies focused on the role of pro-inflammatory cytokines present in the peritoneal fluid (Taketani et al. 1992; Bedaiwy et al. 2002); circulating blood (Pellicer et al. 1998; Sze et al. 2010) and expression by leukocytes on the endometrial epithelial surface (Kyama et al. 2003; Lebovic et al. 2001; van Mourik et al. 2009; Weiss et al. 2009).

1.1.3 Unexplained Infertility

Unexplained infertility (UIF) is diagnosed when all standard diagnostic tests for infertility show no reproductive pathology is identified in either partner. However, patients still have problems conceiving after a year of regular unprotected intercourse. The standard tests include ovulation assessment, analysis of semen quality and quantity, and a hysterosalpingogram. Further testing can establish ovarian reserve or investigative laparoscopy can be conducted. In infertile women approximately 25% are categorised as unexplained infertility (Department of

Health 2009). As there is no uterine and sperm dysfunction found there is currently no treatment. Guidelines advise couples to continue to attempt to conceive and following two years of unsuccessful conception (including a year prior to investigations) then IVF will be offered. Ovulatory stimulation is no longer offered as it has not shown to increase fertility rates. This suggests that an endometrial factor such as receptivity and/or implantation could be a possible cause for infertility. Currently, there are no biomarkers of receptivity identified for unexplained infertility.

1.2 Reproductive Biology

Mammalian reproductive biology focuses on factors that may affect successful reproduction. The reproductive organs, leukocytes, hormones and cytokines are essential to this process. A cascade of events works in harmony for successful reproduction to take place. This process involves gametogenesis, fertilisation, implantation and gestation.

1.2.1 Physiology of the human female reproductive system

The female reproductive organs consist of the ovaries, the fallopian tubes and the uterus (Figure 1-1). From puberty onwards ovaries in women are responsible for ovum production. The fallopian tubes are adjacent to the ovaries and connect to the uterus and provide a functional role in aiding the passage of the ovum to the uterus. The endometrium is a specialised layer of tissue in the uterus wall and has distinct functions in reproduction.

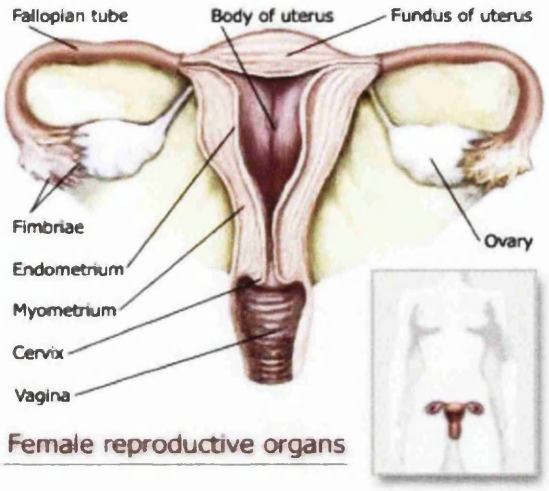

Figure 1-1 Diagram of the structure of the female reproductive organs.

Adapted from (www.wellnessagro.com)

1.2.1.1 Ovaries

The ovaries are dynamic organs where changes in the structure and function can lead to drastic consequences for fertility. The follicular compartment where the follicles develop into ovums is highly specialised, receiving signals from pituitary derived hormones and cytokines throughout the menstrual cycle. This develops primordial follicles to graafian follicles ready for ovulation and regression of the corpus luteum to the corpus albicans are all driven by these signals. Ovulation is where the mature ovum is released from the ovaries. It is also responsible for developing the ovum for implantation and stimulating follicular growth to induce a surge in luteinising hormone expression to induce ovulation. If the ovum is not fertilised within 24 to 26 hours after ovulation it will be degraded by the immune system.

1.2.1.2 Fallopian tubes

The fallopian tubes are lined with ciliated epithelia and connect the uterus to the ovaries, and are typically 8 to 10 cms in length. The ovarian end of the fallopian tubes have feathered like ends, called fimbriae. The fimbriae contain projections which are used to capture the ovum once ovulation from the ovary has taken place

and ensure it can move into the fallopian tube. A specialised ciliated epithelial surface in the fallopian tube allows the ovum to travel from the fallopian tubes into the uterus providing nourishment and lubrication during this process. The ovum first travels into the fimbrial segment, into the infundibular segment, the ampullary segment, isthmic segment and finally into the interstitial segment where it enters the uterine cavity.

1.2.1.3 The uterine cavity

Surrounding the uterus is the peritoneal fluid. This fluid lines the outer surface of the uterus (serosa) providing lubrication between tissue that lines the abdominal wall and the pelvic cavity. This fluid functions to prevent friction between the uterus and digestive organs. The uterus contains three layers of cells; the perimetrium is the outer serosa layer of the uterus, the myometrium which is the muscular layer important for inducing contractions, and the endometrium which is the inner most lining.

1.2.1.4 Endometrium

The endometrium is the inner most lining of the uterus and thickens in response to ovarian derived hormones and cytokine signals to prepare the surface of the endometrium for embryo implantation if fertilisation occurs. This is achieved by the endometrial surface expressing the correct plethora of adhesion proteins which will allow for this attachment to take place. Following this initial attachment the embryo will implant into the endometrium during a preparation process called decidualization. The uterus will then provide the implanted embryo with nutrients and oxygen so that it will develop into a foetus and hence successful pregnancy occurs. However, if fertilisation or implantation does not occur the endometrial tissue will break down and shed as part of the menstrual cycle.

1.2.2 Menstrual cycle

Changes in endometrial morphology throughout the menstrual cycle in response to hormones influence tissue proliferation, differentiation and degradation (Figure 1-2). The menstrual cycle is a cyclic event that occurs in women approximately every 28 days where the endometrial tissue is regenerated under the influence of hormones and cytokines. The endometrium is a highly specialised tissue within the body with the unique ability to differentiate, proliferate and break down. This suggests that cell differentiation and proliferation are highly regulated. Proliferation of the endometrium is driven by estrogen in the proliferative phase (Figure 1-2). Following ovulation the endometrial tissue begins to vascularise and differentiate during the secretory phase, where progesterone is responsible for driving these changes up to approximately day 23 when progesterone levels start to decline. A lack of progesterone in the endometrium results in the constriction of the blood vessels leading to the shedding of the endometrium (menstruation). Days 20-24 of the menstrual cycle have been termed the 'window of implantation'. This is when the endometrial tissue is the thickest and the epithelium is most likely to bind the trophoblast layer of the blastocyst. This begins the implantation process; initially attachment of the blastocyst to the epithelium occurs followed by adhesion of the blastocyst to the endometrial epithelium and finally invasion. Decidualization of the endometrial tissue occurs in preparation for implantation where the blastocyst invades the epithelium and becomes embedded in the stroma where it can begin to differentiation and grow. If successful implantation does not take place the endometrium sheds and the cyclic process initiates again. The primary hormones responsible for these changes in the endometrium are estrogens, progesterone, follicle stimulating hormone and luteinising hormone.

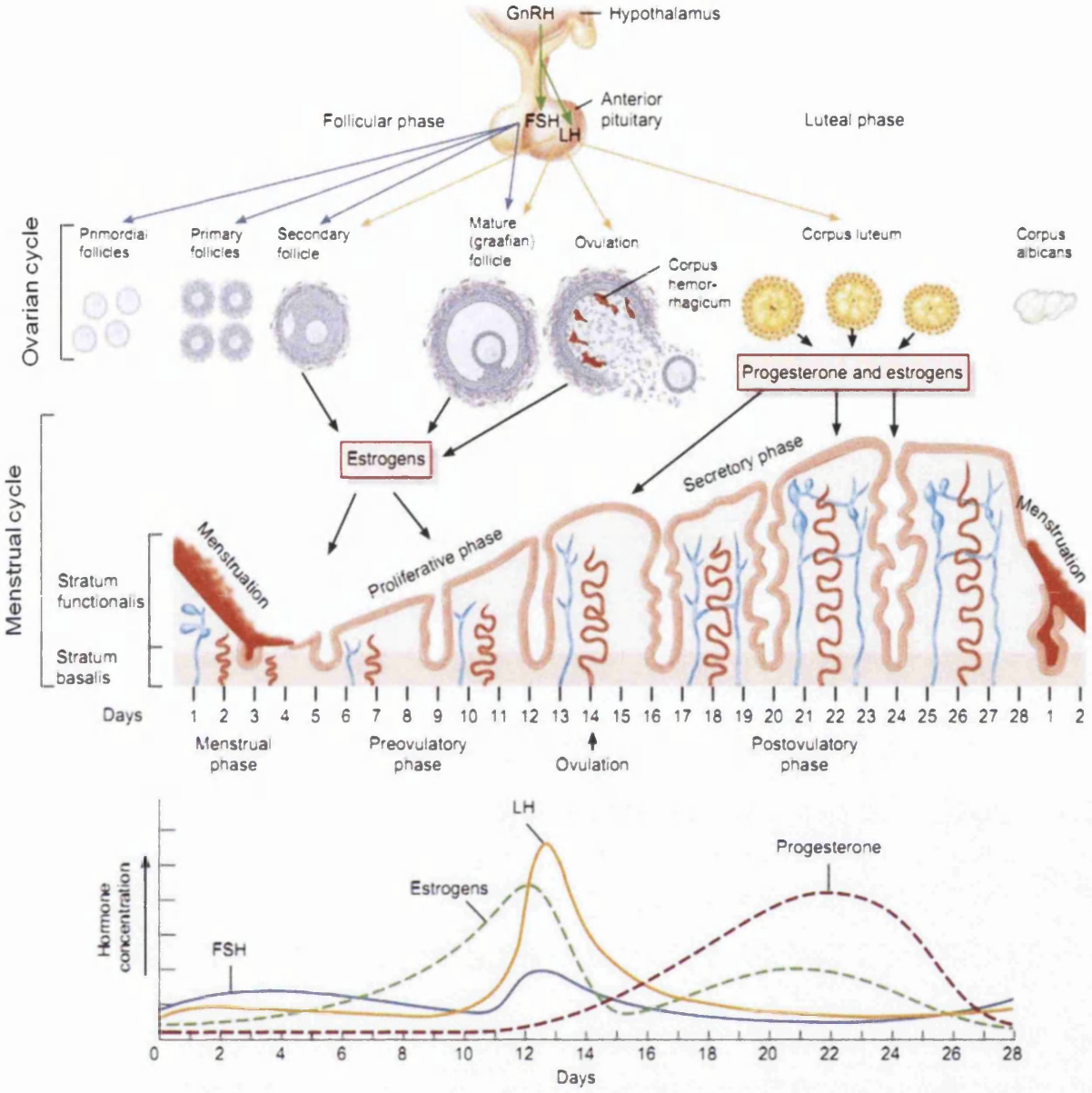

Figure 1-2 Changes in endometrial morphology during the menstrual in response to ovarian derived hormones and pituitary derived gonadotropins.

Endometrial morphology is influenced by ovarian derived hormones estrogen, progesterone, luteinising hormone and follicle-stimulating hormone. Proliferation of the tissue is driven by estrogen and differentiation by progesterone. FSH and LH signal to the ovary to release an egg and provide a negative feedback mechanism for estrogen production. Adapted from (www.antranik.org).

1.3 Endometrial cellular structure and composition

The endometrial lining of the uterus contains two distinct cell types, epithelial and stromal, which interact with each other. The epithelial cells are the outer most cell layer. In these two layers of tissue glandular structures are present. Endometrial glands function to secrete proteins and cytokines to influence the expression of the epithelium in preparation for the blastocyst implantation. The luminal epithelial cells form the endometrial surface that will be in direct contact with the blastocyst. The stromal cells are located between the glandular and luminal epithelium (Figure 1-3). These two distinct cell types utilise paracrine signalling to communicate and an example of this is the regulation of integrin receptor αVβ3 by estrogen and progesterone from the stroma to the endometrial epithelium (Lessey and Arnold 1998). The luminal surface functions to protect the tissue from bacterial infections with columnar epithelia and intracellular tight junctions.

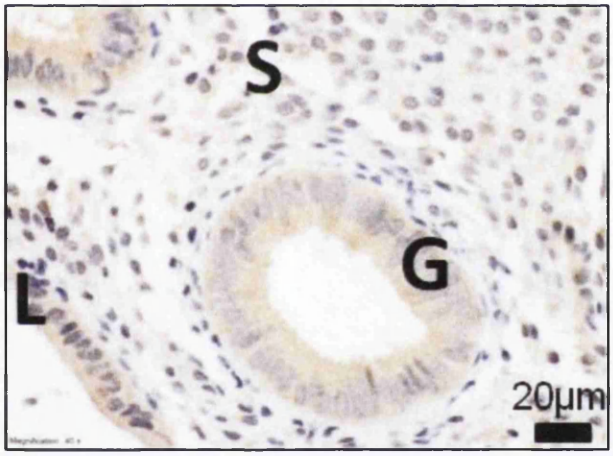

Figure 1-3 IHC biopsy section showing structural elements of endometrium.

The luminal cell surface is indicated (L), along with the glands (G) and the stroma (S). Black bar represents 20µm, magnification, x40.

1.3.1 Signalling mechanism involved in endometrial development.

The hypothalamus releases gonadotropin-releasing hormone (GnRH), resulting in anterior pituitary gland production of follicle stimulating hormone (FSH) and luteinizing hormone (LH). This in turn stimulates the ovaries to produce estrogen. The ovaries also produce inhibin which serves to regulate the ovarian, and therefore menstrual cycle, by forming a negative feedback loop. Estrogen itself then acts as a negative feedback inhibitor of GnRH production by the hypothalamus (Figure 1-4). Different signalling mechanisms are involved in endometrial development including hormone signalling from the pituitary gland. Gonadotropin releasing hormone from the hypothalamus stimulates the pituitary gland to release follicle stimulating hormone (FSH) and luteinising hormone (LH), which act on the ovaries. The anterior pituitary gland secretes FSH and this hormone works synergistically with LH to drive maturation of the developing follicle by increasing FSH in the proliferative phase after levels of progesterone and estradiol fall (Figure 1-4). LH peaks in concentration causing ovulation to occur at day 14. Ovulation is the release of the egg from the mature graffian follicle of the ovaries. This surge also induces a change in the residual follicle to form the corpus luteum (Figure 1-4). Paracrine signalling then takes effect whereby estrogen and progesterone in the epithelium and stroma of the endometrium allow two cell types in the same tissue to communicate. All of these types of signalling are important in the endometrium to maintain its structural morphology and expression of adhesion proteins during implantation.

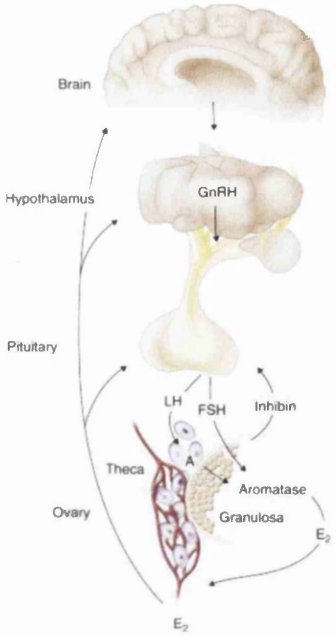

Figure 1-4 The hypothalamic pituitary ovarian axis

The hypothalamic-pituitary-ovarian axis is the culmination of the individual endocrine glands involved in producing and regulating the hormone changes within the body. Importantly, changes to the ovaries and endometrium control reproduction (Goldman and Ausiello 2008).

1.4 Nuclear Hormone Receptor expression levels

The nuclear hormone receptors, estrogen receptor alpha (ERα), estrogen receptor beta (ERβ) and progesterone receptor (PR) drive the essential signalling cascades in the endometrial tissue for adhesion protein expression in the window of implantation. These receptors are activated upon ligand binding in the cytosol, this is followed by receptor dimerisation which allows for translocation to the nucleus where they are able to bind regulatory sites on the gene promoters to mediate gene transcription.

1.4.1 Estrogen

Three main estrogens occur in the body, estrone (E_1), estradiol (E_2) and estriol (E_3). Estradiol is the most potent and predominant estrogen expressed within the body and circulating serum and is involved in influencing the morphological changes in

the endometrium. The developing follicles in the ovaries and the corpus lutea produce estrogens. The biosynthesis of estrogens occurs in the theca cells in the ovaries. Androstenedione is synthesised from cholesterol, this compound is then converted in granulosa cells to estrone or testosterone. Testosterone can then be catalysed by aromatase to estradiol. Estradiol drives the regeneration of the endometrium after degradation (menses) by causing the tissue to proliferate. As such this phase of the menstrual cycle is termed the proliferative phase (Figure 1-2, days 5-14).

1.4.2 Progesterone

Progesterone is synthesized from cholesterol by the removal of a cholesterol side chain to produce pregnenolone, and this is then converted by 3-beta-hydroxysteriod dehydrogenase (3β-HSD) to progesterone. Progesterone can be produced in the ovaries, the adrenal glands and has been shown to be stored by adipose tissue. Progesterone acts on the endometrial surface by differentiating the tissue. This occurs in the 'secretory phase' where glandular structures become more irregular and start to secrete various cytokines, proteins and leukocytes (Figure 1-2, days 15-28).

1.4.3 Steroid hormone receptor expression in the endometrium

Physiological levels of estrogen are around 150 ng/ml at the beginning of the proliferative phase and gradually increase to day 13 where they peak at ~420 ng/ml. Levels then gradually decrease to day 17 before increasing during the secretory phase to peak at 300ng/ml during the window of implantation (Martin and Behbehani 2006). Estrogen signalling however is still active in the mid and late secretory phases. Progesterone concentrations are around 100 ng/ml at the beginning of the proliferative phase and increase to peak at ~350 ng/ml at day 21 before decreasing back to 100 ng/ml at day 28 if pregnancy does not occur (Martin and Behbehani 2006; Francis et al. 2010). During the window of implantation there is a balance between both estrogen and progesterone signalling. After estrogen

peaks in the proliferative phase, progesterone expression increases. This is thought to be through an increase in activator protein 1 (AP-1) which can bind to the promoter and activate transcription of the PR receptor (Petz 2002). ERα and PR expression throughout the menstrual cycle, as determined by immunohistochemistry, demonstrates that maximal expression of both receptors occurs in the mid to late secretory phase (Lessey et al. 1988).

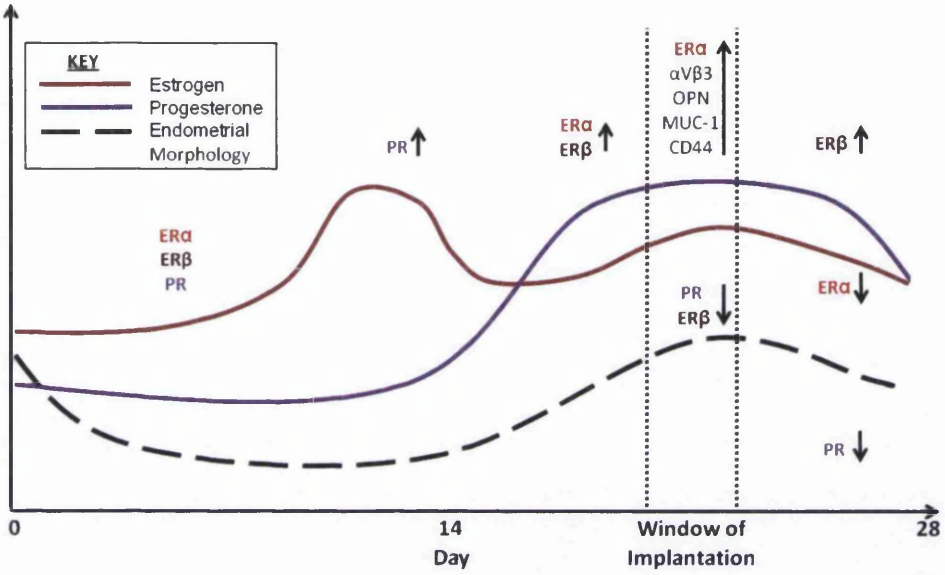

Figure 1-5 Hormone, receptor and adhesion protein expression in menstrual cycle.

Levels of estrogen and progesterone indicate the balance of these hormones throughout the menstrual cycle and the effect of these hormones on endometrial morphology is shown. The changes in ERα, ERβ and PR levels throughout the menstrual cycle are included. In addition to this adhesion molecules up regulated in the window of implantation are indicated. Adapted from (Francis et al. 2010).

Steroid signalling through progesterone and estrogen affects cells directly. The epithelium and stroma both express ER and PR. Expression of ERα, ERβ and PR changes throughout the menstrual cycle as does the levels of estrogen and progesterone (Figure 1-5). Expression of both ER receptors increases from the proliferative phase to the early secretory phase. However, during the mid secretory phase expression of ERα increases while ERβ expression decreases. In the late secretory phase expression of ERα then deceases whilst ERβ increases (Critchley 2002; Lecce et al. 2001). Endometrial PR expression increases in the late

proliferative phase compared to the early proliferative phase. Expression decreases during the mid secretory phase and decreases further in the late secretory phase (Ingamells et al. 1996). The correct expression of estrogen and progesterone throughout the menstrual cycle and crucially during the window of implantation is important where endometrial receptivity is essential to the implantation process.

1.5 Embryo Implantation

The first stage of embryonic implantation is apposition where the trophoblast cells of the blastocyst bind to carbohydrate ligands that are localized on the luminal epithelium during the window of implantation. This is the initial attachment of the blastocyst to the endometrial surface. The adhesion phase is characterised by cellular adhesion molecules including integrin αVβ3 and its ligand osteopontin (OPN) that co-localise and may play a role in endometrium or embryonic signalling, assisting embryo attachment to the apical surface before invasion occurs (Figure 1-6). CD44 is expressed on the endometrial epithelium and trophoblast surface and can bind to OPN (Fazleabas and Kim 2003).

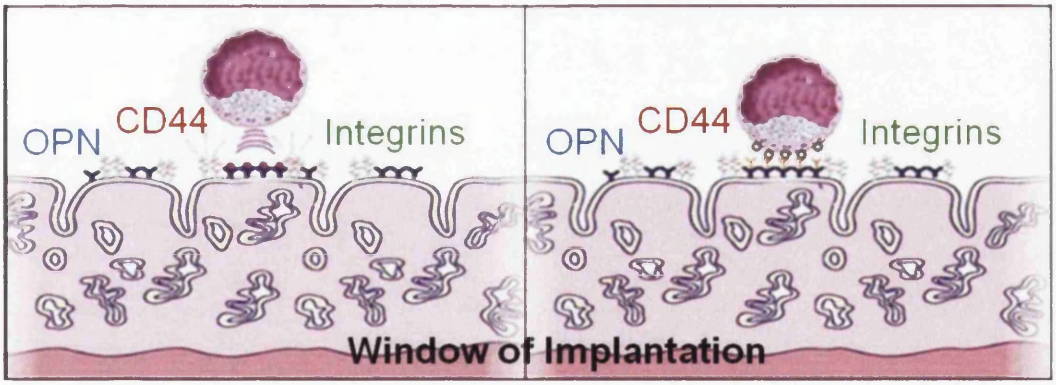

Figure 1-6 Blastocyst implantation.

The attachment of the blastocyst surface (trophectoderm) to the endometrial epithelia, the three stages include apposition, adhesion and invasion for successful implantation. At the three different stages different proteins expressed on the trophectoderm and epithelial surface are key. Adapted from (Achache and Revel 2006).

The last stage of implantation is invasion where the trophoblast adheres to the endometrial epithelial cells and through a paracrine mediated apoptotic reaction the blastocyst will pass through into the epithelial and stromal cell layer. It is crucial that repertoires of genes involved in degradation of the extracellular matrix are activated. The proteolytic enzyme matrix metalloproteinase 9 (MMP-9) has been linked with the invasive phenotype of trophoblasts (Skrzypczak et al. 2007). Finally the blastocyst traverses the basal membrane (Achache and Revel 2006; Geisert et al. 2006).

1.5.1 Uterine receptivity

Endometrial receptivity has been defined as "the capacity for the uterine mucosa to facilitate successful implantation" (Cavagna 2003). Biochemical, structural and molecular events in the endometrium must work in a synchronous fashion for receptivity to be maximal. It is understood for uterine receptivity to be optimal hormone, cytokine signalling and expression of adhesion markers on the endometrial surface is important, however the mechanisms behind their expression are still under investigation (Makker and Singh 2006; Fatemi and Popovic-Todorovic 2013). The expression of adhesion proteins monitored throughout the menstrual cycle and peaking in expression during or around the window of implantation have been considered good candidate molecules to investigate in infertility. Examples of these adhesion proteins are CD44, osteopontin and integrins including αVβ3 (Lessey 2002; Goodison et al. 1999; Apparao et al. 2001).

1.5.2 Extra cellular matrix adhesion molecules

The extra cellular matrix (ECM) functions to provide structural support to cells and regulate communication between cells. The ECM is an interconnected mesh of proteins and polysaccharides, hyaluronic acid is an example of a polysaccharide present in the ECM. Hyaluronic acid, through its specific receptor CD44, can regulate cell behaviour using environmental cues such as in inflammation and the healing process (Goshen et al. 1996; Bellahcène et al. 2008). Collagens and laminins

also make up the ECM and have been found to bind integrins expressed on the cell surface (Ponta et al. 2003). Fibronectins in the ECM contain both a variable region and an arginine-glycine-aspartic acid (RGD) region that has been identified to bind specific integrins such as αVβ3 (Carvalho et al. 1998; Lee et al. 2007). Other molecules containing RGD domains are known as small integrin-binding ligand N-linked glycoproteins (SIBLINGs). These are a family of five identically orientated genes located on chromosome 4 in a region approximately 375,000bp in length (Bellahcène et al. 2008). One of these genes, secreted phosphoprotein 1 (SPP-1), encodes for Osteopontin.

1.6 Osteopontin

Osteopontin is a secreted phosphorylated glycoprotein initially described as a transformation associated phosphoprotein (Senger et al. 1979) and named later as secreted phosphoprotein 1 (SPP-1). During this time it had also been described as 2ar (Smith and Denhardt 1987) and early T-lymphocyte activating gene (Eta-1). The name Osteopontin (OPN) was proposed by Ake Oldberg in 1986, who identified and isolated the protein as a bone sialoprotein from rat osteosarcoma. Hence, it was named osteopontin, which means bone–bridge (Oldberg et al. 1986). In humans, OPN is located on chromosome 4q22.1 and the *SPP-1* gene contains 8 exons (Young et al. 1990) (Figure 1-7). The promoter region of *OPN* contains regulatory elements for nuclear factor kappa B (NFκB), estrogen receptor alpha (ERα), activator protein 1 (AP-1), specificity protein 1 (SP-1) and signal transducer and activator of transcription 1 (STAT1). Previous studies have identified and validated regulatory elements on the *OPN* promoter. An SP-1 site was identified by both Sharma and Wang in independent studies (Wang et al. 2000a; Sharma et al. 2010) an AP-1 site has also been identified (Bidder et al. 2002), in addition to one NFκB site (Samant et al. 2007). Alternate splicing at the mRNA level gives rise to many protein isoforms of OPN.

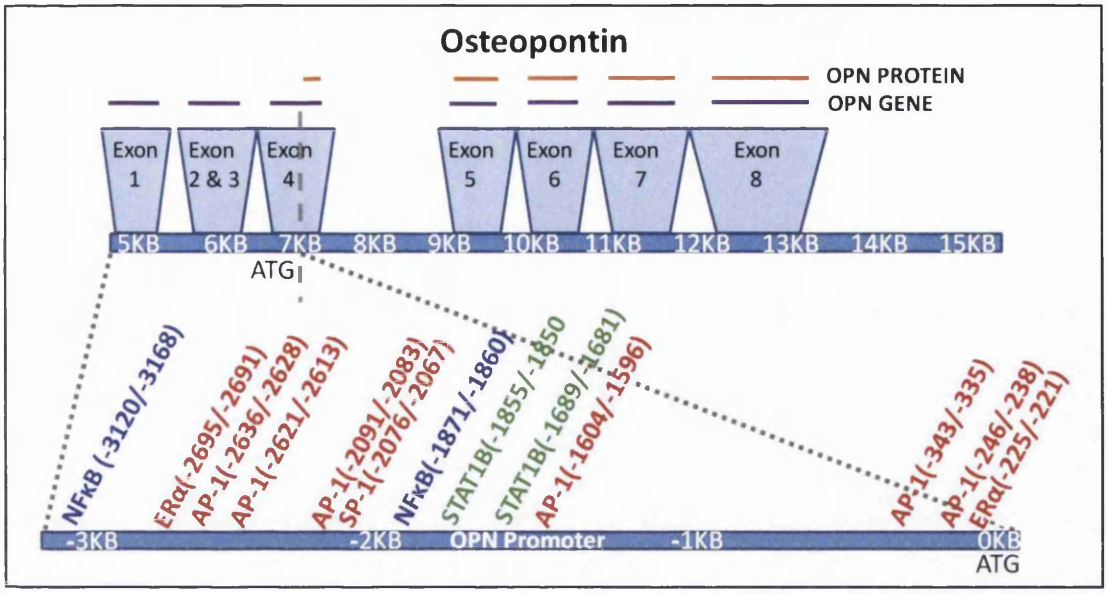

Figure 1-7 Osteopontin gene and promoter structure

1.6.1 Normal physiology, structure, isoforms and function of osteopontin

OPN is expressed throughout the body in many different tissues and there is also evidence that OPN is secreted into body fluids. *OPN* expression has been characterized in luminal epithelia cells in the stomach, small and large intestine, liver, gall bladder, kidney, lung, breast tissue and the endometrium at the mRNA level (Brown et al. 1992). At the protein level OPN expression has been reported in the colon, gallbladder epithelium, pancreas epithelium, kidney distal tubular epithelium, fallopian tube epithelium and endometrial epithelium (Brown et al. 1992). Of note is the involvement of OPN in inflammatory processes and also that it is secreted by macrophages, leukocyte and lymphocytes (Rodrigues et al. 2007). OPN has been shown to exhibit both pro- (promoting IL-12) and anti-inflammatory behaviour during cell injury and infection (Renkl et al. 2005; Mazzali et al. 2002). Based on the diverse expression profile of OPN in the human body, it is thought to play a significant role in wound repair, cell survival, leukocyte recruitment and function, bio-mineralization and iNOS regulation (Mazzali et al. 2002). OPN is a

negatively charged glycoprotein that functions as a component of the ECM (Figure 1-8).

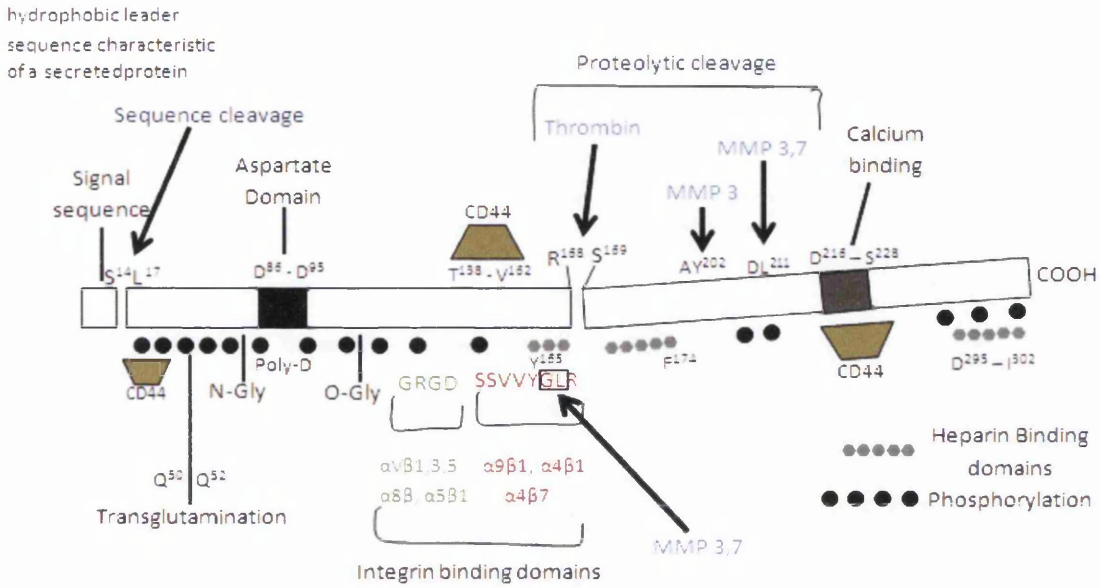

Figure 1-8 Protein structure of OPN.

OPN has a very complex protein structure consisting of multiple proteolytic cleavage, integrin and putative CD44 binding sites. Many heparin binding and phosphorylation sites exist on OPN's protein structure. A calcium binding and aspartate domain has been identified, as well as a transglutamination site.

OPN is a secreted protein that functions in many tissues to promote cell adhesion and cell migration, which are key physiological processes that OPN is involved in and dysfunction of these can lead to pathological processes in many tissues (Section 1.6.2). OPN protein is involved in bone mineralisation through its hydroxyapatite site which is able to bind to collagen (Zurick et al. 2013). OPN protein has many phosphorylation sites and can be heavily phosphorylated (Figure 1-8). OPN phosphorylation in the endometrium is poorly understood however 34 phosphoserine and 2 phosphothreonine site have been identified on OPN's protein structure. OPN protein has multiple cleavage sites for MMP and thrombin. MMPs are a family of proteases involved in the degradation of the extracellular matrix (ECM). They have also been shown to have roles in cell migration, adhesion and proliferation and are often found at sites of tissue regeneration (Kuzuya and Iguchi 2003; Giannelli et al. 2002). Multiple MMP-3 and MMP-7 sites exist on OPN's

protein structure. MMPs -3 and -7 are involved in the decidualization process prior to implantation, where OPN is also thought to play a role (Jones et al. 2006). A thrombin cleavage site located almost in the centre of the protein structure allows cleavage of OPN into two similar molecular weight protein fragments both functional (Grassinger et al. 2009). In addition to this, multiple integrin binding sites exist clustered together (Figure 1-8) (Christensen et al. 2010). Integrin αVβ3 is able to bind to OPN through its RGD tri-peptide domain indicated in green (Casals et al. 2012; Johnson et al. 1999; Peyghambari et al. 2010). Three CD44 binding sites on the OPN protein structure are putative, and are indicated in Figure 1-8. OPN-αVβ3 binding is one of the best characterised binding complexes between OPN and its integrins. OPN protein has also been shown to bind other molecules such as CD44, and in normal tissue physiology this binding functions to provide signal transduction to promote cell adhesion, migration and cell survival as with OPN-αVβ3 binding (Figure 1-9) (Bellahcène et al. 2008). Binding of OPN to membrane bound CD44 initiates a signalling pathway that promotes cell survival in cells. Initial binding activates phospholipase C-γ, protein kinase-C (PKC) and phosphotidylinositol 3-kinase (PI3K) which activates the Akt pathway which in turn activates anti-apoptotic signals in cells. Binding of OPN to integrin αVβ3 initiates two pathways that both up regulate AP-1 expression. This has been linked with cell adhesion and migration through the activation of nuclear factors inducing kinase (NIK), mitogen-activated protein kinase 1 (MAP3K1) and ERK activated AP-1. Alternately MEKK1 also known as MAP3K1 can activate MKK4, c-Jun N-terminal kinase 1 (JNK1) and finally AP-1. These signalling mechanisms in the endometrium have not been elucidated and the effect on endometrial surface expression has not been characterised.

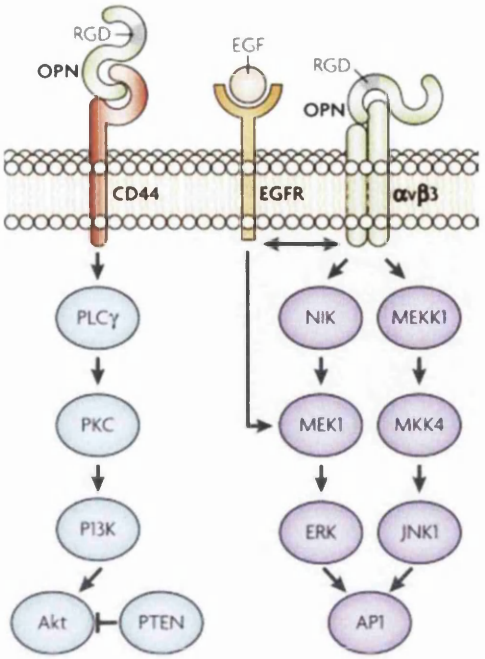

Figure 1-9 Signalling pathways initiated upon cell-matrix interaction.

OPN binding to membrane bound CD44 initiates a signalling complex that activates Akt which is associated with cell survival through anti-apoptotic activation. OPN integrin αVβ3 results in the activation of AP-1 through two distinct pathways, activation of AP-1 is associated with cell adhesion and cell migration. Adapted from (Bellahcène et al. 2008).

1.6.2 Osteopontin Dysfunction

OPN has been implicated in the pathology of many different diseases and disorders including rheumatoid arthritis (Iwadate et al. 2013), asthma (Delimpoura et al. 2010; Samitas et al. 2011), Graves disease (Xu et al. 2011), prostate cancer (Gupta et al. 2013) and breast cancer (Wang et al. 2010). Altered expression levels of OPN in the endometrium have been associated with infertility-related conditions including PCOS (DuQuesnay et al. 2009) and endometriosis (Cho et al. 2009; Wei et al. 2009; Casals et al. 2012).

1.6.3 Osteopontin and Inflammation

OPN is involved in several chronic inflammatory diseases including atherosclerosis (Giachelli et al. 1995; O'Brien et al. 1994), delayed-type hypersensitivity (Yu et al.

1998; Ashkar et al. 2000) granulomatous disease (Ashkar et al. 2000; Yumoto et al. 2002), and arthritis (Nau et al. 1999). Chronic inflammation is marked by consistent presence of macrophages at a site of injury or disease (Lund et al. 2009). This has been found to be increased in tissues undergoing regeneration or at sites of inflammation within tissues (O'Brien et al. 1994; Nau et al. 1999). Secreted levels of OPN in plasma have been linked to many chronic inflammatory and leukocyte derived disorders as well as autoimmune disorders such as Crohn's disease (Agnholt et al. 2007), atherosclerosis (Golledge et al. 2007), lupus (Kariuki et al. 2009), multiple sclerosis (Comabella et al. 2005) and rheumatoid arthritis (Sennels et al. 2008). OPN is responsible for inducing inflammatory responses in many different leukocytes including macrophages, T-cells and dendritic cells (Bruemmer and Collins 2003). A study by Weber concluded that OPN binding to integrins after thrombin cleavage is responsible for the activation and homing of monocytes (Weber et al. 2002). OPN can function in many signalling mechanisms in inflammatory responses and this diverse molecule can be chemotactic to attract the migration of cells of the immune system. There it maintains the cells acting as an adhesive protein. OPN is capable of functioning as a pro-inflammatory cytokine, enhancing Th1 cytokine production and increasing enzymes such as MMPs responsible for degradation of the ECM (Weber et al. 2002; Bruemmer et al. 2003). During the process of macrophage differentiation the expression of OPN is up-regulated however it is not present in circulating macrophages (Krause et al. 1996). Several inflammatory cytokines can induce OPN expression in macrophages including IL-1β, IL-6, IFNγ and TNFα (Nakamachi et al. 2007; Ogawa et al. 2005; Bruemmer et al. 2003).

1.6.4 Expression of Osteopontin in endometrium

OPN expression has been found in the endometrium of healthy cycling women (Casals et al. 2008). Maximal OPN expression is observed during the mid secretory phase in the window of implantation at both the mRNA and protein level (DuQuesnay et al. 2009). OPN expression was localised to the glandular and luminal epithelium (Afify et al. 2006; Albers et al. 1995). Secreted levels of OPN are also

increased in the secretory phase of the menstrual cycle when compared to the proliferative phase (Wolff, Thomas Strowitzki, et al. 2001). It has been proposed that OPN secretion through the endometrial glands is essential to activate integrins on the blastocyst surface to allow for an adhesive surface (Chaen et al. 2012). Secreted OPN is capable of binding to CD44 and integrin αVβ3 separately. It is hypothesized that OPN may act as a bridging molecule between these by binding to both CD44 and integrin αVβ3 simultaneously (Yen and Jaffe 2009). Therefore for the remainder of the study this binding will be referred to as the adhesion complex. CD44 and integrin αVβ3 are both expressed on the endometrial epithelial and trophoblast surface, with maximal expression on the endometrial surface during the window of implantation. Therefore it has been hypothesised that these molecules are involved in the implantation process. These molecules are therefore good candidates for the study of the interaction between the developing blastocyst and the endometrial epithelial surface.

1.7 CD44

The *CD44* gene is located on the short arm of chromosome 11 in region 1 band 3. The promoter region of *CD44* contains regulation elements for ERα, AP-1, SP-1, STAT1, IRF-1 and NFκB (Figure 1-10). Its gene structure is subject to extensive splicing which results in multiple RNA splice variants (up to 20) being produced (Figure 1-11). The standard *CD44* exons include 1-5 and 16-20 and exons 6-15 are variable exons which are alternatively spliced. This results in many possible combinations of exon transcripts, thus giving rise to a variety of different protein structures (Figure 1-11).

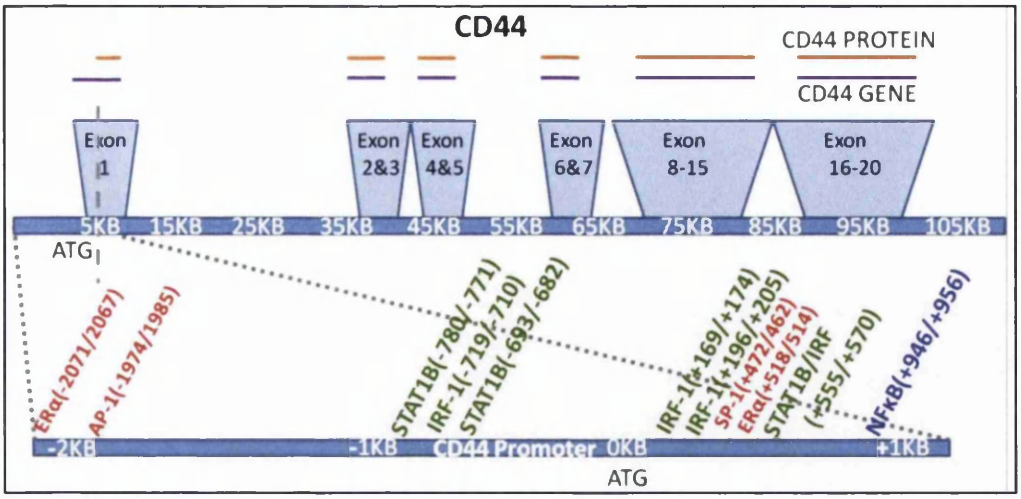

Figure 1-10 CD44 promoter structure.

Regulation elements for ERα, AP-1, SP-1, STAT1, IRF-1 and NFκB are indicated.

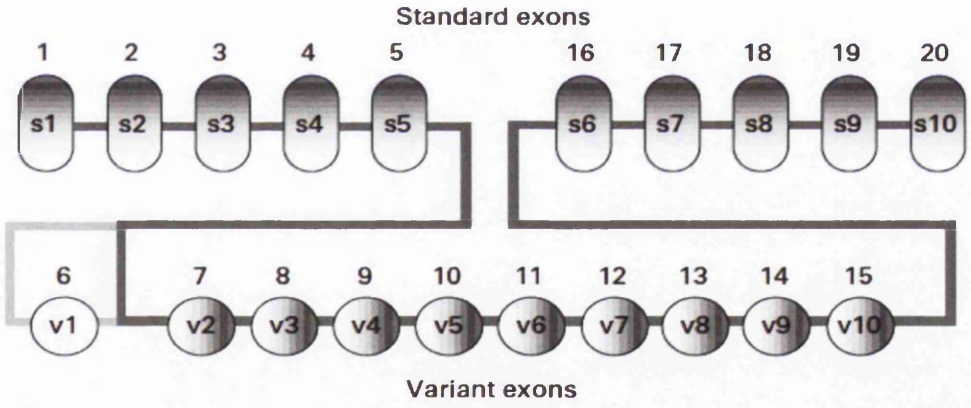

Figure 1-11 CD44 gene structure.

The standard CD44 molecule (CD44s) is coded for by the standard exons (s1-10). Due to alternative splicing a number of variant CD44 protein isoforms exist (v2-10) in humans between s5 and s6. (Goodison et al. 1999) .

1.7.1 CD44 tissue expression

CD44 is a glycoprotein which is membrane bound and expressed on some epithelial cells in humans. Proliferating epithelial cells have been shown to up-regulate the expression of CD44 during tissue repair (Alho and Underhill 1989). Expression of CD44 has been found on migrating mesenchymal stem cells and is markedly increased on chondrocyte cell surfaces, where it plays an important role in cartilage homeostasis (Knudson and Loeser 2002). CD44 expression has been shown in pancreatic duct epithelial cells (Ringel et al. 2001), gastric mucosa (Heider et al. 1993) and breast epithelial tissue (Afify et al. 2008; Hole et al. 1997). At the mRNA level *CD44* expression has been characterised in the retinal corneal epithelia and cervical epithelia (Woerner et al. 1995). Epithelial protein expression of CD44 has been noted in the following tissues: cervix, colon and breast (Woerner et al. 1995; Trejdosiewicz et al. 1998). Furthermore, expression has been demonstrated on a variety of leukocytes including monocytes and intestinal mucosal smooth muscle cells (de La Motte et al. 1999). CD44 binding to OPN has been demonstrated in tissues including the prostate, substantia nigra and kidney (Ailane et al. 2013; Asselman 2003). CD44 expression on the trophoblast surface of the blastocyst has been shown (Goshen et al. 1996).

1.7.2 CD44 protein structure

Splicing at the RNA level results in several different CD44 variant proteins and different variant expression has been associated with different tissues (Figure 1-12). Expression of the standard CD44 (CD44s) has been identified in many cells and tissues throughout the body, whilst expression of CD44 protein variants (CD44v) has been found primarily in epithelial tissues including the oesophagus, skin and small intestine. Expression of CD44v4, CD44v6 and CD44v9 is found in these tissues (Mackay et al. 1994).

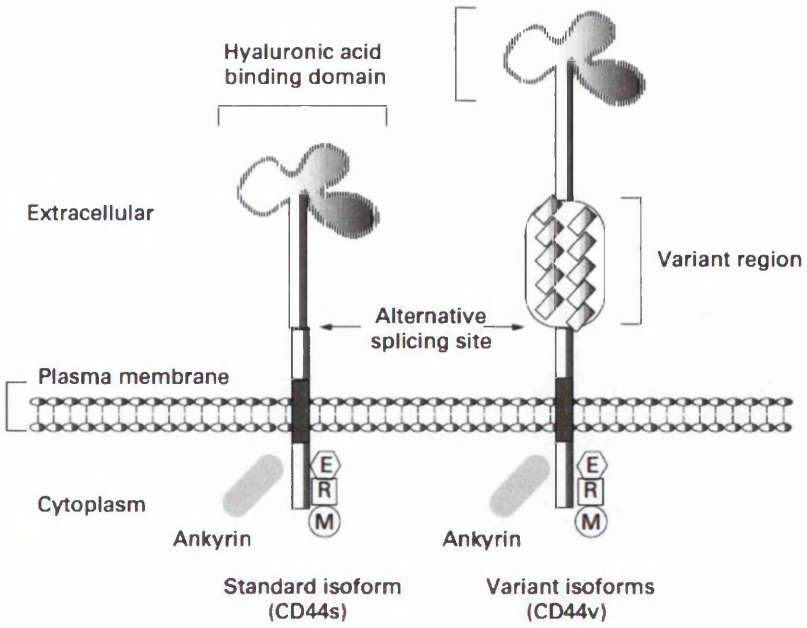

Figure 1-12 CD44 protein structure

The standard form of CD44 protein structure is shown on the left, CD44 primarily binds to hyaluronic acid. The addition of the variant exons reduces its affinity for hyaluronic acid and allows for the binding of other molecules (Goodison et al. 1999).

1.7.3 CD44 function

CD44 is the receptor for hyaluronic acid and through this interaction CD44 is capable of mediating cell-cell and cell-matrix interactions (P. Johnson et al. 2000). Its ability to bind other ligands such as OPN, collagens and MMPs is also thought to have an involvement in CD44 cellular interactions (Goodison et al. 1999). Functionally, CD44 was originally thought to be responsible for tethering cells to extracellular ligands only. However, evidence has shown it is able to monitor changes in the ECM through extracellular ligand binding that can influence cell characteristics such as growth, survival, and differentiation through interactions with associated proteins (Ponta et al. 2003; Lee et al. 2008) (Figure 1-9). CD44 has been shown to be part of the process that activates leukocytes such as lymphocytes and acts as a homing receptor for lymphocytes (Xu 2011).

1.7.4 CD44 dysfunction

When CD44 expression is altered or the protein becomes dysfunctional the consequence can be pathogenic to cells and tissues. Up-regulation of CD44 has been correlated with many cancers such as liver, colon and prostate (Iczkowski 2010; Orian-Rousseau et al. 2002; van der Voort 1999; Desai et al. 2009; Bates et al. 2001). A study that focused on CD44 variants in breast cancer found that a particular isoform CD44v6, when elevated, was correlated positively with ER and PR expression in breast cancer tissue (Friedrichs et al. 1995). CD44 expression has been characterized in the glands of tissues. An example is the mammary glands where CD44 expression is required for the proliferation of the underlying mesenchymal cells (Yu et al. 2002; Hebbard et al. 2000). CD44 expression in the mammary gland is thought to be linked to its role as a mediator of epithelial-stromal signalling in addition to functional roles in proliferation, migration and invasion in cancer cells (Louderbough et al. 2011; Lokeshwar et al. 1995).

1.7.5 CD44 and inflammation

CD44 has been shown to be involved in T-cell recruitment at sites of inflammation, CD44 can activate inflammatory pathways on binding of its ligands (Baaten et al. 2010). CD44 expression is found on most leukocytes in the body and functions to mediate the adhesion of glycosaminoglycans and hyaluronic acid to the ECM (Hutás et al. 2008). Inflammatory responses activate T-cells and induce CD44 binding to hyaluronic acid (Johnson and Ruffell 2009). CD44 is expressed on endothelial cells close to sites of inflammation, where activated T-cells expressing CD44 bind and a rolling interaction is initiated (Nácher et al. 2011; de La Motte et al. 1999). The interaction of these activated T-cells and endothelium activate integrin expression which mediates adhesion to arrest the cells and allows for migration to the site of inflammation. CD44 has a role in limiting the inflammatory response in tissues and aids in the resolution of inflammation in lung models (Johnson and Ruffell 2009). Human chondrocytes *in vitro* when exposed to hyaluronic acid, interact with CD44

to induce NFκB activation, which activates the transcription of pro-inflammatory cytokines TNFα and IL-1β (Campo et al. 2010).

1.7.6 CD44 expression in endometrium

CD44 detected by immunohistochemistry in the endometrium has been described in fertile women and the expression of CD44 variants in the epithelium and stroma appears to differ. CD44 staining has been shown to be more prominent in the stroma than the glands or luminal epithelial cells. However, expression of variants CD44v7-8 was more prominent in the glandular epithelium than the luminal epithelium or stroma (Goshen et al. 1996). Another study of CD44 expression in endometrial epithelial cells identified CD44 expression at high levels and lower expression levels of CD44v9 were detected. The expression of CD44v4 and CD44v6 has not been detected in the endometrial epithelium (Mackay et al. 1994). When the distinct phases of the menstrual cycle are considered in isolation expression of the CD44 variants in the endometrium appears to differ througout the menstrual cycle, in the proliferative phase luminal CD44 expression was lower than the secretory phase (Afify et al. 2006; Poncelet et al. 2010). Protein expression of CD44 and CD44v6 has been detected in the stroma and epithelium respectively of the proliferative phase endometrium (Poncelet et al. 2002). In the secretory phase CD44 expression has been found to be prominent in the endometrium of healthy cycling women (Poncelet et al. 2010; Desai et al. 2007). Expression of CD44 has been identified in secretory phase epithelium and stroma, whilst CD44v6 has only been found in the epithelium during the secretory phase. No expression of CD44v3 was found in the endometrium (Poncelet et al. 2002). CD44 expression in the endometrial stroma in the secretory phase is important in the processes after initial implantation. This is because CD44 is hypothesized to have a role in decidualization through the transcription activation of genes responsible (Wilms tumour-suppressor) for causing cells to decidualize ready for invasion of the developing trophoblast (Kim et al. 2011; Behzad et al. 1994; Goshen et al. 1996). In terms of implantation CD44 expression on the endometrial luminal surface during the

window of implantation is essential to enable the OPN complex to assemble and for attachment of the blastocyst to the epithelia surface (Johnson et al. 2003). Secreted uterine OPN and membrane tethered CD44 have both been shown to be markedly increased in the secretory phase of the menstrual cycle compared to the proliferative phase (Wolff, Thomas Strowitzki, et al. 2001; Afify et al. 2006). The consequence of altered CD44 expression in the epithelia and stroma of endometrial tissue has been linked to the development of endometriotic lesions in women with endometriosis. This is thought to occur through increasing the ability of endometriotic cells to bind the outer peritoneal surface of the endometrium (Lucidi et al. 2005; Poncelet et al. 2002). Expression of CD44 has been shown to be decreased in the proliferative phase of women with infertile PCOS and UIF (Yaegashi et al. 1995; Saegusa et al. 1998).

1.8 Integrin αVβ3

1.8.1 Normal physiology

Integrin αVβ3 is a receptor that is also a component of the extra cellular matrix and has a role in cellular signalling, cell shape, mobility, cell cycle regulation, proliferation and invasion (Desgrosellier and Cheresh 2010; Assoian and Klein 2008; Huttenlocher and Horwitz 2011). Secreted OPN binding to membrane bound integrin αVβ3 can initiate outside-in signalling which allows the cell to respond to external stimuli and initiate signal cascades for cell motility, cell migration or cell survival (Figure 1-9). Integrin αVβ3 is also involved in cell-cell and cell-matrix interactions and communication between cells. Integrins have an important role in the remodelling of the extra cellular matrix through the regulation of localization and activity of proteases. Integrins are widely expressed throughout most tissues in the body but are predominantly expressed in hematopoietic cells such as monocytes and macrophages, as well as angiogenic endothelial cells (Weerasinghe et al. 1998; Hsu et al. 2011).

1.8.2 *Integrin αVβ3 structure*

Integrins consist of an α and β sub-units, there are 18 α sub-units variants and 8 β sub-units variants (Figure 1-13). The α and β sub-units can bind to one another in twenty five identified possible combinations, and are defined by their adhesion properties. Integrins consist of both α and β sub-unit that are transcribed by separate genes. Once the proteins are synthesized they dimerise and can bind a variety of different ECM components.

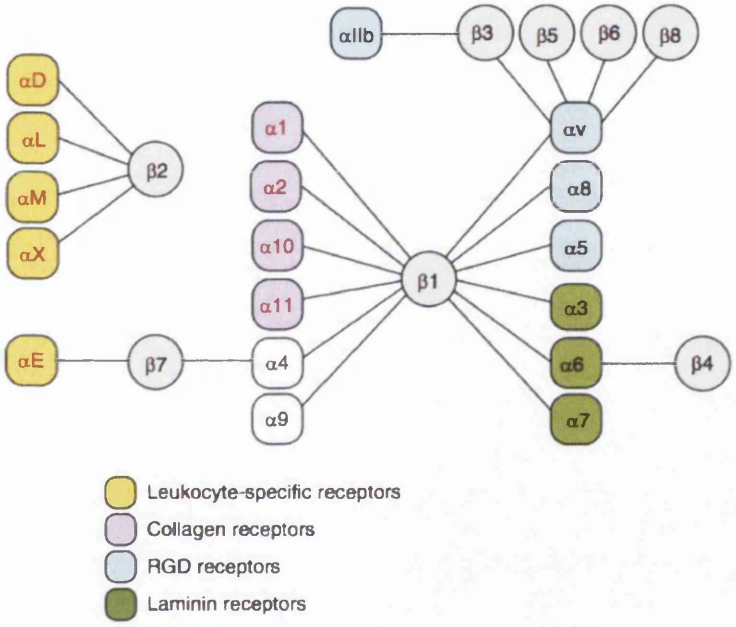

Figure 1-13 Different α and β integrin subunits and possible binding combinations.

Integrins have many different α and β subunits that can bind in multiple combinations. There are four classes of α receptor, those that are specific receptors in leukocytes (yellow), collagen binding (pink), RGD binding (blue) or laminin binding (green) (Srichai and Zent 2010).

The αVβ3 protein is capable of recognising and binding the RGD tri-peptide sequence on ligands. The active ligand recognition site of αVβ3 is thought to be on the area of the protein where the α and β sub-units bind one another to form the extracellular active site. The active RGD binding site is formed by both sub-units equally (Millard et al. 2011). The integrin protein complex is anchored to the cell membrane via the β subunit and kindlin and talin proteins (Figure 1-14). Prior to

ligand binding the inactive integrin conformation has two cytoplasmic tails in close proximity, and the entire structure is folded over (Figure 1-14a). This structure changes, and both subunits extend following kindlin and talin binding. The cytoplasmic tails move apart, extending the sub-units and allowing their active site to become functional. Binding of intrinsic ligands such as tallins activate inside out signalling and aid in this change of conformation, activating the integrin receptors (Figure 1-14b).

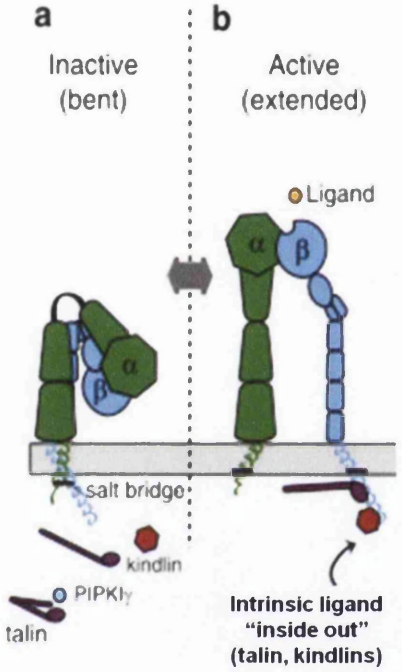

Figure 1-14 Integrin α and β subunits dimerised and expressed at the cell membrane surface.

Conformational change in the integrin structure from inactive to active form. (a) The integrin is inactive when in a bent conformation. (b) This changes to an extended conformation when the receptors are active for ligand binding.

1.8.3 Integrin αVβ3 expression in endometrium

Integrin β3 expression has been monitored throughout the menstrual cycle and found to be markedly increased around day 21. Integrin αVβ3 is well characterized as a marker of implantation, and it is maximally expressed in the secretory phase of the menstrual cycle (DuQuesnay et al. 2009; Lessey and Arnold 1998). The

expression of β3 has been characterised in the fertile endometrium (González et al. 2006) and is considered to be a key adhesion protein that contributes to the receptive state of the endometrium. A study by Lessey found that αVβ3 was up regulated in the secretory phase of healthy, cycling fertile women (Lessey 2002). Other studies that have investigated the levels of αVβ3 in infertile women in comparison to fertile women found no differences in the stromal levels (Ceydeli et al. 2006). In the epithelium of the endometrium maximal expression of αVβ3 has been documented during the window of implantation (Apparao et al. 2001; Wolff, T Strowitzki, et al. 2001). Expression of αVβ3 during implantation has been extensively studied in animal models including rabbit (Illera et al. 2003) and sheep (Wan et al. 2011). In both of these animal models αVβ3 has been shown to be involved in the implantation process and expression has been shown on the trophoblast and the endometrial surfaces.

1.9 Potential factors affecting uterine receptivity

1.9.1 Hormone imbalance

If expression of hormones and secreted hormone receptor levels are increased or decreased this could have undesirable effects on the regulation of ovulation. Variations in estrogen expression in the menstrual cycle can result in delayed ovulation or anovulation (Longcope et al. 1990; Check 2007; Fanta 2013). The development of the egg can also be affected. Complex signalling pathways can be activated upon ER ligand binding to ER (Figure 1-15).

1.9.2 Estrogen receptor signalling

Estrogen signalling can occur through estrogen receptor α or β. Extracellular estrogen enters the cell and on ligand receptor binding in the cytoplasm will dimerise with another ligand-bound estrogen receptor. Once dimerised, the protein complex can then translocate to the nucleus and bind estrogen response elements (ERE) sites on gene promoters to activate or mediate gene transcription. Other signalling mechanisms induced via ER signalling include the up-regulation of AP-1

and SP-1 transcription factors. This initiates a signalling pathway which ultimately leads to their activation (Figure 1-15). OPN and CD44 promoter regions both contain regulatory elements for ERα, AP-1 and SP-1 (Figure 1-7, Figure 1-10). It is possible that hormone imbalance within the endometrium or a decrease in receptor levels could have undesirable consequences on the expression of these genes. If OPN and CD44 expression was to be increased or decreased at the epithelial surface during the window of implantation the receptivity of the uterus could be affected.

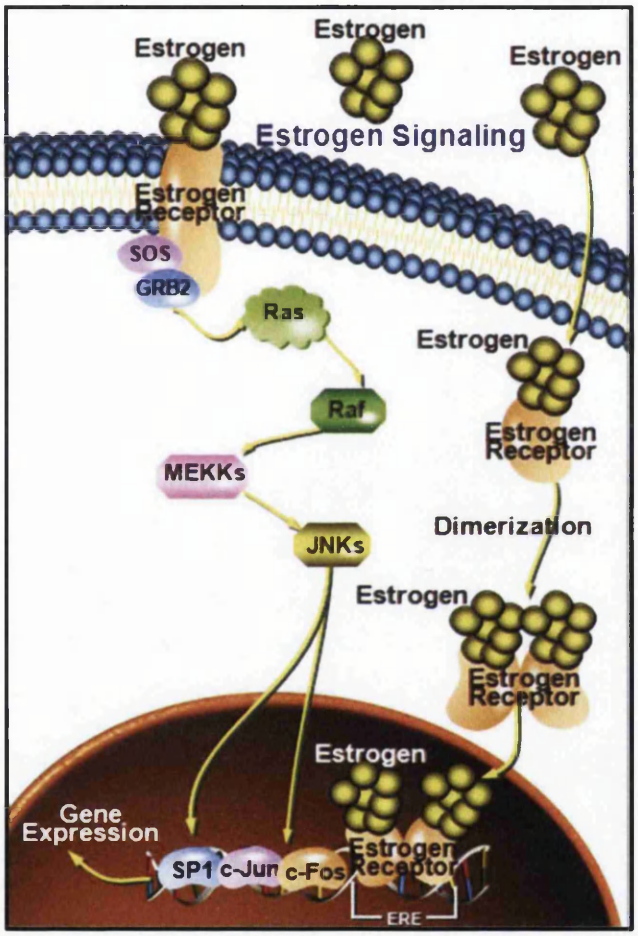

Figure 1-15 Estrogen ligand bound receptor signalling.

Estrogen signalling can activate many signalling pathways which lead to transcription factor activation. Classical Estrogen regulatory elements (EREs), Specificity Protein 1 (SP-1) and Activator Protein 1 (AP-1) transcription factors (Adapted from proteinlounge.com).

1.9.3 Glucose

There is evidence to show that obesity and high body mass index (BMI) increase the risk of diabetes in PCOS women and has been shown to be associated with insulin resistance (Samy et al. 2009). Some of these women will develop type II diabetes. Hyperglycemia could be a factor in infertility and metformin is used as a treatment to suppress glucose production by the liver (Nathan et al. 2009). It is commonly used to treat women who have insulin intolerance as a second medication option after emphasising natural ways to decrease glucose levels such as lifestyle modification (NICE 2012). PCOS women have similar symptoms to those associated with metabolic syndrome and therefore these patients may have excess circulating glucose (Essah et al. 2007). Metabolic syndrome is defined by obesity and two or more of the following factors; raised triglycerides, reduced HDL-cholesterol, raised blood pressure and raised fasting plasma glucose levels (Alberti et al. 2006). Excess levels of glucose may affect the expression of adhesion molecules at the epithelial endometrial surface. High levels of glucose have been shown to regulate OPN expression in mice and rat models (Takemoto et al. 2000; Asaumi et al. 2003). Whilst CD44 has been shown to have a role in insulin resistance (Kang et al. 2013) and in the regulation of glucose metabolism in cancer cells (Tamada et al. 2012).

1.9.4 Cytokines

The Tumour Necrosis Factor alpha *TNFα* gene (TNFA) is located on chromosome 6p21.3 and was first cloned in 1985 (Old 1985). TNFα is a transmembrane protein that is cleaved by TNFα converting enzyme (TACE) to produce soluble TNFα. This is the biologically active form of TNFα expressed on activated macrophages and lymphocytes in addition to other cell types (Horiuchi et al. 2010). In the normal menstrual cycle TNFα and Interleukin 1 beta (IL-1β) play a role in aiding follicular rupture through activation by FSH and LH. In the endometrium TNFα is involved in the proliferative and menses phases of a normal menstrual cycle, with expression peaking in epithelial cells in the secretory phase. However, in the proliferative phase TNFα expression is primarily expressed in the stromal compartment (Junt, Chen &

Hu, 1992). Therefore it is possible that these cell types regulate TNFα differently (Tabibzadeh *et al* 1995; Horiuchi et al. 2010). In the endometrium TNFα is produced by activated cells of the immune system including lymphocytes, macrophages and natural killer cells. In combination with IL-1 it functions to induce the inflammatory response initiating a cascade of cytokines and chemokines (Lebovic et al. 2001). *IL-1B* gene is located on chromosome 2 and codes for the IL-1β protein. This is activated by the cleavage of caspase 1, produced by activated macrophages, endothelial cells, B-cells and fibroblast cells (Burke et al. 2013). IL-1β promotes prostaglandin production (Fakih et al. 1987). While it is important in inflammation, IL-1β is also involved in cell proliferation, differentiation and apoptosis (Kasza 2013). IL-1β is of interest in endometrial biology due to its part in hormonal regulation and its role as an inflammatory mediator. Maximal expression of IL-1β has been detected during the secretory phase of the menstrual cycle at both the mRNA level in tissue and protein level in blood serum (Giudice 1994). IFNγ or type II interferon is encoded for by the *IFNG* gene (Gray and Goeddel 1982). IFNγ protein structure contains six α-helices and is able to dimerise and is secreted by T cells after activation or NK cells (Schroder et al. 2004; Roman et al. 2010). IFNγ is involved with cell proliferation and apoptosis, activation of bacteriocidal activity, and antigen presentation through MHC class I and II molecules (Schroder et al. 2004).

Disrupted expression of these pro-inflammatory cytokines have been found in PCOS and endometriosis (as discussed in section 5.1). PCOS and endometriosis are often associated with chronic inflammation, indicators of which include C-reactive protein (CRP), leukocytes, IL-18, TNFα, IL-1β and IFNγ (Diamanti-Kandarakis, 2007). The disrupted levels of these pro-inflammatory cytokines may lead to increased or decreased signalling pathway activation. This will have consequences on the genes activated downstream of their signalling pathways. *OPN* and *CD44* have shown to contain regulatory elements on their promoter regions for NFκB which can be activated upon TNFα or IL-1β signalling. Furthermore, they both contain STAT1 regulatory elements which can be activated upon IFNγ signalling. When TNFα binds to TNFR2 it initiates a signalling cascade that ultimately leads to the activation of

NFκB (Bouwmeester et al. 2004). Upon ligand binding the following proteins are recruited to TNF Receptor Associated Factor (TRAF2); TRAF, Receptor interacting protein (RIP), and tumour necrosis factor receptor type 1-associated death domain protein (TRADD). This activates NFκB Inducing Kinase (NIK) to recruit inhibitor of NFκB kinase (IKK) which phosphorylates inhibitor of kappaB (Iκβ) and allows for dissociation between Iκβ and NFκB. Iκβ then becomes degraded and NFκB translocates to the nucleus to activate gene transcription (Beg et al. 1993) (Figure 1-16). The genes encoding both *OPN* and *CD44* have NFκB regulatory elements in their promoters and therefore it is possible that their expression could be modulated through the TNFα signalling pathway.

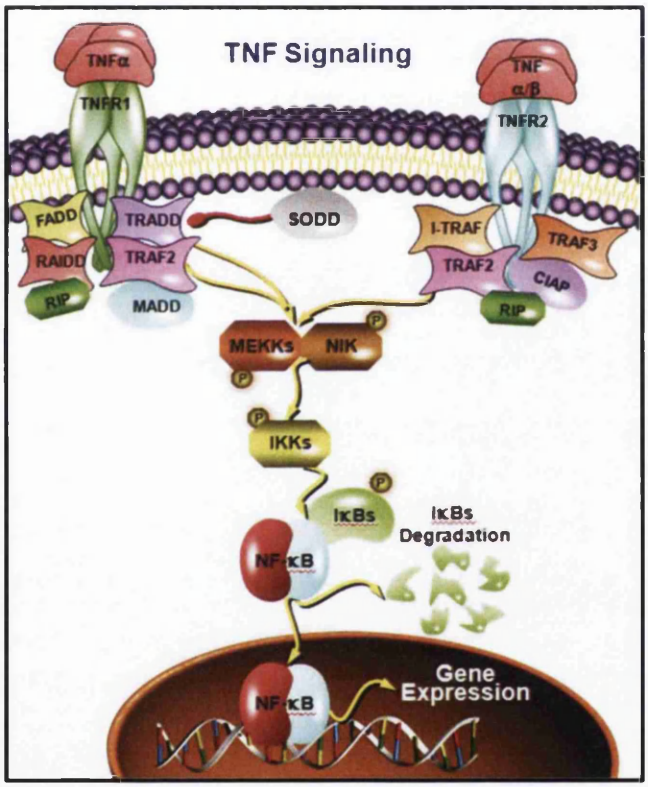

Figure 1-16 TNFα-NFκB signalling pathway

Extracellular TNFα binds to TNFR 1 or 2 to activate a signalling cascade that activates NFκB (Adapted from proteinlounge.com)

Upon IL-1β ligand binding to the IL-1RacP, Toll-interacting Protein (TOLLIP) and Myleloid Differentiation primary response gene-88 (MyD88) are then recruited to

this complex. They then function as adaptors to recruit interleukin-1 receptor associated kinase (IRAK). This is responsible for the recruitment and activation of TRAF6. IRAK then becomes phosphorylated and ubiquitinated. TRAF6 can signal leading to the degradation of IκB through the kinase action of TGF-beta-activating kinase-1 (TAK1) and TAK1 binding protein 1 (TAB1). This complex can then link with TRAF6 initiating the activation of NIK. This leads to the activation of IKK and the subsequent phosphorylation of IκB, finally allowing NFκB to translocate to the nucleus to mediate gene transcription (Figure 1-17).

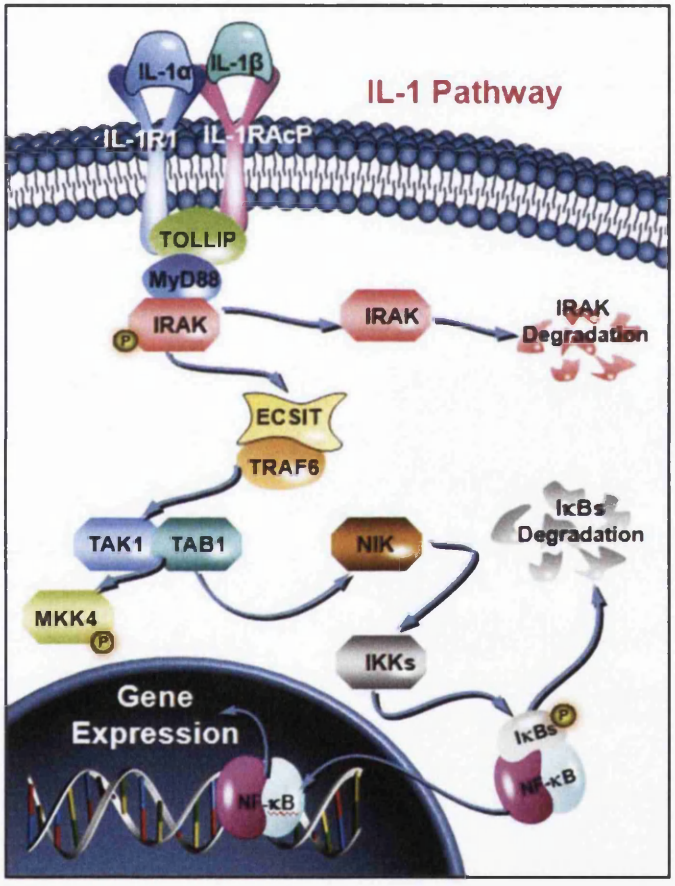

Figure 1-17 IL-1β NFκB signalling.

IL-1β signalling through IL-1RacP induces a signalling cascade that activates NFκB (Adapted from Qiagen.com/pathways).

IFNγ signalling is mediated through the Interferon gamma receptors 1 and 2 which dimerise at the cell membrane. Extracelluar IFNγ binds to the interferon gamma receptor 1-recetor 2 (IFGR1-R2) complex receptor, which is followed by

autophosphorylation and activation of JAK2 (Schroder et al. 2004). Activated JAK2 phosphorylates STAT1 allowing it to dimerise and translocate to the nucleus, there it can bind regulatory elements to influence gene transcription of interferon regulated genes (Figure 1-18). *OPN* and *CD44* promoter regions both contain regulatory elements for STAT1 or IRF-1, to which activated STAT1 dimers can bind and modulate gene transcription. It is possible for IFNγ to regulate the expression of *OPN* and *CD44* through activation of STAT1 (Schroder et al. 2004).

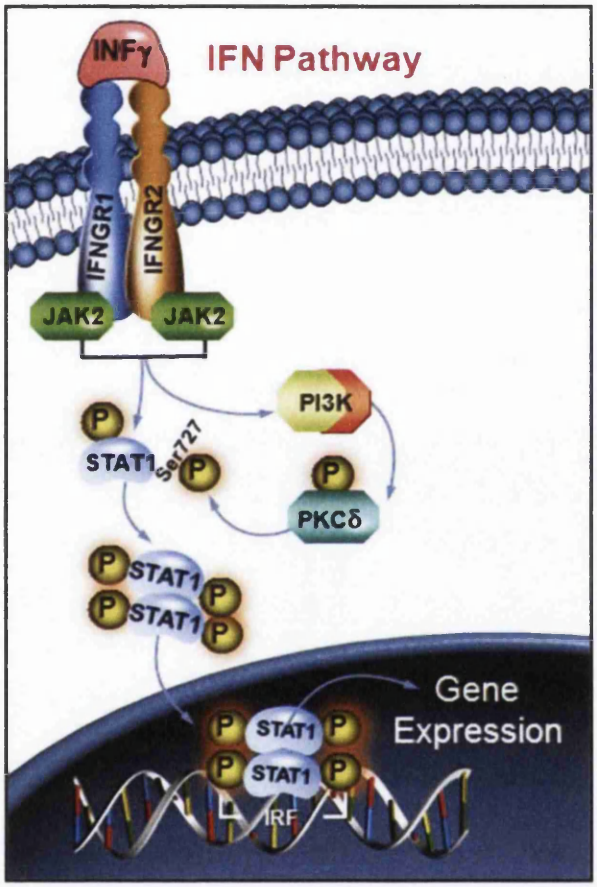

Figure 1-18 IFNγ STAT1 signalling.

IFNγ signalling through the IFGR and IFR2 induces JAK-STAT signalling, activating STAT1 (Adapted from Qiagen.com/pathways).

1.10 Research aims

The purpose of this study is to examine any potential role for the adhesion complex components OPN, CD44 and integrin αVβ3 in infertility. It is hypothesized that the adhesion complex is involved in the attachment process of implantation and that in infertility disrupted levels may be a contributing factor. Therefore, the objectives of this study are:

To establish the expression profile of the adhesion complex components in tissue and supernatant samples obtained from fertile and infertile women. The following techniques are used; to obtain mRNA, intracellular protein and secreted protein levels, quantitative polymerase chain reaction (qPCR), Immunohistochemistry (IHC) and enzyme-linked immunosorbent assay (ELISA) respectively.

To establish if hormones in the healthy menstrual cycle regulate the adhesion complex components. This is carried out by utilising endometrial epithelial cell lines as *in vitro* model to mimic the estrogen and progesterone stimulus in the menstrual cycle. Levels of the adhesion complex expression are then to be measured in response to this at the mRNA, intracellular protein and secreted protein levels. The direct role of ERα in the regulation of the adhesion complex components *OPN* and *CD44* are then investigated using chromatin immunoprecipitation (ChIP).

To determine if common conditions linked to PCOS and endometriosis such as obesity, diabetes, inflammation and elements of metabolic syndrome affected uterine expression of the adhesion complex as may be experienced in a sub set of these women. Treatment with glucose and pro-inflammatory cytokines is conducted to assess their role in regulating the adhesion complex components in an *in vitro* cellular model. Direct regulation by pro-inflammatory pathways is then investigated by ChIP, determining the occupation of STAT1, IRF-1 and NFκB on the promoters of *OPN* and *CD44*.

Chapter 2

Materials and methods

2.1 Collection of primary tissue and supernatants

Endometrial samples were obtained by pipelle biopsy, a standard outpatient procedure, from patients identified by the gynaecological department of Singleton Hospital, Swansea. According to standard clinical procedure all patients were referred to the clinic for laparoscopy, sterilisation or diagnostic purposes to identify pelvic inflammation, endometriosis or ovarian cysts. Trans-vaginal ultrasound identified patients who have a greater than normal endometrial thickness (>5mm) for investigation of menorrhagia and abnormal intermenstrual bleeding. Written consent was obtained for all biopsy samples obtained, subject to ethical approval from the South West Wales Research Ethics Committee (LREC nr. 05/WMW02/45).

Pipelle biopsy obtains a ribbon of endometrial tissue, principally containing epithelial and stromal cells. Once collected, biopsies were placed immediately in 15mls culture medium and kept at 4°C. On receipt of biopsies at Swansea University, the supernatant was removed, centrifuged, and aliquots (0.5mL) were taken and stored at -20°C. Biopsy tissue was either processed for RNA immediately or stored at -80°C. Biopsy material was grouped into four categories according to pathology (Table 2-1). Women with the following conditions were excluded from the qPCR and IHC study: tubular factor, endometrial hyperplasia, endometrial carcinoma, presence of polyps and sexually transmitted diseases. All patient groups were age and BMI matched as closely as possible.

Study group	Diagnosis	Section for reference
1	Fertile control	1.1.1
2	Infertile PCOS	1.1.2
3	Infertile Endometriosis	1.1.3
4	Unexplained Infertility	1.1.4

Table 2-1 Study Groups for clinical study.

Patients were separated to 3 study groups and compared to fertile women who were used as controls.

2.2 Secondary endometrial cell culture

First established in 1968 by Kuramoto, Hec-1A and Hec-1B were both derived from a 71 year old patient with stage 1A endometrial adenocarcinoma (Kuramoto 1972; Kuramoto et al. 1972). Later in 1983 the RL925 cell line was isolated from a 65 year old Caucasian with a grade 2 moderately differentiated adenosquamous carcinoma of the endometrium (Way et al. 1983). Ishikawa is another well differentiated epithelial endometrial adenocarcinoma cell line, which has been used extensively as an epithelial endometrial model for the past 25 years (Nishida et al. 1985). Isolated from a 39 year old Japanese patient with type I, stage 2 endometrial adenocarcinoma in October 1980, a small sample was taken and due to its fragility the epithelial and stroma compartments were easily separated. A further cell line has subsequently been developed, acknowledged in the literature, Hec-50 and nominally called Heraklio in this study (Kuramoto et al. 1991). This is also a type II endometrial epithelial cell line derived from an adenocarcinoma and was obtained from ECACC for this study (Albitar et al. 2007).

All epithelial cells were cultured on plastic culture vessels (Falcon T25, T75, T125) and maintained in Dulbecco's Modified Eagle's Medium; Nutrient Mixture F-12 (DMEM/F12) in a 1:1 with GlutaMAX™ (2.5mM) supplemented with 10% Foetal Bovine Serum (FBS), 1mM sodium pyruvate, 1.5g/L sodium bicarbonate (stock 7.5%) and 1% Penicillin/streptomycin. Cells were incubated at 37°C in a humidified 5% CO_2 atmosphere (Nuaire, UK). Epithelial cells were sub-cultured 1:8 when 70% confluent. For sub-culture, the cells were first washed twice with phosphate buffered saline (PBS) (Lonza-BioWhittaker, UK) to remove serum from the cell monolayer. To detach the cells from the plastic substrate, 0.25% trypsin-EDTA was added and the flasks incubated for 5mins at 37°C. Detachment was confirmed by inverted light microscopy. DMEM/F-12 (10mL) supplemented with FBS was added to the flask to neutralise the trypsin and the cell solution centrifuged for 5mins at 2500g. Cell pellets were re-suspended in 10mL of DMEM/F-12 and split to the

appropriate ratio before seeding to the appropriate culture vessel. All reagents were obtained from Life Technologies unless otherwise stated.

2.3 Cell treatment

All cell treatments for this study were conducted in either 6 well plates (Nunc, UK) or on glass slides for IHC. In each case the cells were grown to 80% confluency and fully supplemented growth media was replaced with charcoal stripped media for a minimum of 24hrs before treatment. This removed any trace steroid and large molecular weight proteins, which may affect the efficiency of cell treatment. Outlined here are the compound preparation and volumes for final required concentration.

Charcoal stripped FBS preparation: Charcoal (Charcoal, Dextran coated Sigma 1g) was add to a 500ml bottle of FBS and inverted 5 times to mix. Incubated at 56˚C for 2 hours and cooled for 1 hour at 25˚C before filtering through a Stericup (Millipore, UK) using vacuum pump system in a lamina flow hood (ScanLife, UK).

2.4 Hormone preparations

Estradiol and Progesterone treatment regimes were chosen at concentrations and time points to the mimic menstrual cycle *in vitro* in a cell line model.

Estradiol (E_2): 0.027g of powdered 17-β Estradiol (Cat: E8875 >98%, Sigma UK) was added to 1mL of absolute ethanol (Fisher Scientific, UK) to make a stock concentration of 1mM. Serial dilutions of 1:10 were then made by removing 100µL of the 1mM stock and adding to 900µL absolute ethanol to give a working stock of 10µM. 3µl of this stock was added to 3mLs of media to obtain a final concentration of 10nM.

Progesterone (P_4): 0.031g of powdered Progesterone (Cat: P0130, Lot# 129K0061, Sigma UK) was added to 1mL of absolute ethanol (Fisher Scientific) to a concentration of 1mM, and serial dilutions of 1:10 were then made by removing

100µL of the 1mM stock and adding to 900µL absolute ethanol to give a working stock at 100µM. 3µl of this stock was added to 3mLs of media to obtain a final concentration of 100nM.

Estradiol (E_2) and Progesterone (P_4) co-treatment: 3µl of 10µM E_2 was added to 3mLs of media to obtain a final E_2 concentration of 10nM plus 3µl of 100 µM of P_4 was added to 3mLs of media to obtain a final P_4 concentration of 100nM

2.4.1 Glucose preparation

Two stocks of media containing different concentrations of glucose were prepared for the experiments in Section 5.2. For high glucose concentration (25mM), 0.09g powdered glucose (α-D-Glucose, Sigma Cat no. 158968 Lot# STBC1731V) was added to 10mLs of appropriate media to obtain 25mM final concentration. For the intermediate concentration of glucose (17mM), 0.0135g was added to 10mLs of appropriate media to obtain 17mM final concentration. Both stocks were then filter sterilised through an acro disc and all Glucose stimulation experiments were performed in basic, DMEM low glucose (5mM) medium phenol free containing 10% stripped serum.

2.4.2 Cytokine preparation

IL-1β: 100µL of deionised filter sterilised water was added to lyophilised IL-1β powder (10µg Miltenyi biotec, GmbH Cat no. 130-093-895, Lot no. 5110831174), to obtain a stock concentration of 100µg/mL. A working stock of 1000ng/mL was made by 1:100 dilution. 5µL of this working stock was added per mL of culture medium to obtain a final concentration of 5ng/mL.

TNFα: 1000µL of deionised filter sterilised water was added to lyophilised TNFα powder (10µg Miltenyi biotec, GmbH Cat no. 130-094-014, Lot no. 5110831175) to obtain a stock concentration of 10µg/mL. 2.5µL of this stock is added per mL of culture medium to obtain a final concentration of 25ng/mL.

IFNγ: 100 µL of deionised filter sterilised water was added to lyophilised IFNγ powder (10µg Miltenyi biotec, GmbH Cat no. 130-096-872, Lot no. 5110831178) to obtain a stock concentration of 100µg/mL. 1µL of this stock is added per mL of culture medium to obtain a final concentration of 100ng/mL (200 IU/mL).

All cytokines were purchased from Miltenyi biotec and are endotoxin free.

2.5 Isolation and quantification of ribonucleic acid

Following cell treatments, total RNA was isolated according to the manufacturer's instructions (RNeasy Kit, Qiagen, UK see appendix A). Briefly, the cell culture media was removed and the cells washed with PBS. RLT (guanidine isothiocycanate lysis) buffer (350µLs) was then added to each sample. The cells were scraped from the 6 well plates and cell lysate collected into clean (RNase/DNase/Pyrogen free) eppendorf tubes, before being added to the Qiashredder spin columns for homogenisation, to break open the cell membranes. RNA was then isolated by processing through a RNeasy column which contains a membrane that RNA binds too and is subject to a DNase digestion for removal of contaminating genomic DNA. After a series of washes in RPE (ethanol salt removal) buffer, RNA was eluted in 25µL of RNase-free water and quantified by spectrophotometer (NanoDrop 2000c – Nucleic Acid program v1.4.2).

2.5.1 Reverse transcription synthesis of complementary ribonucleic acid from ribonucleic acid

RNA was adjusted to the concentration of 100µg/mL in RNase-free water (Qiagen) and 10µL of total RNA was reverse transcribed using random primers according to the manufacturer's protocol (High capacity cDNA conversion Applied Biosciences, UK). A master mix of components was made to avoid small volume pipetting errors. The master mix consisted of 2µL of 10x RT Buffer, 2µL of RT Random Primers, 0.8µL of 25X DNTP Mix (100mM), 3.2µL of nuclease free water (Ambion, UK), 1µL RNase inhibitor and 1µL of MultiScribe™ Reverse Transcriptase per sample. Samples were

added to a 0.2mL thin walled tube (Corning, UK) and 10µL of master mix added (total volume 20µL). Samples were briefly mixed by vortexing and centrifuged. Samples were run on a thermocycler (iCycler, Bio-Rad, UK) using the following programme; samples were heated to 25°C for 10mins then 37°C for 120mins followed by 85°C for 5mins. Samples were then held at 4°C until removed from machine. Samples were stored at -20°C or -80°C for long-term storage. 2µL of the original RNA sample was transferred to a clean (DNase, RNase, pyrogen free) eppendorf for each sample and used as a negative PCR control (un-transcribed template) at a dilution of 1:10. Serial dilutions of cDNA stocks were made at 1:10, 1:100 and 1:1000 from nuclease free water and used to generate standard curves for PCR cycle quantification. Target gene expression was assessed using cDNA at a 1:10 concentration.

2.6 Quantitative Real Time Polymerase Chain Reaction

To obtain qPCR products between 75-150bp for each target gene under investigation cDNA was amplified using gene specific primer pairs (Beacon Design 2.0, Premier Biosoft, USA). Glyceraldehyde 3-phosphate dehydrogenase *(GAPDH)* or Ribosomal Protein 60s L-19 *(RPL-19)* were used as a reference gene, and genomic DNA and RNA were used as positive and negative controls respectively (Table 2.2). Amplification reactions were prepared in a volume of 10µL by adding 5µL of SsoFast evagGreen sSupermix (Bio-Rad, UK), 1µL of each primer (1µM), 2µL of diluted cDNA and 1µL of dH_2O. qPCR amplifications were performed in triplicate on 96-well optical reaction plates and run in the Bio-Rad CFX-96. Samples were first heated to 95°C for 5mins to activate the hot-start DNA Polymerase enzyme and run for 40 cycles of 1secs at 95°C followed by 15secs at the optimal annealing temperature for each primer pair. No amplicons were obtained using RNA directly in the qPCR reaction.

Gene	Primer	Sequence (5'-3')	Ta (°C)	Amplicon length (bp)
GAPDH	F	GTCCACTGGCGTCTTCAC	54.7	145
	R	CTTGAGGCTGTTGTCATACTT		
RPL-19	F	CCTGTACGGTCCATTC	54.3	144
	R	AATCCTCATTCTCCTCATCC		
OPN2	F	ATGGATGATATGGATGATGAAG	53.5	188
	R	TCGGTTGCTGGCGGTC		
CD44	F	GGACCAATTACCATAACTATT	53.9	75
	R	AGGATTCGTTCTGTATTCT		
ITGAV	F	GGAGATTAGACAGAGGAA	53.8	107
	R	CGACTTCAGAGAATAGGA		
ITGB3	F	AAGACTCATATAGCATTG	56.6	200
	R	TGATAGAGATTGACTACA		
ERα	F	CCTCATCCTCTCCCACATCAG	53.5	115
	R	GGCGTCCAGCATCTCCAG		
ERβ	F	TGCTGAACGCCGTGACCGATG	60	75
	R	ATGGATTGCTGCTGGGAGGAGA		
PR B	F	CTGCACTCGGCCTCAACGGG	53.5	119
	R	TGTGGGCTCTGGCTGGCTTC		
GREB1	F	ATCAGCTGCTCGGACTTGCTG	62	135
	R	TGAGCTCCGGTCCTGACAGAT		
AREG	F	TGGACCTCAATGACACCTACTC	55	149
	R	AGGACGGTCACTACTAGAAGG		
SPP1 isoA	F	CTTTACAACAAATACCCAGATGCT	60	113
	R	AAGTCATTGGTTTCTTCAGAGGA		
SPP1 isoB	F	CCTAGCCCCACAGACCCT	60	83
	R	GGTCATCATCATCTTCATCATCC		
SPP1 isoC	F	GGAGTTCTGAGGAACAAGCAGAAT	60	97
	R	TGGTCATGGCTTTCGTTGGA		
SPP1 isoD	F	GACCAAGGAAAACTCACTACCAT	60	131
	R	GACTTACTTGGAAGGGTCTGC		
SPP1 isoE	F	GTACCTACCCCTCCACAACA	60	118
	R	GCCTTTTATTCTGTTCAACTGGAA		

Table 2-2 Quantitative PCR primer pairs for mRNA expression levels.

Primers used to amplify genes from cDNA are shown are with optimal annealing temperature and product amplicon length.

2.6.1 Detection of Real time polymerase chain reaction products

Quantitative real-time PCR is a fluorescent based method allowing for detection and measurement of specific starting quantity of complementary DNA. SYBR green I is a cyanine dye that binds and intercalates double stranded DNA. The DNA-cyanine dye complex is excited with wavelength (λ) 497nm of light and emits green light at λ520. This signal is detected in each cycle and its intensity increases as more PCR product copies are made. This is used to generate a quantitative cycle plot which takes on the appearance of a sigmoid amplification curve (Figure 2-1). The intensity is measured as relative fluorescence units (RFU) and is plotted against cycle number. The quantitative cycle threshold (Qc) value is generated when RFU value is considered to be higher than the background. Where it intersects the cycle number, this is regarded as the Qc.

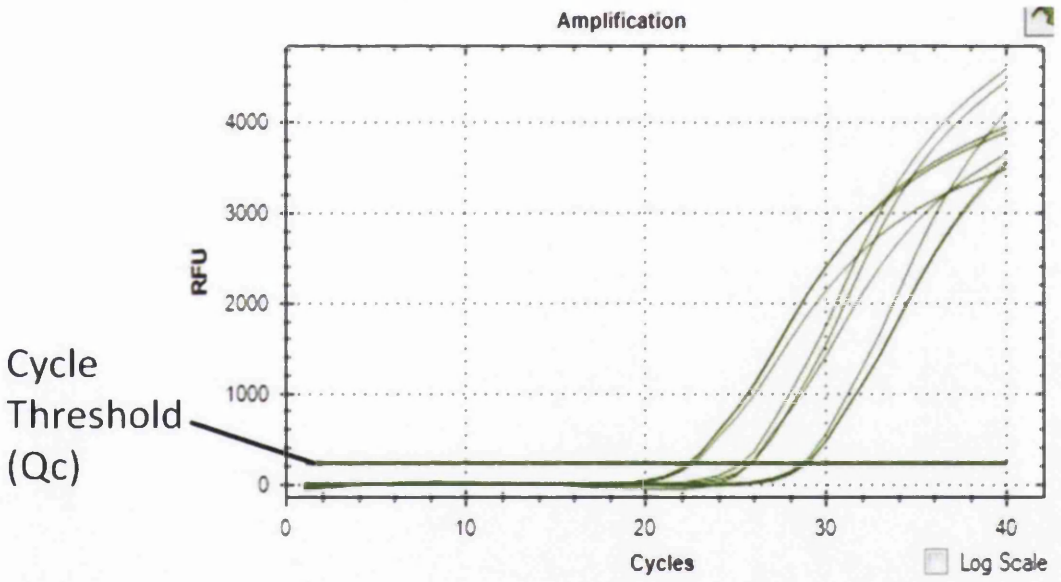

Figure 2-1 Quantitative PCR amplification plot.

A cDNA standard curve from the Ishikawa cell line. Samples were diluted 1/10, 1/100 and 1/1000 in triplicate.

2.6.2 Generation of a standard curve and melt curve

Relative quantification of gene expression data was determined from quantitative cycle (Qc) values for each sample. Serial dilutions of cDNA 1/10, 1/100 and 1/1000 performed in triplicate were used to generate a standard curve and gene expression levels quantified by plotting Qc values on the curve (Figure 2-1). Expression levels were normalized with values obtained for the reference gene (*GAPDH* or *RPL-19*). Once normalized, fold expression was calculated as a ratio of transcript levels between treated and control samples for each gene. This was determined using the $2^{-\Delta\Delta CT}$ method (Livak and Schmittgen 2001) incorporating a Pfaffl modification (Pfaffl 2001) for primer efficiency. After analysis of qPCR data, starting quantities were used to determine if any statistical significance existed between treatment and control for example. This was done using the t-test to measure for variation in a pair wise manner.

To obtain a melting curve for each sample, a final step (after 40 cycles) of 60 cycles was performed for 5secs starting at 65°C and then increasing the set point temperature by 0.5°C per cycle up to a maximum temperature of 95°C. This slowly denatures the bonds between the bases of the product which will change its fluorescent properties. When the change in RFU is plotted against the temperature a peak of fluorescence can be detected at a specific temperature, this can be calculated and used to check the specificity of the reaction.

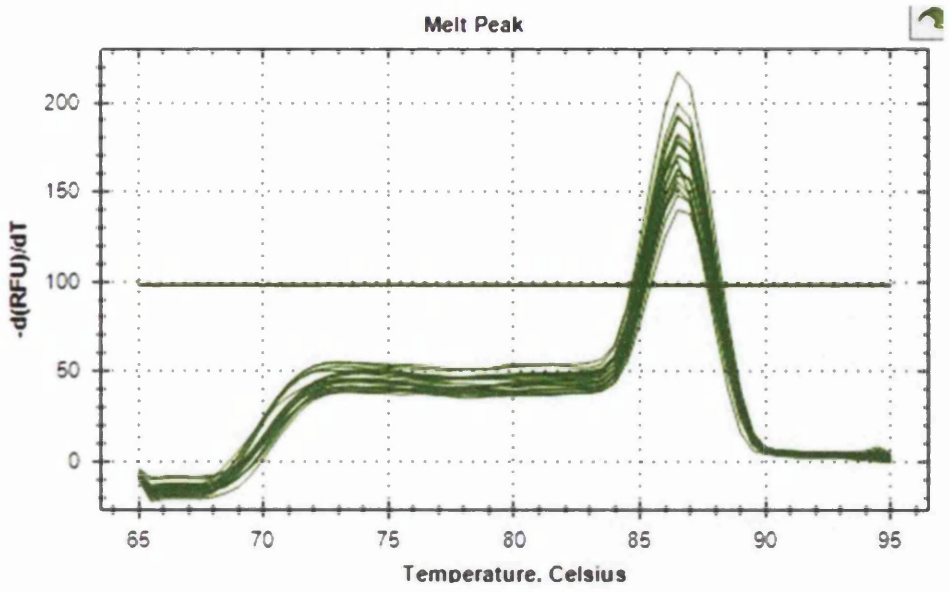

Figure 2-2 Melt curve from a typical Quantitative PCR reaction

The melt curve indicates a peak at 86.5˚C to validate the specificity of reaction product.

2.7 Chromatin Immunoprecipitation

ChIP was conducted using the Chromatrap® solid phase isolation technique, according to manufacturer's guidelines (http://www.chromatrap.com/uploads/documents/Chromatrap_spin_columns_V6_A4.pdf). The ChIP process involved the fixation (cross-linking) and isolation of chromatin (DNA-protein complexes) from the nucleus of cells. Chromatin was then broken into smaller fragments between 100-500bps by sonication. Transcription factor complexes of interest were then selected by immunoprecipitation using a specific antibody for the target transcription factor complex. After reversing the cross-linking and digesting the protein transcription complexes the genomic DNA was detected using qPCR against the relevant positive and negative controls to ensure selective and specific amplification of target DNA (Figure 2-3).

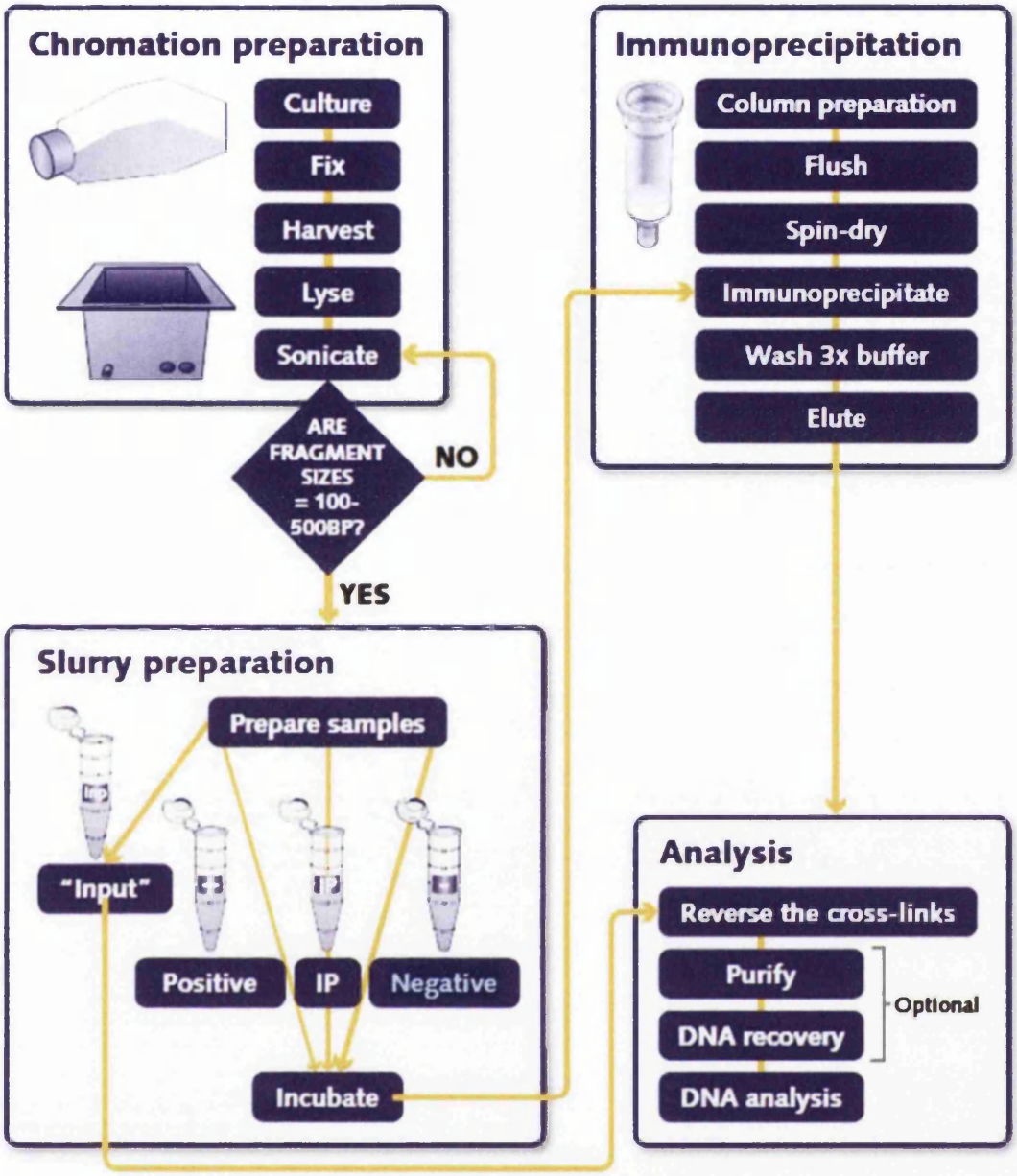

Figure 2-3 Experimental flow of a ChIP procedure

ChIP experimental flow to illustrate chromatin preparation, slurry preparation, Immunoprecipitation and analysis (http://www.chromatrap.com/).

2.7.1 Chromatin Isolation

Following cell treatments the culture media was decanted and the wells washed with 2mLs of PBS warmed to 37˚C. This was decanted and 3mLs of fixation medium (1% formaldehyde in basal stripped media) was added. The cells were incubated in fixative for 10mins at room temperature on a rotating platform to enable the DNA-

protein and protein-protein cross-linking to occur. The fixation media was then replaced with 1.5mL of 0.67M Glycine solution in each well, for 5mins, to quench the fixation reaction. The cells were then harvested by decanting the glycine solution and scraping cells from each well in 1mL of ice-cold PBS, and stored in a clean eppendorf tube. The cells were then pelleted through centrifugation at 3500*x*g (Microcentrifuge 5424R, Eppendorf UK) for 5mins. Following removal of the supernatant, the pellet was re-suspended and cells lysed in 400µL of hypotonic buffer by gentle pipetting and incubation on ice for 10mins. The intact nuclei fractions were then separated by further centrifugation at 5000*x*g for 5mins at 4˚C. Following removal of the supernatant, the nuclei pellet was re-suspended and lysed in 300µL lysis buffer by gentle pipetting and incubated once again for 10mins on ice. To obtain chromatin containing DNA fragments of 100-500bp these samples were then subject to sonication (800R, QSonica, UK) for 15mins using pulses of 30secs at an amplitude of 50 followed by a rest period of 30secs. The chromatin stock samples were then centrifuged at 16000*x*g at 4˚C to remove any nuclear debris material and the supernatant was transferred to a clean eppendorf and 1µL of protease inhibitor cocktail added and mixed by vortex. All chromatin samples were stored at -80˚C.

In order to check the sonication efficiency and quantify the amount for chromatin harvested from each sample, 50µL aliquots of the stock solutions were taken and processed for agarose gel electrophoresis and nanodrop analysis respectively. To process the samples (50µL) they must be reverse cross-linked and then purified. Reverse cross-linking serves to remove any DNA protein bonds by incubating at 65˚C overnight with 5µL of 1M $NaHCO_3$, 5µL of 5M NaCl and 40µL of water to make a total volume of 100µL. After overnight incubation the samples are incubated at 37˚C with Proteinase K to degrade proteins. DNA is then purified to remove protein debris by using the Qiaquick purification kit (Qiagen, UK). 500µL of Buffer PB was then added to the 100µL of sample and adjusted for pH by adding 10µL of 3M sodium acetate at pH 5.0. Following this the sample solution was added to the QIAquick column, allowing DNA to bind to the membrane and cell debris to be

removed by centrifuging at 17900*x*g for 1mins. The flow through is discarded and 750µL of Buffer PE was then added and again the column centrifuged at 17900*x*g for 1min. To elute the DNA 50µL of Buffer EB was added and immediately centrifuged at 17900*x*g for 1mins into a clean eppendorf tube. These samples were then run on a 1% agarose gel to check the size of desired fragments (Figure 4-18).

2.7.2 Immunoprecipitation (IP)

Following chromatin isolation and sonication, stocks were standardised to 400ng of chromatin and added to the IP slurry mixture for each reaction conducted. Briefly, IP slurries were made for each reaction along with an isotype control IgG, (Table 2-3) and a DNA input (which is not processed through the IP columns) sample respectively. ChIP reactions contained 5µL of low salt (LS) Buffer, 1µL of protease inhibitor cocktail (PIC), 5µL of sheared chromatin at 80ng/µL, 25µL of dH2O and 4µL of antibody of interest to make a total reaction volume of 40µLs. The IP slurries were incubated for 3hrs at 4˚C on an end to end rotor. During this time the IP columns were prepared by washing in 600µL of dH_2O, 600µL of ChIP dilution buffer three times and centrifuged dry at 900*x*g. The 40µL target protein (e.g. ERα) and an isotype control IgG slurry were each added to an individual IP column and incubated at 4˚C for a further hour. The input was placed on ice during this time. Columns were then washed with LS buffer three times, MS buffer three times and HS buffer three times and centrifuged to remove any liquid. The IP columns were then placed in clean dry eppendorfs and 50µL of Elution Buffer was added to the columns and incubated for 15mins at room temperature before the chromatin was eluted by centrifuging at top speed for 30 secs. To each sample including the DNA input the following was added; 5µL of 1M NaHCO3, 5M of NaCl and 40µL of dH_2O and they were incubated at 65˚C overnight, to facilitate reverse cross-linking. 1µL of proteinase K solution was added for 1hr at 37˚C to degrade bound antibody-protein complexes. The DNA was then purified using a standard protocol (Appendix B) or the Qiagen DNA purification kit (Qiagen, UK) and the eluted DNA was used directly in the qPCR reaction.

2.7.3 *Chromatin immunoprecipitation validated antibodies*

Antibody	Host & concentration	Supplier	Product Code	Specificity	Reference
Anti-ERalpha (HC-20)	Rabbit 200µg/mL	Santa Cruz	Cat SC-543 Lot# L1911	C-terminus of ERα of human origin	(Shankaranarayanan et al. 2011)
NFκB Anti p65 (C-20)	Rabbit 200µg/mL	Santa Cruz	Cat SC-372 Lot# A1910	C-terminus of NFκB of human origin	(Allison et al. 2012; Liu et al. 2012)
STAT1	Rabbit 200µg/mL	AbCam	Cat ab2415 Lot# GR44902-8	Detects STAT1 alpha p91 & STAT1 beta p84	(Yao et al. 2008)
IgG	Rabbit 200µg/mL	Rockland Ltd	011-0102 Lot# 22557	Precipitated against Anti-Rabbit Serum and IgG	Active Motif Europe
Pol II (H-224)	Rabbit 200µg/mL	Santa Cruz	Cat SC-9001	Raised against amino acids 1-224 of Pol II of human origin	(Montes et al. 2012)

Table 2-3 Table of antibodies used in Chromatin Immunoprecipitation reactions

Antibodies ERα, NFκB, STAT2, IgG and Pol II were used in chromatin immunoprecipitation reactions. All antibodies had been previously validated for ChIP by the supplier.

2.7.4 *Promoter analysis for identification of regulatory elements*

The promoter sequence of human *OPN* (NG_030362.1) and *CD44* were identified from a web programme (mybioinfo.info). These sequences were downloaded in FASTA format and entered into the Alggen-Promo web programme (http://alggen.lsi.upc.es/cgi-bin/promo_v3/promo/promoinit.cgi?dirDB=TF_8.3) to identify human putative regulatory elements. In addition to this a literature search identified positive sites confirmed by electrophoretic mobility shift assay or luciferase assay for SP-1 (Sharma et al. 2010; Wang et al. 2000a; Bidder et al. 2002) and NFκB on the *OPN* promoter (Samant et al. 2007). The following sites were searched; ERα [T00261], AP-1 [T00029], SP-1, NFκB [T00593], STAT1B [T01573], IRF-

1 [T00432]. Following this primers were designed using Beacon Designer (Premier Biosoft, UK) for regions of the *OPN* and *CD44* promoter where regulatory elements were identified. The coordinates for these response elements are listed relevant to the position of the transcription start site.

2.7.5 Quantitative polymerase chain reaction post chromatin immunoprecipitation

qPCR reactions were set up using the following master mix; 5µL of SsoFast evagreen sSupermix, 2µL DNA, 1µL forward primer, 1µL reverse primer and 1µL nuclease free dH_2O to make a total volume of 10µL per well. All reactions for each sample were performed in triplicate in natural Multiplate Low-Profile 96-Well un-skirted PCR plates. Plates were heated at 98˚C for 2mins to irreversibly denature antibody-bound Sso-7-fusion polymerase to fully activate it. The samples were then denatured for 30secs at 98˚C and annealing and extension performed in one step at the annealing temperature of the specific primer pair for 5secs (listed in Table 2-4). Primers were optimised for annealing temperature by running at three different temperatures and best annealing temperature chosen by melt curve analysis (Appendix D). Denaturation and anneal-extension is performed 40 times. The plate is then heated from 65˚C to 95˚C by 0.5˚C increments for 1sec to generate a melt curve.

2.7.6 Genomic primers for quantitative polymerase chain reaction post chromatin immunoprecipitation

Site	Transcription Factor	Sequence	Ta (°C)
GAPDH 1	Pol II **F**	TCGACAGTCAGCCGCATCT	60
	Pol II **R**	CTAGCCTCCCGGGTTTCTCT	
XBP1 1	ER **F**	ATACTTGGCAGCCTGTGACC	60
	ER **R**	GGTCCACAAGCAGGAAAAA	
OPN 1	ER AP1 AP1 **F**	ATGGATGAGGGAACAAGGATAGG	52.3
	ER AP1 AP1 **R**	GCAGAAGTAAAGCAGTTTC	
OPN 2	AP-1 **F**	TCTTCCTGGATGCTGAATGC	52.3
	AP-1 **R**	CCAAGCCCTCCCAGAATTTA	
OPN 3	AP1 **F**	GGAAACCACCGATGCTAATCAG	60
	AP1 **R**	AGCAGTGGCATATTCAGAAAGG	
OPN 4	AP1 AP1 ER **F**	TGTATGATGAGTTATCGCATGTAAG	48.5
	AP1 AP1 ER **R**	ACAAACAGCACACATAGACTTTC	
OPN 5	NFKB **F**	CACAACTGAGAAAGCAAATGAAG	60
	NFKB **R**	TCCCAAGGTATGTAAAGTAGGC	
OPN 6	NFκB **F**	TCAGCCAAACGCCGACCAAG	52.3
	NFκB **R**	CTAGACACCTTTGTTCCAGGAGACC	
OPN 7	OPN STAT1 **F**	GCTACTGGGTTGTGCATTC	48.5
	OPN STAT1 **R**	TTCTGATTAGCATCGGTGG	
CD44 1	ER AP1 **F**	AGGCAAGGTCACACAACTAAGAAGC	60
	ER AP1 **R**	ACCATTCCTAGAGAAGGGAGTCAC	
CD44 2	SP1 ER **F**	GCACAGTCGTTGTCTGGACT	60
	SP1 **R**	ACCCATTGCCAGCTAGTC	
CD44 3	STAT1 IRF **F**	ACACTGGCTTGAACACATGGGTTAG	48.5
	STAT1 IRF **R**	GCTGGAGAGAGGGCGAGGTC	
CD44 4	IRF **F**	TGGGTGCG GGGTGCTCAG	60
	IRF **R**	TGCTTCCACAGACACATTCTCCAAC	
CD44 5	IRF STAT1B **F**	TGTGTCTAGGCAGGGCAGAG	60
	IRF STAT1B **R**	GCTTTGGAACAAGGCTCAGTG	
CD44 6	NFκB **F**	GCCTGGCAGCCTCAGAGCAGAGAG	55.1
	NFκB **R**	CGCAGCCCCTCCCCTCCATAGC	

Table 2-4 Primer pairs used to amplify genomic DNA.

Transcription factor binding sites from genomic DNA with location relevant to start site and optimal annealing temperature.

2.7.7 *Analysis of quantitative polymerase chain reaction post chromatin immunoprecipitation*

All post qPCR analysis was conducted in the same manner for all antibodies. The average Cq for the antibody, isotype control IgG, and input were calculated from the triplicate wells. An antibody % signal relevant to the input amplification and PCR efficiency was calculated along with the equivalent isotype control IgG percentage value. The real signal was simply calculated by deducting the IgG % from the antibody % (Figure 2-4). The real signal percentage was used to assess the basal differences between ERα in the Ishikawa and Heraklio cell lines. All other data comparing treatment to controls used fold data. All statistical analysis was conducted on a minimum of three independent biological repeats as stated using a two tailed t-test of unequal variance to compare treatment to control or cell line to cell line.

$$TF(\%) = 100\left\{2^{(C_q^i - C_q^t)}\right\}$$

$$B(\%) = 100\left\{2^{(C_q^i - C_q^b)}\right\}$$

$$R(\%) = TF(\%) - B(\%)$$

Figure 2-4 Formulae for real signal from ChIP

Where TF is the transcription factor, B is the background, R is the real signal, C_q^i is the input cycle quantity, C_q^t is the transcription factor cycle quantity and C_q^bs the background cycle quantity.

2.8 *Immunohistochemistry for osteopontin and CD44*

2.8.1 *Endometrial sampling*

The pipelle endometrial sampling method is used to obtain a sample of the endometrial tissue for diagnostic or research purposes. This technique was developed in 1984 (Cornier 1984) and involves a flexible plastic tube with piston that is used to create a vacuum for sampling. A hole at the distal end allows for the endometrial tissue to fill the tube as the piston is withdrawn and rotated. The sample obtained is then fixed in formalin for diagnostics or placed in media for research purposes.

2.8.2 *Gold standard diagnostics*

The gold standard diagnostic procedure for endometrial pathology is examination of haematoxylin and eosin (H&E) staining followed by immunohistochemistry to characterise tumour development. This involves a formalin fixed sample, embedded in paraffin wax and sectioned using a microtome. These thin sections (4μm) of preserved tissue are placed on to slides and stained with H&E to visualise the nucleus and cytoplasm. Structural elements of the tissue still intact can now be visualised under the microscope. The tissue structure is important to the pathologist to help identify the phase of the menstrual cycle, hyperplasia and cancer in the tissue.

2.8.3 *Immunohistochemistry for paraffin embedded blocks*

Samples were fixed in 10% buffered formalin for 24hrs, embedded in paraffin and 3-4μm thick sections cut and placed on positively charged slides before immunohistochemical studies. The sections were incubated with a rabbit anti-CD44 or anti-OPN antibody (Table 2-5). Deparaffination was achieved by incubating at 72°C and antigen retrieval was performed by incubating slides in cell concentration 1 (CC1) buffer (Ventana) for 8mins on heated plates at 98°C on a Benchmark XT (Ventana) processor. Primary peroxidase inhibitor was added before the primary

antibody was incubated for 60mins at 1:200 dilution at 36°C. Detection of positive immunostaining was obtained through the interaction of avidin-biotin peroxidase complex with a biotinylated secondary antibody using a Ventanna I View DAB detection kit (Ventana BioTek Solutions, Tucson, AZ, USA). After 4min amplification stage at 36°C the slides were stained with haematoxylin for 8mins at 36°C. The slides were then dehydrated, cleared and mounted in DPX.

Antibody	Host & concentration	Supplier	Product Code	Specificity	Reference
Anti- OPN	Rabbit 200µg/mL	Millipore	Cat AB1870 Lot# NG1827385	Amino acid 75-90 of human OPN (SwissProt Acession # P10451; PSKSNESHDHMDD MDD)	(Tsai et al. 2012)
Anti-CD44 [H-CAM], clone EPR1013Y	Rabbit 200µg/mL	Millipore	Cat 04-1123 Lot# NG1883338	Residues in human CD44	(Tanabe et al. 1990)

Table 2-5 Table of antibodies used for immunohistochemistry

2.8.4 Dating of menstrual phase

Dating of endometrial biopsies is conducted using the Noyes criteria: the proliferative phase of the endometrium is classically characterized by the morphological thinness (4-8mm) of the regenerating epithelium (Barker et al. 2009; Aflatoonian and Mashayekhy 2011). The endometrial tissue in the secretory phase is typically between 8 to 16mm in thickness as measured by ultrasound. Histological sections are characterized by the shape of the glands; straight, short, narrow glands are of proliferative type while the mid proliferative phase is identified by columnar surface epithelium, longer, curving glands. The secretory phase post ovulation is characterized by sub-nuclear vacuolation of the gland epithelium while glandular changes are key in dating the first half of the secretory phase such as mitosis, pseudostratification, basal vacuolation and secretion (Noyes et al. 1950). All

samples were dated using the first day of the last menstrual period as day 1 and proliferative or secretory phase confirmed by criteria above.

2.8.5 Scoring and statistical analysis for paraffin embedded blocks

Using a light microscope three independent observers scored all slides blinded to the diagnosis, demographic or menstrual cycle stage. Two of the observers were trained gynaecological doctors in addition to myself, this ensured that the scoring was consistent between observers. The endometrial samples were scored (H-score) by compartment, the stroma and the epithelium containing the glands and lumen. Intensity and distribution of staining were scored separately with the following criteria intensity (0-4.5); 0-absent, 1-weak, 2-moderate, 3-intermediate, 4-strong, 4.5-very strong. Distribution (0-4.5); 0-absent, 1-<25%, 2-25%-50%, 3–50%-75%, 4–75%-95%, 4.5-100%. This criteria allows for robust and reproducible assessment. The more red-brown staining observed in the sections, indicating positive antibody staining, was reflected in a higher score for staining intensity and distribution. The sum of these scores was obtained and all subsequent analysis was conducted on the sum H-score. All data were represented in box and whisker plots. The median data point represented by a crossed circle, the upper and lower quartiles of the data in the boxes each side and the whiskers representing the upper and lower quarter extremes of the data.

2.8.6 Statistical analysis

Due to the heterogeneity of the patient samples obtained from each group the Anderson Darling test (Appendix C) for normality was conducted on the data in order to identify the correct statistical method to employ for analysis of variation between fertile and infertile groups (Margarit et al. 2010; Darling 1952). Each group of data was tested for normality and several were observed to be significantly different from the normal distribution ($p \leq 0.05$). All data were therefore treated as non-parametric. In the first instance the Kruskal-Wallace (K-W) test was applied to all groups in each category (i.e. all proliferative gland groups) to assess if any

significant total variation in the data existed. If a result was significant for the K-W test ($p \leq 0.05$) a Mann-Whitney U (M-WU) test was used to conduct a pairwise comparison of an individual infertile group to the fertile (control) group. This was conducted for each compartment and target retrospectively (Kruskal and Wallis 1952; Mann and Whitney 1947).

Due to the small patient sample number and small number of comparisons applied to the data, a correction for multiple testing was not considered appropriate for the data set. Correcting for multiple testing, while reducing possible type I errors potentially increased the risk of type II errors if the expected type I error rate is below one (Lieberman and Cunningham 2009; Green and Britten 1998; Gelman et al. 2012). No more than four comparisons were made simultaneously (e.g. OPN (IHC), across 4 groups, Figure 3-5) during the study therefore the theoretical risk of a type I error at the 5% significance level would be 0.2, considerably lower than one.

2.9 Isolation and quantification of Secreted Protein

All secreted proteins were harvested from the cell cultures, for both primary and secondary cell culture by decanting off the media. Following centrifugation at 600*x*g for 5mins all cell debris is removed. Supernatants containing secreted proteins were then transferred to a clean labelled eppendorf and stored at -80°C.

2.10 Enzyme linked immunosorbent assay

Cells were cultured as described in section 1.3; at the end time point of each experiment the supernatants were collected and aliquots were separated into 1.5mL eppendorf tubes. The amount of secreted OPN in the supernatant was determined using a commercially available ELISA kit. All antibodies described below were included in the kit (R&D Systems, Inc., Minneapolis, MN, USA). The ELISA method uses a monoclonal (capture) antibody that is bound to a 96-well plate, which targets the C-terminal sequence of OPN common to all identified isoforms. ELISA plates were blocked using 1% BSA to remove non-specific binding of the

sample to the micro-well plate. Samples were then added and allowed to bind to the OPN capture antibody for 2hrs before being decanted and each well washed (wash buffer 0.05% Tween® 20 in PBS) to remove any unbound sample. The biotinylated detection antibody was added to bind OPN and on the addition of Streptavadin-horseradish peroxidase, following the addition of a substrate, an enzymatic reaction occured. The substrate containing hydrogen peroxide and tetramethylbenzidine was transformed in to a blue product that was directly proportional to the amount of OPN present in each well. Sulphuric acid (1M) was then added to stop this reaction so that the absorbance can be measured at 450nm on a spectrophotometer (FluoSTAR, BMG Labtech, UK). Known concentrations of OPN were used to produce serial dilutions and generate a standard curve (concentrations of 4000, 2000, 1000, 500, 250, 125 and 62.5pg/mL). A blank of the reagent diluent was added to account for background and subtracted from each reading. Using the Mars data analysis software (BMG Labtech, UK) optical density of all samples and standards are deduced from the blank optical density before further analysis to compare control and treatment values. A standard curve using the four parameter logistic curve-fit was generated and all optical densities from unknown samples were compared to this.

Chapter 3

Expression of Osteopontin and CD44 in fertile and infertile endometrium

3.1 Introduction

The endometrium is a complex network of cells comprising of epithelia, stroma, endothelia and migrating leukocytes, and displays orchestrated phases of proliferation, differentiation and shedding (Tabibzadeh, 1991). These phases are driven by responses to ovarian steroid hormones, pituitary derived gonadotropins, growth factors and cytokines. The endometrial tissue functions to provide optimal conditions for fertility (Makrigiannakis et al. 2006). Multiple complex signalling patterns including autocrine, paracrine and endocrine signalling occur, affecting cell proliferation and differentiation. Increased ovarian steroid hormone receptor levels (estrogen and progesterone) observed in pathologies such as PCOS and endometriosis could contribute to the disrupted expression levels of various embryo adhesion proteins (Margarit et al. 2010; Igarashi et al. 2005). This makes the adhesion gene and protein expression levels strong candidates as biomarkers for determining what contributes to infertile endometrial pathology.

Candidate embryo-epithelial adhesion proteins OPN, CD44 and integrin $\alpha V\beta 3$ are hypothesized to form an adhesion complex at the epithelial surface, which may be crucial for blastocyst attachment during the window of implantation (Yen and Jaffe, 2009; Singh and Aplin, 2009). Literature suggests that maximum expression of OPN in the glands and lumen of the endometrium is during the mid-secretory phase. When secreted from the glands, OPN can bind to luminal CD44 or $\alpha V\beta 3$ (Afify et al. 2006; Albers et al. 1995). Integrin $\alpha V\beta 3$ is well characterized in the literature as a marker of implantation and it is maximally expressed in the secretory phase of the menstrual cycle (DuQuesnay et al. 2009; Lessey and Arnold 1998). The roles of OPN and CD44 as markers of implantation have not been studied extensively in the human endometrium in the context of infertile pathology, although some literature exists which hypothesizes their role during implantation. Secreted uterine OPN and membrane tethered CD44 have both been shown to be markedly increased in the secretory phase of the menstrual cycle when compared to the proliferative phase (Wolff, Thomas Strowitzki, et al. 2001; Afify et al. 2006).

In this chapter a comprehensive analysis of the expression levels of candidate biomarkers for infertile pathologies was performed. In a cohort of 178 women attending the gynaecology clinic at ABMU HB Singleton Hospital. A total of 91 women were included in the IHC study, 28 in the secreted OPN study and a further 59 in the mRNA study. OPN and CD44 expression was assessed at the intracellular protein level, and secreted OPN levels analyzed in the culture media in which the biopsies were placed immediately following collection. Gene expression analysis was conducted in order to facilitate the understanding of *OPN* and *CD44* gene regulation. The aim of this study was to characterize the expression of constituent components of this adhesion complex in the endometrium of a fertile cohort, and then compare them to an infertile cohort presenting with distinct pathologies. Samples were grouped by pathology and phase of menstrual cycle to ascertain the expression as a result of menstrual cycle development. It is important to note that the PCOS group has been sub-divided into two groups, anovulatory PCOS and ovulatory PCOS as defined by the Rotterdam criteria and confirmed using LMP and Noyes criteria. Therefore all women in the anPCOS group are in the proliferative phase of the menstrual cycle whilst the ovPCOS are in the secretory phase.

3.2 Results

3.2.1 IHC analysis of OPN and CD44 protein expression in the endometrium

OPN and CD44 expression throughout the menstrual cycle in healthy fertile controls and infertile pathologies were observed in a retrospective study of archived uterine material, in relation to patient age and BMI. A pattern of OPN and CD44 expression levels from this fertile group was then compared to patients diagnosed with various endometrial disorders including; anovulatory PCOS (anPCOS), ovulatory PCOS (ovPCOS), endometriosis and unexplained infertility (UIF). Formalin fixed paraffin-embedded (FFPE) uterine tissue sections were grouped by pathology according to their recorded patient profiles and clinical diagnosis by pathology staff at Singleton Hospital. Samples were characterized and dated by Noyes (Noyes et al. 1950)

criteria and separated into stages of the menstrual development. All samples were scored and statistical analysis conducted as in section 2.8.6.

3.2.2 Clinical Data and patient demographics

In order to ensure a robust comparison between groups, a strict selection criterion was employed. Patients who were over 42 years of age or with a BMI of 36 or over were deemed ineligible. The BMI limit of 36 was chosen as it included only the first class of obese women (BMI 30-35, Obese Class I) however most women in the study fell into the overweight category (BMI 25-29). Women with pathological features such as tubular defects and hyperplasia were excluded. Although every attempt was made to age and BMI match patients, a significant variation was observed in the age of the ovPCOS and secretory phase UIF patients compared to the fertile group, when analysed using the student t-test ($p=0.001$) (Table 3-1). Early onset of infertility in young women with ovPCOS (mean age 27.5) and UIF (mean age 30.8) are noted in this study. The fertile women included in this study were recruited whilst undergoing sterilization or hysterectomy and therefore tended to be older (mean age 35.6) than the infertile groups. Of the 91 patients selected for this study, 53 were in the proliferative phase of the menstrual cycle; 18 had anPCOS, 6 had endometriosis and 19 were UIF, with 10 women in the fertile group (Table 3-1). Similarly in the secretory phase, a total of 38 women were available; 8 ovPCOS, 6 endometriosis, 12 UIF and 12 fertile.

3.3 Osteopontin protein expression in fertile endometrium

OPN and CD44 have both been shown to be up-regulated in the secretory phase endometrium of healthy cycling women and could therefore be useful as predictive markers of fertility (DuQuesnay et al. 2009; Poncelet et al. 2010). OPN protein expression was analyzed in the endometrial tissue of healthy, fertile patients and separated into the proliferative and secretory phases of the menstrual cycle. OPN expression was first assessed in fertile women in the two distinct phases of the menstrual cycle. The staining patterns for OPN expression were separated into

three compartments; glands, lumen and stroma to assess where OPN is expressed within the tissue (Figure 3-1). Significant differences were detected in OPN protein expression between the compartments (K-W p=0.000) and therefore a M-W U test was conducted to determine which compartments were significantly different in the secretory phase when compared to the proliferative phase by pairwise comparisons. OPN staining in the glands and luminal epithelium of the fertile group was stronger in the secretory phase when compared to the proliferative phase (Figure 3-1). Stromal staining meanwhile appeared similar between the two phases. The glandular expression of OPN was significantly increased in the secretory phase (H = 7.5) compared to the proliferative phase (H = 6.4; M-WU p=0.021). Luminal expression was not significantly increased, but rose from a median H-score value of 6.7 to 7.3. No significant alteration in the stromal staining pattern of OPN was observed where consistent median H-score values (H = 5.5 and 5.4) were observed in the proliferative and secretory phases respectively (p=0.56). In both phases glandular and luminal OPN staining were more abundant than stromal expression (DuQuesnay et al. 2009; Franchi et al. 2008).

IHC	Fertile		PCOS		Endometriosis		Unexplained Infertility	
	Pro	Sec	Anov	Ov	Pro	Sec	Pro	Sec
AGE	34 ± 7.7	37.2 ± 4.6 p=0.27	28.4 ± 5.2 p=0.06	27.5 ± 5.7 p=0.002	33.3 ± 7.7 p=0.87	31.5 ± 6.5 p=0.09	30.9 ± 4.7 p=0.27	30.8 ± 4.1 p=0.001
BMI (kg/m^2)	28.8 ± 4.7	25.8 ± 3.8 p=0.19	28.1 ± 6.3 p=0.80	27.4 ± 8 p=0.63	28.4 ± 5.6 p=0.90	26.3 ± 5.5 p=0.90	25 ± 5.4 p=0.11	24 ± 2.5 p=0.25
n=	10	12	18	8	6	6	19	12
n= cum	22		26		12		31	

Table 3-1 Patient demographics for IHC study.

Retrospect IHC study using tissue biopsy material from a cohort of patients undergoing investigation for infertile pathology. Recorded parameters of age, BMI and total number of grouped patients, were statistical analyzed for variation between groups. Mean values, standard deviation and probability calculations (student's t-test) are displayed. Pro-proliferative; Sec-secretory; Anov-anovulatory; ov-ovulatory; BMI-body mass index; n-number; cum-cumulative.

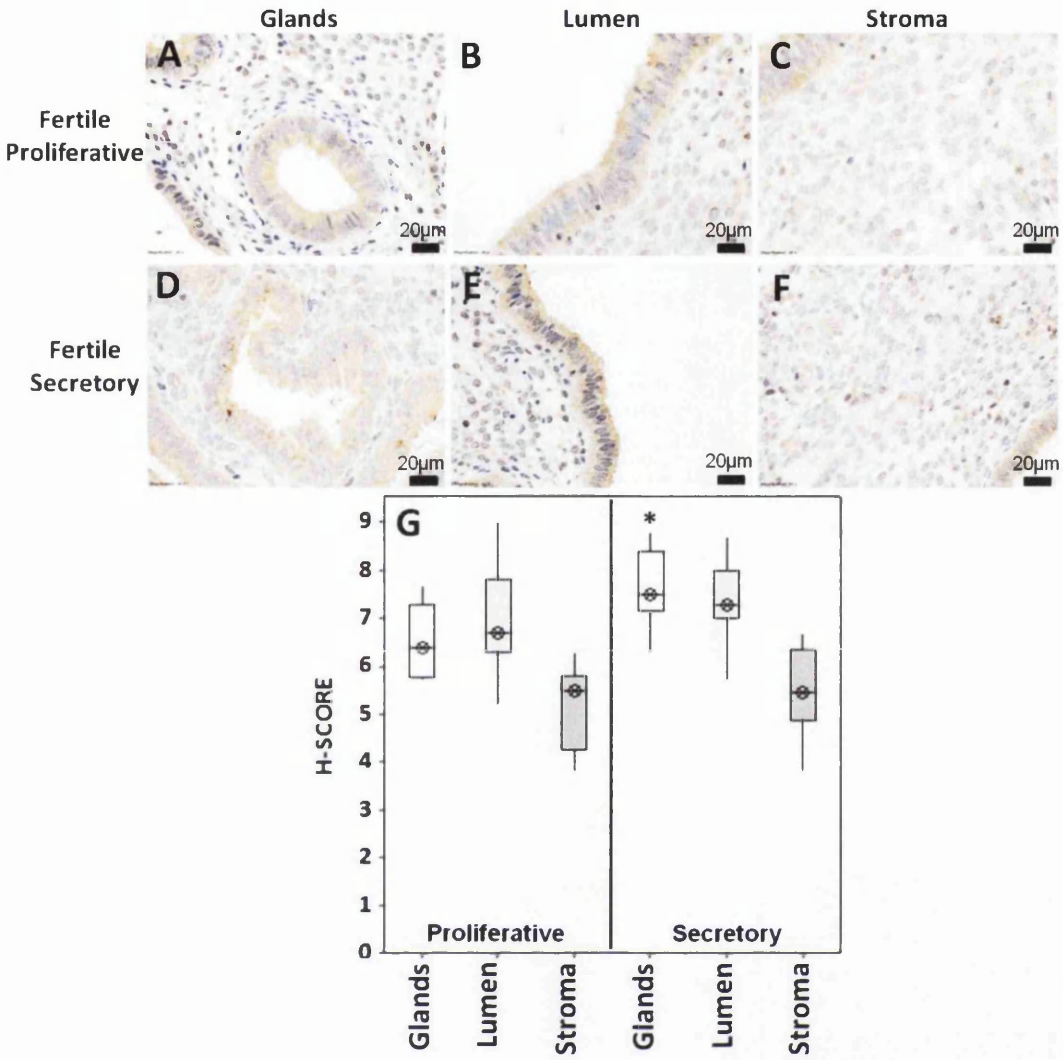

Figure 3-1 OPN protein expression in the proliferative and secretory phase of fertile endometrium.

OPN expression in fertile endometrium by compartment; (A-C) proliferative phase (n=10), (D-F) secretory phase (n=12). Sections of fertile endometrium were stained with OPN antibody and slides scored by three independent scorers at 40x magnification, scale bar (black) represents 20µm. A significant increase in glandular OPN expression was noted in the secretory phase when compared to the proliferative phase endometrium (M-WU p=0.02). (G) H-scores were grouped per compartment and semi-quantitative H-score used for statistical analysis performed using the Kruskal-Wallis (p≤0.05) test followed by the Mann-Whitney U test (proliferative versus secretory)* P≤0.05.

3.3.1 Osteopontin protein expression in proliferative phase infertile endometrium

In order to assess the median level of OPN protein expression in infertile groups, the staining patterns were compared directly to those obtained in the healthy cycling fertile patients. Groups compared to the proliferative phase fertile group were anPCOS, endometriosis and UIF. Only the anPCOS group was compared to the proliferative phase fertile group as patients in this group were confirmed as proliferative phase. The ovPCOS group retrospectively chosen had been histologically confirmed as in the secretory phase and therefore were included in the secretory phase study only. To further understand how the two PCOS pathologies differed, anPCOS was also compared to the secretory phase.

3.3.2 Osteopontin glandular expression in proliferative phase endometrium

The staining patterns observed in the glands of the proliferative phase (Figure 3.2) showed increased OPN expression in the anPCOS (Figure 3-2B) and endometriosis (Figure 3-2C) groups when compared to the fertile group (Figure 3-2A). No change in staining intensity or distribution was observed in the glands of UIF women (Figure 3-2D). These subtle changes in staining patterns were reflected in the H-scores obtained (Figure 3-2E). H-scores increased in women with anPCOS (H=7.7) and endometriosis (H=7.7) in the proliferative phase endometrium when compared directly to the fertile group (H=6.4). In women with unexplained infertility, the H-score decreased (H=6.0). However, no significant differences were detected between groups (K-W $p>0.05$) and therefore no further pairwise comparisons were conducted. The H-score values for all infertile groups were similar.

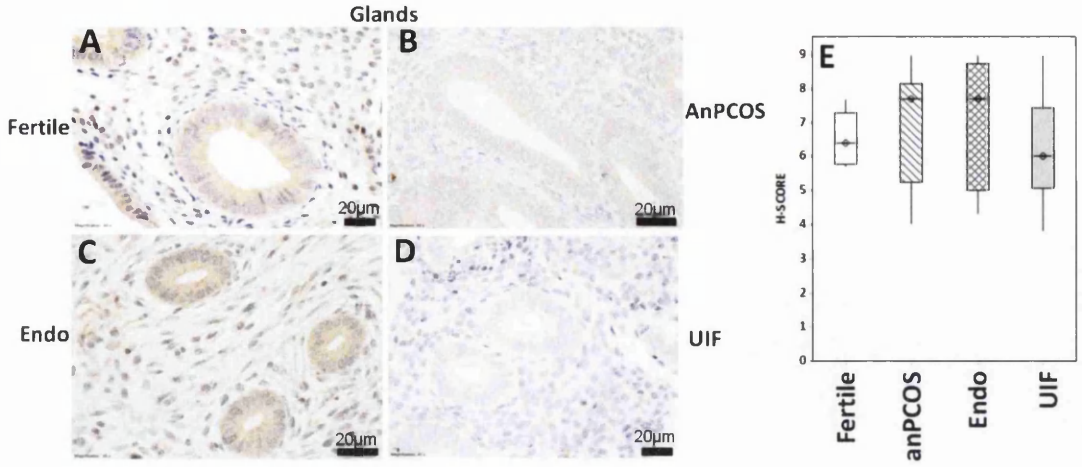

Figure 3-2 Proliferative phase OPN protein expression in endometrial glands.

Proliferative phase endometrium from fertile (n=10), anPCOS (n=18), endometriosis (Endo) (n=6) and UIF (n=19) patients stained for OPN. (A) fertile, (B) anPCOS, (C) endometriosis, (D) UIF x40 magnification, scale bar (black) represents 20µm. No significant alterations in OPN staining were observed between the fertile and infertile groups. (E) scores for OPN were plotted by group and expression analyzed using semi-quantitative H-scores. Statistical analysis was performed using the Kruskal-Wallis test (K-W; p=0.34).

3.3.3 Osteopontin luminal expression in proliferative phase endometrium

Similar patterns of altered OPN expression to the glands were observed in the luminal epithelial compartment of the endometrium (Figure 3-3). In the anPCOS (Figure 3-3B) and endometriosis (Figure 3-3C) groups increased intensity and distribution of OPN staining was observed when compared to the fertile group (Figure 3-3A). No change in staining was observed in the UIF group (Figure 3-3D) when compared to the fertile group. This was reflected in H-scores (Figure 3-3E). These observed differences were not significant (K-W p=0.42); as differences in OPN were not detected between groups therefore no further pairwise comparisons were conducted.

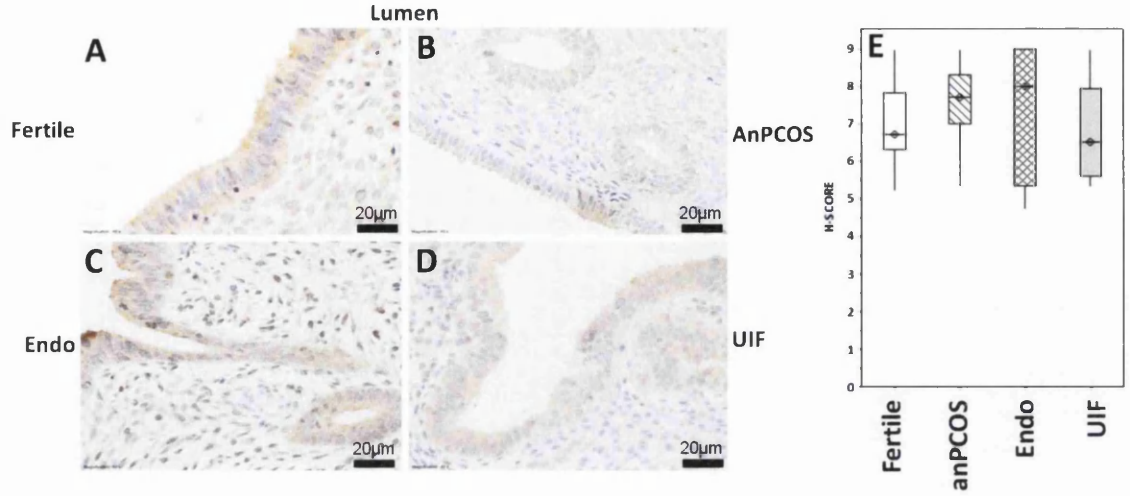

Figure 3-3 Proliferative phase OPN protein expression in endometrial luminal epithelium.

Proliferative phase endometrium from fertile (n=10), anPCOS (n=18), endometriosis (Endo) (n=6) and UIF (n=19) patients stained for OPN. (A) fertile, (B) anPCOS, (C) endometriosis, (D) UIF x40 magnification, scale bar (black) represents 20µm. No significant alterations in OPN staining were observed between the fertile and infertile groups. (E) scores for OPN were plotted by patient group and expression analyzed using semi-quantitative H-scores. Statistical analysis was performed using the Kruskal-Wallis test (K-W p=0.42).

3.3.4 Osteopontin stromal expression in proliferative phase endometrium

Altered patterns of OPN stromal staining were observed between the fertile group and those observed in each of the infertile groups (Figure 3-4). Stronger staining was evident in the stroma of anPCOS (Figure 3-4B) and endometriosis (Figure 3-4C) groups when compared to the fertile group (Figure 3-4A). In contrast the stromal compartment of the UIF group showed weaker staining for OPN when compared to the fertile group (Figure 3-4D). These changes are reflected in the H-scores (Figure 3-4E) and statistical comparisons. Significant variation was observed in OPN expression between the groups when the Kruskal-Wallis test was applied (K-W p=0.015). Therefore, the Mann-Whitney U test was conducted to determine which groups were significantly different to the fertile group by pairwise comparison. Stromal OPN expression was significantly increased in women with endometriosis (H = 7.0) when compared to the fertile group (H = 5.5; p=0.04). Women with

anPCOS (H = 5.3) showed no significant alteration in OPN staining (H = 5.3) when compared to the fertile group (M-WU p=1), although it is noteworthy that the data were highly variable. UIF patients (H=4.4) displayed decreased stromal OPN expression and a tight distribution of data compared to the fertile group (H=5.5) but was insignificant (M-WU p=0.07).

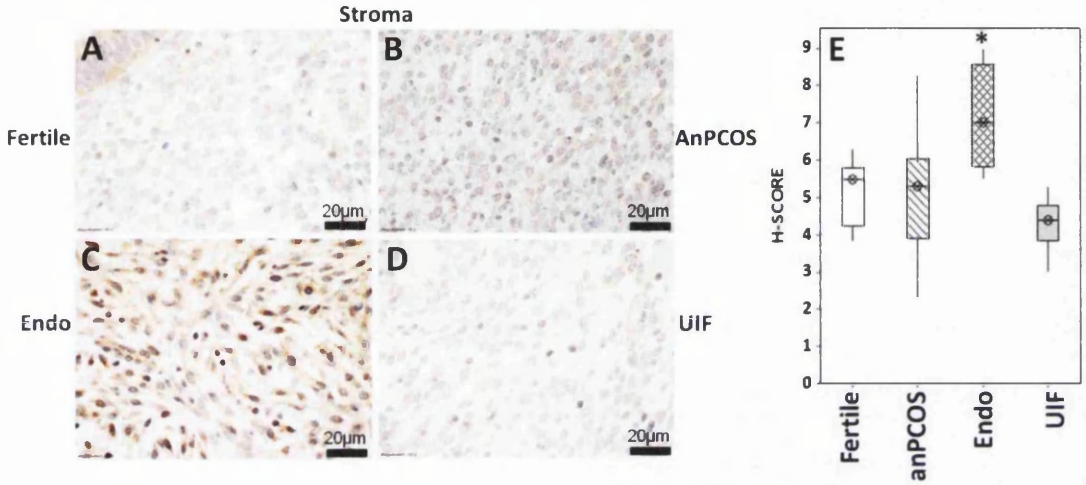

Figure 3-4 Proliferative phase OPN protein expression in endometrial stroma.

Proliferative phase endometrium from fertile (n=10), anPCOS (n=18), endometriosis (Endo) (n=6) and UIF (n=19) patients stained for OPN. (A) fertile, (B) anPCOS, (C) endometriosis and (D) UIF x40 magnification, scale bar (black) represents 20µm. Significant alterations in OPN staining were observed between the fertile and infertile groups. (E) The scores for OPN were plotted by patient group and expression analyzed using semi-quantitative H-scores. Statistical analysis was performed using the Kruskal-Wallis test (K-W p=0.02) followed by a Mann-Whitney U test. A significant up-regulation of OPN expression was noted in the endometriosis group (M-WU p=0.04). * P≤0.05

3.4 Osteopontin protein expression in secretory phase endometrium

3.4.1 Osteopontin glandular expression in secretory phase endometrium

It has been proposed that OPN secretion through the endometrial glands is essential to activate integrins on the blastocyst surface, to allow it to become adhesive (Chaen et al. 2012). In this study, altered OPN staining intensity and distribution was observed in the glandular epithelium of some infertile groups when compared directly to the fertile group (Figure 3-5). (Figure 3-5B) In the anPCOS

group OPN patterns of staining intensity were more abundant than those of the fertile group (Figure 3-5A), while the most abundant staining patterns were clearly observed in the tissue sections obtained from ovPCOS patients (Figure 3-5C). Tissue sections of endometriosis (Figure 3-5D) and UIF (Figure 3-5E) groups appeared to have less abundant OPN staining than the fertile group, reflected in H-scores (Figure 3-5F). Despite this clear staining pattern, no statistically significant variations in the OPN H-scores between all groups were observed when the Kruskal-Wallis test was applied (K-W p=0.13); therefore no further pair-wise comparisons for statistical significance were conducted.

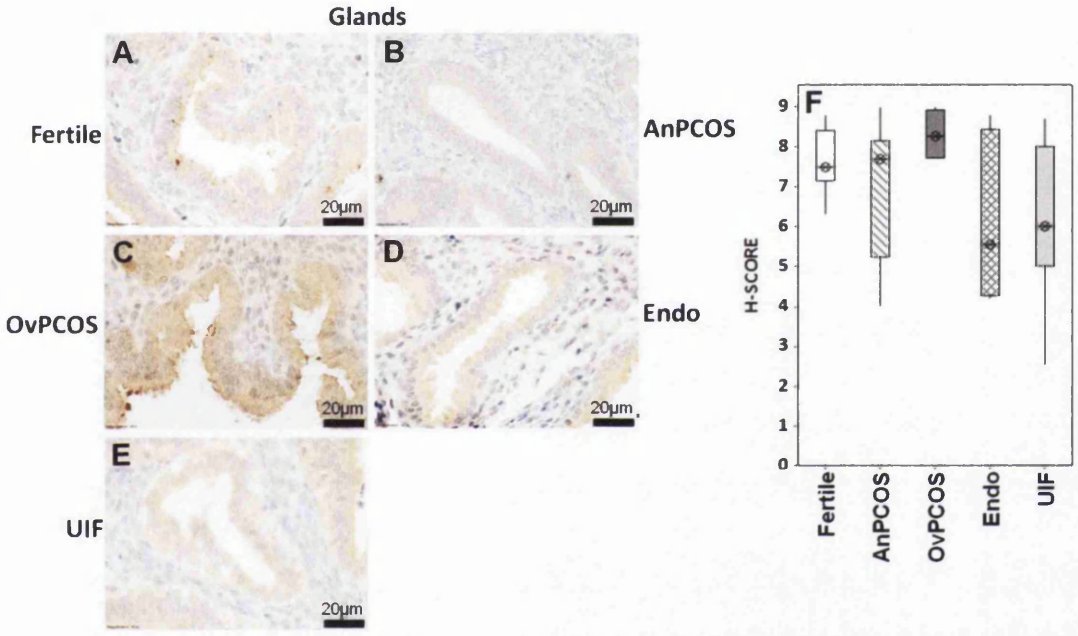

Figure 3-5 Secretory phase OPN expression in endometrial glands.

Secretory phase endometrium from fertile (n=12), anPCOS (n=18), ovPCOS (n=8), endometriosis (Endo) (n=6) and UIF (n=12) patients stained for OPN. (A) fertile, (B) anPCOS, (C) ovPCOS, (D) endometriosis, (E) UIF x40 magnification, scale bar (black) represents 20µm. No significant alterations in OPN staining were observed between the fertile and infertile groups. (F) Scores for OPN were plotted by patient group and expression analyzed using semi-quantitative H-scores. Statistical analysis was performed using the Kruskal-Wallis test (K-W p=0.13).

3.4.2 Osteopontin luminal expression in secretory phase endometrium

Luminal staining of OPN showed very similar patterns of expression to those observed in the glandular epithelium (Figure 3-6). Stronger staining was observed in the luminal epithelium of anPCOS group (Figure 3-6B) and more so in the ovPCOS (Figure 3-6C) group when compared to the fertile group (Figure 3-6A). In contrast, sections obtained from the endometriosis group (Figure 3-6D) seemed to exhibit a less abundant staining intensity and distribution compared to the fertile group (Figure 3-6A). This pattern of less abundant staining was also observed in the UIF patients (Figure 3-6E). These patterns were reflected in the H-score values obtained (Figure 3-6F).

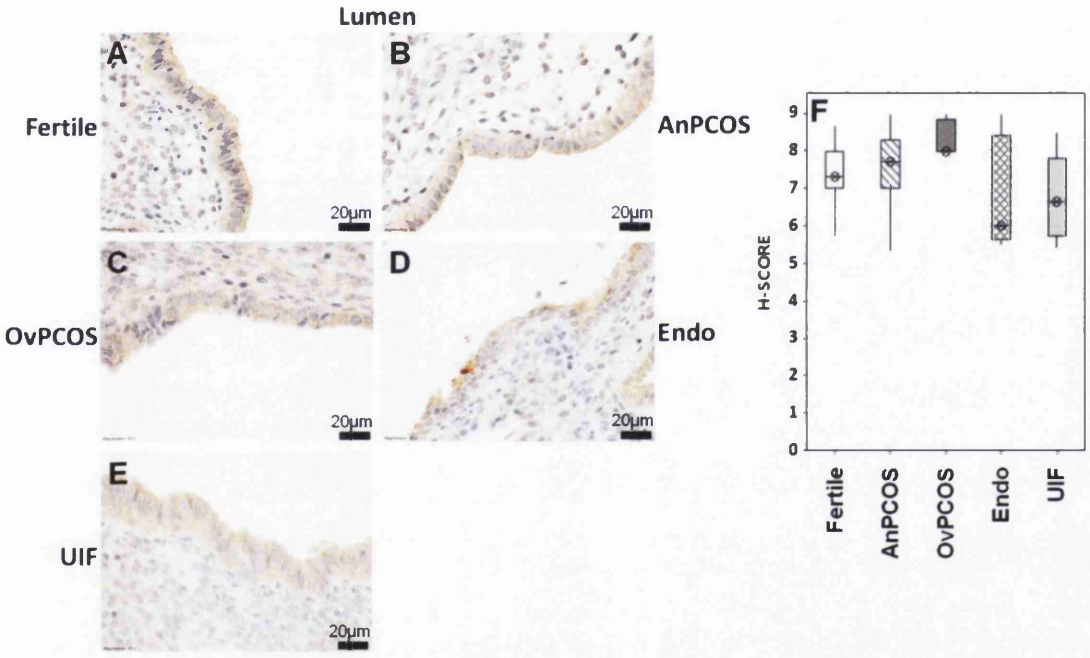

Figure 3-6 Secretory phase OPN expression in endometrial luminal epithelium.

Secretory phase endometrium from fertile (n=12), anPCOS (n=18), ovPCOS (n=8), endometriosis (Endo) (n=6) and UIF (n=12) patients stained for OPN. (A) fertile, (B) anPCOS, (C) ovPCOS, (D) endometriosis and (E) UIF x40 magnification, scale bar (black) represents 20µm. (F) The scores for OPN were plotted by patient group and expression analyzed using semi-quantitative H-scores. Statistical analysis was performed using the Kruskal-Wallis test (K-W p=0.07).

No significant differences were detected in OPN protein expression between the patient groups (K-W $p>0.05$), therefore no further statistical analysis was conducted. The ovPCOS patients (H=8.0) had a very tight data distribution resulting from consistently strong staining patterns and an increase in OPN expression when compared to the fertile group (H=7.3). No significant variation was detected between anPCOS (H=7.7) and the fertile group (H=7.3). The endometriosis (H=6) and UIF (H=6.7) groups both exhibited decreased H-scores, neither of these however were significant changes, probably due in part to the variation observed in staining pattern within these groups.

3.4.3 Osteopontin stromal expression in secretory phase endometrium

Less abundant staining patterns for OPN were observed in the stromal compartment for all infertile groups when compared to the other endometrial compartments (Figure 3-7). Consistent staining was observed in each of the PCOS groups (Figure 3-7B and C) when compared to the fertile group (Figure 3-7A). No significant variations were observed in the data when the Kruskal-Wallis test was applied (K-W $p=0.097$) and therefore no further statistical analysis was conducted. Less abundant staining was observed in the endometriosis group (Figure 3-7D) as well as the UIF group (Figure 3-7E). The staining patterns observed were reflected in the H-score values obtained (Figure 3-7F). Consistent H-scores were obtained for the anPCOS (H=5.5) and fertile group (H=5.5). Women with endometriosis appeared to exhibit a decreased level of OPN expression in the stroma (H=3.4), obtaining a decreased H-score value and less variation within the data set. The UIF (H=4.3) group appeared to have a decreased expression however this decrease was not significant, possibly a result of the variable distribution of the data.

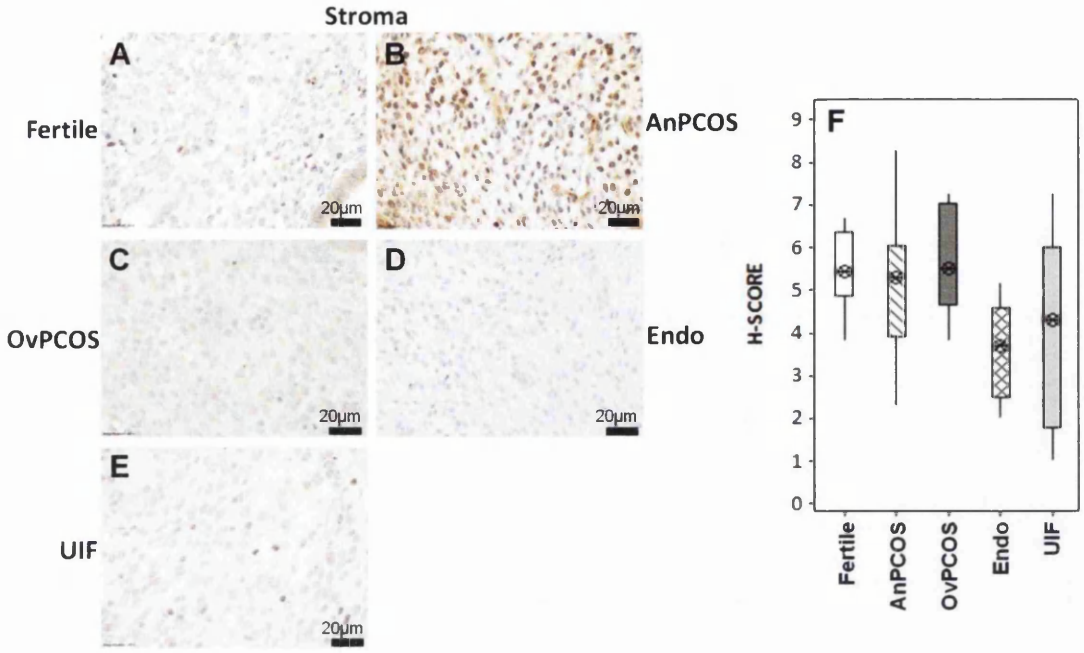

Figure 3-7 Secretory phase OPN expression in endometrial stroma.

Secretory phase endometrium from fertile (n=12), anPCOS (n=18), ovPCOS (n=8), endometriosis (Endo) (n=6) and UIF (n=12) patients stained for OPN. (A) fertile, (B) anPCOS, (C) ovPCOS, (D) endometriosis, (E) UIF x40 magnification, scale bar (black) represents 20µm. No significant alterations in OPN staining were observed between the fertile and infertile groups. (F) scores for OPN were plotted by patient group and expression analyzed using semi-quantitative H-scores. Statistical analysis was performed using the Kruskal-Wallis test (K-W p=0.1).

3.5 Secreted osteopontin from fertile and infertile endometrium

A pilot study was conducted to investigate whether the secreted OPN levels observed in the biopsies obtained from Singleton Hospital could be correlated to the data obtained in the IHC study (Section 3.1). Pipelle biopsy samples obtained from 20 women attending the infertility clinic were transferred to Swansea University and kept in media at 4˚C (maximum 4hrs) before culture. The media was aspirated, centrifuged and aliquots were taken in order to assess the secreted levels of OPN by ELISA. Samples were not separated into phase of menstrual cycle due to their limited number in this preliminary study. These samples included 6 fertile women, 3 diagnosed with anPCOS, 5 diagnosed with endometriosis and 6 with UIF

(Table 3.2). Patient grouping and statistical analysis were conducted using the identical methodology as the IHC study. All data are presented as box plots with the crossed circle indicating the median value of secreted OPN (pg/mL).

	Fertile	anPCOS	Endometriosis	UIF
AGE	33.8 ± 10.1	36.0 ± 8.5 p=0.7	36.4 ± 6 p=0.6	34.6 ± 3.2 p=0.9
BMI	26.8 ± 3.9	28 ± 4.4 p=0.7	28.7 ± 6.3 p=0.5	21.7 ± 4.8 p=0.2
n=	6	3	5	6

Table 3-2 Patient demographics for secreted OPN pilot study.

Media samples containing biopsy material while being transferred from Singleton Hospital to Swansea University were analyzed using ELISA to detect secreted OPN levels. Recorded parameters of age, BMI and total number of grouped patients, were analyzed and any statistical variation between groups recorded show mean values standard deviation and probability calculations, using a student's t-test. Total number of samples n=20. anPCOS, anovulatory, BMI, body mass index, n, number.

3.5.1 Secreted osteopontin

Secreted OPN has been identified in uterine flushings from animal models (Johnson et al. 1999; Chaen et al. 2012). Here we aimed to measure secreted OPN in the media surrounding the biopsy. Levels of secreted OPN detected by ELISA showed secreted OPN levels for fertile controls were 238 pg/mL (Figure 3-8). In the anPCOS group there was a large decrease in secreted OPN with a median value of 168 pg/mL obtained. The distribution of OPN in this group showed less variation, possibly due to the smaller sample size (n=3) than the fertile group. The endometriosis group exhibited similar data variation and a similar median value of 213pg/mL to the fertile group was recorded. The UIF group had a decreased median value of 169 pg/mL, however this was not significant when compared to the fertile group. This could be due to more variation in the data set. No significant differences

in secreted OPN were detected between groups and therefore no further pairwise comparisons were conducted (K-W p>0.05).

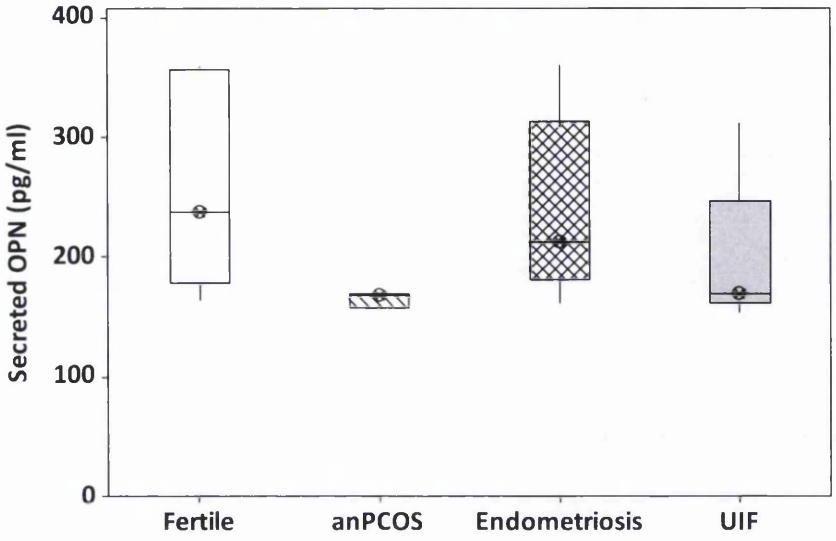

Figure 3-8 Secreted OPN levels in culture media of biopsies.

Secreted OPN levels measured by ELISA in fertile and infertile groups. Fertile (n=6), anPCOS (n=3), Endo (n=5) and UIF (n=6) groups. A decrease in secreted OPN was observed in the anPCOS (164pg/mL) and UIF (198 pg/mL) groups when compared to the fertile group (238pg/mL). No significant alterations in secreted OPN were observed between the fertile and infertile groups when analyzed for statistical variation in a pairwise manner using a student's t-test (p>0.05).

3.6 CD44 expression in the fertile endometrium

There have been no previous studies simultaneously measuring the expression of OPN and CD44 throughout the menstrual cycle in the human endometrium. In this study, the protein expression of CD44 was evaluated in the same patient cohort as for OPN in order to correlate the expression of both markers in the endometrium. CD44 expression on the epithelia is essential to enable OPN to form a complex with $\alpha V\beta 3$. CD44 expression is up regulated in the secretory phase, concurrent with the window of implantation, and has shown to bind OPN in other tissues and cell types such as the prostate, substantia nigra and kidney (Desai et al. 2009; Desai et al. 2007; Bellahcène et al. 2008; Lee et al. 2007).

Data presented here indicate CD44 expression in the proliferative phase endometrium was most abundant in the stroma when compared to the glands and luminal epithelium (Figure 3-9). Secretory phase glandular CD44 expression showed stronger staining than in the proliferative phase (Figure 3-9A and D). Luminal CD44 staining was similar in the proliferative and secretory phase (Figure 3-9B and D) whilst stromal staining was decreased in the secretory phase when compared to the proliferative phase (Figure 3-9C and F). Staining was quantified by H-score analysis (Figure 3-9G). Significant differences were detected in CD44 protein expression between the different compartments and therefore a Mann-Whitney U test was conducted to determine which compartments were significantly different in the secretory phase when compared to the proliferative by pairwise comparisons (K-W $p=0.001$). Secretory phase glandular CD44 expression showed a significant 3-fold increase ($H = 4.6$) when compared to the proliferative phase ($H = 1.5$; M-WU $p=0.02$). Stromal CD44 expression decreased significantly in the secretory phase when compared to the proliferative phase ($H = 5.7$; $H= 4.8$ respectively; M-WU $p=0.04$). No significant variation in luminal CD44 expression was observed between the two phases; H-scores of 2.3 and 2.7 in the proliferative and secretory phases were obtained respectively (M-WU $p=0.55$).

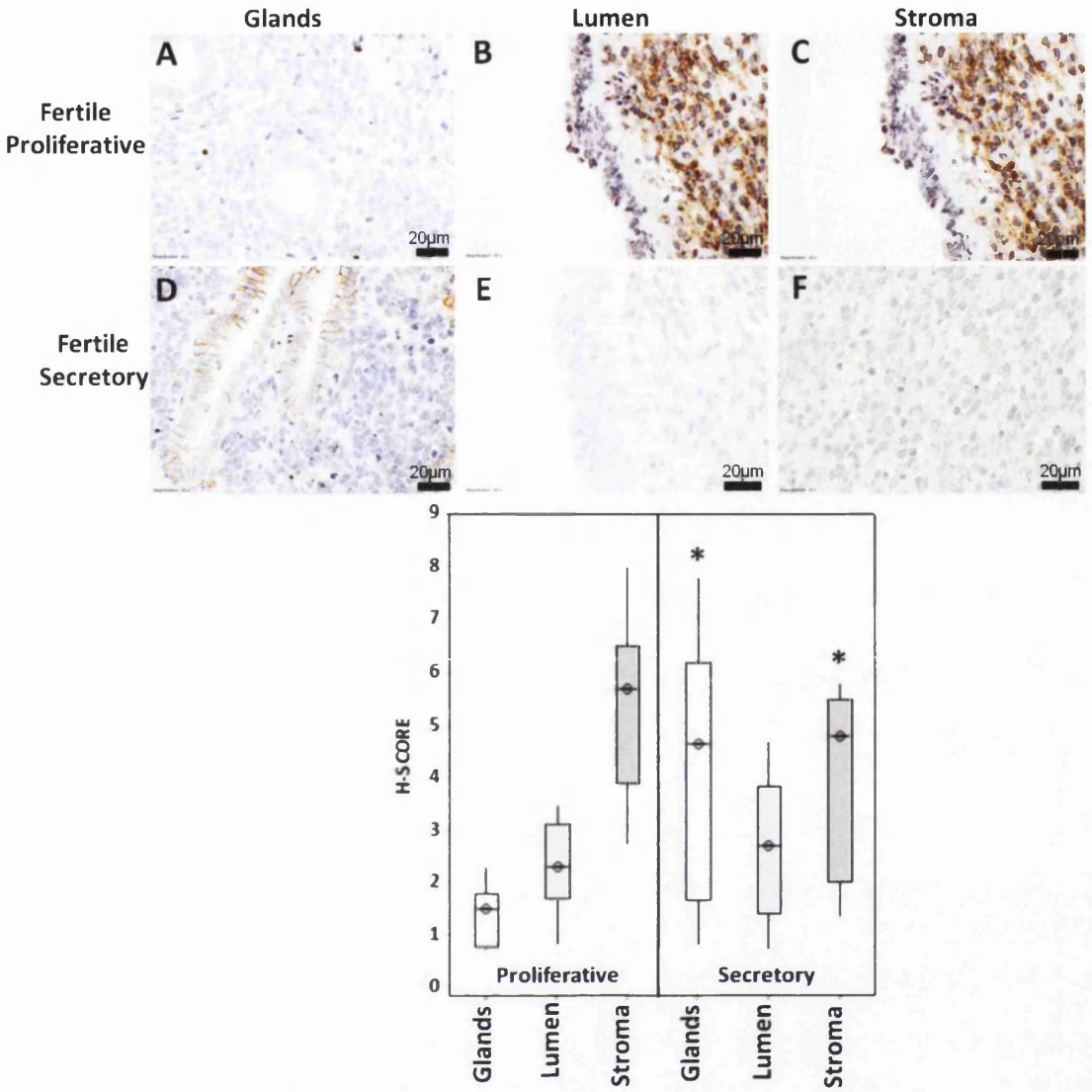

Figure 3-9 CD44 protein expression in the proliferative and secretory phase of the fertile endometrium.

CD44 expression in fertile endometrium by compartment; (A-C) proliferative phase (n=10), (D-F) secretory phase (n=12). Sections of fertile endometrium were stained with CD44 antibody and slides scored by three independent scorers at x40 magnification, scale bar (black) represents 20µm. A significant increase in glandular CD44 expression was noted in the secretory phase when compared to the proliferative phase endometrium (M-WU p=0.02), whilst stromal CD44 expression significantly decreased in the secretory phase (p=0.04). (G) All H-scores were grouped and plotted. * P≤0.05

3.6.1 CD44 expression in the proliferative phase infertile endometrium

CD44 expression has been found to be less abundant in the secretory phase endometrium of healthy cycling women (Poncelet et al. 2010). CD44 expression in the endometrium was found to be different in endometrial pathologies. Up or down-regulation of CD44 expression in endometrial tissue has been shown in the epithelia and stroma and has been linked to the development of endometriotic lesions in endometriosis. This is thought to occur through an increasing ability to bind the outer peritoneal surface of the endometrium (Lucidi et al. 2005; Poncelet et al. 2002). Therefore, CD44 expression in infertile groups is compared to the fertile group to assess if any differences exist.

3.6.2 CD44 glandular expression in proliferative phase endometrium

Glandular staining of CD44 appeared to be stronger in the anPCOS (Figure 3-10B), endometriosis (Figure 3-10C) and UIF (Figure 3-10B) infertile groups compared to the fertile group (Figure 3-10A). This difference in staining was reflected in the H-scores (Figure 3-10E). No significant difference between groups was observed when the Kruskal-Wallis test (K-W $p=0.17$) was applied and therefore no further statistical analysis was conducted. Glandular CD44 expression measured by H-score in anPCOS and UIF groups was very similar to the fertile group with both obtaining H-score values of 2 compared to the fertile group ($H = 1.5$). No significant differences were observed in the endometriosis group, possibly due to the wide data distribution when compared to the fertile group. With the exception of the endometriosis group, CD44 expression was very low in fertile and infertile pathologies in the proliferative phase endometrium as expected (Yaegashi et al. 1995; Saegusa et al. 1998).

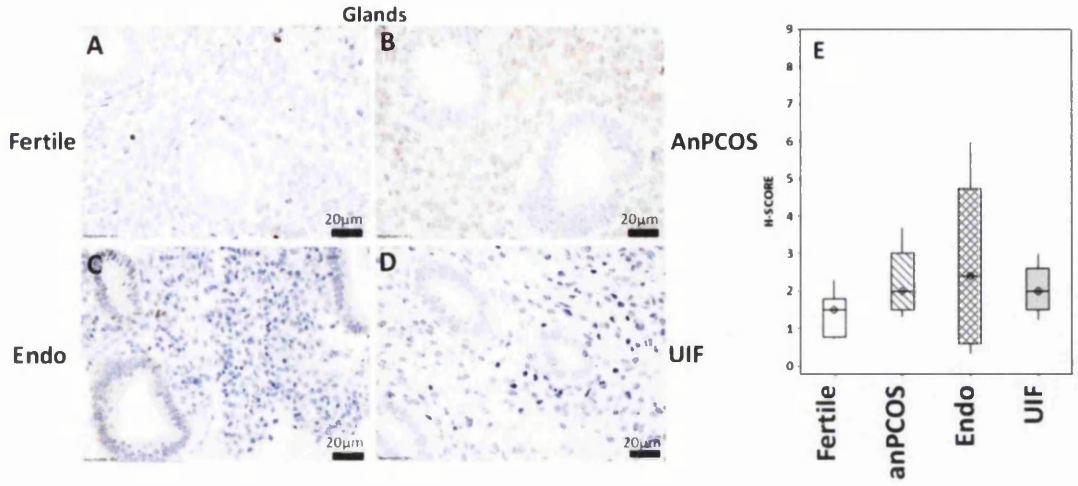

Figure 3-10 Proliferative phase CD44 expression in the endometrial glands.

Proliferative phase endometrium from fertile (n=10), anPCOS (n=18), endometriosis (Endo) (n=6) and UIF (n=12) patients stained for CD44. (A) fertile, (B) anPCOS, (C) endometriosis, (D) UIF x40 magnification, scale bar (black) represents 20µm. No significant alterations in CD44 staining were observed between the fertile and infertile groups. (E) scores for CD44 were plotted by patient group and expression analyzed using semi-quantitative H-scores (E). Statistical analysis was performed using the Kruskal-Wallis test (K-W p=0.2).

3.6.3 CD44 luminal expression in proliferative phase endometrium

In the proliferative phase, CD44 staining in the luminal compartment of the endometrium in anPCOS (Figure 3-11B), endometriosis (Figure 3-11C) and UIF (Figure 3-11D) exhibited similar patterns to the fertile group (Figure 3-11A). Quantitated by H-score values (Figure 3-11E), all groups displayed similar median H-score values and data distributions. No significant differences in CD44 expression were detected between groups (K-W $p>0.05$), therefore no further pair-wise comparisons were conducted. Luminal CD44 expression in the proliferative phase is expected to be decreased in agreement with current literature (Afify et al. 2006).

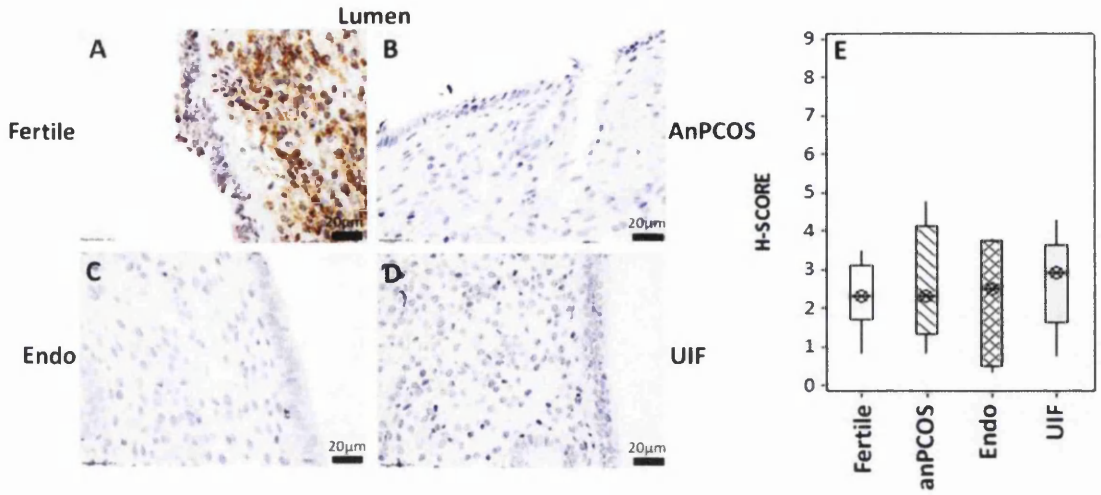

Figure 3-11 Proliferative phase CD44 expression in the endometrial luminal epithelium.

Proliferative phase endometrium from fertile (n=10), anPCOS (n=18), endometriosis (Endo) (n=6) and UIF (n=12) patients stained for CD44. (A) fertile, (B) anPCOS, (C) endometriosis, (D) UIF x40 magnification, scale bar (black) represents 20µm. No significant alterations in CD44 staining were observed between the fertile and infertile groups (E). Scores for CD44 were plotted by patient group and expression analyzed using semi-quantitative H-scores. Statistical analysis was performed using the Kruskal-Wallis test (K-W p=0.8).

3.6.4 CD44 stromal expression in proliferative phase endometrium

CD44 staining in the stroma of the infertile groups was not as strong as in the fertile group (Figure 3-12). Weaker CD44 staining was observed in anPCOS (Figure 3-12B), endometriosis (Figure 3-12C) and the UIF (Figure 3-12D) group when compared to the fertile group (Figure 3-12A). This was additionally reflected in semi-quantitative H-scores (Figure 3-12E). Significant differences were detected in CD44 protein expression between the groups (K-W p=0.02), and therefore a Mann-Whitney U test was conducted to determine whether any of the infertile groups demonstrated a significant difference to the fertile group via a pairwise comparison. CD44 expression in the UIF group was significantly decreased 1.7-fold when compared to the fertile group (H = 3.3; H = 5.7 respectively, M-WU p=0.009). The anPCOS and

endometriosis groups displayed a similar level of CD44 expression to the fertile group (4.8 and 5.4 respectively; M-WU p=0.77 and p=0.64 respectively).

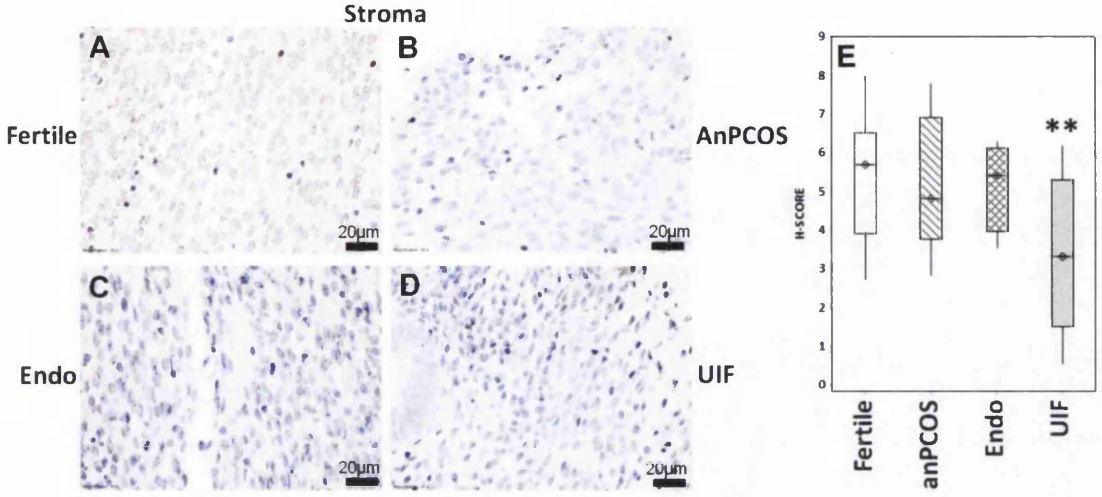

Figure 3-12 Proliferative phase CD44 expression in the endometrial stroma.

Proliferative phase endometrium from fertile (n=10), anPCOS (n=18), endometriosis (Endo) (n=6) and UIF (n=19) patients stained for CD44. (A) fertile, (B) anPCOS, (C) endometriosis, (D) UIF x40 magnification, scale bar (black) represents 20µm. Significant alterations in OPN staining were observed between the fertile and infertile groups. (E) Scores for CD44 were plotted by patient group and expression analyzed using semi-quantitative H-scores. Statistical analysis was performed using the Kruskal-Wallis test (K-W p=0.02). CD44 decreased significantly in the stroma of the UIF group compared to the fertile group (M-WU p=0.009). ** P≤0.01

3.6.5 CD44 expression in the secretory phase endometrium of infertile women

Expression of CD44 in human endometrium has been linked to a role in the outcome of fertility. Endometrial CD44 expressed at the apical surface of luminal epithelium forms a complex with OPN to bind the integrin αVβ3 presented by the blastocyst promoting embryo attachment. There are no studies describing the expression of CD44 in the endometrium of women with different pathological conditions associated with infertility. Our hypothesis is that CD44, through its function as OPN receptor, may contribute to the attachment of the embryo to the receptive endometrium during implantation. If expression of CD44 is an important

factor in determining endometrial receptivity, then alteration in CD44 expression could contribute to endometrium-related infertility.

3.6.6 CD44 glandular expression in secretory phase endometrium

CD44 expression has been characterized in the glands of other tissues, such as mammary glands where CD44 expression is required for the proliferation of the underlying mesenchymal cells (Yu et al. 2002; Hebbard et al. 2000). CD44 expression in the mammary gland is thought to be linked to its role as a mediator of epithelial-stromal signalling in addition to functional roles in proliferation, migration and invasion in cancer cells (Louderbough et al. 2011; Lokeshwar et al. 1995). CD44 staining in the endometrium has been described in fertile samples and shown to be less pronounced in the glands and luminal epithelium compared to the stroma (Goshen et al. 1996). In this study CD44 expression in the secretory phase of the endometrium was measured in the glandular compartment of fertile and infertile groups. Glandular CD44 staining appeared weaker in anPCOS (Figure 3-13B), ovPCOS (Figure 3-13C) and endometriosis (Figure 3-13D) infertile groups when compared to the fertile group (Figure 3-13A). No differences in staining patterns were observed in the UIF group (Figure 3-13E). These changes in staining patterns were quantified using H-score analysis (Figure 3-13F). Significant differences were detected in glandular CD44 protein expression between the groups (K-W p=0.03) and the Mann-Whitney U test was therefore conducted to determine which infertile groups were significantly different to the fertile group by pairwise comparison. A significant decrease in glandular CD44 staining was observed in the ovPCOS group and H-score values showed a significant decrease of 3.6-fold (H = 4.7) when compared to the fertile group (H = 1.3; M-WU p=0.04). CD44 expression in the anPCOS group was similar to the fertile group, however there was larger variation within the data resulting in a decrease of CD44 expression. This was not judged to be significant (H = 2.0). The endometriosis group also had a lower H-score (H=2.5) but the variation in the data was very similar to that of the fertile group. No

significant variation was observed in the UIF group when compared to the fertile group (H=4.2, M-WU p=0.68).

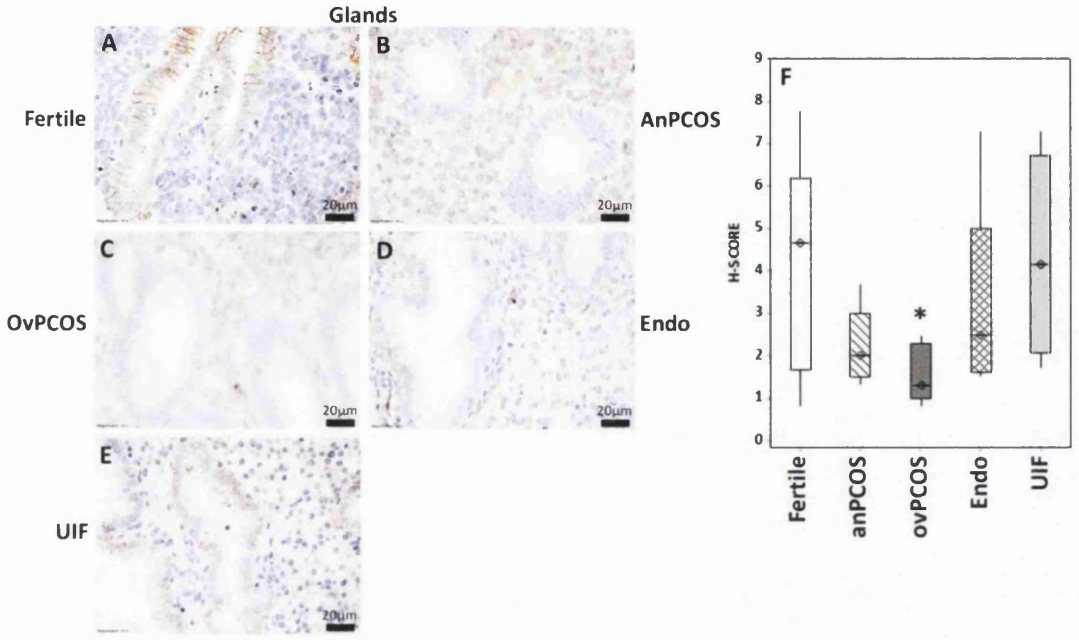

Figure 3-13 Secretory phase CD44 protein expression in endometrial glands.

Secretory phase endometrium from fertile (n=12), anPCOS (n=18), ovPCOS (8), endometriosis (Endo) (n=6) and UIF (n=12) patients stained for CD44. (A) fertile, (B) anPCOS, (C) ovPCOS, (D) endometriosis, (E) UIF x40 magnification, scale bar (black) represents 20µm. Significant alterations in CD44 staining were observed between the fertile and infertile groups. (F) Scores for CD44 were plotted by patient group and expression analyzed using semi-quantitative H-scores. Statistical analysis was performed using the Kruskal-Wallis test (K-W p=0.03). CD44 decreased significantly in the glands of the ovPCOS group compared to the fertile group (M-WU p=0.04). * P≤0.05

3.6.7 CD44 luminal expression in secretory phase endometrium

CD44 expression on the endometrial luminal surface during the window of implantation is essential to enable OPN complex to assembly and attachment of the blastocyst to the epithelia surface (Johnson et al. 2003). The lumen cells of the epithelium is the first point of contact with the developing trophoblast; a process known as apposition. This is followed by adhesion and molecules such as CD44 are involved in stabilizing the attachment of the trophoblast to the endometrium allowing the subsequent invasion of the developing blastocyst into the

endometrium. The luminal expression of CD44 was assessed in the secretory phase of the endometrium in fertile and infertile groups (Figure 3-14). Luminal CD44 staining in anPCOS (Figure 3-14B), ovPCOS (Figure 3-14C), endometriosis (Figure 3-14D) and UIF (Figure 3-14E) infertile groups appeared to be decreased compared to the fertile group (Figure 3-14A). This was confirmed by H-scores analysis (Figure 3-14F). No significant difference in CD44 expression was detected between the fertile and infertile groups (K-W $p>0.05$) and therefore no further pairwise comparisons were conducted.

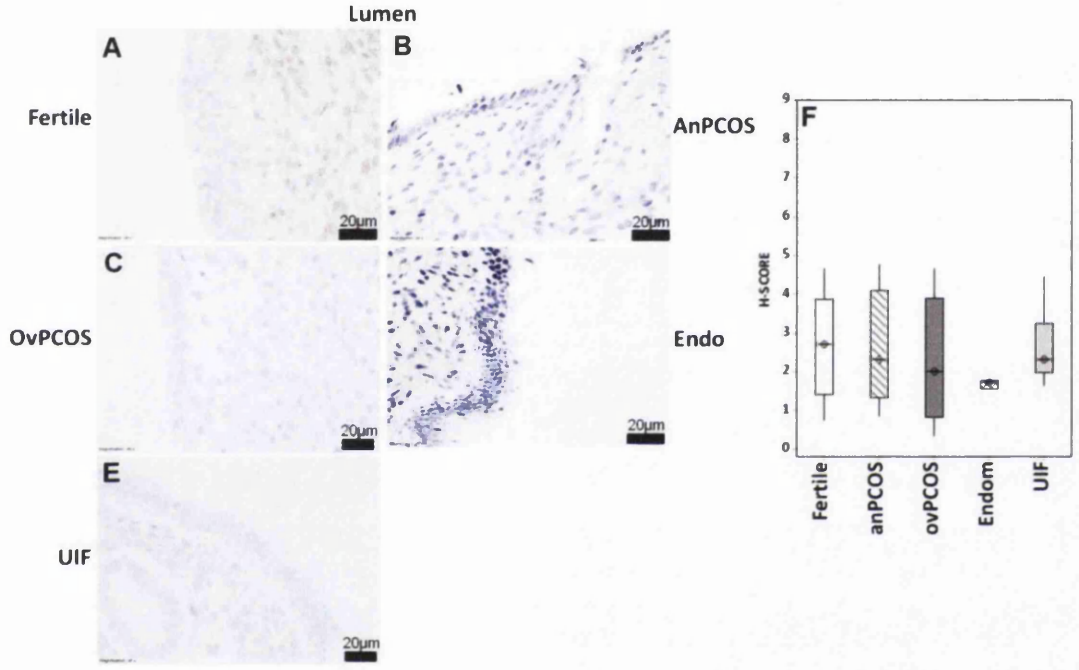

Figure 3-14 Secretory phase CD44 protein expression in endometrial luminal epithelium.

Secretory phase endometrium from fertile (n=12), anPCOS (n=18), ovPCOS (8), endometriosis (Endo) (n=6) and UIF (n=12) patients stained for CD44. (A) fertile, (B) anPCOS, (C) ovPCOS, (D) endometriosis, (E) UIF x40 magnification, scale bar (black) represents 20µm. No significant alterations in CD44 staining were observed between the fertile and infertile groups. (F) H-scores for CD44 were plotted by patient group and expression analyzed using semi-quantitative H-scores. Statistical analysis was performed using the Kruskal-Wallis test (K-W p=0.03).

The endometriosis group exhibited less variation in data distribution and a similar H-score to the fertile group (H=1.7). Similar variations in the data distribution and

staining were observed between the fertile (H = 2.7), anPCOS (H = 2.3) and ovPCOS (H = 2) groups. The UIF group had a tighter data distribution than the fertile group and a similar H-score value (H=2.3).

3.6.8 CD44 stromal expression in secretory phase endometrium

CD44 expression in the endometrial stroma in the secretory phase is important in decidualization, a process that allows endometrial differentiation to sustain pregnancy. CD44 has been described to be expressed in decidual cells, that are differentiated stromal cells, and highly expressed in pregnant decidua (Behzad et al. 1994; Goshen et al. 1996). In this study CD44 staining in the stroma of the secretory phase appeared similar in the anPCOS (Figure 3-15A), ovPCOS (Figure 3-15B) and endometriosis (Figure 3-15C) groups compared to the fertile group (Figure 3-15). Stromal staining in the UIF group appeared to be stronger (Figure 3-15E). This was confirmed by the H-score analysis (Figure 3-15F). Significant differences were detected in stromal CD44 protein expression between the groups (K-W p=0.03). A Mann-Whitney U test was therefore conducted to determine which infertile groups were significantly different to the fertile group by pairwise comparisons. In the UIF group (H=5.5) a significant increase in CD44 staining was observed in the secretory endometrium, reflected by a higher H-score than the fertile group (H= 4.8; M-WU p=0.018). H-score values obtained for both PCOS (anPCOS and ovPCOS, H = 4.8 and 3.9 respectively) groups were very similar to the fertile group (H = 4.8). No significant variation was observed. In the endometriosis group (H=5.5) however, the spread of the data was similar to the fertile group and therefore it was not statistically different.

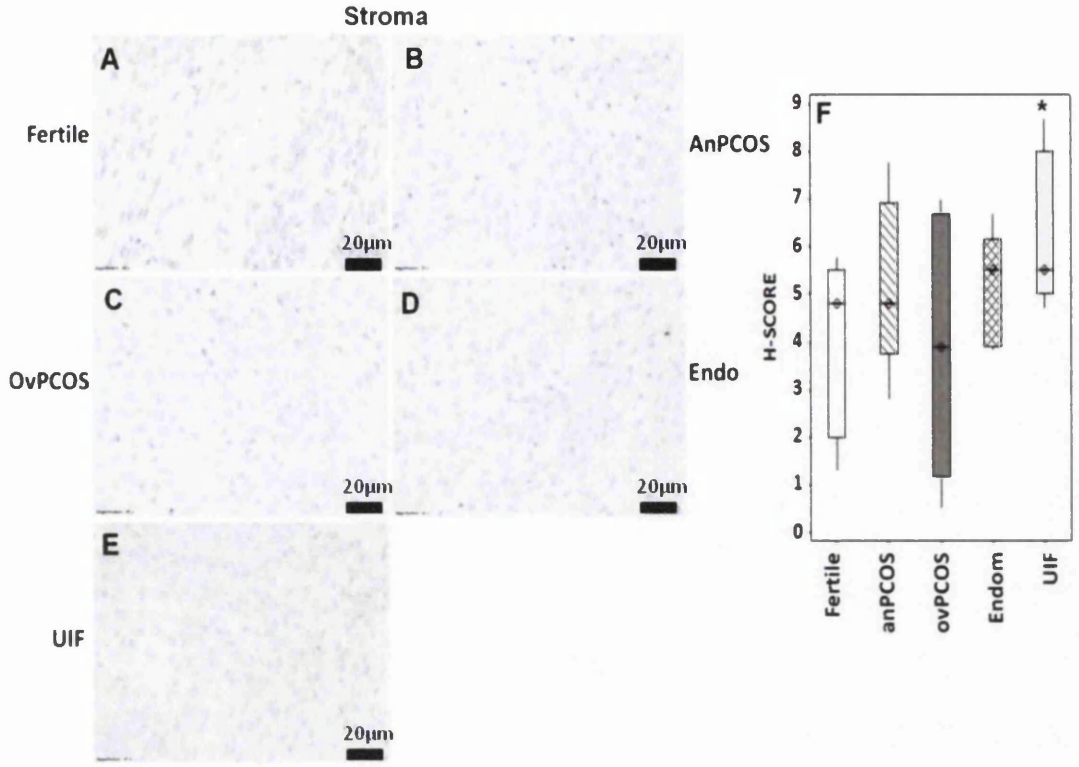

Figure 3-15 Secretory phase CD44 protein expression in endometrial stroma.

Secretory phase endometrium from fertile (n=12), anPCOS (n=18), ovPCOS (n=8), endometriosis (Endo) (n=6) and UIF (n=12) patients stained for CD44. (A) fertile, (B) anPCOS, (C) ovPCOS, (D) endometriosis, (E) UIF x40 magnification, scale bar (black) represents 20µm. Significant alterations in CD44 staining were observed between the fertile and infertile groups (F). Scores for CD44 were plotted by patient group and expression analyzed using semi-quantitative H-scores. Statistical analysis was performed using the Kruskal-Wallis test (K-W p=0.03). CD44 decreased significantly in the stroma of the UIF group compared to the fertile group (M-WU p=0.02). * P≤0.05

3.6.9 Immunohistochemistry summary

Spatial distribution of CD44 (Figure 3-9) in the fertile endometrial tissue differs from that of OPN (Figure 3-1) in both phases of the menstrual cycle. OPN expression is up regulated in the glands and luminal epithelium when compared to the stroma in both phases of the menstrual cycle. CD44 expression is up-regulated in the glands in the secretory phase when compared to the proliferative phase. In both phases stromal expression of CD44 was higher than for the other two compartments,

stromal expression in proliferative phase was higher than secretory phase. In the proliferative phase CD44 glandular expression is 3.8-fold lower than stromal CD44. In the secretory phase however, CD44 expression in the glands and stroma was similar; reflected in similarity in variations of data and H-scores.

Glandular proliferative expression of CD44 was very low when compared to OPN staining in the glands (Figure 3-3). Although OPN luminal expression (Figure 3-4) in the proliferative phase was higher than CD44 expression (Figure 3-11), the same observation was made in the expression patterns between the infertile and fertile group. Stromal OPN and CD44 expression in the proliferative phase indicated similar staining and H-scores patterns with both OPN and CD44 showing decreased expression in the UIF group (Figure 3-5; Figure 3-12). This observation of altered stromal expression of both molecules suggests a role for OPN/CD44 complex during stromal proliferation.

In the secretory phase, glandular expression of CD44 (Figure 3-13) was less abundant than glandular OPN expression (Figure 3-5) in all fertile and infertile groups. This could be due to CD44 being most abundantly located in the cell membrane with little cytoplasmic and nuclear staining being observed. Therefore as the distribution of CD44 was lower, a low H-score was obtained. In comparison with CD44, luminal expression of OPN in the secretory phase (Figure 3-6) is more abundantly expressed in fertile and infertile groups. However, the expression of CD44 is much more varied in terms of data distribution than OPN expression, which is much tighter (Figure 3-14).

Stromal OPN expression in the secretory endometrium (Figure 3-7) was similar to CD44 (Figure 3-15) in terms of abundance with H-score values within the same range. However different patterns of expression of the two markers were noted in each pathology group. OPN expression decreased in the stroma of endometriosis patients while CD44 expression increased (compared to fertile group). However, both proteins showed decreased stromal expression in UIF patients. Although the differences observed for the UIF and endometriosis groups were not statistically

significant, they indicated the need for a larger study to separate the different degrees of endometriosis and a larger cohort for the UIF group. Taken together, these subtle differences in both proteins may impact on the coordination of the events taken place during the secretory phase. For example, successful decidualization relays in the coordinate paracrine signalling between the glands and stroma to take place.

3.7 Clinical data and patient demographics for gene expression study

In order to investigate if the gene expression of *OPN* and *CD44* was a major factor involved in the observed protein expression changes, a small study was designed to measure the mRNA levels from a small group of tissue samples. Total RNA was extracted from fresh frozen biopsies obtained from women attending infertility clinics at Singleton Hospital. Quantitative Polymerase Chain Reaction (qPCR) was performed to determine the levels of mRNA present in pipelle biopsies of total endometrium. In addition, expression analysis was conducted for integrin αVβ3 at the mRNA level. Each αVβ3 sub-unit was analyzed separately with primers designed specifically for the αV *(ITGAV)* and β3 *(ITGB3)* genes which protein products form a dimer (αVβ3).

3.7.1 Demographics and statistics

Women with proven fertility (at least 2 full term births) were recruited to the study; 3 were in the proliferative phase and 6 in the secretory phase and they were selected according to the inclusion criteria in section 3.3.1. 15 women with PCOS were recruited and separated into anovulatory (13) and ovPCOS (2) groups (Table 3-3). Nine women with endometriosis were recruited in each phase of the menstrual cycle. Sixteen women with unexplained infertility were recruited; 8 proliferative and 9 secretory phase. A total of 57 women were included in this study. Significant differences were found between the mean age of the women in anPCOS and the proliferative UIF groups when compared to the fertile proliferative group ($p=0.002$; $p=0.046$ respectively). Despite limiting the effectiveness of this

study, no significant outliers were found and therefore none were removed so that patient numbers for the study were preserved. All statistical analyses were conducted following the same methodology as the IHC study and data presented as box plots (section 3.3.1).

RNA	Fertile		PCOS		Endometriosis		Unexplained Infertility	
	Pro	Sec	Anov	Ov	Pro	Sec	Pro	Sec
AGE	36.0±0	32.0±5.5 p=0.18	28.2±6.0 p=0.002	24.0±7.1 p=0.3	33.9±5.2 p=0.26	30.8±6.4 p=0.75	29.3±4.1 p=0.046	28.6±1.9 p=0.25
BMI (kg/m)	23.3±9.2	23.3±1.2 p=0.16	23.4±3.4 p=0.16	35.5±4.9 p=0.17	26.6±4.1 p=0.25	27.0±5.6 p=0.13	24.2±4.3 p=0.17	25.4±5.5 p=0.41
n=	3	6	13	2	9	9	8	9
cum n=	9		15		18		17	

Table 3-3 Patient demographics for total RNA extraction study.

Total RNA was extracted from fresh frozen tissue biopsy material and assessed for OPN, CD44, ITGAV and ITGB3 gene expression. Recorded parameters of mean age (standard deviation), BMI, and total number of grouped patients were analyzed and any statistical differences between groups recorded using mean values standard deviation and probability calculations, using a student's t-test. Total number of samples n=59. Pro, proliferative, Sec, secretory, Anov, anovulatory, ov, ovulatory, BMI, body mass index, n, number, cum, cumulative.

3.8 Gene expression of adhesion complex components

3.8.1 Endometrial adhesion partner expression in fertile endometrium

Expression of all adhesion partner genes at the mRNA level was first assessed in the fertile proliferative and secretory phases. No significant variation in expression was observed between the groups when the Kruskal-Wallis test was applied and consequently no further pairwise comparisons were conducted (K-W p=0.34). It was noted that *OPN* expression increased in the secretory phase compared to the proliferative phase (Figure 3-16). This increase was not found to be statistically

significant. No significant change in the expression of *CD44* was observed between the distinct phases of the menstrual cycle despite an increase in the median value (0.05 to 0.09) in the secretory phase. Increased expression of *ITGAV* and *ITGB3* integrin subunits was observed in the secretory phase of the menstrual cycle when compared to the proliferative phase. *ITGAV* demonstrated a 3.8-fold (0.05 to 0.19) increase. A 10-fold increase in expression was observed for the *ITGB3* subunit (0.05 to 0.5) in the secretory phase. These differences were not found to be statistically significant however.

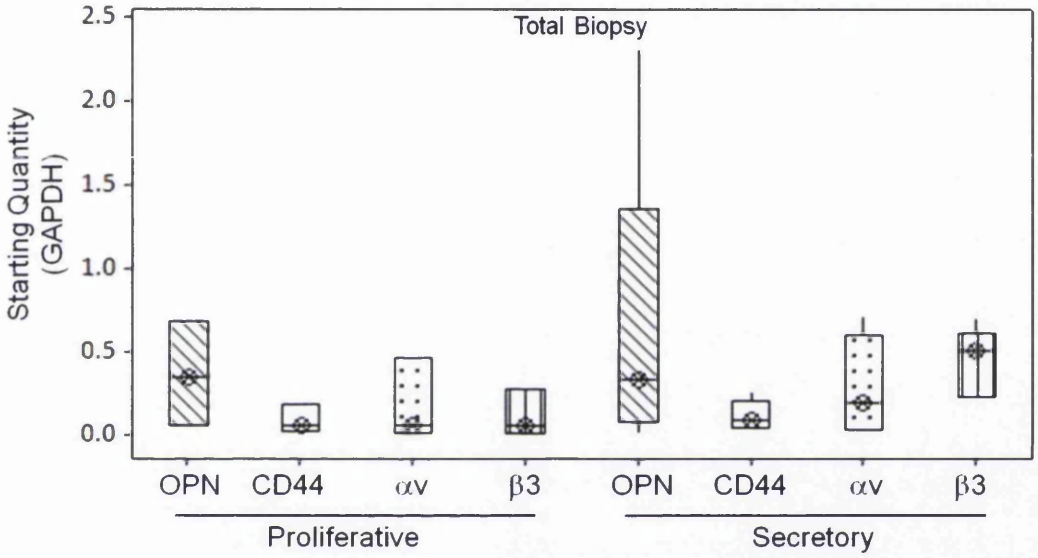

Figure 3-16 Total RNA expression levels throughout the menstrual cycle.

Total biopsy tissue analyzed for OPN, CD44, ITGAV and ITGB3 transcript levels in the proliferative (n=3) and secretory phase (n=6) of the menstrual cycle. All starting quantity values are absolute and normalized against GAPDH. Values are represented in box plots. Statistical analysis was performed using a Kruskal-Wallis test.

3.8.2 Adhesion complex components proliferative phase expression in infertile endometrium

Expression levels of the adhesion complex components were measured in the proliferative phase (Figure 3-17) of the menstrual cycle in infertile women and compared to fertile women. No significant variation in mRNA expression was

observed between the groups when the Kruskal-Wallis test was applied and therefore no further pairwise comparisons were conducted (K-W p=0.4).

3.8.3 Osteopontin proliferative phase expression in endometrium

OPN expression decreased in each of the three infertile groups compared to the fertile group however this trend was not statistically significant (Figure 3-17A). More variation in the 50% interquartile region of the data was observed in the fertile and endometriosis groups compared to the anPCOS and UIF groups. Despite this variation, the median scores for the data set obtained are indicative of large decreases in *OPN* gene expression. When compared to the fertile group expression decreased 13-fold in the anPCOS, 12-fold in the endometriosis group and 11-fold in the UIF group. Due to the small sample size these differences were not significant.

3.8.4 CD44 proliferative phase expression in endometrium

Decreased absolute starting quantities of *CD44* gene expression levels were observed in the infertile groups when compared to the fertile group (Figure 3-17B). *CD44* expression in the proliferative phase of the endometrium of anPCOS and UIF groups showed a decrease of 2.5 and 5.6-fold respectively when compared to the fertile group, but differences were not significant. A similar starting quantity was observed in *CD44* expression in the endometriosis group compared to the fertile group.

3.8.5 Integrin AV proliferative phase expression in endometrium

ITGAV expression showed decreases in absolute starting quantities in the infertile groups when compared to the fertile group (Figure 3-17C). Expression of *ITGAV* exhibited a 2-fold decrease in anPCOS, a 2.3-fold decrease in endometriosis and a 2.7-fold decrease in the UIF group.

3.8.6 *Integrin B3 proliferative phase expression in endometrium*

ITGB3 exhibited a decrease in absolute starting quantity at the RNA level in each of the infertile groups (Figure 3-17D). A 2-fold decrease in *ITGB3* expression is observed in the anPCOS group. This was higher in the UIF group where a 2.5-fold decrease was observed. The endometriosis group showed a similar expression pattern to the fertile group.

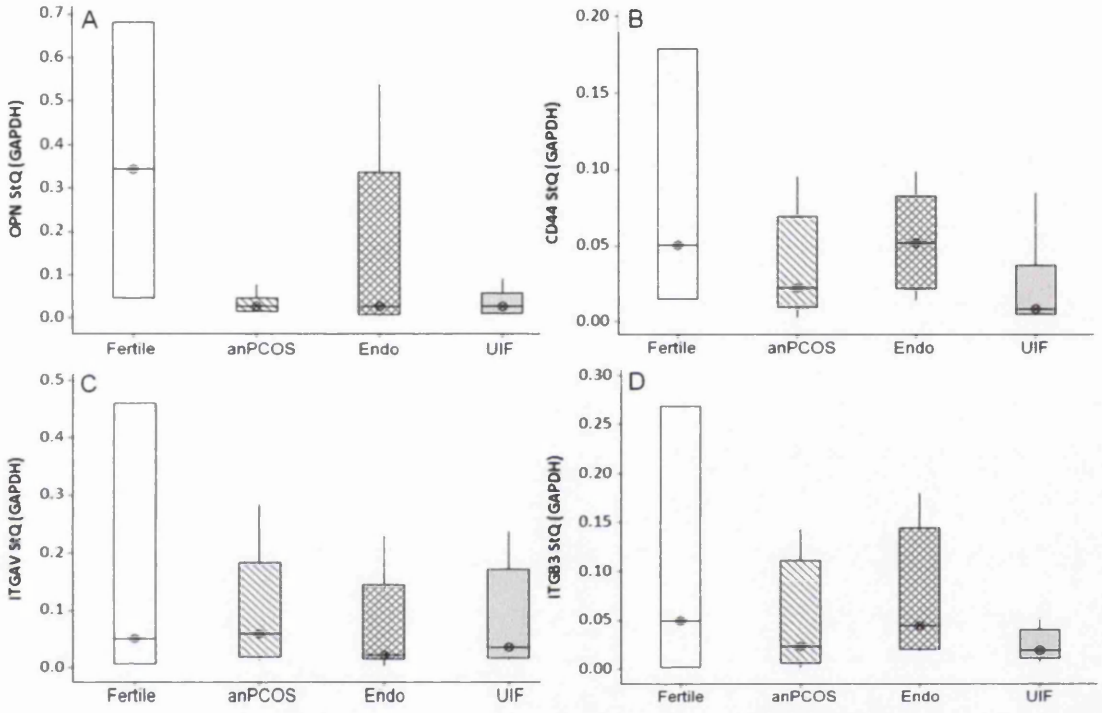

Figure 3-17 Proliferative phase adhesion complex partner expression.

Quantitative PCR was conducted on total RNA reverse transcribed to cDNA in, fertile (n=3), anPCOS (n=13), endometriosis (Endo) (n=9) and UIF (n=8) for (A) OPN, (B) CD44, (C) ITGAV and (D) ITGB3 mRNA expression. All starting quantity values are absolute and normalized against the GAPDH housekeeping gene. No significant differences in expression were observed between fertile and infertile groups for all genes analyzed.

3.8.7 *Proliferative phase correlation analysis*

To identify if expression of the adhesion complex could be correlated in the proliferative phase of infertile women, a Spearman's rank order correlation was used to determine the relationship between gene products. A strong positive

correlation was found between the expression of *CD44* and *ITGB3* in the endometriosis group of the proliferative phase (Spearman's rho =0.667 p=0.05). No other significant correlations were detected.

3.8.8 Adhesion complex secretory phase expression in infertile endometrium

Expression levels of the adhesion complex compartments were assessed in the secretory phase of the menstrual cycle in fertile and infertile women (Figure 3-18). Significant differences were detected by qPCR in mRNA expression between the infertile and fertile group and therefore a Mann-Whitney U test for pairwise comparison was conducted.

3.8.9 Osteopontin secretory phase expression in endometrium

In order to assess the significance of *OPN* gene expression in the secretory phase, the expression levels in the fertile group were compared directly to the four infertile groups (K-W p=0.007) (Figure 3-18A). When compared to the fertile control group, levels of *OPN* RNA were decreased significantly by 13-fold in anPCOS (M-WU p=0.007). In the ovPCOS group a 5-fold difference was detected but was not found to be statistically significant (M-WU p=0.9). In contrast *OPN* levels in the endometriosis and UIF groups were similar to the fertile control group (M-WU p=0.93; p=0.44).

3.8.10 CD44 secretory phase expression in endometrium

CD44 expression in the secretory endometrium of fertile and infertile groups of total biopsies (K-W p=0.044) (Figure 3-18B). *CD44* expression is significantly reduced 4.5-fold in the anPCOS group compared to the fertile group (M-WU p=0.024). A further significant 5-fold decrease in *CD44* expression was observed in the UIF group compared to the fertile control (M-WU p=0.008). A 2-fold decrease was noted in the ovPCOS group while expression was decreased 4.7-fold in the endometriosis group however these decreases were not statistically significant (M-WU p=0.1).

3.8.11 Integrin AV secretory phase expression in endometrium

ITGAV expression in all infertile groups was decreased compared to the fertile group (K-W p=0.001) (Figure 3-18C). The UIF group has significantly less *ITGAV* expression; 48-fold less compared to the fertile group (M-WU p=0.002). ITGAV expression was decreased in expression in both the PCOS sub groups 8 and 11-fold in the anPCOS and ovPCOS groups respectively, however this was not statistically significant (M-WU p=0.22). The endometriosis group displayed a 6-fold decrease in *ITGAV* expression but it was not statistically significant when compared to the fertile group (M-WU p=0.17).

3.8.12 Integrin B3 secretory phase expression in endometrium

αVβ3 complex partner *ITGB3* illustrated a decrease in expression in the secretory phase of the menstrual cycle in all infertile groups (K-W p=0.006) (Figure 3-18D). When compared to the fertile group significant decreases in *ITGB3* were observed, in the anPCOS group a significant 17-fold decrease in *ITGB3* was observed (M-WU p=0.003), the endometriosis group a significant 32-fold decrease in *ITGB3* (M-WU p=0.008) and the UIF group a significant 26-fold decrease in *ITGB3* expression was observed compared to the fertile group (M-WU p=0.003). The ovPCOS group displayed a 6-fold reduction in *ITGB3* expression which was not statistically significant.

3.8.13 Secretory phase correlation analysis

To identify if expression of the adhesion complex could be correlated in infertile women a Spearman's rank order correlation was used to determine the relationship between gene products. In the endometriosis group a very strong positive correlation between *OPN* and *CD44* was noted in the secretory phase (Spearman's rho =0.857, p=0.014). In the secretory phase of women diagnosed with UIF, a strong positive correlation was observed between *OPN* and *ITGAV* (Spearman's rho =0.738 p=0.037). As expected expression of *ITGAV* and *ITGB3* was very strongly correlated

in the secretory phase of the fertile group (Spearman's rho =0.900, p=0.037). No other significant correlations were detected.

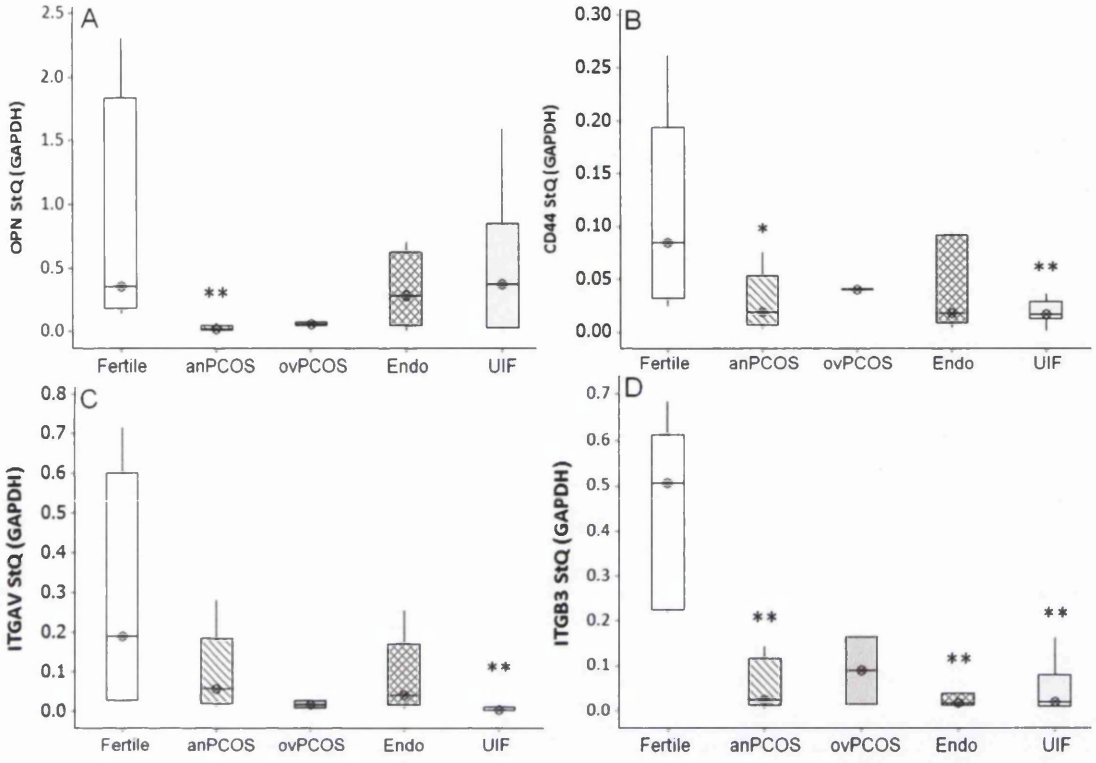

Figure 3-18 Secretory phase adhesion complex partner expression.

Quantitative PCR was conducted on total RNA reverse transcribed to cDNA in, fertile (n=6), anPCOS (n=13), ovPCOS (n=2), endometriosis (Endo) (n=9) and UIF (n=9) for (A) OPN, (B) CD44, (C) ITGAV and (D) ITGB3 mRNA expression. All starting quantity values are absolute and normalized against the GAPDH housekeeping gene. Significant variations in expression were observed between fertile and infertile groups for all genes analyzed. All genes showed a decrease in expression in some infertile groups when compared to the fertile group. * P≤0.05 ** P≤0.01

3.9 Summary

A summary (Table 3-4) of all findings in the three studies measuring RNA, intracellular and extracellular protein were utilized to explore the different expression patterns of the adhesion complex in the endometrium of infertile pathologies compared to fertile endometrium.

Genes	*OPN*				*CD44*				*ITGAV*	*ITGB3*
Pathology	mRNA	Glands	Lumen	Stroma	mRNA	Glands	Lumen	Stroma	mRNA	mRNA
AnPCOS	**Down-regulated p=0.007**	ns K-W p=0.3	ns K-W p=0.07	ns K-W p=1	**Down-regulated p=0.02**	ns pro phase K-W p=0.2	ns K-W p=0.8	ns K-W p=1	ns K-W p=0.2	**Down-regulated** p=0.003
OvPCOS	ns K-W p=0.9; p=0.4				ns K-W p=1	**Down-regulated** in sec phase **p=0.04**				ns p=0.08
Endometriosis				**Up-regulated** in pro phase **p=0.04**		ns pro phase K-W p=0.2				**Down-regulated** p=0.008
UIF				ns p=0.07	**Down-regulated p=0.008**			**Down-regulated** in pro phase **p=0.009** **Up-regulated in** sec phase **p=0.02**	**Down-regulated** p=0.002	**Down-regulated** p=0.03

Table 3-4 Summary of adhesion complex expression in each infertile group.

The expression at the mRNA and protein level broken down by compartment displayed by infertility group in comparison to the fertile group. Mann Whitney-U p values unless stated otherwise.

The results of this study indicate that expression differences in the adhesion complex exist in infertile pathology compared to fertile endometrium. Expression differences at the mRNA and protein level suggest that the adhesion complex may be a good candidate to explore infertility. Further work will be conducted to understand the regulation of these genes in fertile and infertile endometrium.

3.10 Discussion

In this study a detailed IHC analysis to investigate protein expression patterns was undertaken. It was demonstrated that the levels of OPN expressed in fertile women in the glandular compartment increased significantly in the secretory phase of the menstrual cycle compared to the proliferative phase. This is in agreement with previous studies (Franchi et al. 2008). CD44 expression in the glands was significantly up-regulated in the secretory phase when compared to the proliferative phase, which has been noted (Goshen et al. 1996). In the stromal compartment, CD44 expression in the secretory phase was decreased compared to the proliferative phase and again these findings have been noted previously (Albers et al. 1995). An important observation was that the levels of CD44 as measured by H-score were lower across all compartments when compared to OPN. Interestingly, the spatial distribution of OPN and CD44 differed in the three distinct cellular types. In glands and luminal epithelium OPN levels were higher than in the stroma, conversely, CD44 levels were higher in the stroma than the glands and luminal epithelium. In contrast to the IHC study mRNA levels of OPN and CD44 isolated from whole tissue samples were not significantly different between the two phases of the menstrual cycle (Figure 3-18) which is consistent with previous reports. This observation is likely due to the analysis not being conducted on the different component structures individually (DuQuesnay et al. 2009; Behzad et al. 1994). Although separating the epithelial cells from the stroma cells can be achieved, the limited amount of tissue collected in this study prohibited this and therefore lead to evaluation at the mRNA level of the glands, lumen and stroma simultaneously.

In anPCOS, little published literature exists that evaluates the expression of OPN and CD44 in the human endometrium by individual molecules. The findings in this study suggest that at the RNA level there appears to be differential expression of *OPN*, *CD44* and *ITGB3*, in whole biopsy tissues and that expression is decreased in anPCOS. It has been demonstrated previously that anPCOS women have decreased levels of αVβ3, although the study group were taking the therapeutic drug clomiphene citrate which may have influenced the expression (Apparao et al. 2002). Clomiphene citrate is a drug commonly used to stimulate ovulation in PCOS women. By blocking the effect of estrogen, other hormones such as FSH and LH increase to induce ovulation. Blocking estrogen signalling would also induce progesterone signalling, which has been shown to regulate αVβ3 expression (Apparao et al. 2001). The difference in expression of αVβ3 in the anovulatory PCOS groups in this study could suggest a role in regulation of these adhesion genes by ER, as these women do not ovulate and therefore ER continually influences the endometrial tissue.

OPN expression has been analysed previously in a cohort (n=10) of ovPCOS women, where the study illustrated that glandular and luminal OPN protein expression (measured by IHC) was significantly decreased compared to fertile women (DuQuesnay et al. 2009). Here we present data showing that OPN protein expression is similar in the luminal epithelium and glands of ovPCOS and fertile women. It is possible that the small sample number in each study and differences in mean age and sample collection timing (day of cycle) have resulted in these differing observations. Additionally, all biopsies were taken during the window of implantation (around day 21-22) in the previous study. In this study samples range from day 15-28 as these were the only samples available from the tissue archives. CD44 expression in the ovPCOS group showed that glandular expression was significantly decreased. OPN is thought to be secreted from the glands (Chaen et al. 2012) allowing it to form the adhesion complex with CD44 and αVβ3 (Singh and Aplin 2009). Therefore, glandular expression differences of OPN may have a

SWANSEA LIBRARY UNIVERSITY

significant consequence on the adhesion complex of OPN-CD44-αVβ3 in implantation.

This study presents data that support a trend of increased expression (non-significant) of OPN in the glands of both PCOS cohorts with no differences in CD44 expression compared to fertile women. This probably reflects functions of OPN other than regulating implantation. It has been described that neutralization of OPN with specific antibodies improves insulin sensitivity (Kiefer et al. 2010). A recent publication provided evidence that genetic OPN deficiency improves diet-induced insulin resistance (Nomiyama et al. 2007). In this context, a slight up-regulation of OPN may reflect the insulin sensitivity status of the PCOS patient's recruited. Insulin resistance is one of the features of the PCOS syndrome, among others like obesity which has also been linked with high OPN expression (Gómez-Ambrosi et al. 2007). Our patient cohort did not differ significantly in BMI, excluding this factor as an influence to OPN expression in these women. Further studies will clarify whether the observed changes in endometrial OPN expression correlate to the insulin sensitivity of patients.

In the endometriosis group, this study found that stromal expression of OPN was significantly increased in the proliferative phase and significantly decreased in the secretory phase when compared to the fertile group. This suggests a pattern of disrupted regulation throughout the menstrual cycle may occur in the endometriosis group. A study conducted by Cho indicated that at the mRNA level endometrial OPN was increased in endometriosis women when compared to fertile controls, although this was not observed when the data was split into proliferative and secretory phase expression. However, systemic levels of secreted OPN in blood plasma were significantly increased in both phases of the menstrual cycle when compared to fertile controls (Cho et al. 2009). Collectively this indicates that OPN levels are increased in women with endometriosis and this could be linked to inflammation. OPN has been shown to have a role in inflammatory diseases such as Crohn's disease, atherosclerosis, lupus and rheumatoid arthritis (Lund et al. 2009;

Uede 2011; Cho et al. 2009). Moreover, OPN has been associated with roles in cell migration, cell survival and metastasis. It has also been hypothesised that endometriosis may be caused by dysregulation of stem cell function through spreading of endometrial progenitor cells (Maruyama and Yoshimura 2012). Although endometriotic cells are not characterised by uncontrolled differentiation, they show some features of malignant tissues such as invasion, induction of metastasis and the ability to evade apoptosis. In this context, our data describing increased OPN expression in eutopic endometrium of endometriosis patients may reflect the migratory and anti-apoptotic properties of these cells in the ectopic lesions and supports a common progenitor cells origin (Laganà et al. 2013; Aznaurova et al. 2014).

In the secretory phase, *ITGB3* mRNA expression is down regulated in women with endometriosis when compared to fertile women in agreement with findings from González (González et al. 2006). This further indicates disrupted adhesion complex expression throughout the menstrual cycle. This could impact on the receptivity of the endometrium during the window of implantation. Lessey found that αVβ3 to be up regulated in the secretory phase of healthy cycling fertile women (Lessey 2002). This study also demonstrated that αVβ3 complex partner *ITGB3* was decreased in expression in the secretory phase of the menstrual cycle in all related infertile pathologies.

We hypothesise that differences in OPN and CD44 expression in PCOS and endometriosis pathologies could be related to inflammatory environments in these patient groups. Inflammation is present at the systemic and local levels and low-grade chronic inflammation and pelvic inflammatory disease are common in these two pathologies (Ruan and Dai 2009; González et al. 2006; Diamanti-Kandarakis et al. 2006; Weiss et al. 2009). In both pathologies inflammatory cytokines are present in the peritoneal fluid that surrounds the reproductive organs, effectively bathing the uterus in a pro-inflammatory environment (Halis and Arici 2004). This could affect how cytokines are regulated locally in addition to increasing the amount of

pro-inflammatory cytokines in the uterine environment. Obesity is common in patients with PCOS and it is a contributing factor to the disease, a BMI of 36 was noted in the ovPCOS group of the gene expression study. This association has been linked to insulin resistance, which has been observed in these women (Dhindsa et al. 2004). As described previously, several reports have shown that OPN is responsive to glucose, insulin resistance, obesity-induced adipose tissue inflammation and pro-inflammatory cytokines in animal models (Gong et al. 2009a; Nomiyama et al. 2007). In addition *CD44* has been described to be a target gene of WT1, a key transcription factor that mediates the decidualization process in the human uterus (Kim et al. 2011, Makrigiannakis et al. 2001; Anthony et al. 2003). Our group has recently published that WT1 targets the expression of genes in the uterine epithelial and stromal compartments and that WT1 expression is significantly downregulated in ovPCOS patients (Gonzalez et al., 2012). Accordingly we observed a statistically significant decrease of CD44 expression in ovPCOS glands suggesting a link between CD44 expresion and the WT1 signalling pathway and a role for CD44 in the decidualization process.

OPN and CD44 have not been studied extensively in patients with unexplained infertility. Here the novel observations that women diagnosed with unexplained infertility have significantly less *CD44* expression at the mRNA level and significantly more OPN expression in the stroma of the secretory phase endometrium has been made. In the stromal cells of the secretory phase CD44 protein expression was significantly down regulated in the proliferative phase and significantly up regulated in the secretory phase in the UIF group when compared to the fertile group. These differences at the protein level suggest that expression of CD44 may be altered throughout the menstrual cycle and functionally could lead to disrupted CD44 signalling in the stroma cells. The WT1 gene has been identified as having a key role in the decidualization process of the endometrial tissue (Makrigiannakis et al. 2001; Anthony et al. 2003). WT1 gene encodes the WT1 protein, a transcription factor that regulates the expression of many genes including CD44 (Kim et al. 2012). Although a specific role for CD44 during decidual transformation has not been

attributed its expression has been described in pregnant decidua implying a role for CD44 to sustain pregnancy. In this context, a significantly lower expression of CD44 may influence the successful decidualization of the endometrium and the immunological dialogue between maternal and embryo tissues (endometrium/blastocyst) resulting in poor maternal support of the embryo, poor placentation and ultimately infertility. This is further supported by our data at the mRNA level. In the UIF group the adhesion complex expression at the mRNA level was significantly decreased in the secretory phase; *CD44* was decreased 5-fold, *ITGAV* was decreased 48-fold and *ITGB3* 26-fold compared to the fertile women. The decreased levels of *ITGAV* and *ITGB3* in UIF are consistent with previous observations showing integrin αVβ3 was significantly decreased in expression at the protein level in unexplained infertility (Tei et al. 2003).

The secreted protein study was conducted in order to correlate data with the IHC study. A study that used an intrauterine device to collect endometrial secretions found that secreted OPN increased in the secretory phase of the menstrual cycle when compared to the proliferative phase (Wolff, Thomas Strowitzki, et al. 2001). As OPN is a linker molecule between αVβ3 and CD44 examining the secreted levels provided information on the levels of OPN that could become functional components of the protein complex involved in recruiting the trophoblast to the endometrium. If a profile of secreted OPN could be built for each pathology it could then be possible to develop this technique for use as a less invasive diagnostic technique using uterine flushing's. In this pilot study decreased levels of OPN were detected in PCOS and UIF samples. However, due to access to limited numbers of samples these preliminary observations were not shown to be significant.

Of note is the imbalance of OPN and CD44 expression in the infertile pathologies included in this study. As OPN can only bind to the endometrial epithelium via αVβ3 or CD44, disrupted CD44 expression in the luminal epithelium cells combined with disrupted glandular secretion of OPN could lead to the inability of the αVβ3-OPN-CD44 complex to form between the embryo and endometrial epithelia. OPN and

CD44's interaction on the surface influences signalling patterns (autocrine and paracrine signalling) for cell survival, cell proliferation, homing and migration (Bellahcène et al. 2008). Altered expression of OPN and CD44 could result in these signalling events being disrupted and perturbation of cell homeostasis leading to increased proliferation, migration, cell survival, poor embryo recognition and deficient endometrial differentiation, all ultimately leading to infertility and poor pregnancy outcome.

The work conducted in this chapter indicates that the expression of the αVβ3-OPN-CD44 adhesion complex components is altered in infertile pathologies compared to fertile endometrium. These differences could be a result of different hormone, metabolite and cytokine expression described for these pathologies which all have an inflammatory component. Therefore, an *in vitro* model system was employed to examine the effects of hormones (Chapter 4) and glucose and cytokines (Chapter 5) on the adhesion complex components expression in the endometrium.

Chapter 4

Hormonal regulation of adhesion complex components

4.1 Introduction

The proposed functions of OPN to form an adhesion complex with CD44 and αVβ3, and adhere the blastocyst to the endometrial lining make it an excellent candidate to study in terms of fertility. Expression of this adhesion complex peaks on the endometrial epithelial surface during the window of implantation, where the correct hormone expression could be important to its regulation (Figure 1-5). Regulation of OPN by sex steroid hormones has been investigated in a diverse range of human and animal tissues such as the ovine uterus (G. Johnson et al. 2000), murine uterus (Peyghambari et al. 2010), bovine uterus (Johnson et al. 2003) and human uterine tissue (Lessey 2003; Brown et al. 1992; Qu et al. 2008). It has been shown in renal tissue of male rats that testosterone promotes kidney stone formation, through suppression of OPN. Conversely, in female rats estrogen appeared to inhibit urinary stone formation by increasing OPN expression in the kidneys (Yagisawa et al. 2001). The binding partner of OPN, CD44 and its many variants, is also expressed in a range mammalian of tissues (Section 1.7.6) however regulation of its expression by sex steroid hormones in normal tissues has only been studied in the human endometrium. Expression of CD44 has been characterised in the menstrual cycle of healthy women (Goodison et al. 1999; Saegusa et al. 1998; Koo et al. 2013; Afify et al. 2005). The expression of αVβ3 has also been extensively studied in the endometrium, with the β3 subunit in particular being regarded as a marker of implantation (Section 1.8.3).

There is evidence to suggest that estrogen and progesterone are key regulators of OPN and CD44 in the endometrium. OPN has been found to be expressed throughout the duration of the menstrual cycle, with low expression patterns observed in the proliferative phase, and high expression in the secretory phase (Wolff, Thomas Strowitzki, et al. 2001). Micro-array analysis conducted in three independent studies all found OPN expression to be significantly increased in the mid-secretory phase in endometrial tissue when compared to the early secretory phase (Carson et al. 2002; Kao et al. 2002; Riesewijk 2003). A potential

consequence of these observations is that OPN is involved in implantation. Spatial distribution of OPN expression is localized to the glandular, luminal and stromal tissue. In addition, OPN expression was found to be increased in endometrial leukocytes and in uterine secretions (Wolff, Thomas Strowitzki, et al. 2001). Again, expression was increased in the mid- and late-secretory phase of the menstrual cycle in healthy cycling women (Apparao et al. 2001). CD44 expression has also been reported throughout the endometrium (Behzad et al. 1994). In the healthy cycling endometrium the expression pattern of CD44 was found to be similar to that of OPN, although CD44 is additionally expressed in the early secretory phase. CD44 has many isoforms, and recent studies have found and focused on the expression of CD44v6 in the endometrium (Yaegashi et al. 1995; Afify et al. 2005; Poncelet et al. 2002). There is however evidence in the literature that other isoforms are also expressed in the endometrium. CD44v3 expression has also been observed in the endometrium (Saegusa et al. 1998). Whereas CD44v7-8 isoform variants have been shown to be expressed on the trophoblast surface (Goshen et al. 1996).

The correct expression of these molecules could be key in the receptivity of the endometrium; infertility could therefore be caused by ovarian dysfunction where disrupted menstrual cycles could reduce endometrial receptivity. An example of this is amenorrhea; when a woman of reproductive age does not menstruate. The primary cause has been linked to a lack of ovulation. A sub group of women who suffer from PCOS experience problems with ovulation. Disrupted hormonal expression has been linked to secondary causes of amenorrhea. It has also been found to cause very heavy and prolonged menses in addition to abnormal blood clotting in some women, this is associated with dysmenorrhea (Proctor and Farquhar 2006). This is a common complaint in women who are diagnosed with endometriosis, which is often associated with pelvic pain. Therefore the correct balance of E_2 and P_4 signalling in the endometrium is crucial for maintenance of tissue morphology, ovulation and the secretion of cytokines and proteins from the endometrial surface to prepare for embryo implantation.

E_2 and P_4 are the ligands for the ER and PR receptor. These nuclear receptors contain DNA binding domains that are capable of interacting with receptor specific DNA promoter elements to enhance or repress transcription of a gene (Section 1.9.2). In this chapter, the role of E_2 and P_4 signalling through their respective steroid hormone receptors is investigated using endometrial epithelial cell line models and treatment regimes representative of healthy cycling women. Of particular interest is the effect on the expression and location of OPN and CD44 during the window of implantation. OPN and CD44 expression following treatment with physiologically relevant concentrations of E_2 and P_4 was monitored. CD44 protein expression patterns were detected using IHC. Additionally, secreted OPN protein levels were established to determine its expression in relation to the adhesion complex as a linker molecule, at the basal levels and in response to E_2 and P_4 treatment. Finally, the direct involvement of ERα in the regulation of these expression patterns was monitored using ChIP.

The work presented in this chapter aims to establish an appropriate cell line model using physiological E_2 and P_4 concentrations to mimic conditions in healthy cycling women, to determine the regulation of OPN and CD44 by these hormones, and in addition to understanding the role of ERα in the expression patterns of these genes in Ishikawa and Heraklio cells.

4.2 Results

4.2.1 Basal expression levels in endometrial cell lines

To determine which were the most appropriate cell models for the regulation of *OPN* and its adhesion complex partners, the basal expression of *OPN*, *CD44* and αVβ3 was investigated in the epithelial endometrial cell lines Ishikawa, Heraklio, HEC-1A, HEC-1B and RL925. A suite of techniques was used to determine the basal expression level of *OPN* mRNA, tissue localized protein and secreted proteins. *CD44* expression was determined at the mRNA and protein level. The expression of αVβ3 was investigated at the mRNA level by studying *ITGAV* and *ITGB3*. To quantify the

basal gene expression levels of *OPN*, *CD44* and *ITGAV* and *ITGB3*, total RNA was extracted from the endometrial epithelial cells Heraklio, Ishikawa, HEC-1A, HEC-1B and RL925. All five endometrial epithelial cell lines expressed OPN and its adhesion complex partners (Figure 4-1, panels A-E). As anticipated, expression patterns differed between the cell lines, with Heraklio displaying the highest expression levels of each tested gene relative to the other cell lines. The Ishikawa and Heraklio cell lines were chosen for further investigations due to the differential expression of genes of interest between the cell lines. These cell lines were selected based on their relative expression levels of the adhesion complex components. The cell lines are established in the literature to differentially express ERα (and ERβ). These cell lines are therefore useful models to relate to endometrial pathology where high expression of the adhesion complex components (Heraklio) is present but infertility persists where levels of *OPN* in Ishikawa resemble the fertile women. The difference in ER receptor expression allows for investigations into regulation of the adhesion complex components by ER.

The highest level of basal (untreated) *OPN* mRNA expression was in Heraklio cells (Figure 4-1). A significant 1000-fold higher expression of *OPN* was observed in Heraklio cells compared to Ishikawa cells ($p<0.01$). Hec-1A and Hec-1B cells also exhibited higher *OPN* levels than Ishikawa cells; 274 and 556-fold greater respectively ($p<0.001$; $p<0.05$). RL925 cells expressed significantly less *OPN* compared to Ishikawa ($p\leq0.05$).

CD44 was found to be expressed most abundantly in Heraklio cells (Figure 4.1B). When compared to Ishikawa expression was 11-fold higher ($p<0.01$). *CD44* expression in the HEC-1A and HEC-1B cells was 3 and 4-fold higher than Ishikawa ($p<0.01$; $p<0.05$). Expression of *CD44* was also higher in RL925 compared to Ishikawa ($p<0.01$).

The highest expression level of *ITGAV* was observed in Heraklio cells (Figure 4.1C), where expression levels were 2.4-fold higher than in Ishikawa ($p<0.01$). HEC-1A and RL925 cells had similar basal expression levels of *ITGAV* to Ishikawa cells ($p>0.05$).

HEC-1B cells had a 3-fold lower levels of *ITGAV* expression compared to Ishikawa ($p \leq 0.05$).

ITGB3 was expressed at the greatest level in the Heraklio cells; when compared to Ishikawa cells the expression was 12-fold higher ($p < 0.01$) (Figure 4.1D). HEC-1A cells showed no significant difference in *ITGB3* expression pattern compared to Ishikawa cells ($p > 0.05$). *ITGB3* expression was significantly lower in both HEC-1B and RL925 cells (4 and 2054-fold respectively) compared to Ishikawa cells ($p < 0.001$; $p < 0.001$).

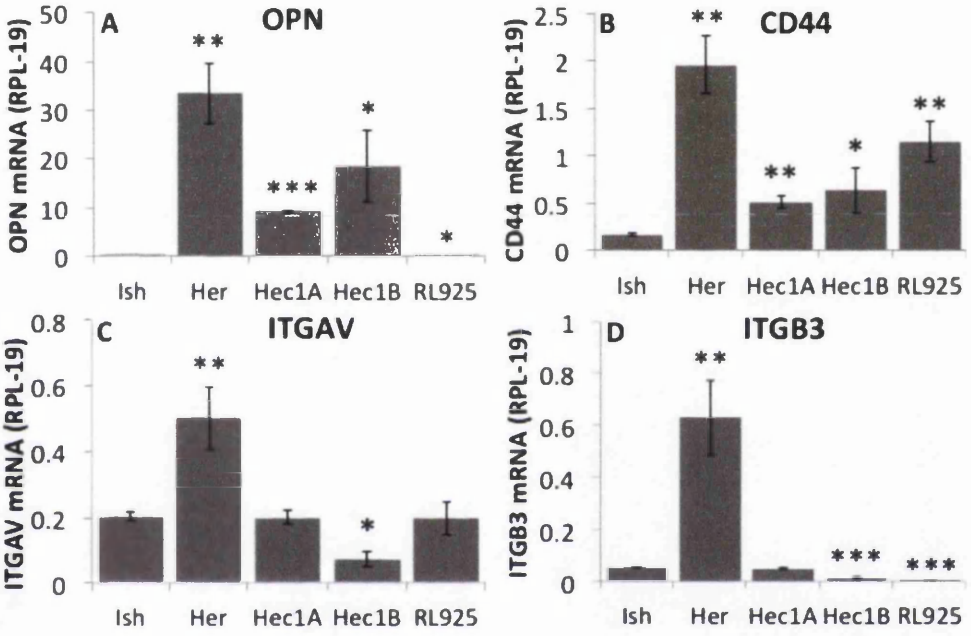

Figure 4-1 Basal OPN and adhesion partner gene expression in EEC lines.

Quantitative PCR was conducted to measure basal gene expression in absolute starting quantities of OPN, CD44, ITGAV and ITGB3. Analysis was conducted in five ECC lines (A) Ishikawa, (B) Heraklio, (C) HEC-1A, (D) HEC-1B and (E) RL925. All five cell lines showed variable expression levels of the four target genes. Values are average and SD. Statistical analysis of the data was performed using a Student's t-test (e.g. OPN cell line X Vs. OPN cell line Ishikawa). *, P≤0.05, **, P≤0.01 and ***, P≤0.001 are considered significant. Results are representative of three biological repeats.

4.2.2 Basal expression of osteopontin isoforms

The expression of *OPNs* five splice isoforms at the mRNA level has not been previously characterized in the human endometrium. To assess if the differential

expression of *OPN* observed between Ishikawa and Heraklio was due to differences in the expression of *OPN* splice isoforms, each was measured using primers designed to specifically amplify each isoform individually (Figure 4-2). The expression patterns of the individual isoforms were very similar in both cell lines, despite Heraklio cells expressing significantly higher amounts of each isoform, Ishikawa is graphed separately to emphasise the difference in scale of expression (Figure 4-2B). Isoform D was expressed at the highest level in both cell lines. Isoform B had the second highest expression in both cell lines. Levels of isoform C and E were low in both cell lines; both isoforms about 20-fold less than isoform A. Due to the similarity in the ratio of isoform expression pattern observed between the cell lines primers were designed spanning a region common to all five isoforms in order to evaluate total *OPN* expression in all subsequent experiments.

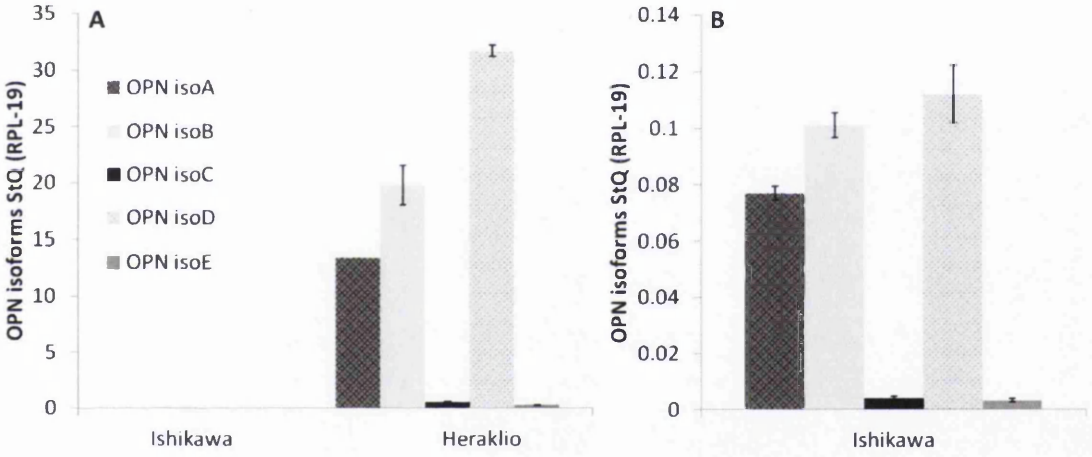

Figure 4-2 Absolute starting quantities of OPN splice isoforms in Ishikawa and Heraklio cells.

Quantitative PCR was used to measure basal gene expression of OPN variants using isoform specific primers to amplify OPN isoforms A-E in (A) Ishikawa and Heraklio (B) Ishikawa alone. Values are average and SD. Statistical analysis of the data was performed using a Student's t-test (Isoform X Ishikawa Vs. Isoform X Heraklio). No significant differences in the isoform expression pattern were observed between the cell lines.

4.2.3 Basal osteopontin protein expression

Immunohistochemistry and ELISA were conducted to assess the cellular and secreted levels of OPN protein in Ishikawa and Heraklio cells (Figure 4-3). OPN staining in Ishikawa cells appeared strong in the nucleus and cytoplasm compared to Heraklio cells (Figure 4-3A,B). Ishikawa cells exhibited significantly more nuclear and cellular OPN at the basal level when compared to Heraklio cells ($p<0.001$) (Figure 4-3C). The level of OPN secreted by the cells when in culture was determined using ELISA. Heraklio cells secreted 370-fold more OPN than Ishikawa cells ($p>0.01$). Secreted OPN levels in Heraklio cells measured 741 ng/mL of OPN, compared to 2 ng/mL in Ishikawa cells (Figure 4-3D).

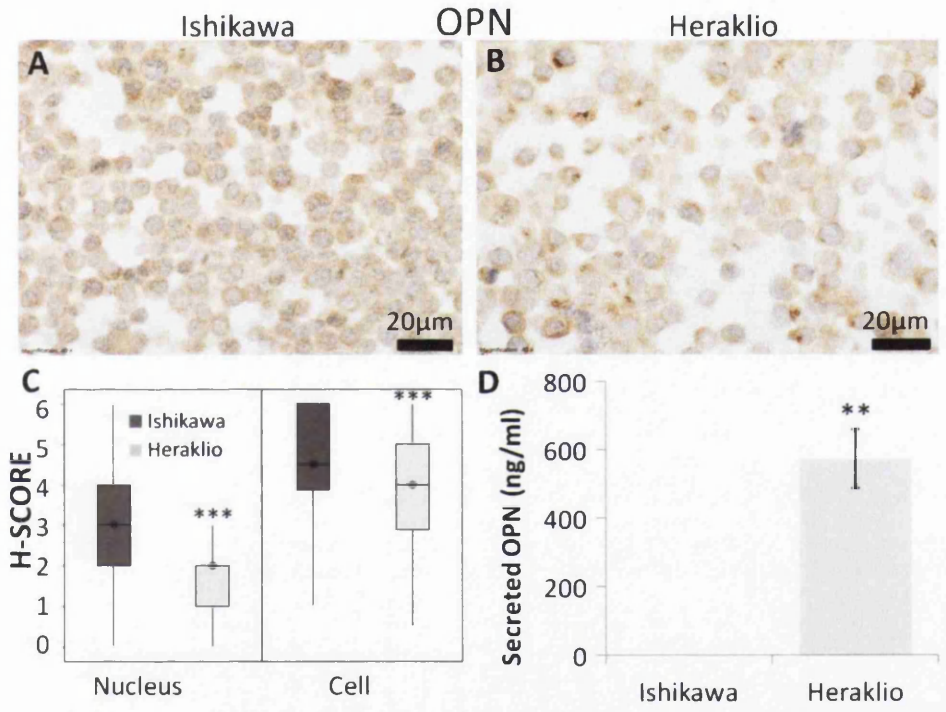

Figure 4-3 Basal expression of OPN in the Ishikawa cell line.

IHC stained slides for OPN (A) Ishikawa and (B) Heraklio cells. Magnification, X40, black scale bar represents 20µm. (C) Nuclear OPN was increased in Ishikawa (H = 3) compared to Heraklio (H = 2). Cellular component OPN expression increased in Ishikawa (H = 4.5) compared to Heraklio (H = 4). (D) Secreted OPN, Heraklio cells secreted 370-fold more OPN protein compared to Ishikawa cells ($P<0.01$). Values are average and SD. Statistical analysis of the data was performed using a Student's t-test (Ishikawa Vs. Heraklio). **, $P\leq0.01$ and ***, $P\leq0.001$ are considered significant.

OPN expression measured at the mRNA level correspond with those found at the secreted level for Ishikawa and Heraklio. The intracellular levels are very similar between the cell lines and do not reflect this difference in expression. Thus, for the remainder of the experiments secreted OPN was used as a measure of protein expression.

4.2.4 Basal CD44 protein expression

Immunohistochemistry was conducted on cell lines to measure the basal levels of CD44 protein expression (Figure 4-4). CD44 staining in Ishikawa (Figure 4-4A) was less abundant than in Heraklio (Figure 4-4B) where expression was clearly identified around the cell membrane. H-SCORE analysis showed that Heraklio CD44 expression (H = 8) was significantly higher than in Ishikawa cells (H = 2; $p<0.05$) (Figure 4-4C).

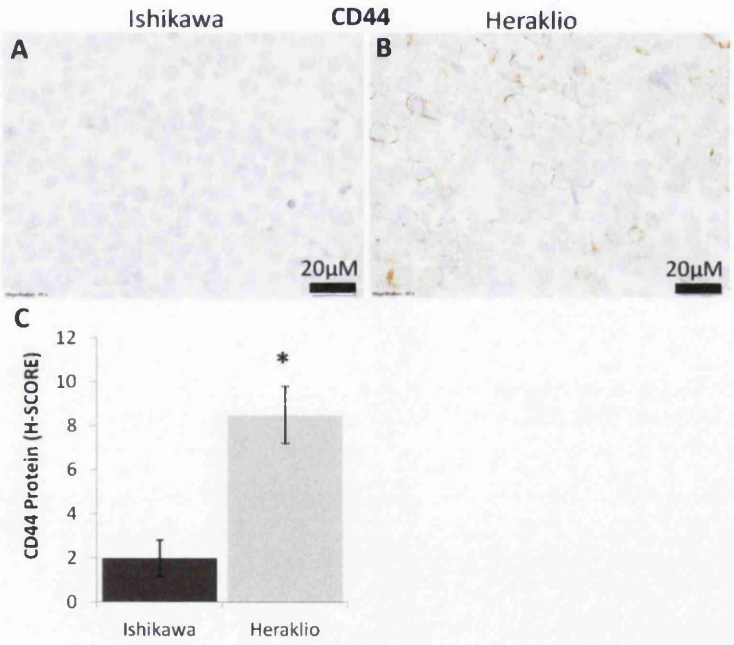

Figure 4-4 Basal expression of CD44 in the Ishikawa cell line.

IHC stained slides for CD44 on (A) Ishikawa and (B) Heraklio cells. Magnification, X40, black scale bar represents 20μm. (C) Cellular CD44 was 4-fold lower in Ishikawa (H = 2) compared to Heraklio (H = 8). Values are average and SD. Statistical analysis of the data was performed using a Student's t-test (Ishikawa Vs. Heraklio). *, P≤0.05 **, P≤0.01 and ***, P≤0.001 are considered significant.

4.3 *Hormonal regulation of osteopontin, CD44 and integrin αVβ3*

Having established the basal expression levels for the three target molecules at the mRNA and protein levels, the hormonal regulation of these molecules was investigated. To better understand any hormonal response, hormone receptor expression patterns of *ERα*, *ERβ* and *PR* were measured at the mRNA level in both cell lines (Figure 4-5). *ERα* expression was undetectable in Heraklio cells compared to Ishikawa cells ($p \leq 0.05$). *ERβ* expression was significantly higher (2-fold) in Heraklio than Ishikawa ($p \leq 0.05$). PR expression was 12-fold lower in Heraklio cells compared to Ishikawa cells ($p \leq 0.05$). This confirms the ERα negative status of Heraklio and suggests that *ERβ* may play more of a role in signalling in this cell line therefore any E_2 responses will be attributed to *ERβ* in this cell line. Therefore, for the remainder of the study, the role of *ERα* in the regulation of the adhesion complex components will be conducted using Ishikawa as a model for ERα +ve expression and Heraklio as ERα -ve expression. Ishikawa cells had more prominent expression of PR than Heraklio cells ($p \leq 0.05$).

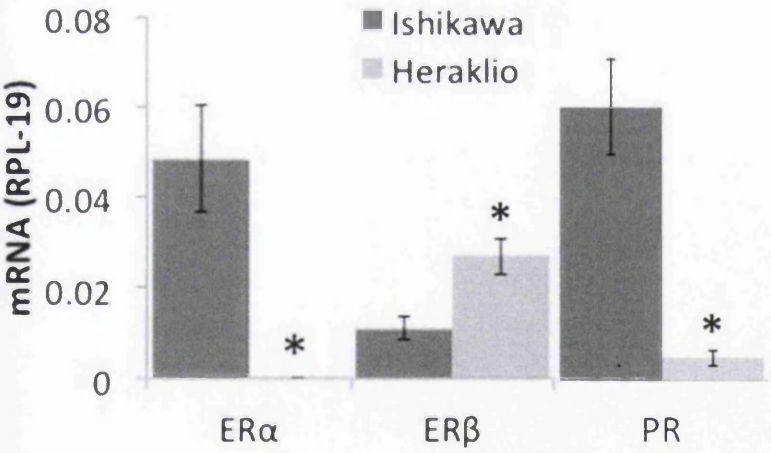

Figure 4-5 Basal hormone receptors levels in Ishikawa and Heraklio.

Quantitative PCR was conducted to measure basal gene expression in absolute starting quantities of ERα, ERβ and PR in Ishikawa and Heraklio cells. Significant differences in each hormone receptor were observed between Ishikawa and Heraklio cells. Values are average and SD. Statistical analysis of the data was performed using a Student's t-test (Ishikawa Vs. Heraklio). *, $P \leq 0.05$, was considered significant.

4.3.1 Hormonal regulation models

During the secretory phase of the menstrual cycle P_4 expression is dominant with reduced expression of E_2. In order to model *in vitro* the effect of E_2 and P_4 on the regulation of OPN and CD44 during the secretory phase, two *in vitro* culture models were established. The first model tested involved treating cells with E_2 (10nM), P_4 (100nM) or E_2 and P_4 (10nM; 100nM) in combination. A 48hr treatment period was used to imitate the secretory phase window of implantation. First, to establish the effectiveness of hormonal treatments on ER and PR signalling, downstream target genes of both signalling pathways were measured in response to estradiol and progesterone treatment.

GREB1 is a gene that is activated early in estrogen receptor response to E_2 and expression has been found in hormone responsive tissues (Hnatyszyn et al. 2010; Bourdeau et al. 2004; Stossi et al. 2004). *AREG* is a progesterone regulated paracrine growth factor that is increased in response to PR receptor signalling (Khan et al. 2012; Byun et al. 2008). *GREB1* expression in Ishikawa cells increased by 8-fold following treatment with E_2, and 4-fold with E_2+P_4 in combination ($p<0.01$; $p<0.01$) (Figure 4-6). Expression of *AREG* was significantly increased 4.8 and 2.4-fold following treatment with P_4 alone and E_2+P_4 ($p<0.01$). In Heraklio cells, *GREB1* expression was significantly increased by 5.4-fold after E_2 treatment and increased by 4-fold after E_2+P_4 ($p<0.01$). Expression levels of AREG in Heraklio cells increased 3-fold following P_4 treatment and 2-fold following E_2+P_4 treatment ($p<0.01$; $p<0.01$). After establishing that hormone receptor signalling was active in Ishikawa (ERα +ve) and Heraklio cells (ERα -ve), the hormonal regulation of OPN and its adhesion partners was investigated. Gene expression levels in Ishikawa (Figure 4-7) cells were analyzed in response to the treatment with physiological concentrations of E_2 and P_4. Both cell lines, despite differing ER expression, responded similarly to estradiol and progesterone stimulation of known ER and PR target genes.

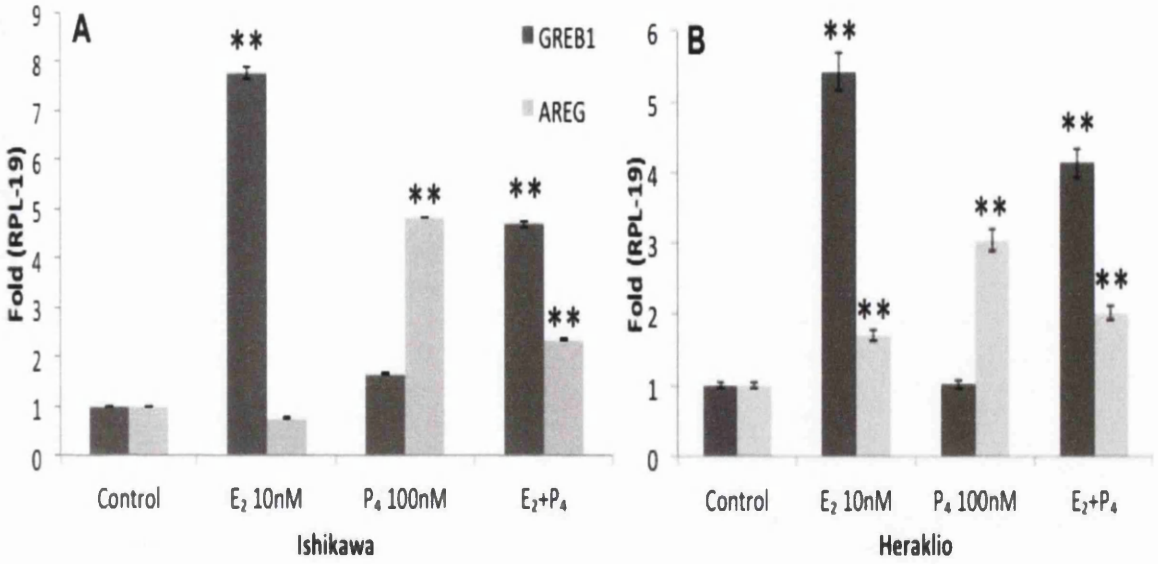

Figure 4-6 Gene expression of GREB1 and AREG in response to hormones.

Quantitative PCR was conducted to measure hormone stimulated fold increases in GREB1 and AREG in Ishikawa and Heraklio cells. Significant differences in the expression levels were observed after treatment with hormones compared to control. Values are average and SD. Statistical analysis of the data was performed using a Student's t-test (control Vs. treatment). **, P≤0.01, was considered significant.

4.3.2 Secretory phase model

Due to the very similar expression patterns observed in both cell lines the secretory phase model was initially evaluated using only Ishikawa. In Ishikawa cells (ERα +ve) *OPN* expression was significantly increased 2.6-fold in response to E_2 treatment alone ($p<0.001$) (Figure 4-7). P_4 treatment alone increased *OPN* expression 1.6-fold and when the two hormones were combined an additive effect was observed with a 3.3-fold increase in expression ($p<0.001$; $p<0.001$ respectively). Similarly, *CD44* expression increased with all three treatments, expression increased 2.3-fold in response to E_2 alone and 3-fold in response to P_4 ($p<0.001$; $p<0.001$ respectively). A 4-fold increase in *CD44* expression was observed with the combined E_2 and P_4 treatment ($p<0.001$). A similar response was observed with *ITGAV* expression where a 2-fold increase was observed after treatment with E_2 alone ($p<0.01$). When treated with P_4 alone a 3-fold increase was noted ($p<0.001$). The combination of

both hormones increased *ITGAV* expression 9-fold ($p<0.001$). ITGB3 expression was increased in response to E_2 treatment by 1.3-fold ($p>0.05$). A further 2.2-fold in response to P_4 treatment ($p<0.001$) and 3.6-fold in response to the combination of E_2 and P_4 treatment in Ishikawa cells (ERα +ve) ($p>0.01$).

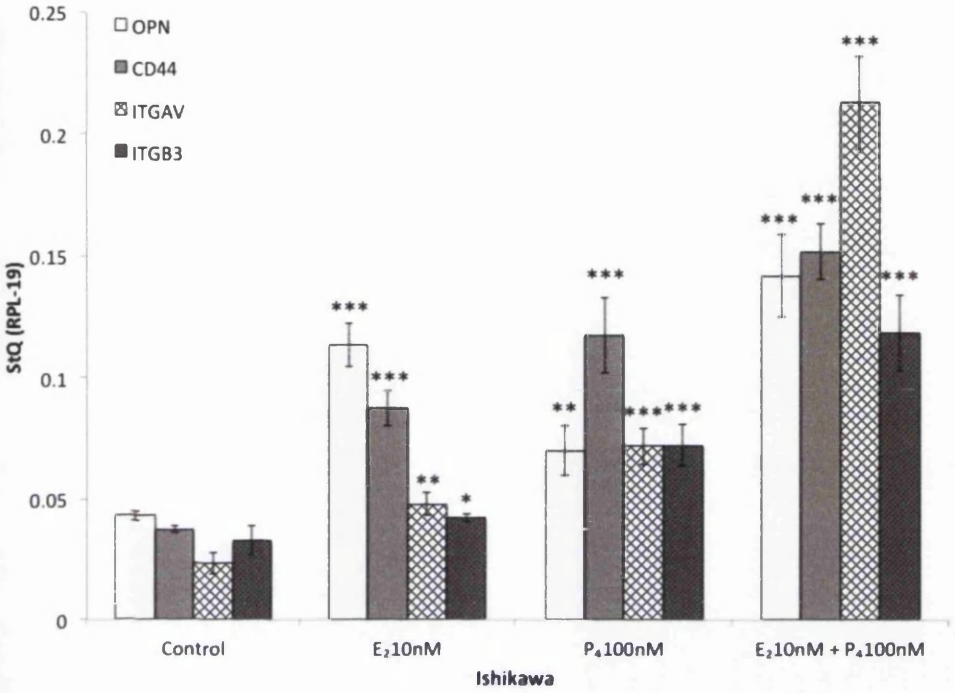

Figure 4-7 Gene expression of the adhesion complex in response to steroid hormone treatments in Ishikawa cells (ERα +ve).

Quantitative PCR was conducted to measure hormone stimulated levels of OPN, CD44, ITGAV and ITGB3 in Ishikawa cells (ERα +ve) after 48hrs. Significant differences in each gene occur between treatment with hormones and the control. Values are average and SD. Statistical analysis of the data was performed using a Student's t-test (control Vs. treatment). *, P≤0.05 **, P≤0.01, ***, P≤0.001 was considered significant.

4.3.2.1 Secreted osteopontin in response to hormone treatments

To determine the secreted levels of OPN in response to hormone treatments an ELISA was conducted using the samples collected after 48hrs. IHC was not conducted on treated cells as the basal levels of OPN in both cell lines was high (H = 5-6) therefore detecting any increases from treatment would be difficult (

). Additionally the secreted levels detected reflected the differences found at the mRNA level (Figure 4-7). Ishikawa cells showed no increase in OPN expression following treatment with E_2 or P_4 treatment (Figure 4-8). However when E_2+P_4 were combined, levels of secreted OPN increased significantly 1.5-fold ($p \leq 0.05$).

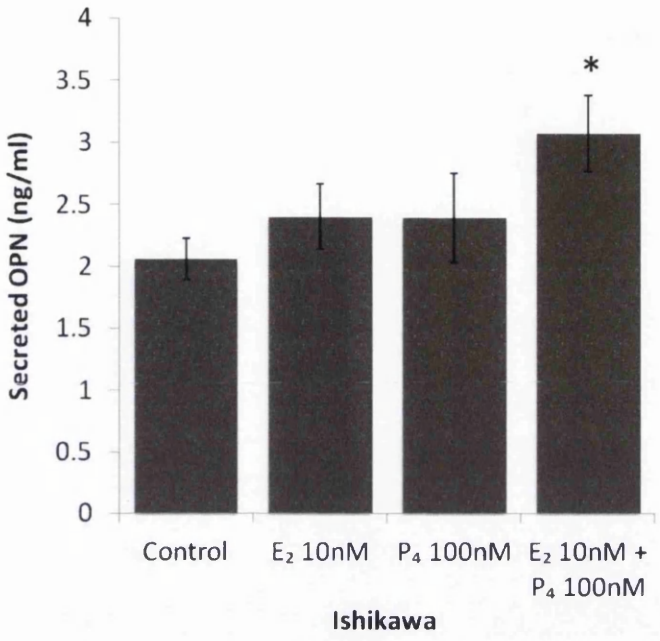

Figure 4-8 Secreted OPN levels secretory phase model in Ishikawa (ERα +ve).

ELISA was conducted to measure sex steroid hormone stimulated levels of expression of OPN in Ishikawa cells (ERα +ve). Values are average and SD. Statistical analysis of the data was performed using a Student's t-test (control Vs. treatment). *, P≤0.05 was considered significant.

4.3.2.2 CD44 protein expression

CD44 protein expression was assessed by IHC in response to sex steroid hormone treatments (Figure 4-9). CD44 staining in Ishikawa cells (ERα +ve) was stronger in response to E_2+P_4 treatment. E_2 treatment increased CD44 protein expression 2-fold however this increase was not significant ($p>0.05$). P_4 treatment increased CD44 expression 2.8-fold however this increase was not significant ($p>0.05$).

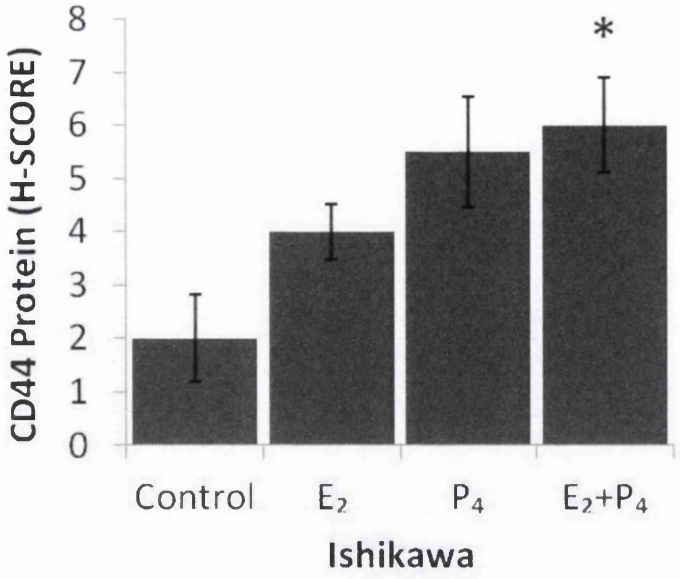

Figure 4-9 Ishikawa (ERα +ve) expression of CD44 protein in response to sex steroid hormone stimulation after 48hrs.

IHC was used to semi-quantitatively assess the effect of hormones on CD44 protein expression. CD44 protein H-SCORE for Ishikawa cells (ERα +ve indicated that CD44 expression increased with treatment regimes however only the treatment with E_2+P_4 was significant. Values are average and SD. Statistical analysis of the data was performed using a Student's t-test (control Vs. treatment). *, P≤0.05 was considered significant.

4.3.3 Estrogen priming model

An alternate model that aimed to mimic *in vitro* the complete menstrual cycle from proliferative to secretory phase, involving E_2 and P_4 signalling prior to and during the window of implantation was investigated. This was done in order to determine whether early signalling effects in the cycle had an important role in regulating the expression of the adhesion complex components. Ishikawa cells (ERα +ve) were first primed with E_2 (10nM) for a 24hr period and then treated with P_4 (100nM) or E_2+P_4 (10nM;100nM) for a further 48hrs. This treatment regime attempted to recreate the up-regulation in E_2 signalling in the proliferative phase of the menstrual cycle before P_4 signalling becomes predominant in the secretory phase (Figure 1-5). Treatment with P_4 post priming represents the physiological E_2 and P_4 levels in the early secretory phase. Treatment with E_2+P_4 post priming was representative of the

mid- and late- secretory phase. The adhesion complex gene targets were analyzed in the estrogen primed model in Ishikawa cells (ERα +ve) previously shown to respond to hormones (Figure 4-10). *OPN* expression increased 1.3-fold after E_2 priming alone and 1.2-fold after E_2 priming followed by 100nM of P_4, however these expression changes were not significant ($P>0.05$; $P>0.05$ respectively). A 1.3-fold increase in *OPN* was observed after E_2 priming and the combination treatment of E_2+P_4, which was not significant ($p>0.05$). *CD44* expression was significantly increased by all treatment regimes. *CD44* was increased 1.7-fold by E_2 priming alone ($P<0.01$). A 1.9-fold increase was observed after treatment to E_2 priming plus 100nM of P_4 ($p<0.01$). After E_2 priming and the combination of E_2 and P_4 a significant 2.2-fold increase in *CD44* expression was observed ($p\leq0.05$). *ITGAV* expression in Ishikawa cells (ERα +ve) was increased in the E_2 priming model. E_2 priming alone increased *ITGAV* expression 1.2-fold, however this was not significant ($p>0.05$). E_2 followed by P_4 treatment, significantly increased *ITGAV* expression 2.5-fold ($p<0.01$). E_2 combined with P_4 following E_2 priming significantly increased ITGAV expression 1.6-fold ($p<0.01$). *ITGB3* expression is unchanged with E_2 priming alone however after exposure to 100nM of P_4 *ITGB3* expression is significantly increased 1.7-fold ($p<0.01$). When E_2 and P_4 were combined after priming *ITGB3* expression was significantly decreased 2-fold compared to the control ($p<0.01$).

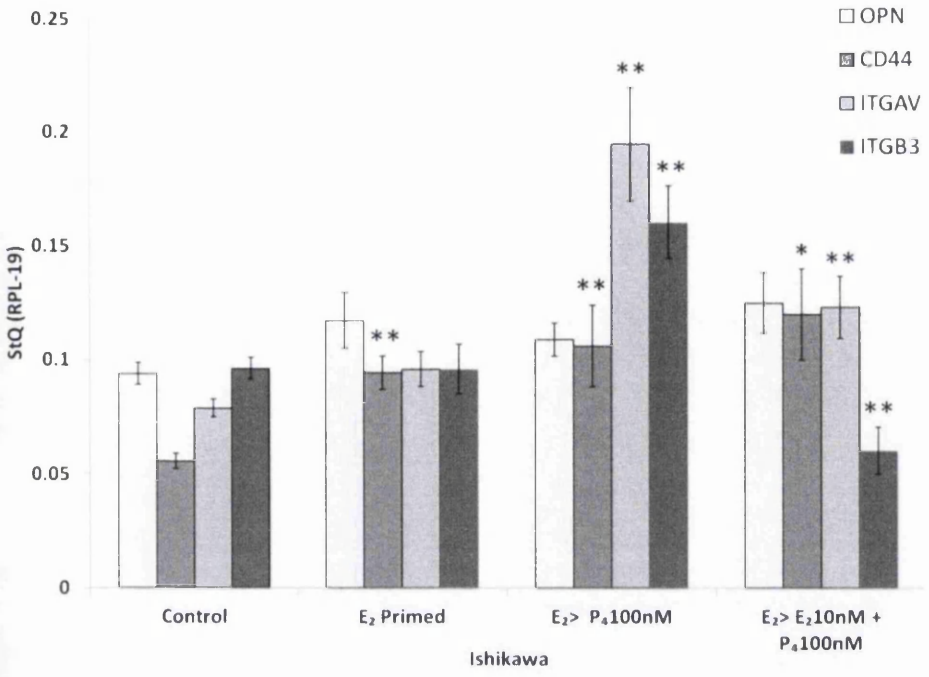

Figure 4-10 Ishikawa cell (ERα +ve) gene expression in response to E_2 primed model.

Quantitative PCR was conducted to measure hormone stimulated levels of expression of OPN, CD44, ITGAV and ITGB3 in Ishikawa cells after 72hrs. Significant differences in each gene occur between treatment with hormones and the control. Values are average and SD. Statistical analysis of the data was performed using a Student's t-test (control Vs. treated). *, P≤0.05 **, P≤0.01, was considered significant.

4.3.3.1 Secreted osteopontin expression

Cells were first primed with E_2 for 24hrs and then exposed to E_2 or P_4 alone or in combination for 48hrs (Figure 4-11). Secreted OPN, was measured by ELISA and was found to have increased 1.2-fold in response to treatment with E_2 priming alone ($p<0.001$). Post priming treatment with P_4 alone for 48hrs resulted in a 1.2-fold decrease in secreted OPN expression ($P<0.001$). No significant changes were observed in secreted OPN with the combination of E_2+P_4 after priming ($p>0.05$).

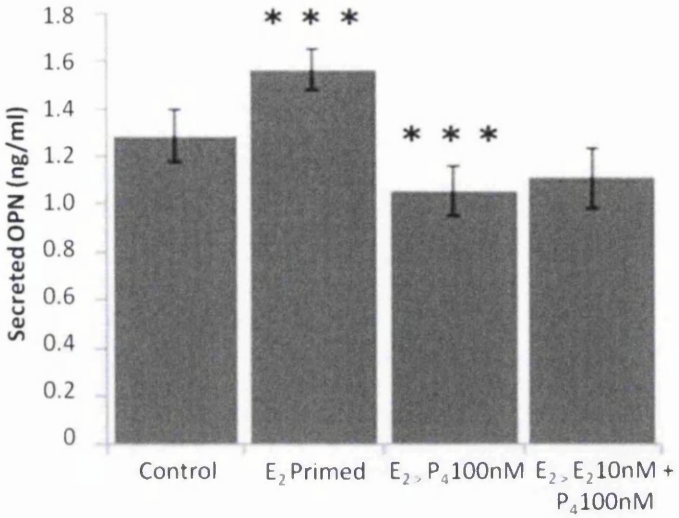

Figure 4-11 Secreted OPN levels in response to E_2 primed model in Ishikawa.

The ELISA technique was conducted to measure hormone stimulated levels of expression of OPN in Ishikawa cells. Significant differences in each gene occur between treatment with hormones and the control. Values are average and SD. Statistical analysis of the data was performed using a Student's t-test (control Vs. treated). *, P≤0.05 **, P≤0.01, was considered significant.

4.3.3.2 Intracellular CD44 expression

CD44 protein expression was assessed by IHC in response to sex steroid hormone treatments (Figure 4-12). CD44 staining in Ishikawa (ERα +ve) was stronger in response to all treatments, however these expression changes were not significant ($p>0.05$). In response to E_2 priming CD44 expression increased 1.4-fold ($H = 8.5$) when compared to the control ($p>0.05$). Treatment with P_4 after E_2 priming increased CD44 expression 1.3-fold ($H = 8$), however treatment with E_2+P_4 after E_2 priming further increased CD44 expression 1.6-fold ($H = 9.5$) ($p>0.05$; $p>0.05$).

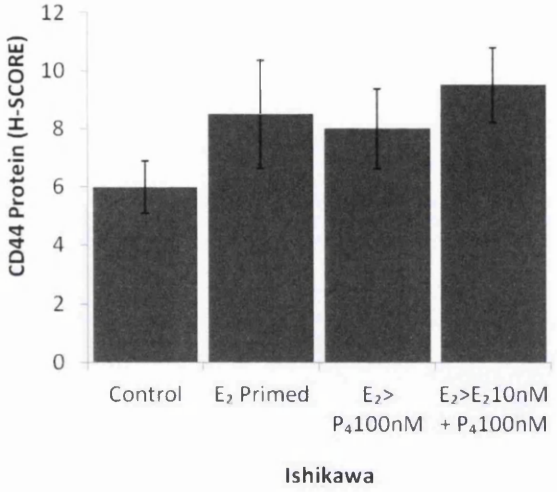

Figure 4-12 CD44 protein expression in Ishikawa cells (ERα +ve) in response to E_2 primed model.

IHC was used to semi-quantitatively assess the effect of hormones on CD44 protein expression. Values are average and SD, statistical analysis of the data was performed using a Student's t-test (control Vs. treatment) data are representative of three biological repeats.

4.3.4 Heraklio (ERα -ve) hormone regulation

The Ishikawa (ERα +ve) cell line showed greater increased expression of the adhesion complex components after the secretory phase treatment regime. Therefore, this treatment regime was used to establish the requirement for ERα and any role of ERβ in the regulation of the adhesion complex. To achieve this Heraklio (ERα -ve) cells were treated with identical concentrations and treatment periods (Figure 4-13), and a markedly different response to hormone stimulation was observed when compared to Ishikawa (ERα +ve). *OPN* mRNA expression in the Heraklio cell line was 10-50-fold greater depending on the specific treatment than the other adhesion complex components. For this reason *OPN* is graphed separately (Figure 4-13A). *OPN* expression was significantly increased 1.2-fold after treatment with E_2 alone and with the combination of E_2 and P_4 ($p \leq 0.05$). This increase was much less than that observed in Ishikawa in terms of fold change. This suggests an important role for ERα in the regulation of *OPN*. *CD44* expression was

significantly decreased when exposed to E_2 alone and with the combination of E_2+P_4 ($p \leq 0.05$) (Figure 4-13B). *ITGAV* expression was significantly decreased by 1.5 fold in response to E_2 ($p<0.01$). In the presence of P_4, *ITGAV* expression increased 1.4-fold and with the E_2+P_4 combined treatment by 1.5-fold ($p<0.01$; $p<0.01$ respectively). No changes in ITGB3 expression were observed in Heraklio cells.

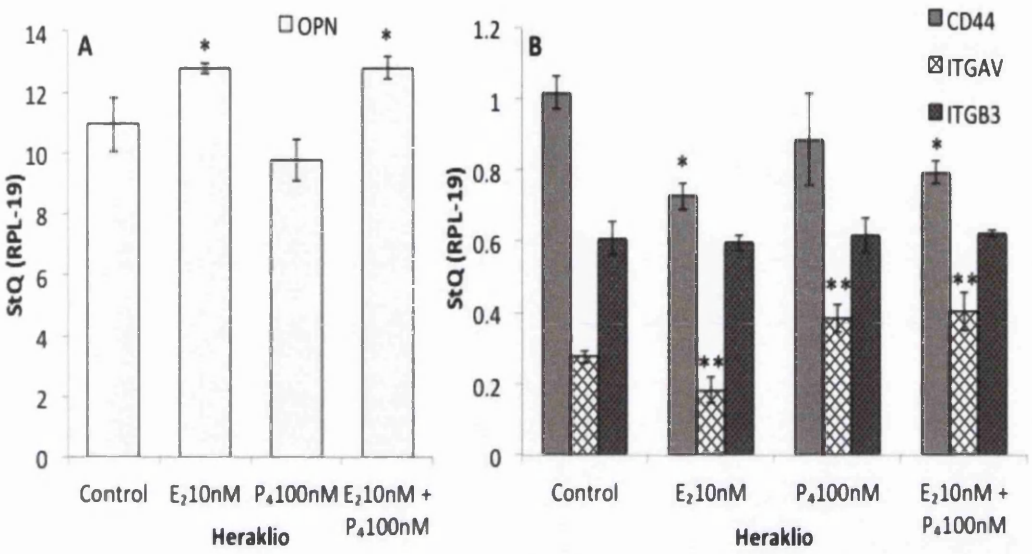

Figure 4-13 Gene expression analysis of OPN and its complex targets in the Heraklio (ERα -ve) model of secretory phase endometrium.

Quantitative PCR was conducted to measure hormone stimulated levels of absolute starting quantities of OPN, CD44, ITGAV and ITGB3 in Heraklio cells. Significant differences in each gene occur between treatment with hormones and the control. Values are average and SD. Statistical analysis of the data was performed using a Student's t-test (control vs. treatment). *, P≤0.05 **, P≤0.01, was considered significant.

4.3.4.1 Secreted osteopontin expression

In Heraklio cells, secreted OPN levels altered following all treatments (Figure 4-14). Treatment with P_4 alone resulted in a decrease of 1.7-fold in the level of secreted OPN ($p \leq 0.05$). This was consistent with the trend observed at the mRNA level. The combination of E_2+P_4, increased secreted OPN levels 1.6-fold ($p \leq 0.05$). Whilst E_2 treatment resulted in an increase similar to E_2+P_4, this increase was not significant.

The general trends seen at the secreted protein level reflect the trends observed at the mRNA level after each treatment.

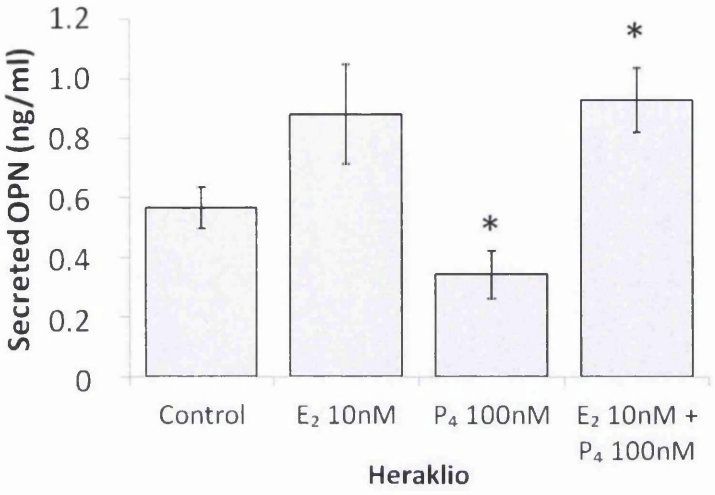

Figure 4-14 Secreted OPN expression levels in a secretory phase model in Heraklio (ERα -ve) cells.

ELISA was conducted to measure hormone stimulated levels of expression of OPN in Heraklio cells. Significant differences in each gene occur between treatment with hormones and the control. Values are average and SD. Statistical analysis of the data was performed using a Student's t-test (control vs. treatment). *, P≤0.05, was considered significant.

4.3.4.2 CD44 protein expression

CD44 protein expression in response to the secretory phase treatment regime in Heraklio (ERβ +ve) cells (Figure 4-15) was considerably different to the response in Ishikawa (ERα +ve). In response to E_2 treatment, CD44 expression decreased 1.2-fold (H = 7) when compared to the control (H = 8.5). However, this was not significant ($p>0.05$). Treatment with both P_4 alone and in combination with E_2 decreased CD44 expression 1.3-fold (H = 6.5), this decrease in expression was not statistically significant ($p>0.05$; $p>0.05$ respectively).

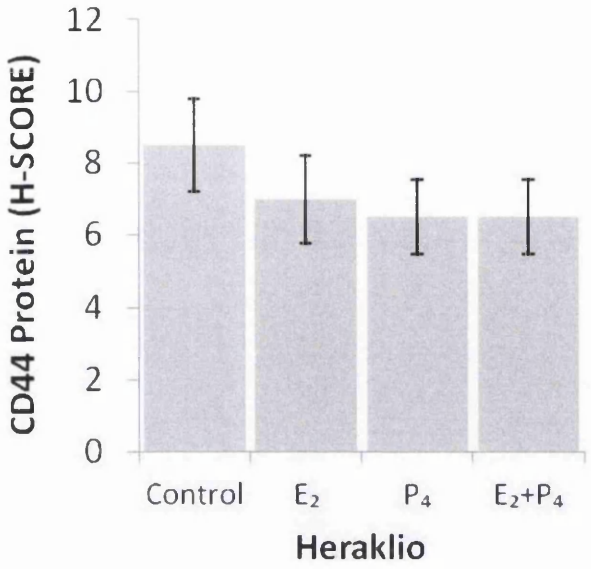

Figure 4-15 CD44 protein expression in a secretory phase model in Heraklio (ERα -ve) cells.

IHC stained slides for CD44 protein expression in response to secretory phase model treatments in Heraklio cells (ERα -ve). Values are average and SD. Statistical analysis of the data was performed using a Student's t-test (Control Vs. treatment), data are representative of three biological repeats.

4.4 Osteopontin and CD44 promoter analysis

The hormonal regulation models of adhesion complex components suggested that *OPN* and *CD44* were most responsive to hormone stimulation in Ishikawa cells, which could be a result of ERα expression. The Heraklio cell line had negligible expression levels of ERα suggesting that ERβ may have a more prominent role in the Heraklio cell line. It should also be noted that the levels of *OPN* in Heraklio were very high (>300-fold) than in Ishikawa, suggesting a very different mode of regulation. Therefore to understand the regulation of *OPN* and *CD44* in the Ishikawa cell line by ERα, a promoter analysis was conducted to establish which ERE existed on each gene's promoter (Figure 4-16 and Figure 4-17). Following this, ChIP was conducted to measure the transcriptional activity of estrogen response element on the *OPN* and *CD44* promoters at the basal level in Ishikawa. The absent ERα in the Heraklio cell line allowed for this to be used as a background control.

4.4.1.1 *Osteopontin promoter*

Analysis of the *OPN* promoter revealed 7 putative and 1 previously described regulatory element (site 2) (Sharma et al. 2010; Wang et al. 2000a; Bidder et al. 2002) that qPCR primers were designed to amplify (Figure 4-16). Primers sets were designed to amplify 4 regions on the *OPN* promoter that contained 2 ERα, 6 AP-1 and 1 SP-1 spanning from -2.7KB to -200bp before the translation start site in exon 4. Each primer set is identified by a site (Figure 4.16, sites 1-4).

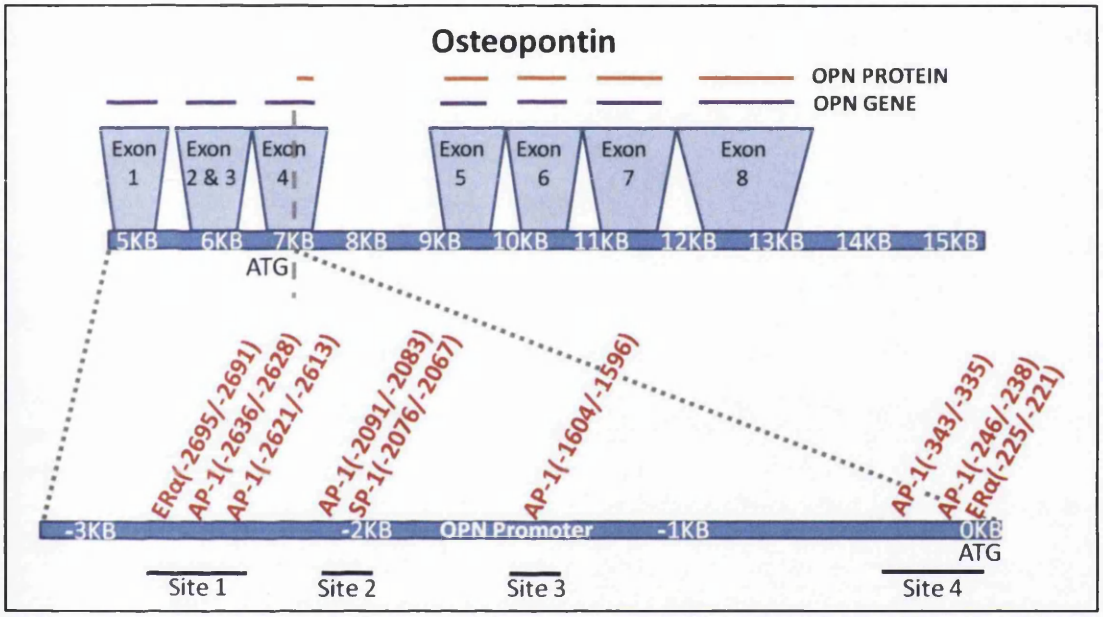

Figure 4-16 Promoter analysis of the human *OPN* gene.

The OPN promoter was analysed for ERα, AP-1 and SP-1 binding sites, -3KB from the translation start site to +0.5KB after the start site. Primers were designed to amplify two putative regulatory elements for ERα, five for AP-1 and one SP-1 element.

4.4.1.2 *CD44 promoter*

The *CD44* promoter included 5 putative ER regulatory elements that primers were designed to amplify (Figure 4-17). The *CD44* promoter contained fewer estrogen responsive elements than *OPN* and primers were designed to amplify regions containing 2 putative regulatory elements for ERα, 1 AP-1 site in addition to one SP-

1 site. Each primer set is identified by a site (Figure 4.17, sites 1 and 2). The *CD44* promoter contained estrogen regulatory elements downstream of the translation start site in exon 1.

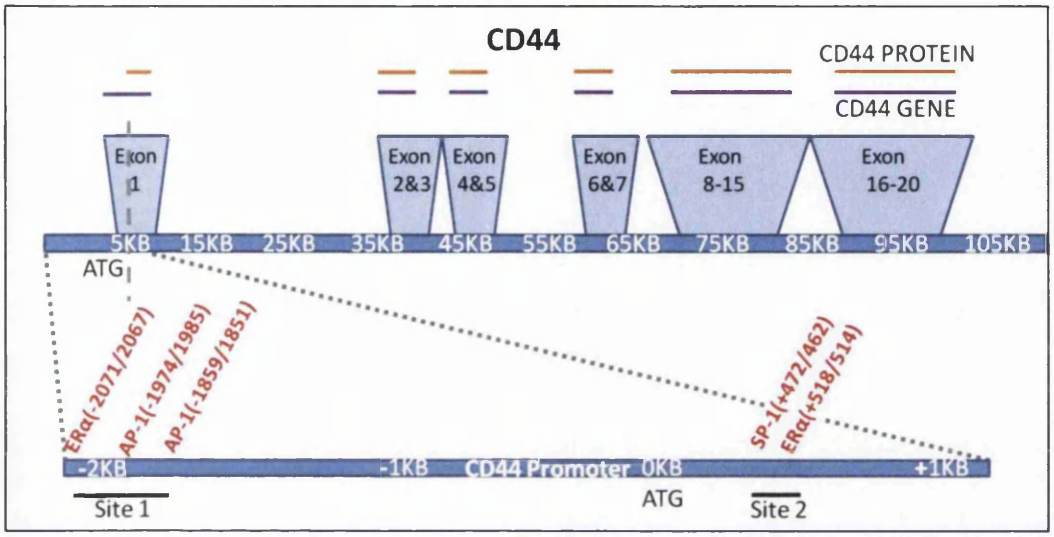

Figure 4-17 Promoter analysis of the human *CD44* gene promoter.

The CD44 promoter was analysed for ERα, AP-1 and SP-1 binding sites, -2KB from the translation start site to +1KB after the start site. Primers were designed to amplify two putative sites for ERα, two for AP-1 and one for SP-1.

4.4.2 Chromatin immunoprecipitation

To validate the enrichment of chromatin (Figure 4.18) a high abundance target, RNA polymerase II was selected and qPCR primers designed to determine binding to a known site on the *GAPDH* promoter (Figure 4-19A). Polymerase II enrichment showed no difference between the two cell lines, demonstrating consistent regulation between cell lines of a positive control target. ERα recruitment to a region of the promoter sequence of X-box binding protein *(XBP1)*, a known ERα target, was also evaluated. ERα enrichment clearly demonstrated in the ERα66 Ishikawa cells, and as expected no recruitment was seen in Heraklio cells which are ERα -ve (Figure 4-5).

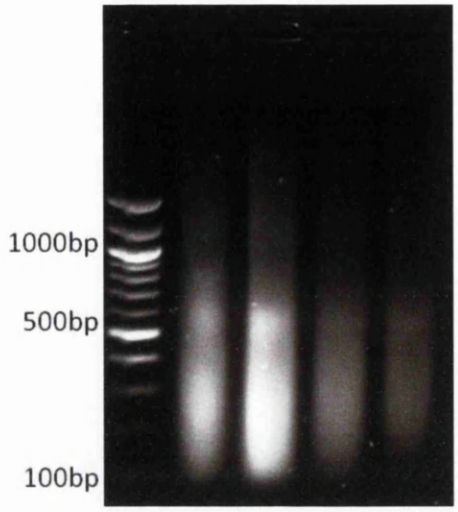

Figure 4-18 Sheared chromatin from Heraklio cells.

1% agarose gel of sheared chromatin from Heraklio cells using 800R sonicator (QSonica, UK). The first lane on the left has a 1KB ladder, the next four lanes show the fragment sizes of sheared chromatin ranging from 800-100bps.

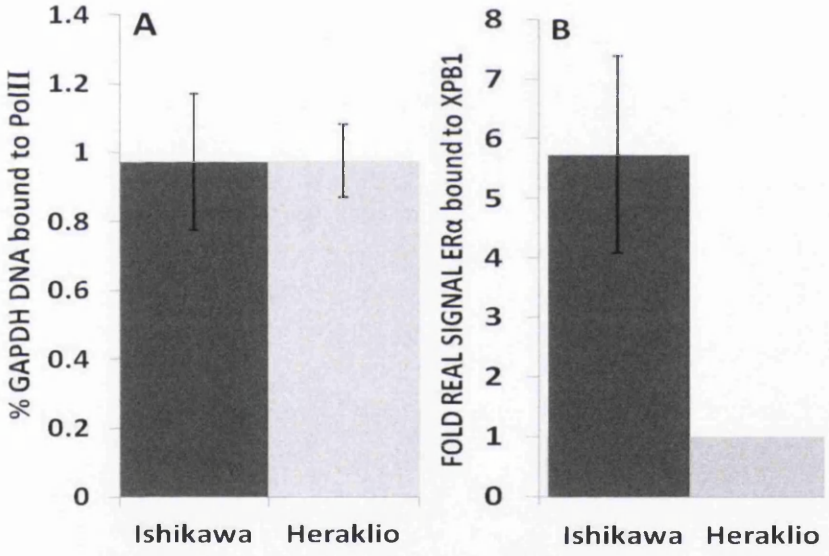

Figure 4-19 Chromatin immunoprecipitation for positive control targets.

Quantitative PCR was conducted on GAPDH and XBP1 promoter regions for Pol II or ERα occupancy respectively. Values are average and SD for Pol II and fold for ERα.

4.4.2.1 *ChIP for estrogen receptor α on osteopontin promoter regions*

ERα ChIP was performed for the sites identified (Figure 4-16 and Figure 4-17) in the *OPN* and *CD44* promoters (Figure 4-20 and Figure 4-21). Heraklio (ERα -ve) was used to establish background IP levels as it does not express ERα for the Ishikawa (ERα +ve) cell line. The binding sites in the first ERα site (containing ERα/AP-1/AP-1 elements approximately 2.5K upstream) identified in this study are indistinguishable by ChIP due to its 500bp resolution. There was a 25 fold increase in ERα recruitment signal in Ishikawa. This indicates that ERα is recruited to these sites even in the absence of E_2. In contrast at site 2 containing a previously identified SP-1 regulatory element at approximately 2KB upstream (Wang et al. 2000a; Sharma et al. 2010) no recruitment of ERα was observed. Sites 3 and 4 also showed no occupancy. Therefore a novel binding site for ERα on *OPN* has been identified. High resolution mapping would be necessary to determine the exact binding site.

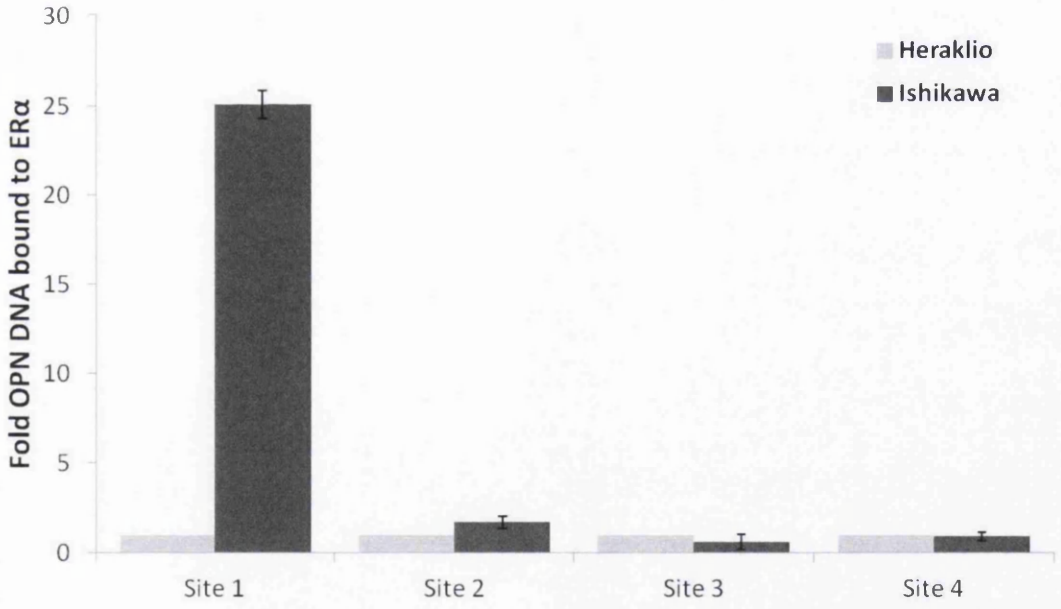

Figure 4-20 ERα chromatin immunoprecipitation on the OPN promoter.

Quantitative PCR was conducted for ERα on OPN promoter to measure, in fold, ERα occupancy in Ishikawa (ERα +ve) normalised to Heraklio (ERα -ve). Values are fold normalised to Heraklio (ERα -ve).

4.4.2.2 CD44 estrogen receptorα chromatin immunoprecipitation

Similar ChIP analysis was conducted for ERα on the *CD44* promoter in the Ishikawa (Figure 4-21). For the first set of regulatory sites, there was a significant increase in ERα recruitment by 9-fold to the *CD44* promoter in Ishikawa cells, and an 8-fold increase in the binding levels of the second set of sites between the cell lines. Again, a novel binding site for ERα has been identified, this time in the *CD44* promoter at approximately 2KB upstream. High resolution mapping would be necessary to determine the exact site involved in ERα recruitment.

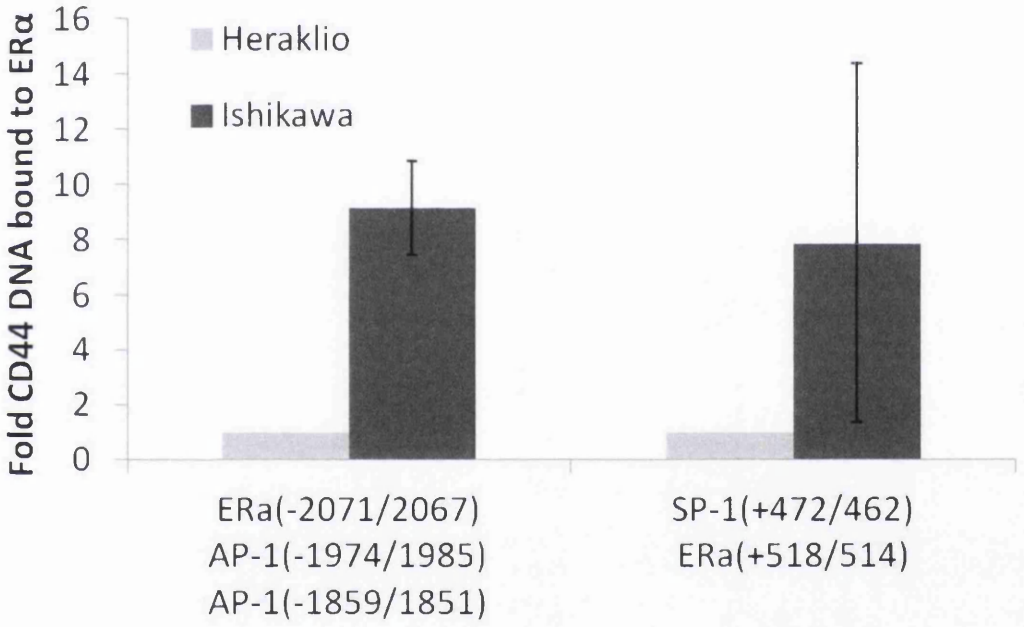

Figure 4-21 ERα chromatin immunoprecipitation on the CD44 promoter.

Quantitative PCR was conducted for ERα on CD44 promoter to measure, in fold, ERα occupancy in Ishikawa (ERα +ve) normalised to Heraklio (ERα -ve). Values are fold normalised to Heraklio (ERα -ve).

4.5 Discussion

The work conducted in this chapter aimed to determine if OPN and CD44 expression in the endometrial epithelium was regulated by the ovarian derived hormones, estrogen and progesterone. The cell lines Ishikawa and Heraklio were utilised to deduce the role of ERα and possible contribution of ERβ in the estrogen signalling pathway regulation of the adhesion complex components. They were also used to determine potential contributions of PR signalling. Both cell lines were shown to have active estrogen and progesterone signalling by measuring downstream targets of ER and PR signalling *GREB1* and *AREG*. *GREB1* induction at 48hrs through the ERα and ERβ receptors are consistent with previous reports (Stossi et al. 2004). In the secretory phase model, induction of OPN and CD44 through E_2 and P_4 signalling in the Ishikawa cell line saw larger fold changes in gene expression than in the Heraklio cell line. It is important to note that αVβ3 was used only in the regulation studies, it has been well documented in the literature and served to provide a control for hormone induction in cell lines.

The first important observation of the adhesion complex components was the differential basal expression levels in Ishikawa (ERα +ve) and Heraklio (ERβ +ve) cells. The high levels of ERα in the Ishikawa cell line (or more prominent ERβ expression in the Heraklio cell line suggests a role in the regulation of the adhesion complex components; OPN, CD44 and αVβ3) correlate with decreased adhesion complex expression. Basal expression levels of OPN and CD44 in the cell lines Ishikawa and Heraklio differed markedly. Low expression patterns were observed in the Ishikawa cell line, and very high levels of expression for OPN were observed in the Heraklio cell line which correlate with hormone receptor expression in each cell line. Ishikawa cells expressed ERα, whereas ERβ was predominately expressed in Heraklio. PR expression was observed in both cell lines with the Ishikawa cell line expressing higher levels of PR.

When the cell lines were treated with hormones, OPN expression in the Ishikawa cell line was significantly increased by 10nM of estradiol (2.6-fold) in agreement

with previous work (DuQuesnay et al. 2009). *OPN* mRNA has been shown to localise to the glandular epithelium of the sheep endometrium, upon stimulation with progesterone. The study hypothesised that PR had a function in regulating OPN however a down-regulation of PR in the epithelium is required for secretory glands to up regulate protein expression of OPN (G. Johnson et al. 2000).

Different expression in the *OPN* isoforms between the cell lines was ruled out as a cause of this differential expression pattern. The relative expression levels of *OPN* isoforms A-E were similar between the two cell lines whilst the expression in Heraklio was higher overall, although the expression levels of *OPN* were ~300-fold greater in Heraklio than Ishikawa. To explore these interesting findings, ChIP was conducted to establish if ERα binding to the promoter regions of both genes differed between the cell lines. Distinct patterns of ERα, AP-1 and SP-1 regulatory elements were observed on the *OPN* and *CD44* promoters in Ishikawa, with the ERα negative cell line Heraklio used as a background control. Site 1 on the *OPN* promoter had significantly increased ERα binding in Ishikawa. This site flanks a previously identified site (Site 2) shown active through luciferase and electrophoretic gel shift assays (Sharma et al. 2010; Wang et al. 2000a). However no ERα binding was detected in either of the cell lines on this site of the *OPN* promoter. Sites 3 and 4 also had no ERα occupancy as they had the same occupancy in both ERα +ve and ERα -ve cells.

It appears that ERα plays a very prominent role in the regulation of OPN. The presence of ERα in cells maintains OPN at very low levels. However treatment of these ERα +ve cells with E_2 causes an increase in the expression of OPN. ERα may therefore modulate OPN expression by activating the expression of a potent repressor of OPN expression which E_2 treatment counteracts. This has been observed by the increased levels of ERα binding to the *OPN* promoter in Ishikawa cells (Figure 4-20), in addition to the increase in OPN expression as a result of E_2 treatment (Figure 4-7). To determine which of the three potential sites (ERα, AP-1

or SP-1) ERα is binding to, high resolution EMSA mapping or promoter detection analysis could determine the precise binding sites.

ChIP analysis also revealed that the *CD44* promoter was occupied ERα, where it was observed bound to site 1 and site 2 in Ishikawa cells. These novel sites suggest that ERα also plays an important role in the regulation of CD44 in endometrial cells. Again the data suggests that ERα maintains CD44 expression at low levels as CD44 expression was ~ 10-fold higher in ERα -ve Heraklio cells. This repression is likely to be indirect, as treatment in Ishikawa cells with E_2 results in increased CD44 expression (Figure 4-7).

CD44 expression has been shown previously to be up-regulated in ER negative breast cancer cell lines (Hole et al. 1997). However it is also possible that the affect observed is ERβ driven.

The hormone driven regulation of OPN, CD44 and other adhesion complex molecules has been shown here. Whilst E_2+P_4 drive only subtle changes in expression of these target molecules, it is likely that they play an important role in preparing the endometrial surface in a receptive state. Excitingly novel ERα regulatory elements have been identified in the promoters of both OPN and *CD44* genes. Further characterisation of these elements in clinical samples using emerging technologies such as formalin fixed paraffin embedded tissue for ChIP analysis will determine their importance in the endometrium. It would be possible to establish if any differences through this potential regulatory mechanism can be detected in fertile and infertile women.

Chapter 5

Glucose and pro-inflammatory cytokine regulation of Osteopontin and CD44

5.1 Introduction

The hormone driven process of the regenerative menstrual cycle has parallels to that of the inflammatory response in tissues. The changes that occur in the vascular compartment of the endometrium mirror that of the inflammatory response in tissue regeneration (King and Critchley 2010). Migratory peripheral blood leukocytes such as monocytes and tissue resident macrophages that differentiate form monocytes have also been shown to have a role on the epithelial surface to protect the epithelium from pathogen invasion in addition to communicating with the epithelium to maintain its integrity (Sze et al. 2010). Monocytes and macrophages expressed on the epithelial surface have the ability to phagocytose pathogens, whilst other mechanisms for pathogen defence involve steric hindrance, provided by mucins, which are also expressed on the luminal epithelial surface (Ransohoff et al. 2003; Déchaud et al. 1998).

Noyes first described immune cell trafficking into the endometrium during the secretory phase in 1950. In the mid to late secretory phase macrophages and natural killer cells have been found to accumulate in the tissue. It has been hypothesized by Mueller et al that cyclic recruitment and turnover of uterine immune cells is achieved through endocrine signals inducing chemokines and immunomodulatory proteins (Mueller et al. 2000).

Cytokines released by the leukocytes such as monocytes, macrophages and lymphocytes include TNFα, IL-1β and IFNγ (Bliss et al. 1999; Cole et al. 2007). In the endometrial vasculature monocytes have shown to increase secretion of cytokines IL-1β and TNFα after ovulation in the menstrual cycle in healthy, cycling women (Willis 2003; Desai 2007). This suggests that the epithelial and stromal cells are surrounded by cytokine expressing leukocytes (Figure 5-1). The resulting paracrine signalling through the stroma and epithelial components in the endometrial tissue may have consequences on the expression of adhesion proteins on the epithelial surface. Expression of cytokines such as TNFα and IL-1β have been shown during

the implantation process and these are thought to aid uterine receptivity however the function of these cytokines is yet to be elucidated (Makrigiannakis et al. 2006).

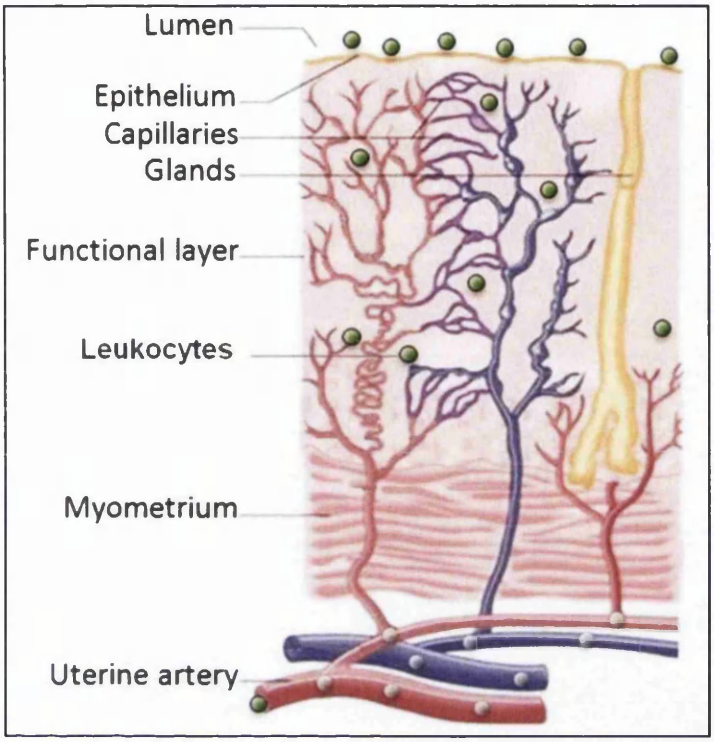

Figure 5-1 Leukocyte expression in the uterus.

Leukocyte expression on the luminal epithelia and in the epithelia tissue. Leukocytes such as monocytes (shown in green) migrate from the circulatory blood into the endometrial tissue where they mature into macrophages. Adapted from (The Feria Journal of Medicine, 2011).

Pro-inflammatory cytokines have also been shown to be up regulated in endometrial pathology (Weiss et al. 2009). Peritoneal fluid in women with endometriosis showed an increased level of white blood cell populations and specifically macrophages and these are thought to be linked with endometriosis-associated pelvic inflammation. Peritoneal fluid aspirated from women with endometriosis during laparoscopy had increased levels of pro-inflammatory cytokines IL-1 and TNFα (Taketani et al. 1992; Fakih et al. 1987; Montagna et al. 2008). Similarly, another study indicated that peritoneal levels of TNFα could be used to predict endometriosis in women (Bedaiwy et al. 2002). Levels of TNFα have

been shown to be increased in circulating blood of patients suffering with endometriosis, which may lead to increased TNFα induced proliferation, cell adhesion or angiogenesis. Further to this endometriotic lesions have been found to secrete TNFα and IL-1 (Kyama et al. 2003).

Women with PCOS have been found to have elevated levels of C-reactive protein, a standard test for inflammation (Ruan and Dai 2009; Kelly et al. 2001). Described as a low-grade inflammatory disorder, higher levels of TNFα and IL-6 have been found in circulating blood and follicular fluid in women with PCOS when compared to healthy, fertile controls (Amato et al. 2003).

Insulin resistance, commonly associated with PCOS is often found to exacerbate the syndrome along with other metabolic disorders including obesity and elevated fasting plasma glucose (Fanta 2013; Essah et al. 2007). In hyperglycaemic conditions (10 and 15mM), as experienced by a sub-set of PCOS women, TNFα expression is increased in the mononuclear cells isolated from peripheral blood of obese (ovulating, oligoamenorrhea) PCOS women (González et al. 2006). A study conducted to measure circulating TNFα levels in PCOS women had found that as BMI increased, TNFα expression too increased when compared to BMI matched fertile controls (Gonzalez et al. 1999). The interplay between inflammatory and metabolic environments in PCOS and endometriosis women suggest that they may be key in influencing the expression of the adhesion complex. Chronic exposure to TNFα has been shown to decrease functionality in GLUT4 or to decrease the levels of transporter proteins for example (Gonzalez et al. 1999).

Over expression of adhesive proteins which could impact on the receptivity of the endometrium during the window of implantation has been suggested as a factor impacting receptivity in endometrial pathology (Weiss et al. 2009). OPN has been shown to be up-regulated in the blood plasma of inflammatory diseases such as Crohn's disease (Agnholt et al. 2007) and cancer (El-Tanani et al. 2006). The expression of OPN has been shown to be modulated by IL-1β, TNFα and IFNγ cytokines in pancreatic cells of rat cell line models (Gong et al. 2009b; Foster et al.

1998). IL-1β, TNFα and IFNγ have all been shown to up-regulate the expression of CD44 at the gene level in rat aortic smooth muscle cells (Foster et al. 1998). Additionally OPN and CD44 expression has been shown to be directly or indirectly (as discussed in section 1.9.3) regulated by glucose expression in many different tissues (Kawamura et al. 2004; Takemoto et al. 2000; Tamada et al. 2012; Weiss et al. 2008). Shown to be associated with disrupted metabolic environments and high BMI, PCOS women have complications such as insulin resistance (Dunaif et al. 1989; Legro et al. 1998; Tan et al. 2010).

Differential OPN and CD44 expression was detected in the target pathology groups of this study, at both the mRNA and protein level (Chapter 3), leading to an investigation into the uterine environments of these patients. Cell culture models (Chapter 4) indicated that estradiol and signalling through ERα is important in the regulation of OPN and CD44. Other studies show that a decrease in the circulating blood levels of IL-1β and IL-6 were found to coincide with an increase in E_2 levels, suggestive of a link between E_2 signalling and inflammation (Pellicer et al. 1999).

In this chapter, the role of altered glucose and pro-inflammatory cytokine environments on levels of OPN and CD44 expression are investigated in an *in vitro* model. Glucose concentrations and time course experiments were chosen based on the study conducted by Gong *et al.,* 2009, which had shown modulation of OPN expression. The glucose levels chosen also reflect those in previous studies and are matched to distinct physiologies. Concentrations of 5.6mM are considered the cut off for detecting abnormal glucose tolerance in PCOS women therefore the 5mM concentration represents healthy non diabetic women (Gagnon and Baillargeon 2007). The World Health Organisation classes fasting glucose levels over 7mM as diabetic (type II) (Heuck et al. 2002) and represented in this study by 17mM a heightened level of glucose as in diabetics, where 25mM represents an extreme level and serves as a positive control level proven to initiate an OPN response (Gong et al. 2009b). The Ishikawa and Heraklio cell line were treated with varying

concentrations of glucose and the effect on OPN and CD44 expression quantified by qPCR, IHC for CD44 and ELISA for secreted OPN.

Both cell lines are also grown in the presence and absence of pro-inflammatory cytokines (IL-1β, TNFα and IFNγ), according to previous studies conducted to investigate expression of adhesion molecules in the endometrium (Dharmaraj et al. 2010). After establishing the effect of pro-inflammatory cytokines on OPN and CD44 expression, investigation into the regulatory mechanisms of these genes was conducted. NFκB and STAT1 are transcription factors activated through IL-1β, TNFα and IFNγ signalling. The promoters of *OPN* and *CD44* were analysed, revealing regulatory elements for both NFκB and STAT1 binding within both the promoters of OPN and CD44 respectively.

5.2 Results

5.2.1 Glucose regulation of osteopontin and CD44

Glucose concentrations of 4-7.8mM in the blood after eating are observed in healthy patients and are considered to be normal, while patients with Type II diabetes can experience levels up to 25mM (Kelly et al. 2001; American Diabetes Association 2011). To assess the effect of these altered glucose levels on OPN and CD44 expression, Ishikawa and Heraklio cells were grown in culture media supplemented with 5, 17 and 25mM of glucose respectively. The lowest dose of 5mM replicating the situation in normal, healthy, non-diabetic women and higher than normal levels (17 and 25mM of glucose), to mimic the conditions of insulin resistance observed in those with type II diabetes (American Diabetes Association 2011). OPN and CD44 expression levels were assessed at the gene and protein level, with secreted OPN protein measured using ELISA, while the intracellular expression of CD44 was measured using IHC.

5.2.2 *Osteopontin gene expression*

No significant alteration in *OPN* expression at the RNA level was observed in Ishikawa cells in the presence of 17mM glucose at 4 or 24 hours compared to the 5mM reference treatment (Figure 5-1). When higher levels of glucose (25mM) were present, a significant increase in *OPN* expression was detected after 4hrs (p=0.006) and this effect was not observed after 24hrs. In the Heraklio cell line *OPN* mRNA expression levels showed a significant 2.6-fold increase after a 4-hour treatment with 25mM of glucose compared to the normal levels (5mM of glucose; p=0.0001). After twenty-four hours however, this effect was lost, with *OPN* expression showing no significant alteration in the presence of either 4 or 25mM of glucose.

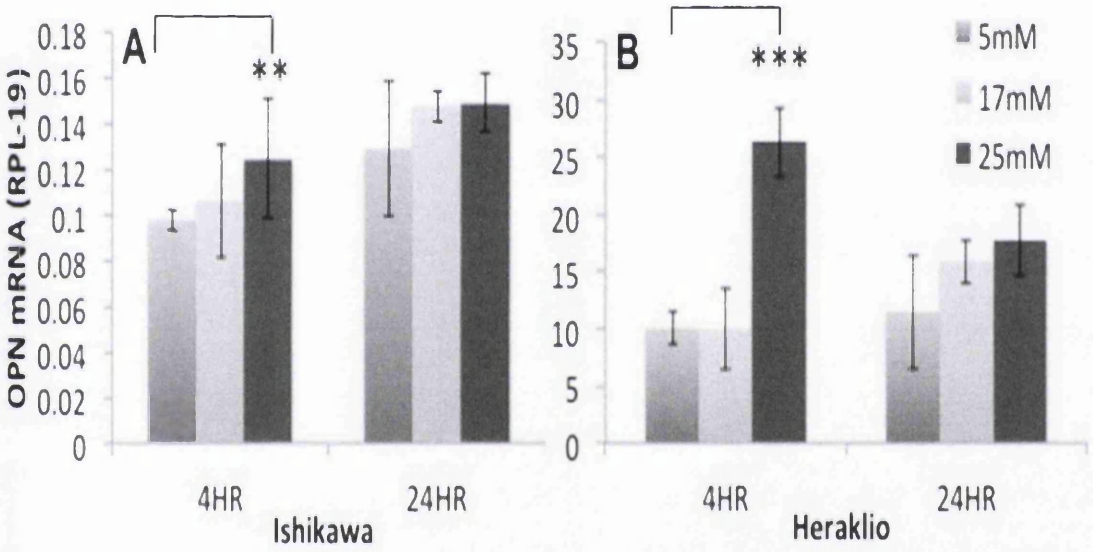

Figure 5-2 *OPN* gene expression in endometrial epithelial cell lines following glucose treatment.

Quantitative PCR was conducted to measure the levels of OPN expression in response to 5mM, 17mM and 25mM of glucose for 4 and 24hrs in (A) Ishikawa and (B) Heraklio. Values are average and SD of a minimum 3 independent biological repeats. Statistical analysis of the data was performed using a Student's t-test (control Vs. treatment). **, P≤0.01 and ***, P≤0.001 are considered significant.

Under basal conditions, grown in the presence of normal (5mM) levels of glucose, the ERα Heraklio cells demonstrated significantly higher levels of *OPN* expression at

the mRNA level (100-fold; $p<0.0001$). This suggests that the observed glucose response is likely to be ERα independent. Despite the observed expression pattern, the levels of *OPN* were reduced after 24 hours, even at the higher glucose concentration, suggesting a short lived temporal effect.

5.2.3 Secreted osteopontin expression

The ELISA method was used in order to establish the basal levels of OPN protein secretion from both cell lines and to compare them to those observed in the presence of increasing glucose concentrations over both a 4 and 24hr period. This allowed the comparison between secreted protein expression levels and those observed at the RNA level.

In contrast to the RNA level, secreted OPN levels decreased in the presence of increasing concentration of glucose, in both cell lines (Figure 5-3). In the ERα +ve Ishikawa cells levels of secreted OPN following 24hrs increased ~5-fold from when compared to the 4hr group in the presence of all glucose concentrations. While the presence of 17mM of glucose did not significantly alter levels of OPN expression at 4 or 24 hours, secreted OPN showed significant decreases (2 and 1.4-fold respectively) in response to treatment with 25mM of glucose, when compared directly to the 5mM reference point ($p=0.03$; $p=0.02$).

No significant change in secreted OPN levels were detected in the ERβ +ve Heraklio cell line after four hours in the presence of either 17 or 25mM glucose (Figure 5-3B; $p>0.05$). A significant 17-fold increase in secreted OPN was observed after 24hrs in the presence of all glucose concentrations. At twenty-four hours the levels of OPN were significantly decreased by both 17mM and 25mM (1.5 and 1.4-fold respectively) relative to 5mM sample ($p=0.001$; $p=0.001$).

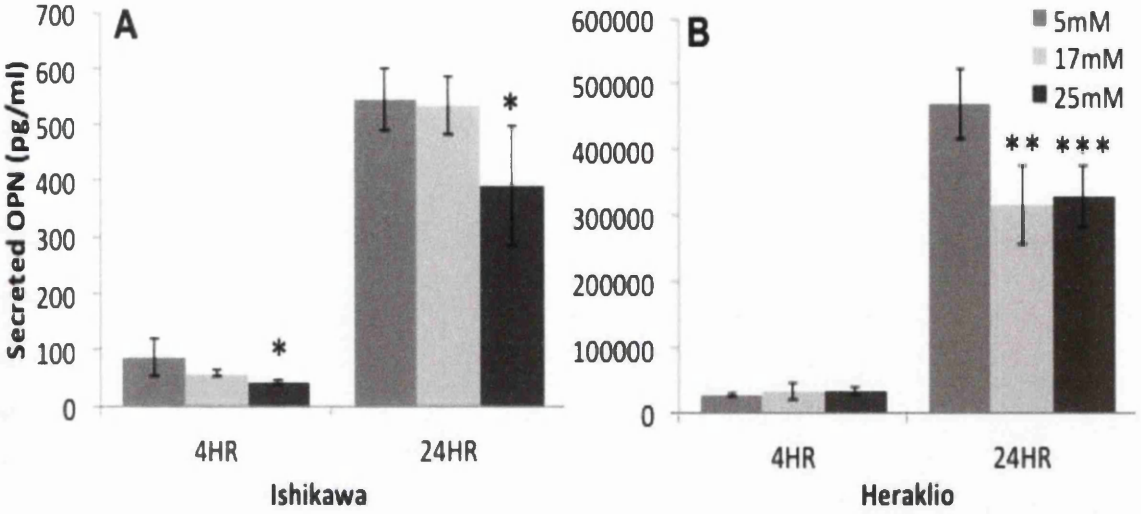

Figure 5-3 Secreted OPN expression in endometrial epithelial cell lines following glucose treatment.

The ELISA technique was conducted on cell supernatants to measure the levels of secreted OPN expression in response to treatment with 17mM and 25mM of glucose for 4 and 24hrs in (A) Ishikawa and (B) Heraklio. Glucose levels at 5mM are used as the reference point. Values are average and SD. Statistical analysis of the data was performed using a Student's t-test (control Vs. treatment). *, P≤0.05, **, P≤0.01 and ***, P≤0.001 are considered significant.

5.2.4 CD44 expression

CD44 expression was investigated at the RNA level, in order to further understand the role of increased glucose concentration, relative to that observed in PCOS patients with increased BMI, on its regulation. The levels of *CD44* mRNA were analysed by qPCR differences in ERα +ve (Ishikawa) and ERβ +ve (Heraklio) cells in response to glucose (Figure 5-4).

Similar to OPN, the expression levels of *CD44* detected were significantly 10-fold higher in the ERα -ve Heraklio cells when compared to Ishikawa cells ($p<0.0001$). In the Ishikawa cell line the levels of *CD44* detected in the presence of 5mM glucose decreased after twenty four hours when compared to 4hrs (Figure 5-4A). Significant increases in *CD44* expression (1.4 and 1.3-fold respectively) were detected in the presence of 17mM and 25mM of glucose for 4hrs ($p=0.006$; $p=0.01$). At 24 hours

this pattern was exaggerated with 17mM of glucose inducing a significant 2.5-fold increase in *CD44* expression and 25mM inducing a 2.9-fold increase (p=0.000001; p=0.002).

A significant 1.5-fold increase in *CD44* expression was observed after 4hrs in the presence of 17mM of glucose (Figure 5-4B; p=0.0006). Similar to that observed in OPN RNA expression, this inducible effect was not observed after 24hrs, where no significant change was detected (p>0.05). When treated with 25mM of glucose for 4hrs, no significant alteration in *CD44* expression was observed when compared to the 5mM reference point (p>0.05). However after a twenty-four hour treatment with 25mM of glucose *CD44* expression significantly decreased 1.2-fold (p=0.02).

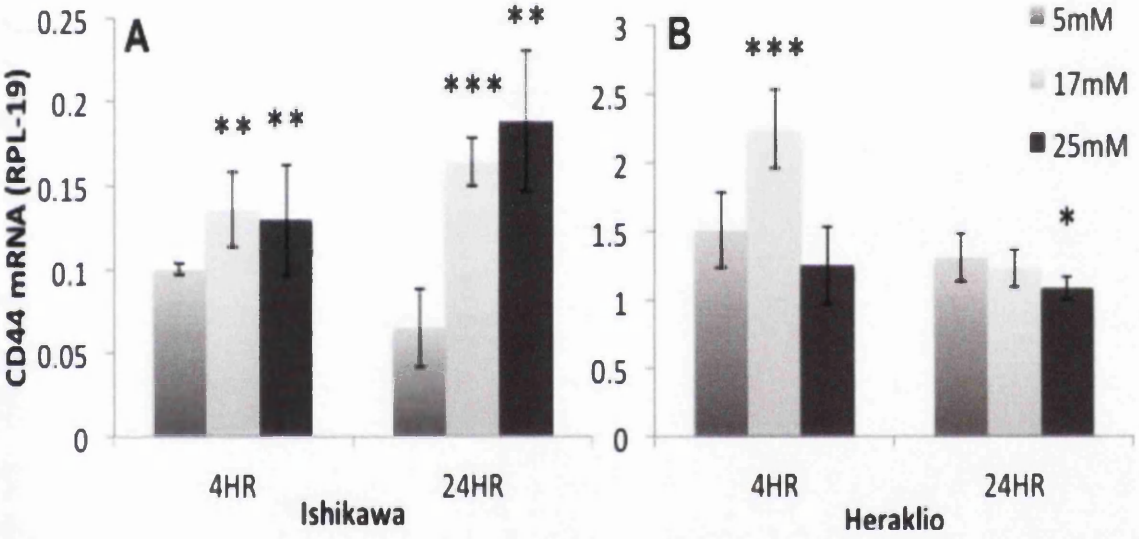

Figure 5-4 CD44 gene expression in ERα +ve and ERα -ve cells following glucose treatment.

Quantitative PCR was conducted to measure the levels of CD44 expression in response to 5mM, 17mM and 25mM of glucose for 4 and 24hrs in (A) Ishikawa ERα +ve and (B) Heraklio ERβ +ve. Values are average and SD. Statistical analysis of the data was performed using a Student's t-test (control Vs. treatment). *, P≤0.05, **, P≤0.01 and ***, P≤0.001 are considered significant.

5.3 Cytokine regulation of osteopontin and CD44

Pro-inflammatory cytokines IL-1β, TNFα and IFNγ were chosen to study their effect on the regulation of OPN and CD44, due to their increased expression in women with infertile pathologies such as PCOS and endometriosis. Again to assess the role of ERα and ERβ signalling in inflammatory environments the cell lines Ishikawa and Heraklio cells were used and grown in the presence of IL-1β, TNFα and IFNγ alone or in combination. Cells were exposed to cytokines for 48hrs and qPCR was used to quantify *OPN* and *CD44* expression at the RNA level. Once again, ELISA technology was used to determine secreted OPN levels while IHC was used to determine the protein expression levels of CD44.

5.3.1 Osteopontin gene expression

Ishikawa cells were treated with IL-1β over a forty eight hour period, showed a significant 1.4-fold decrease in *OPN* expression at the RNA level compared to the untreated control ($p<0.05$; Figure 5-5A). Similarly, a 4-fold decrease in *OPN* expression was observed following treatment with TNFα for 48hr compared to the untreated control ($p<0.001$). No significant effect on *OPN* expression was observed in the Ishikawa cells when treated with IFNγ alone ($p>0.05$). When treated with combinations of cytokines, differential *OPN* expression patterns were observed, suggesting that multiple signalling pathways may affect *OPN* regulation in these cells. TNFα treatment in combination with IFNγ resulted in a significant 2-fold down-regulation of *OPN* expression at the RNA level ($p<0.001$), suggesting that IFNγ is capable of suppressing the effect of TNFα alone. IL-1β treatment in combination with TNFα and IFNγ resulted in a significant 3-fold reduction in *OPN* expression compared to the untreated control ($p<0.001$) and interestingly enhanced the effect compared to IL-1β treatment in isolation.

While basal, untreated control levels of *OPN* expression at the RNA level are significantly lower in Ishikawa cell compared to Heraklio cell lines, Heraklio cells treated with exactly the same combinations and concentrations of pro-

inflammatory cytokines over a 48hr period exhibited markedly different responses. The differential regulation of *OPN* by cytokines between the cell lines suggests the ERα signalling pathway may interact with cytokine signalling.

Treatment with IL-1β and TNFα in isolation, resulted in no significant change in *OPN* expression at the RNA level when compared to the untreated control samples (Figure 5-5B; $p>0.05$). Interestingly when treated with IFNγ only, significant 2.4-fold increases in *OPN* expression were observed ($p<0.001$). This effect was dampened when IFNγ treatment was combined with TNFα, where a small but significant 1.3-fold up-regulation of *OPN* was observed compared to the untreated control sample ($p\leq0.05$). This effect was lost when IL-1β was administered in combination with TNFα and IFNγ where no significant difference in *OPN* expression was observed when compared to the control ($p>0.05$). Despite the high levels of *OPN* expression in the Heraklio cell line, levels of *OPN* were significantly increased by IFNγ treatment ($p\leq0.05$).

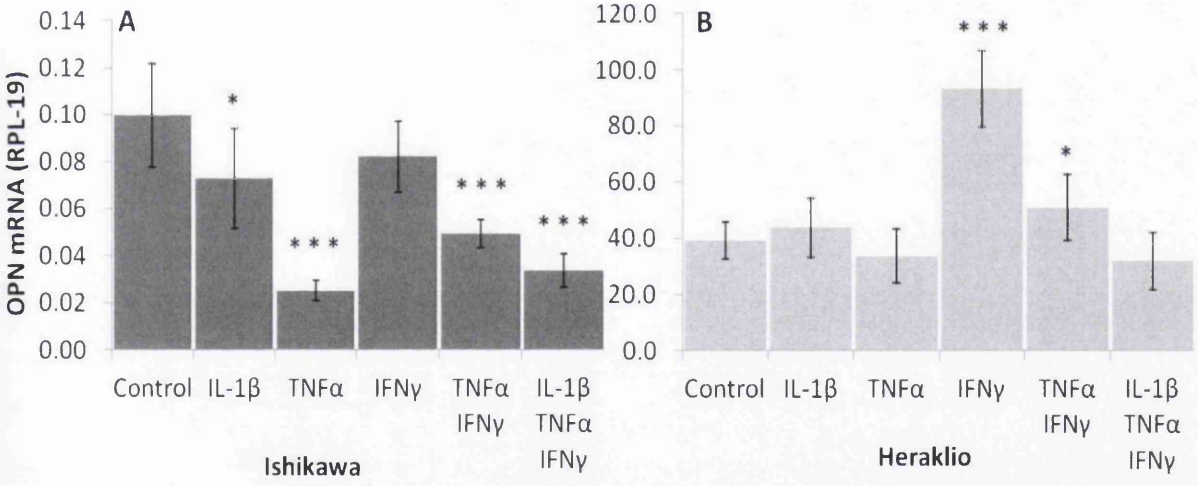

Figure 5-5 Expression of OPN in response to treatment with pro-inflammatory cytokine in Ishikawa and Heraklio cells.

Quantitative PCR was conducted on reverse transcribed total RNA after exposure to cytokines IL-1β, TNFα and IFNγ for 48hrs. (A) in the Ishikawa cell line and (B) in the Heraklio cell line. Values are average and SD. Statistical analysis of the data was performed using a Student's t-test (control Vs. treatment). *, P≤0.05, and ***, P≤0.001 are considered significant.

5.3.2 Osteopontin protein secretion

As was the case at the RNA level, significantly higher secreted *OPN* expression was detected in the ERα -ve Heraklio cells when compared to the ERα +ve Ishikawa, in the untreated control sample. Significantly, the patterns of secreted OPN expression as a result of cytokine treatments were dramatically altered in both the cell lines, when compared to the RNA level.

Ishikawa cells treated with IL-1β, TNFα and IFNγ in isolation, over 48hrs, showed significantly decreased levels of secreted OPN (Figure 5-6A; $p<0.05$). 1.2, 2 and 1.4-fold decreases in secreted OPN expression were detected respectively ($p<0.01$; 0.001 and 0.001). Co-treatment with TNFα and IFNγ, had a synergistic effect, resulting in a further 4-fold decreased expression of OPN ($p<0.001$). When IL-1β was added to this combination the effect was greater with a 6-fold decrease in OPN secretion observed ($p<0.001$).

In contrast to the RNA level once again, a differential response profile was observed in the Heraklio cell line after 48hr treatments with the same cytokine combinations (Figure 5-6B). 1.6 and 1.5-fold increases in OPN secretion were observed in response to IL-1β and TNFα treatment alone when compared to the untreated control samples ($p<0.001$; $p<0.001$ respectively). A slight but significant 1.2-fold increase in OPN secretion was observed when Heraklio cells were exposed to IFNγ alone OPN ($p\leq0.05$). The co-treatment of TNFα and IFNγ resulted in a 1.4-fold decrease in OPN secretion and when all three cytokines were added in combination, a 3.3-fold decrease in secreted OPN was observed ($p<0.001$).

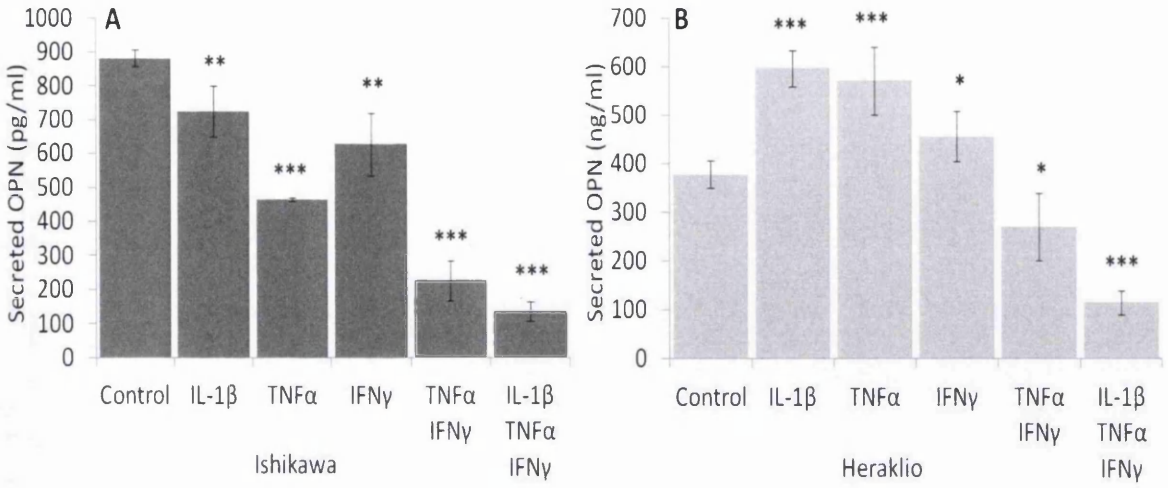

Figure 5-6 Secreted OPN in response to treatment with pro-inflammatory cytokines in Ishikawa and Heraklio cells.

ELISA was conducted on media samples from cell lines after exposure to cytokines IL-1β (5ng/mL), TNFα (25ng/mL) and IFNγ (200IU) for 48hrs. (A) in the Ishikawa (pg/ml) and (B) in the Heraklio cell lines (ng/ml). Values are average and SE. Statistical analysis of the data was performed using a Student's t-test (control Vs. treated). **, P≤0.01, and ***, P≤0.001 are considered significant.

5.3.3 CD44 gene expression

All cytokines when administered alone exhibited a different effect in the both cell lines. In Ishikawa cells, decreased OPN expression was observed, however in Heraklio their presence resulted in increased expression, suggesting a possible interaction between ERα and cytokine signalling.

CD44 expression was analysed by qPCR in response to cytokine treatment in the Ishikawa and Heraklio cells using the same treatment regime as for OPN (Figure 5-7). In the Ishikawa cell line *CD44* expression was increased by all cytokines alone and in combination (Figure 5-7A). Treatment with IL-1β alone resulted in *CD44* expression increasing 1.6-fold (p=0.001). When treated with TNFα, *CD44* expression significantly increased 1.5-fold (p=0.02) and when treated with IFNγ *CD44* expression was significantly increased 1.4-fold (p=0.01). The combination of cytokines TNFα and IFNγ resulted in a small additive effect and *CD44* expression significantly increased 1.7-fold (p=0.001). When all three cytokines were used in

combination, again a small additive effect was observed, *CD44* expression significantly increased 2-fold (p=1.6-11). In the Heraklio cell line (Figure 5-7B) when treated with the same cytokines in combination or isolation only TNFα increased *CD44* expression 1.2-fold (p=0.05). Treatment with IL-1β, IFNγ alone or in combination with TNFα did not significantly change *CD44* expression (p>0.05).

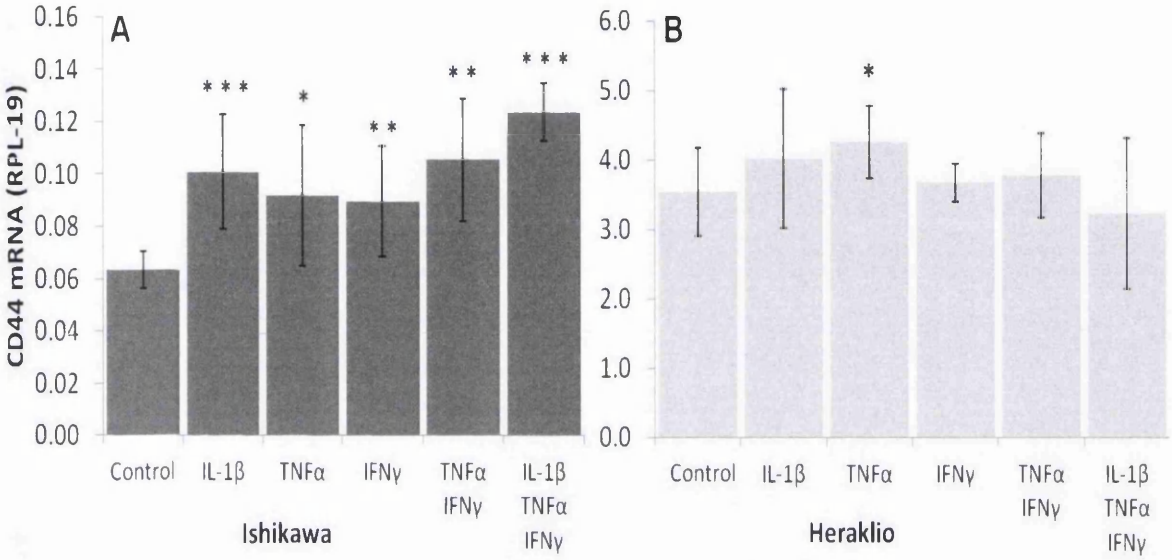

Figure 5-7 Expression of CD44 in response to treatment with pro-inflammatory cytokine in Ishikawa and Heraklio cells.

Quantitative PCR was conducted on reverse transcribed total RNA after exposure to cytokines IL-1β (5ng/mL), TNFα (25ng/mL) and IFNγ (200IU) for 48hrs. (A) in the Ishikawa (ERα +ve) and (B) Heraklio (ERβ +ve) cell lines. Values are average and SD. Statistical analysis of the data was performed using a Student's t-test (control Vs. treatment). *, P≤0.05, **, P≤0.01 and ***, P≤0.001 are considered significant.

5.3.4 CD44 protein expression

Detected by IHC, significant alterations in the level of CD44 protein expression were detected in response to the cytokine treatments, in both cell lines (Figure 5-8). In the Ishikawa cells, CD44 expression was increased following cytokine treatment (Figure 5-8A). Each cytokine, administered in isolation resulted in increased CD44 expression IL-1β (H = 5), TNFα (H = 7) and IFNγ (H = 6.5) when compared to the untreated control (H = 4), however these increases were not statistically significant (p>0.05). When cytokine treatments were administered in combination, TNFα+ IFNγ

(H = 6.5) and TNFα+IFNγ+IL-1β (H = 6.5) each resulted in increased CD44 expression, however, again these increases were not statistically significant compared to the untreated control (p>0.05).

In the Heraklio cell line treatment with cytokines alone had different effects on CD44 expression. When treated with IL-1β (H = 4) or TNFα (H = 6) alone, decreased levels of CD44 expression levels were detected compared to the untreated control (H = 7), however this decrease was not significant (p>0.05). When treated with IFNγ alone, increased CD44 expression (H = 11) was observed, however when TNFα and IFNγ were combined, CD44 expression decreased (H = 5). Once again however, none of these detectable alterations in protein expression were statistically significant (p>0.05). Combined treatment of IL-1β, TNFα and IFNγ resulted in increased CD44 expression (H = 7.5; p>0.05).

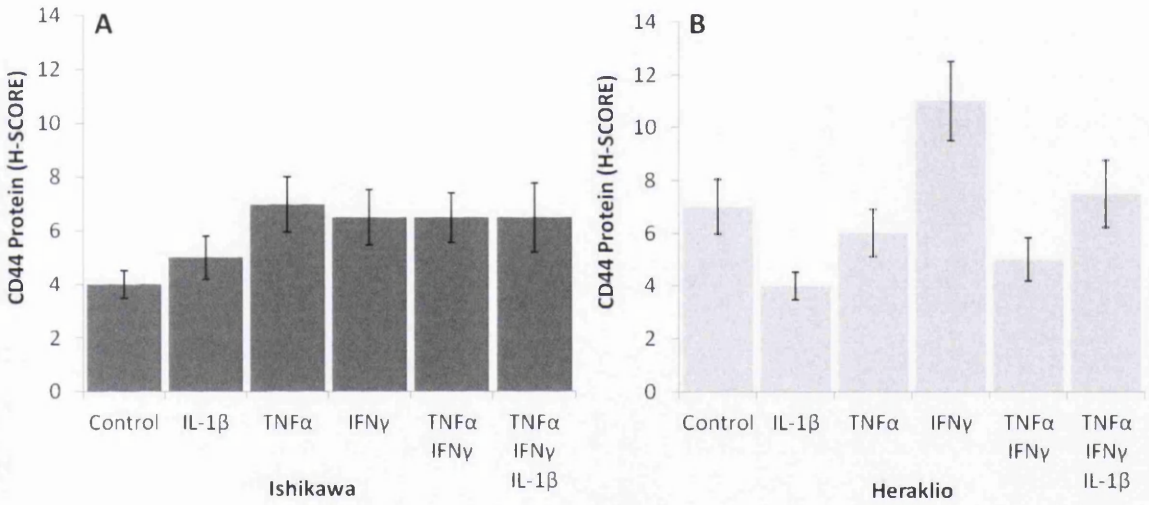

Figure 5-8 CD44 intracellular protein expression following treatment with pro-inflammatory cytokine treatment in Ishikawa and Heraklio cells.

IHC stained slides for CD44 protein expression in response to pro-inflammatory cytokine treatments IL-1β (5ng/mL), TNFα (25ng/mL) and IFNγ (200IU) for 48hrs in Ishikawa (ERα +ve) and Heraklio (ERα -ve) cells. H-SCORE values are average and SD. Statistical analysis of the data was performed using a Student's t-test (Control Vs. treatment), data is representative of three biological repeats.

5.4 Chromatin Immunoprecipitation

Treatment by pro-inflammatory cytokines indicated that OPN and CD44 expression could be regulated through TNFα and IFNγ signalling. The regulation appeared to differ between the Ishikawa and Heraklio cell lines, suggesting an additional role, via ERα signalling. NFκB and STAT1 transcription factors have been shown to be activated through TNFα and IFNγ signalling. To determine therefore if TNFα and IFNγ signalling directly influences the transcriptional regulation of *OPN* and *CD44* through NFκB and STAT1, putative promoter analysis was conducted to identify appropriate response element positions with the promoters of *OPN* and *CD44*, followed by ChIP assays to detect binding.

5.4.1 Osteopontin regulation

To determine if transcription factors known to be activated in response to pro-inflammatory cytokine signalling were capable of regulating *OPN* and *CD44*, through binding to appropriate response elements, a promoter analysis was conducted. The *OPN* promoter region spanning from 3KB upstream to the transcription start site (ATG site) was analysed for identified regulatory elements. In this region, one putative (site 5) and one previously identified NFκB site (site 6) (Samant et al. 2007) were identified in addition to a putative STAT1 site (site 7) (Figure 5-9). Primers were then designed to amplify identified regions containing these sites for specific amplification via qPCR following ChIP isolation of DNA fragments through NFκB and STAT1 specific antibodies respectively.

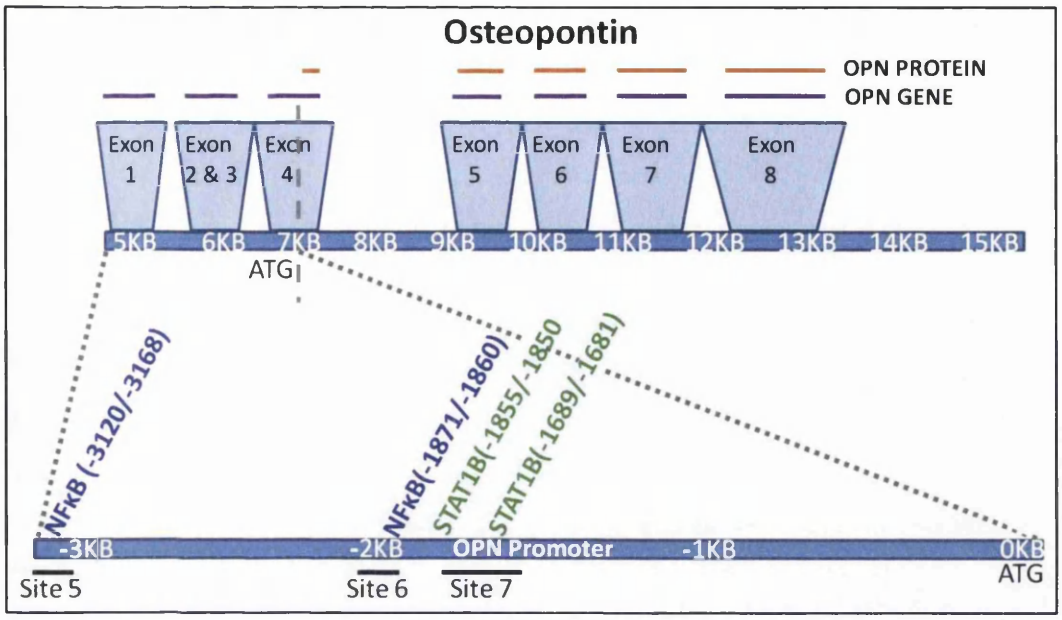

Figure 5-9 Promoter analysis of the human *OPN* gene promoter.

The Osteopontin promoter was analysed using Alggen Promo for NFκB and STAT1 binding sites, -3KB from the translation initiation start site to +0.5KB after the start site. Additional primers were designed to amplify two putative regulatory elements for NFκB and two STAT1 binding sites in addition to previously described estrogen regulatory sites.

After establishing that these direct regulation elements were present on the *OPN* and *CD44* promoter, identical cytokine treatments as those in section 5.3 were conducted on both cell lines. To determine the role of ERα the Ishikawa and Heraklio cells were utilised to investigate if ERα has a role in cytokine signalling. The cells were fixed, and chromatin was extracted and immunoprecipitation conducted (Section 2.7). After reverse cross-linking to separate DNA from antibody/protein complexes, qPCR was performed and amplification Cq values were calculated, directly proportional to the amount of transcription factor binding in any given treatment or control, at the time of fixation. This was used to analyse the role of NFκB and STAT1 signalling in the action of pro-inflammatory cytokines on the expression levels of OPN and CD44 in endometrial epithelial cell lines.

5.4.2 *NFκB ChIP*

ChIP for NFκB signal binding to the *OPN* promoter showed that TNFα administered in isolation over a 48hr period resulted in increased NFκB binding in Ishikawa cells (Figure 5-10). At site 5 and site 6 on the OPN promoter, significant 2.9 and 1.8-fold-increased levels of NFκB binding were detected respectively (p=0.01; p=0.02). When administered in combination, TNFα+IFNγ induced significant 1.9-fold increase in NFκB binding at site 5, however at site 6, significant 0.7-fold decreased NFκB binding was detected (p=0.04; p=0.002 respectively).

In the Heraklio cell line, treatment with TNFα alone resulted in significantly decreased NFκB occupancy of the *OPN* promoter at site 5 (p=0.007). This was also observed when TNFα was administered in combination with IFNγ (p=0.006). However, in contrast to site 5, significant 7-fold increased NFκB binding was detected at site 6 at site 6 on the *OPN* promoter compared to the control, in response to the combined TNFα+IFNγ treatment (p=0.04; Figure 5-10).

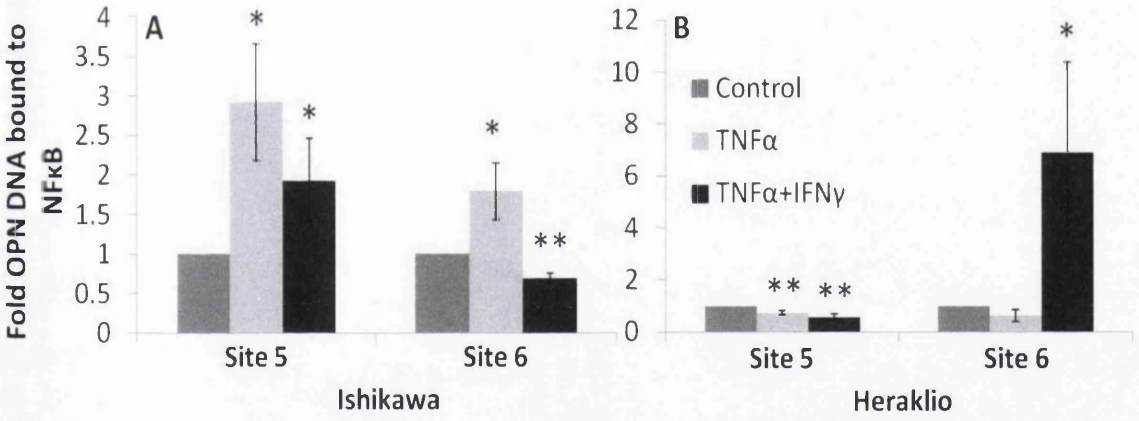

Figure 5-10 NFκB ChIP on the OPN promoter.

Quantitative PCR was conducted on NFκB immunoprecipitated promoter of OPN to measure, in fold, NFκB occupancy in Ishikawa and Heraklio cells after cytokine treatment TNFα (25ng/mL) and IFNγ (200IU) for 48hrs. Significant differences in occupation on regulatory sites occurred between the control and treatment. Values are average and SD. Statistical analysis of the data was performed using a Student's t-test (Control Vs. treatment). *, P≤0.05 **, P≤0.01, was considered significant.

5.4.3 STAT1 ChIP

ChIP for STAT1 presence at the *OPN* promoter in Ishikawa cells, in the presence of IFNγ demonstrated an average 8-fold increase in NFκB recruitment to site 7, however due to the variation in the three biological replicates this effect was not significant (P>0.05;Figure 5-11). The combination treatment of TNFα+IFNγ however, resulted in significant 3.4-fold increased STAT1 occupancy at site 7 (p=0.01). In the Heraklio cells, no significant alteration in the level of STAT1 occupancy of the *OPN* promoter was observed following treatment with IFNγ alone. When administered in combination however, a combined TNFα+IFNγ treatment resulted in a significant 2.5-fold increase in STAT1 occupancy on site 7 (p=0.006).

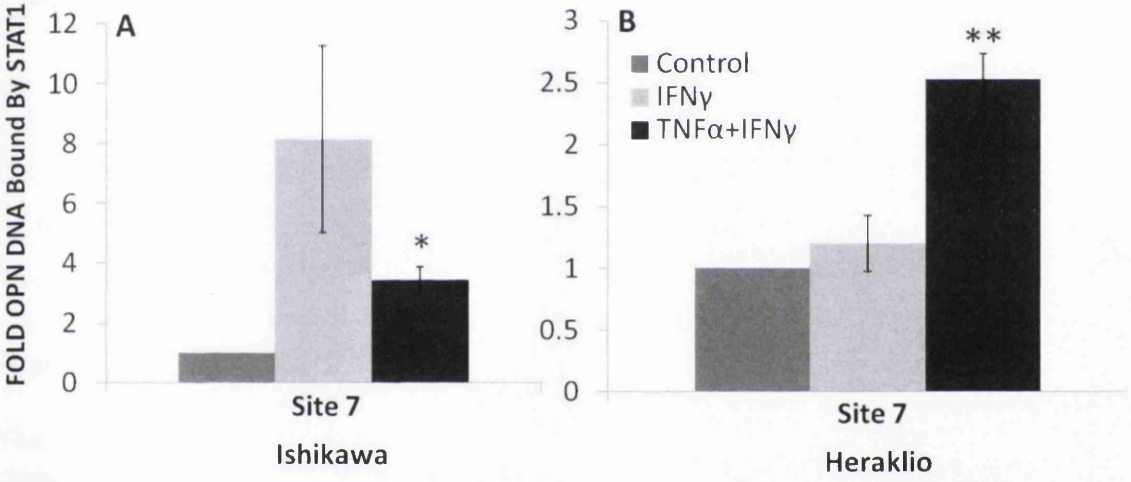

Figure 5-11 STAT1 ChIP on the OPN promoter.

Quantitative PCR was conducted on STAT1 immunoprecipitate of OPN promoter to measure, in fold, STAT1 B occupancy in Ishikawa and Heraklio cells after cytokine treatment TNFα (25ng/mL) and IFNγ (200IU) for 48hrs. Significant differences in occupation on regulatory sites occurred between the control and treatment. Values are average and SD. Statistical analysis of the data was performed using a Student's t-test (Control Vs. treatment). *, P≤0.05 **, P≤0.01, was considered significant.

5.4.4 *CD44 regulation*

The *CD44* promoter site was analysed from 2KB upstream of the ATG site to 1Kb downstream (+). One putative NFκB (site 6) binding site and six putative STAT1 binding sites (sites 3-5) were identified on the *CD44* promoter. Primers were then designed around these sites to specifically amplify these identified regions for qPCR after the ChIP procedure (Figure 5-12).

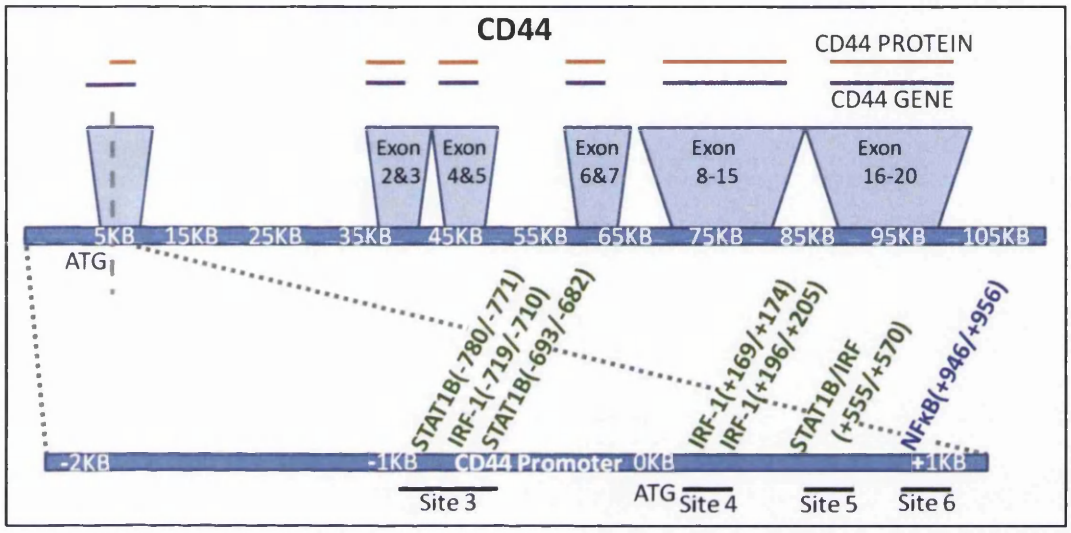

Figure 5-12 Promoter analysis of the human *CD44* gene promoter.

The CD44 promoter was analysed using Alggen Promo for NFκB and STAT1 binding sites, -2KB from the translation initiation start site to +1KB after the start site. Additional primers were designed to amplify one putative regulatory element for NFκB and six STAT1 binding sites in addition to previously described estrogen regulatory sites.

5.4.5 *NFκB ChIP*

NFκB binding to the *CD44* promoter (Figure 5-13) is increased in both cell lines in response to cytokine treatment. In the Ishikawa cell line NFκB binding was significantly increased 10-fold upon treatment with TNFα alone ($p=0.03$). Although binding was increased 3-fold with the combined cytokine treatment was not significant ($P>0.05$). In the Heraklio cell line treatment with TNFα significantly increased NFκB occupancy to the *CD44* promoter 2.8-fold ($p<0.001$). TNFα+IFNγ significantly increased NFκB occupancy 2.2-fold ($p<0.001$).

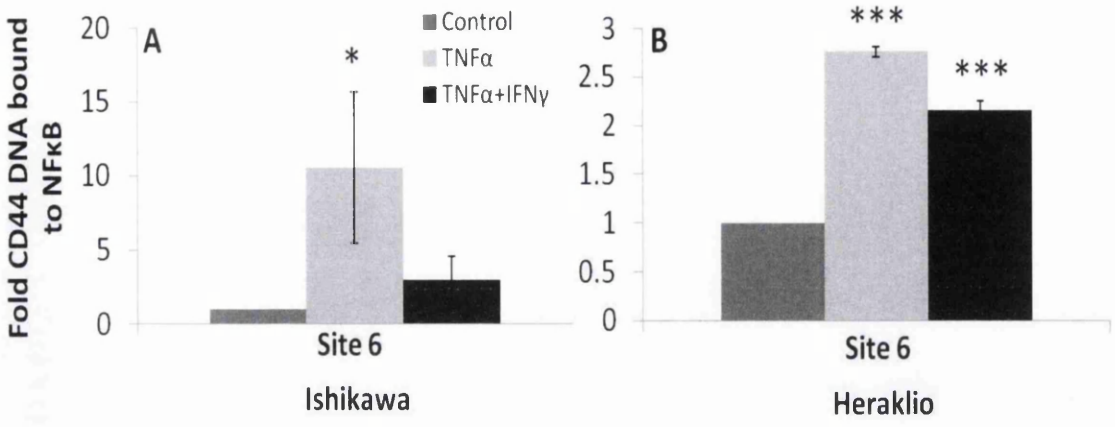

Figure 5-13 NFκB ChIP on the CD44 promoter.

Quantitative PCR was conducted on NFκB immunoprecipitate of OPN promoter to measure, in fold, NFκB occupancy (site 6) in Ishikawa and Heraklio cells after cytokine treatment TNFα (25ng/mL) and IFNγ (200IU) for 48hrs. Significant differences in occupation on regulatory sites occurred between the control and treatment. Values are average and SD. Statistical analysis of the data was performed using a Student's t-test (Control Vs. treatment). *, P≤0.05 ***, P≤0.001, was considered significant.

5.4.6 STAT1 ChIP in Ishikawa

ChIP performed to assay for the presence of STAT1 binding on the *CD44* promoter in Ishikawa resulted in differential binding patterns in response to the cytokine treatments (Figure 5-14). No significant changes in STAT1 binding were observed between the treated and untreated control group at site 3, although IFNγ treatment appeared to increase STAT1 occupancy ($p>0.05$). Significantly, 2-fold decreased STAT1 occupancy was observed at site 4 on the *CD44* promoter following treatment with IFNγ ($p=0.01$). In contrast, a significant 2.5-fold increase in STAT1 occupancy of the *CD44* promoter following IFNγ treatment was observed at site 5 ($p=0.002$). The combination treatment of TNFα+IFNγ had no influence on STAT1 occupancy to the *CD44* promoter in the regions tested.

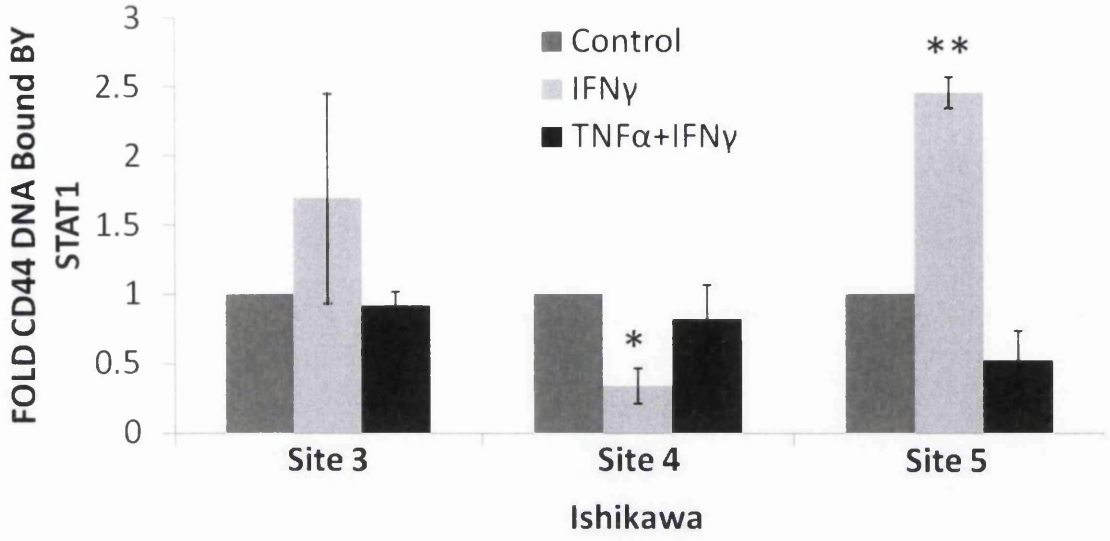

Figure 5-14 STAT1 ChIP on the CD44 promoter in Ishikawa cells.

Quantitative PCR was conducted on STAT1 immunoprecipitate of the CD44 promoter to measure, in fold, STAT1 occupancy (sites 3-5) in Ishikawa cells after cytokine treatment TNFα (25ng/mL) and IFNγ (200IU) for 48hrs. Significant differences in occupation on regulatory sites occurred between the control and treatment. Values are average and SD. Statistical analysis of the data was performed using a Student's t-test (Control Vs. treatment). *, P≤0.05 **, P≤0.01, was considered significant.

5.4.7 STAT1 ChIP in Heraklio

Treatment with pro–inflammatory cytokines influenced STAT1 binding to the *CD44* promoter in the Heraklio cell line (Figure 5-15). Both pro-inflammatory cytokine treatment regimes decreased STAT1 binding to site 3 on the *CD44* promoter. Significant 1.5 and 2-fold decreases in STAT1 binding were observed following treatment with IFNγ and TNFα+IFNγ respectively (p≤0.05). At site 4 both treatments resulted in 1.4-fold (P>0.05) and 1.6-fold (p=0.03) significantly increased STAT1 occupancy. IFNγ treatment alone resulted in significant 2.4-fold increased STAT1 binding to the *CD44* promoter, at site 5 (p=0.0002). When TNFα+IFNγ were administered in combination, an increase in STAT1 occupancy was observed at site 5, however this increase was not significant (P>0.05).

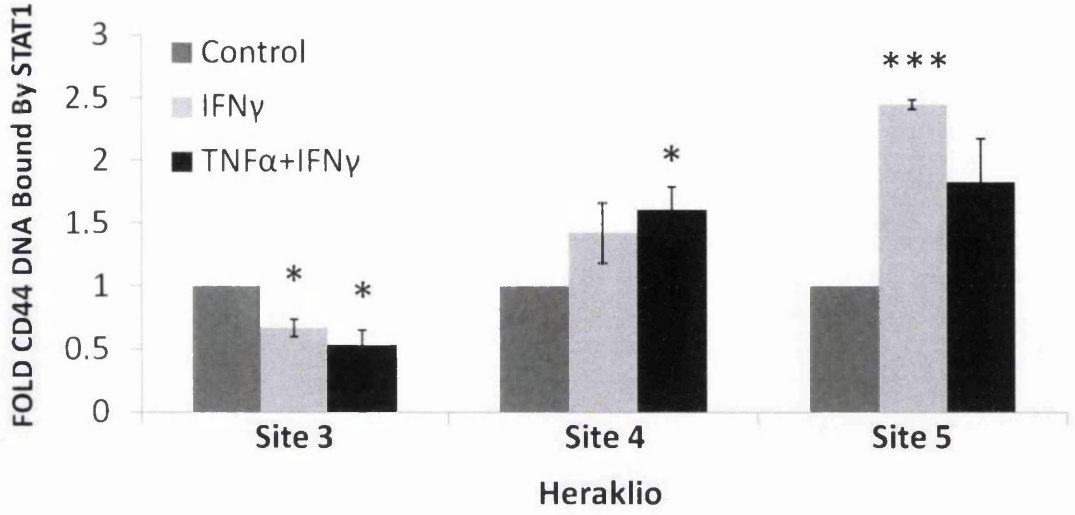

Figure 5-15 STAT1 ChIP on the CD44 promoter in Heraklio cells.

Quantitative PCR was conducted on STAT1 immunoprecipitate of CD44 promoter to measure, in fold, STAT1 occupancy (site 3-5) in Heraklio cells after cytokine treatment TNFα (25ng/mL) and IFNγ (200IU) for 48hrs. Significant differences in occupation on regulatory sites occurred between the control and treatment. Values are average and SD. Statistical analysis of the data was performed using a Student's t-test (Control Vs. treatment). *, P≤0.05 **, P≤0.01, was considered significant.

5.5 Discussion

Common characteristics of PCOS and endometriosis include disrupted cytokine expression levels, released by both leukocytes, such as monocytes, macrophages and lymphocytes and the endometrial vasculature monocytes (Dimitriadis et al. 2005; Dominguez et al. 2005). While the expression of cytokines such as TNFα and IL-1β has been detected during the window of implantation and is thought to aid implantation, their functions are not fully elucidated (Laird et al. 1996; Sarapik et al. 2012). Their detected elevated expression levels in both circulating blood and local peritoneal fluid, associated with pelvic inflammation, may indeed disrupt the expression levels of key adhesion molecules involved in the implantation cascade (as discussed in Section 5.1).

In this chapter the effect of elevated glucose and pro-inflammatory cytokine treatment on the expression of OPN and CD44 in selected endometrial epithelial cell lines was monitored in an *in vitro* model, mimicking the disrupted cytokine environment observed in endometrial pathology. ERα positive and ERα negative cell lines Ishikawa and Heraklio were grown in the presence of increasing glucose concentrations, to mimic the levels hypothesized in those suffering with type II diabetes. Levels of *OPN* increased at the mRNA level in response to 25mM of glucose in both cell models after four hours however this was not observed at the secreted protein level. CD44 expression too increased in response to 17mM of glucose in both cell lines after four hour treatment.

Bioinformatic analysis of both the *OPN* and *CD44* gene promoters revealed known and putative binding sites for NFκB and STAT1, prominent transcription factors, known to be induced in the presence of pro-inflammatory cytokines IL-1β and TNFα and IFNγ. Primers were designed to amplify regions of the promoters around these regulatory sites identified in this study along with sites previously identified. Treatment with TNFα, IFNγ and IL-1β over a 48hr period resulted in differential expression levels of OPN and CD44 at the RNA and protein level, dependent on the presence of ERα. The two cell line models responded differently to treatment with pro-inflammatory cytokines, the most striking differences were the response of OPN to TNFα and IFNγ. TNFα treatment in the Ishikawa decreased levels of *OPN* mRNA, while no effect on OPN was observed in Heraklio cells. Whilst IFNγ treatment in the Ishikawa cell line had no effect on altering OPN expression however in the Heraklio cell line, expression of *OPN* mRNA was increased. In order to elucidate the signalling mechanisms being induced in the presence of TNFα and IFNγ, ChIP analysis was conducted. In response to TNFα treatment in the Ishikawa cell line NFκB occupancy increased at site 5 and 6 whilst in the Heraklio cell line no increase in occupancy was observed by NFκB. *CD44* mRNA in response to pro-inflammatory cytokines increased in the Ishikawa cell line however TNFα was the only cytokine to increase CD44 expression in the Heraklio cell line. NFκB occupation on the *CD44* promoter is increased in response to treatment with TNFα in the

Ishikawa and Heraklio cell lines. In response to treatment with IFNγ, STAT1 occupancy on the *CD44* promoter in the Ishikawa cell line increases at site 3 and 5. In the Heraklio cell line occupancy by STAT1 on the CD44 promoter at site 5.

In the Ishikawa and Heraklio cell line the effect observed in response to 25mM of glucose at 4hrs was diminished by 24hrs possibly in response to the cells metabolising the glucose by the 24hr time point. Alternatively levels of OPN may not increase further in response to this treatment as a negative feedback mechanism. This is suggestive of *OPN* transcription being activated quickly following glucose stimulation and the effect lost after 24hrs. In the Heraklio cell line, where there was no ERα expression, a 2.6-fold increase in expression was observed compared to a 1.3-fold increase in Ishikawa. These changes were not reflected at the secreted protein level, which could be a result of the short time period, not allowing enough time for protein secretion to occur to a detectable level.

In the Ishikawa cell line, levels of CD44 increase after four and twenty four hours in response to 17mM and 25mM of glucose. However the levels after 24hrs did not increase as they did for OPN. This suggests a role for CD44 in glucose metabolism. However in the Heraklio cell line levels of *CD44* mRNA only increase in response to 17mM at four hours. It could therefore be possible that CD44 could have a requirement for ERα in sustaining the elevated levels of CD44 following glucose treatment. It may therefore be important to determine the ERα status in patients with infertility.

A study conducted by Von Wolf *et al* in 2003 showed the presence of glucose transporter facilitators in the human endometrium throughout the menstrual cycle (Wolff 2003) thus, suggesting the healthy cycling endometrium may be responsive to glucose. Increased *CD44* expression was also observed at the RNA level, as a result of increasing glucose concentrations in the Ishikawa cell line. CD44 has been indicated to play a role in glucose metabolism (Tamada et al. 2012; Kodama et al. 2012) and therefore the increase in CD44 observed could be due to a negative

feedback mechanism, leading to decreased glucose in the cells. CD44 levels have also been shown to be increased in obese insulin resistant mice compared to healthy mice (Kodama et al. 2012). This effect has been observed in animal models (mice), when *CD44* cDNA was introduced to peripheral circulating blood (Weiss et al. 2008). Insulin resistance and diabetes observed in PCOS patients with high BMI, may have higher levels of circulating glucose. This in turn may increase OPN and CD44 expression if glucose levels were above those tested here (17mM to 25mM), disrupting the adhesion protein patterning of the uterine surface. It may therefore be possible for patients prescribed regular insulin, to control their levels of glucose, according to the data shown here should also control their expression of both OPN and CD44.

Under conditions of high glucose and therefore chronic exposure, as represented by the 25mM group, OPN expression may be decreased, as shown after 24 hours. In comparison, the expression of CD44 in these circumstances may be constantly increased, in an attempt to lower the cellular glucose levels and thus disrupting the ratio of adhesion protein present at the surface of the endometrium. In addition, GLUT4 RNA expression in adipocytes has been shown to be decreased in PCOS women compared to fertile controls (Jensterle et al. 2008). If GLUT4 levels are decreased then the transport of glucose into the cells would decrease, therefore lowering the cellular glucose concentration and that of CD44 expression, but increase secreted OPN resulting in altered adhesion complex balance once again.

In the Ishikawa cell line IL-1β and TNFα treatment decreased OPN expression, and this is likely to be through the NIK→IKK→IκB pathway (Figure 1-16). IκB is degraded by IKKs, which release NFκB allowing it to dimerise and translocate in the nucleus to alter gene transcription. Binding of NFκB in the nucleus to the novel site 5 response element, as well as the previously identified site 6 at the OPN promoter is clearly demonstrated here (Samant et al. 2007). Binding to the novel NFκB site in the *OPN* promoter significantly increased after TNFα treatment. OPN signalling can influence the phosphorylation of NIK and IKKβ, which are involved in activating NFκB, which

in turn leads to IκB degradation and NFκB activation (Wang and Denhardt 2008). High levels of OPN could therefore result in high levels of NFκB, a negative feedback mechanism in Heraklio, which may explain the lack of OPN gene activation upon dual treatment with both TNFα and IL-1β treatment. However the turnover of OPN at the protein level may not be very rapid and added to the high levels of OPN protein observed result in no significant alteration in OPN secretion within the 48hrs of the experiment.

IFNγ shows no determinable regulatory effect on OPN after a 48hr treatment in Ishikawa cells, however a significant 6-fold increase in secreted protein levels are observed. This could be a result of gene transcription of OPN in response to IFNγ STAT1 signalling being very rapid and therefore not observed in the forty eight hour time frame observed. This is supported by the presence of increased STAT1 occupancy on the OPN promoter following dual treatment with TNFα and IFNγ, in Ishikawa cells. The STAT1 sites (OPN site 7) are located in close proximity to an NFκB site (OPN site 6), suggesting the possibility that NFκB is bound to the OPN promoter at site 6 preferentially. This would in turn lead to an inability of STAT1 binding at site 7 due to steric hindrance blocking the response element and resulting in no induction of signal.

In Heraklio cells there is a significant increase in OPN expression at both the RNA and secreted protein levels in response to IFNγ. This effect is also noted with the co-treatment of TNFα+IFNγ, however the response in slightly diminished at both the RNA and secreted protein level. No other cytokines alone or in combination significantly affected OPN transcript levels. This may be due to the fact that a negative feedback system for OPN expression may result in its decreased expression after 48hrs. However protein secreted into the media in the 48hr period is increased when compared to the control by all treatments, except when all three are used in combination.

The occupancy of NFκB and STAT1 transcription factors differed from that observed in Ishikawa, and a decrease in NFκB occupancy was observed at the OPN promoter

at site 5 in Heraklio. As a result, no change in the RNA level of OPN was detected when treated with TNFα after forty-eight hours. However when TNFα and IFNγ treatment were administered together, NFκB occupancy on the *OPN* promoter increased significantly at site 6. This suggests a role for the control of *OPN* gene transcription by NFκB as an increase in *OPN* mRNA levels were observed.

This mechanism supports the mRNA data, where Heraklio cells treated with IFNγ or TNFα+IFNγ show an up-regulation in *OPN* expression. The ChIP data for STAT1 suggests that it may be responsible for this increase in gene activation. STAT1, IFNγ and OPN expression has been co-localised in the lumina cells in cross sections of a porcine model (Bazer et al. 2008). Re-enforcing the IFNγ signalling pathway, phosphorylation of STAT1 occurs via TYK2 and JAK1 pathway resulting in STAT1 activation by allowing dimerization to occur. The resultant translocation into the nucleus enables STAT1 to bind and activate the transcription of *OPN*. In the Heraklio cells OPN expression is only modulated by IFNγ signalling. When treated with IFNγ alone, OPN expression is increased 2.4-fold. STAT1 binding to the *OPN* promoter is increased upon IFNγ treatment and at the mRNA level *OPN* expression is increased. When co-treatment of IFNγ and TNFα was used in combination, no change in the binding of STAT1 was observed, at the *OPN* promoter and the RNA level remained unchanged.

NFκB has been shown previously to bind the *CD44* promoter (Hinz et al. 2002) and this result is suggestive of a similar mechanism of gene regulation in the endometrium, in the presence of increased TNFα. Increased expression of CD44 expression was observed with all treatments and this was enhanced with combined treatments. ChIP detected significantly increased NFκB binding at the *CD44* promoter following TNFα treatment, when compared to the control. This however, was not observed following co-treatment with TNFα+IFNγ; suggesting NFκB is not solely responsible for the increase in gene activation observed following dual treatment STAT1 binding to the *CD44* promoter changed significantly. At STAT1 site 3, a trend of increased binding was observed, while a significant decrease in STAT1

occupancy was observed at site 4 on the *CD44* promoter. However a significant increase in STAT1 occupation/binding to the *CD44* promoter was observed site 5.

In contrast to Ishikawa cells, a significant increase in NFκB occupancy on the *CD44* promoter was observed as a result of both TNFα and combined TNFα+IFNγ treatments in the Heraklio cells. This is supportive of NFκB activation of *CD44* expression and that the mechanism is through traditional, accepted NFκB response elements. STAT1 occupancy was affected by treatment with IFNγ alone and when added in combination with TNFα. At site 3 on the *CD44* promoter STAT1 occupancy significantly decreases in response to treatment with IFNγ alone or TNFα+IFNγ in combination. At site 4 STAT1 occupancy is increased as a result of IFNγ treatment alone and significantly increased as a result of the combination treatment of TNFα+IFNγ. At site 5 STAT1 occupancy is significantly increased as a result of IFNγ treatment alone and a similar effect was observed following dual treatment with TNFα+IFNγ. Although at the mRNA level *CD44* expression was not increased in response to these treatment regimes, it suggests that the interplay between the pathways may have the effect of decreasing gene transcription of *CD44* in Heraklio cells. Alternatively this lack of gene activation could be linked with the ERα/ERβ/PR status of this cell line, which differs from the hormone status of the Ishikawa cell line.

Regulation of *OPN* and *CD44* appears to differ at the transcriptional level by NFκB and STAT1 in the Ishikawa (ERα +ve) and Heraklio (ERα -ve) cell lines. This suggests a role for ERα in the regulation of these adhesion complex genes in addition to a cross talk between the signalling pathways investigated, this is discussed further in chapter 6.

Chapter 6

General Discussion

The work described in this thesis furthers the existing knowledge of the expression of the adhesion complex components by evaluating their expression in infertility simultaneously. OPN and CD44 were shown to be differentially expressed in the endometrium of fertile and infertile women. The mechanisms of regulation of OPN and CD44 have started to become elucidated and may provide an insight into the adhesion complex regulation in infertile pathology. Chapter 3 demonstrated the levels of adhesion complex expression in infertile women relative to women of proven fertility. The first observation was that in UIF the adhesion complex expression was decreased in the secretory phase the expression of adhesion complex components CD44, ITGAV and ITGB3 were decreased in whole biopsy tissue samples obtained from infertile women. Down-regulation of ITGAV and ITGB3 are consistent with previous observations indicating that at the protein level integrin $\alpha v\beta 3$ was decreased in UIF (Tei et al. 2003). CD44 stromal protein expression was down regulated in the secretory phase endometrium of UIF, down-regulation of CD44 has not been demonstrated previously at the mRNA or protein level proving to be an exciting novel result. In the anovulatory PCOS women it was observed that expression of OPN, CD44 and ITGB3 mRNA were decreased in the secretory phase endometrium. Consistently, decreased levels of $\alpha v\beta 3$ in anovulatory PCOS have previously been reported in the literature (Apparao et al. 2002). In addition women diagnosed with ovulatory PCOS showed that levels of CD44 protein were down regulated in the endometrial glands of the secretory phase, an observation not reported previously. This work has demonstrated that in women with endometriosis stromal OPN protein expression in the proliferative phase was decreased. Whilst this contrasts to a previous study that indicated endometrial mRNA endometrial levels and blood plasma levels of OPN were increased in endometriosis (Cho et al. 2009), tissue protein levels were measured in this study and this may suggest that regulation of OPN in tissues is post transcriptional. In the endometriosis group ITGB3 expression was decreased at the mRNA level in the secretory phase, again another novel observation as levels of ITGB3 have not been described previously in endometriosis throughout the menstrual cycle (Chapter 3). To relate these observations to ER status, increased

ERα expression has been identified in PCOS and endometriosis pathologies in the glands, lumina cells and stroma (Margarit et al. 2010). This study has shown that high ERα expression could impact on the regulation of OPN and CD44, resulting in decreased expression of the adhesion complex. This may affect its function as a linker complex between the epithelial and trophoblast cells during implantation (Yen and Jaffe 2009; Singh and Aplin 2009).

6.1 Regulation of adhesion complex components by nuclear receptor signalling

This study has indicated, using an *in vitro* model that OPN and CD44 are regulated by hormones E_2 and P_4; and that expression is ERα dependent in endometrial epithelial cells Ishikawa and Heraklio (Chapter 4). The markedly different expression of OPN and CD44 between the Ishikawa and Heraklio cell lines could be due to their differential expression of ERα, ERβ and PR (Table 6-1).

	Ishikawa	Heraklio
ERα	+++	-
ERβ	+	++
PR	+++	-
OPN	+	+++
CD44	+	++

Table 6-1 Summary of Ishikawa and Heraklio cell line expression status

Ishikawa cells are characterised as ERα/ERβ/PR +ve, whilst Heraklio are ERα/PR -ve, ERβ +ve. As no PR regulatory elements on the *OPN* or *CD44* promoter have been identified in the literature, our studies have focused on the role of EREs, ERα, SP-1 and AP-1 found in the *OPN* promoter (Sharma et al. 2010; Wang et al. 2000b; Bidder et al. 2002). At the basal level (i.e. in the absence of exogenous E_2) more ERα was found to bind to the *OPN* binding site 1 for ERα and the CD44 binding sites 1 and 2 for ERα in Ishikawa when compared to Heraklio suggesting that ERα is required in Ishikawa to maintain OPN and CD44 basal expression levels. OPN

promoter analysis revealed that ERα binding to site 1 was preferential to site 2 (Sharma et al. 2010; Wang et al. 2000b; Bidder et al. 2002) suggesting that in endometrial epithelial cells site 1 is highly important in the regulation of OPN.

Preliminary data has shown that following E_2 treatment the occupancy of ERα on site 1 of the *OPN* promoter was increased 40-fold (Figure 6-1). This indicates that the increase in *OPN* mRNA expression observed in chapter 4, was likely due to E_2 driven binding of ERα at this site. Site 1 contains 1 ERE and two AP-1 elements and it remains to be determined which of these sites is key for E_2 regulation of OPN.

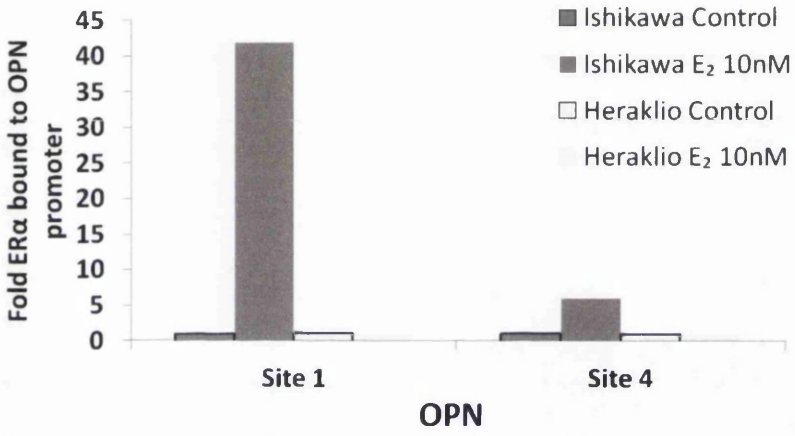

Figure 6-1 E_2 induced ERα occupancy on the OPN promoter.

ChIP was conducted on ERα precipitate of the OPN promoter to measure, ERα occupancy in Ishikawa and Heraklio cells after treatment with E_2 (10nM). Values from one biological repeat.

Regulation of OPN and CD44 expression by hormones E_2 and P_4 was demonstrated in ERα positive Ishikawa cells. Both cell lines were shown to be responsive to E_2 and P_4, as well characterised targets of ER and PR signalling pathway were shown to be activated. A study by Stossi evaluated the expression of levels of genes regulated by ERα and ERβ in response to E_2 (10nM) in cell lines transfected to stably express ERα or ERβ. Of the four genes measured *GREB1* expression increased in a time dependant manner with expression peaking at 48hrs. The levels of *GREB1* expressed were also very consistent between the ERα and ERβ stable cells (Stossi et al. 2004). In this study increases in *GREB1* (Figure 4-6) were shown to be consistent

at 48hrs with that of Stossi's study re-enforcing the active signalling of ERα in Ishikawa cells, and ERβ in Heraklio cells. The increases noted in the Ishikawa cells in response to hormones were not mirrored in Heraklio cells. In the context of the findings from chapter 4 this suggests a very different role for OPN and CD44 by the ERα and ERβ receptors.

6.2 Regulation of the adhesion complex by glucose

Glucose regulation of *OPN* and *CD44* was demonstrated in chapter 5 and shown to be ERα independent for *OPN* and ERα dependent for *CD44*. Similar responses were observed in OPN and CD44 expression in both the Ishikawa and Heraklio cells as a result of glucose treatments (Chapter 5). In response to 25mM of glucose *OPN* mRNA expression increased in both cell lines after 4hrs. This effect was lost at 24hrs in both cell lines possibly due to decreased glucose levels following cellular metabolism. The expression of *CD44* was modulated by glucose treatment; however levels were still high at 24hrs, this maybe a result of *CD44* regulating glucose expression in cells. A recent study suggested that ablation of *CD44* increased the levels of glucose and its related metabolites in the glycolysis pathway suggesting that CD44 could have a role in the regulation of glucose (Tamada et al. 2012).

6.3 Regulation of the adhesion complex by pro-inflammatory cytokines

The regulation of OPN and CD44 by pro-inflammatory cytokines was explored in chapter 5 and demonstrated that both OPN and CD44 expression were regulated by TNFα, IL-1β and IFNγ. Further to this, the direct regulation of NFκB and STAT1 through TNFα and IFNγ signalling was characterised. The direct modulation of these transcription factors was shown to differ between the ERα +ve and -ve cell lines. Treatment of cells with TNFα and IFNγ showed the most striking differences between the cell lines, and suggested a role for ERα. TNFα treatment in the Ishikawa cells decreased levels of *OPN* mRNA, while no effect on *OPN* was observed

in Heraklio cells. Whilst IFNγ treatment in the Ishikawa cell line had no effect on altering *OPN* expression however in the Heraklio cell line, expression of *OPN* mRNA was increased. Therefore these treatments were chosen to investigate the direct regulation of *OPN* and *CD44* utilising ChIP. Putative regulatory elements on the *OPN* promoter were identified. These sites include ERα/AP-1 (site 1), NFκB (site 5) and STAT1 (site 7). A binding site for NFκB on the *OPN* promoter (site 6) had been identified previously to contain 9 conserved and 3 non-conserved bases (GGG GAA GTC CAA) when compared to the consensus NFκB sequence (GGG AAA GTC CCC). Using EMSA and ChIP to demonstrate that the p65 unit of NFκB was capable of binding to this sequence (Samant et al. 2007). A novel NFκB site (site 5) was identified in this study, and positive binding by NFκB was demonstrated by ChIP (CGG ACT TTC CCT). Putative regulatory elements were also identified in the CD44 promoter. These include sites for ERα, AP-1 and SP-1 (Site 1 and 2), STAT1 (site 5) and NFκB (site 6). The putative *CD44* NFκB site 5 (GGG GAG GGG CTG) was bound by NFκB following TNFα treatment suggesting this site plays an important role in *CD44* regulation in response to TNFα signalling in the endometrium. Novel binding sites for ERα, AP-1, NFκB and STAT1/IRF-1 have been identified.

6.4 Conclusion

The main aim of this study was to understand the regulation of the adhesion complex components OPN and CD44 in clinical samples and cellular models.

The study of clinical samples clearly demonstrated that the expression patterns of both OPN and CD44 were perturbed in the tissues of patients diagnosed with PCOS, endometriosis and UIF. Using the adhesion complex component expression as a panel of markers enables the distinction of different infertile pathologies. For the first time a specific marker was unveiled for UIF, where levels of CD44 were down regulated in stroma of these patients. As this change is unlikely to directly affect trophoblast attachment, further investigations to determine effects on signalling to the uterine surface, or establishment of implantation will be required. Nevertheless, it is now important to conduct a larger study of UIF patients to

determine whether CD44 can be used as an effective marker to characterise and potentially stratify these patients.

The study of three distinct signalling pathways; hormones (E_2 and P_4), glucose and pro-inflammatory cytokines (IL-1β, TNFα and IFNγ), revealed that regulation of OPN and CD44 was incredibly complex, with each pathway having a subtle role in the control of these key adhesion complex components. This is the first time that the three pathways have been investigated simultaneously in an unbiased way in a single study. This approach has demonstrated the need to now investigate the regulation of OPN and CD44 in model systems that even more closely mimic the local environment experienced by endometrial cells in healthy tissue, as well as samples originating from PCOS, endometriosis, and UIF patients. This notion is further supported by the analysis that was undertaken to consider the direct regulation of OPN and CD44 by the key transcription factors ERα, NFκB, and STAT1, that are known to control the response to E_2, and the pro-inflammatory cytokines TNFα and INFγ. The detailed observations made in this study revealed that these transcription factors occupied the promoters of both *OPN* and *CD44*. More importantly this analysis revealed novel regulatory elements within the promoter region of the genes encoding these two proteins (Figure 6-2).

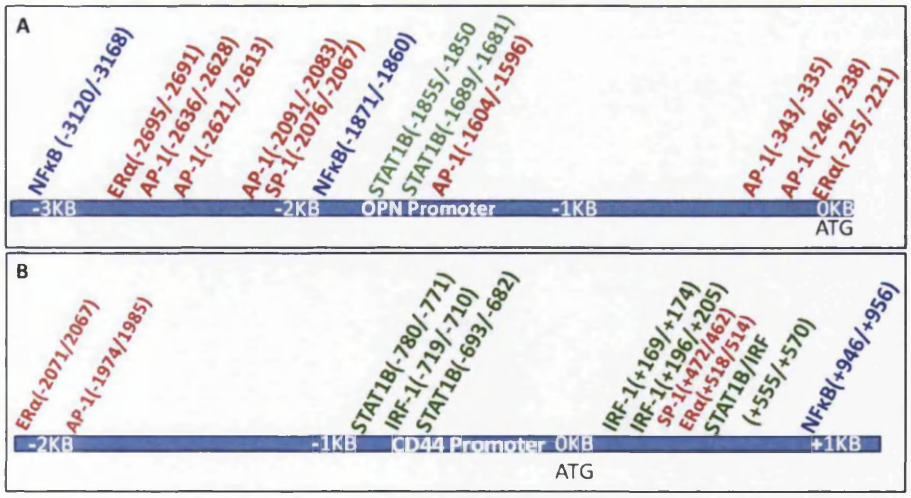

Figure 6-2 OPN and CD44 promoter regulatory elements.

These elements had adjacencies to one another which further supports the suggestion of a subtle balance of co-regulation (or dysregulation) by hormones and cytokines of OPN and CD44. Close monitoring of circulating levels of cytokines, hormones and blood glucose, the regulation of these factors by treatment with combinations of anti-inflammatory, insulin sensitising, and hormone balancing therapies could result in the re-balancing of the expression levels of adhesion complex components, and contribute to restoring fertility. However there is much work to be done before reaching this point.

6.5 Further work

To establish the role ERα plays in the regulation of OPN and CD44 the Ishikawa cell line could be transfected with RNAi to knock out the expression of ERα, similar results to that of Heraklio regulation of OPN and CD44 would suggest regulation via ERα. Alternatively, the Heraklio cell line could be transfected to express ERα and results similar to that in Ishikawa would hint to regulation via ERα.

High resolution mapping or EMSA would distinguish which of multiple sites detected by some primer sequences were responsible for the regulation of OPN and CD44, allowing further work to be conducted.

To determine if the co-factors associated with ERα, AP-1, SP-1, STAT1 and NFκB play a role, sequential ChIP could be conducted. This would involve an initial ChIP for example on ERα, this would be subject to ChIP again but for a co-factor such as SRC. This would establish which of the transcription factors are bound to co-activators and may elucidate the interplay between co-factors and transcription factors that are located very close to one another on the promoter sequence (Figure 6-2).

Finally results from these experiments would inform more specific regulation tests that could be conducted on biopsy samples, leading to a greater understanding of

the mechanisms of expression and possibly to a therapeutic solution to restore receptivity.

Appendicies

A: RNA Protocol for RNeasy Kit Qiagen

1. Cells grown in a monolayer (do not use more than 1 x 10^7 cells): Cells can be either lysed directly in the cell-culture vessel (up to 10 cm diameter) or trypsinized and collected as a cell pellet prior to lysis.

2. Disrupt the cells by adding Buffer RLT. For pelleted cells, loosen the cell pellet thoroughly by flicking the tube. Add the appropriate volume of Buffer RLT (see Table 5). Vortex or pipette to mix, and proceed to step 3.

3. Pipette the lysate directly into a QIAshredder spin column placed in a 2mL collection tube, and centrifuge for 2min at full speed. Proceed to step 4.

4. Add 1 volume of 70% ethanol to the homogenized lysate, and mix well by pipetting. Do not centrifuge.

5. Transfer up to 700µL of the sample, including any precipitate that may have formed, to an RNeasy spin column placed in a 2mL collection tube (supplied). Close the lid gently, and centrifuge for 15 s at 8000*xg* Discard the flowthrough.

6. Add 700µL Buffer RW1 to the RNeasy spin column. Close the lid gently, and centrifuge for 15s at 8000*xg* to wash the spin column membrane. Discard the flow-through.

7. Add 500µL Buffer RPE to the RNeasy spin column. Close the lid gently, and centrifuge for 15s at 8000*xg* to wash the spin column membrane. Discard the flow-through.

8. Add 500µL Buffer RPE to the RNeasy spin column. Close the lid gently, and centrifuge for 2min at 8000*xg* to wash the spin column membrane.

9. Optional: Place the RNeasy spin column in a new 2mL collection tube (supplied), and discard the old collection tube with the flow-through. Close the lid gently, and centrifuge at full speed for 1min.

10. Place the RNeasy spin column in a new 1.5mL collection tube (supplied). Add 30–50µL RNase-free water directly to the spin column membrane. Close the lid gently, and centrifuge for 1min at 8000*xg* to elute the RNA.

B: Qiaquick DNA purification

1. Add 5 volumes of Buffer PB to 1 volume of the PCR sample and mix. For example, add 50µL of Buffer PB to 100µL PCR sample.

2. If pH Indicator I has been added to Buffer PB, check that the color of the mixture is yellow. If the color of the mixture is orange or violet, add 10µL of 3M sodium acetate, pH 5.0, and mix. The color of the mixture will turn to yellow.

3. Place a QIAquick spin column in a provided 2mL collection tube.

4. To bind DNA, apply the sample to the QIAquick column and centrifuge for 30–60s.

5. Discard flow-through. Place the QIAquick column back into the same tube. Collection tubes are re-used to reduce plastic waste.

6. To wash, add 0.75mL Buffer PE to the QIAquick column and centrifuge for 30–60s.

7. Discard flow-through and place the QIAquick column back in the same tube. Centrifuge the column for an additional 1min.

IMPORTANT: Residual ethanol from Buffer PE will not be completely removed unless the flow-through is discarded before this additional centrifugation.

8. Place QIAquick column in a clean 1.5mL microcentrifuge tube.

9. To elute DNA, add 50µL Buffer EB (10 mM Tris·Cl, pH 8.5) or water (pH 7.0–8.5) to the center of the QIAquick membrane and centrifuge the column for 1min. Alternatively, for increased DNA concentration, add 30µL elution buffer to the center of the QIAquick membrane, let the column stand for 1min, and then centrifuge.

Note: All centrifugation steps are carried out at 17,900*xg*

C: RNA normality test

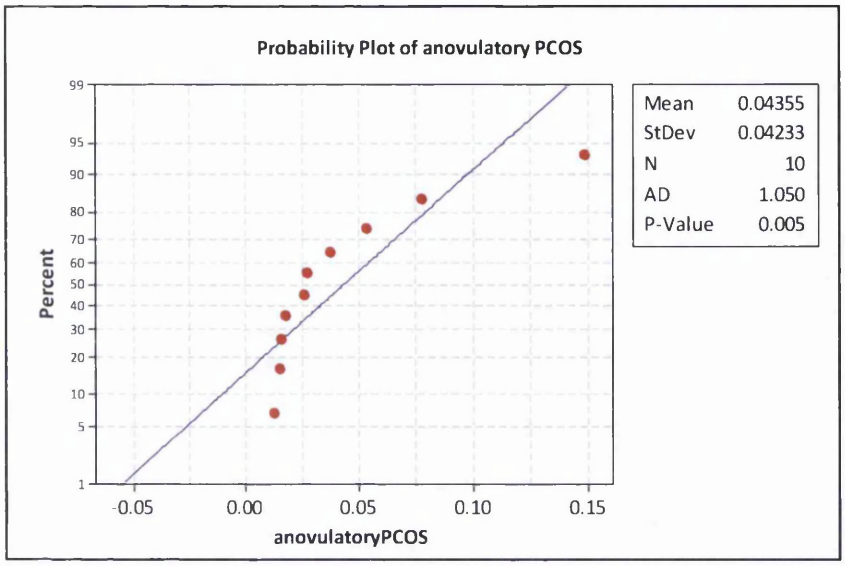

Normality testing using the Anderson Darling test. Data distribution analysis for each patient cohort group. All data obtained for RNA starting quantity were grouped and the normality of the distribution of the data assessed. The data for anovulatory PCOS patients is shown here and is significantly different from a normal distribution ($p<0.005$). This example is representative and indicative of the observed heterogeneity in the clinical data obtained.

D: Melt curve analysis for optimal annealing temperature for qPCR

Primer Name	Sequence	Location	Amplicon	Primer length (bp)	Beacon Rating	Ta (°C)	Tm (°C)
OPN 3 F	ATGGATGAGGGAACAAGGATAGG	4322-4344	155	23	79.4	52.4	89.6
OPN 3 R	GCAGAAGTAAAGCAGTTTC	4458-4476	155	19	74.9	52.4	89.6

Run at 52.3˚C:

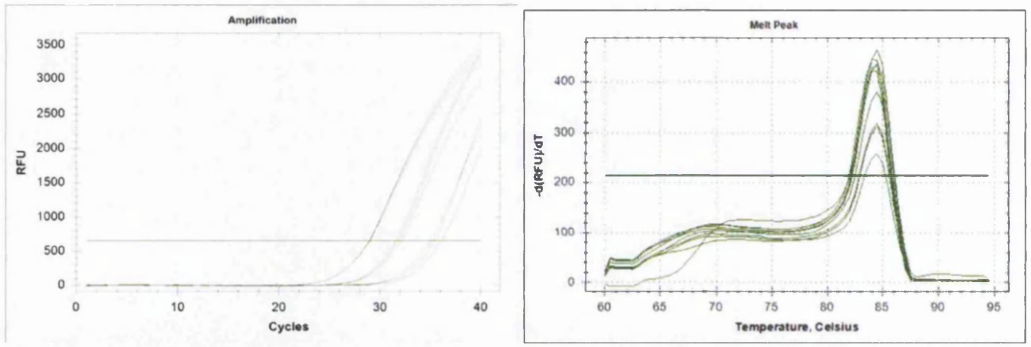

Run at 59.4˚C:

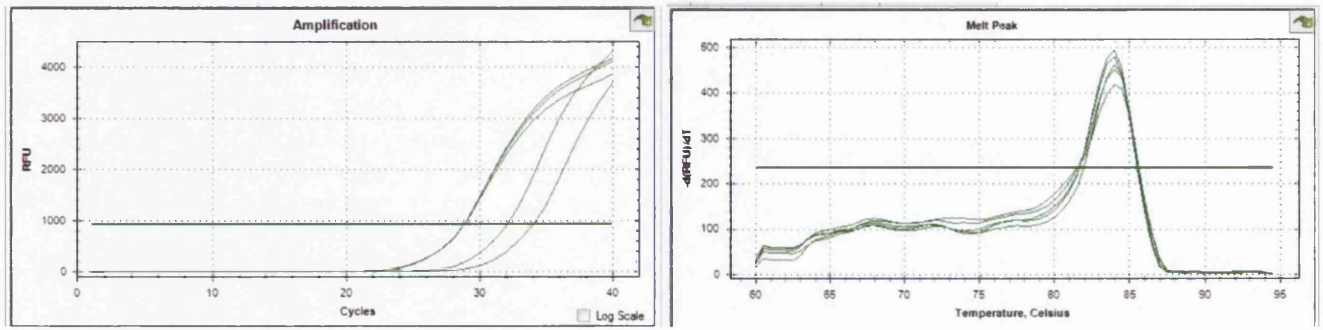

Primer Name	Sequence	Location	Amplicon	Primer length (bp)	Beacon Rating	Ta (°C)	Tm (°C)
OPN 4 F	TCTTCCTGGATGCTGAATGC	4807-4826	250	20	79	52.8	88
OPN 4 R	CCAAGCCCTCCCAGAATTTA	4036-5056	250	20	55.5	52.8	88

Run at 52.3˚C:

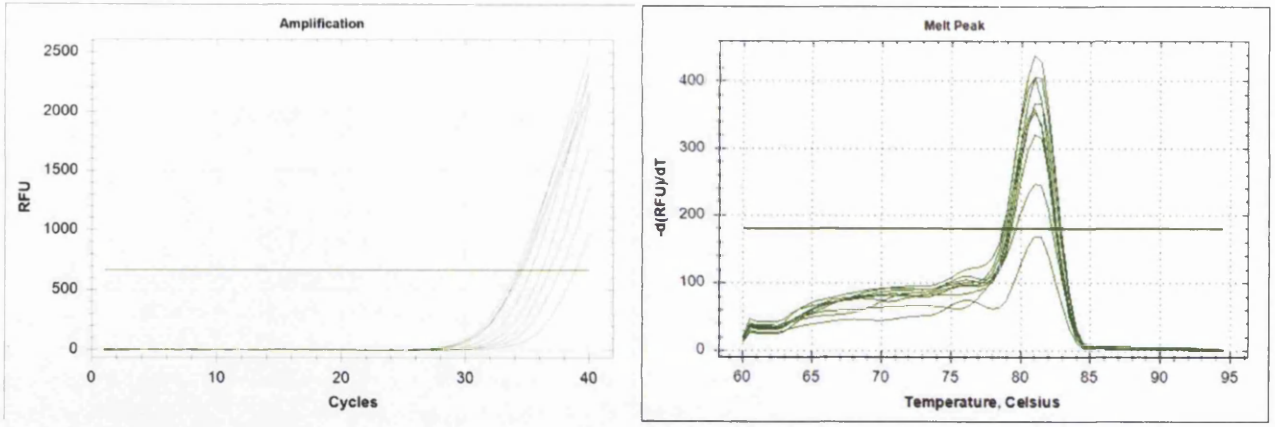

When run at 59.4˚C:

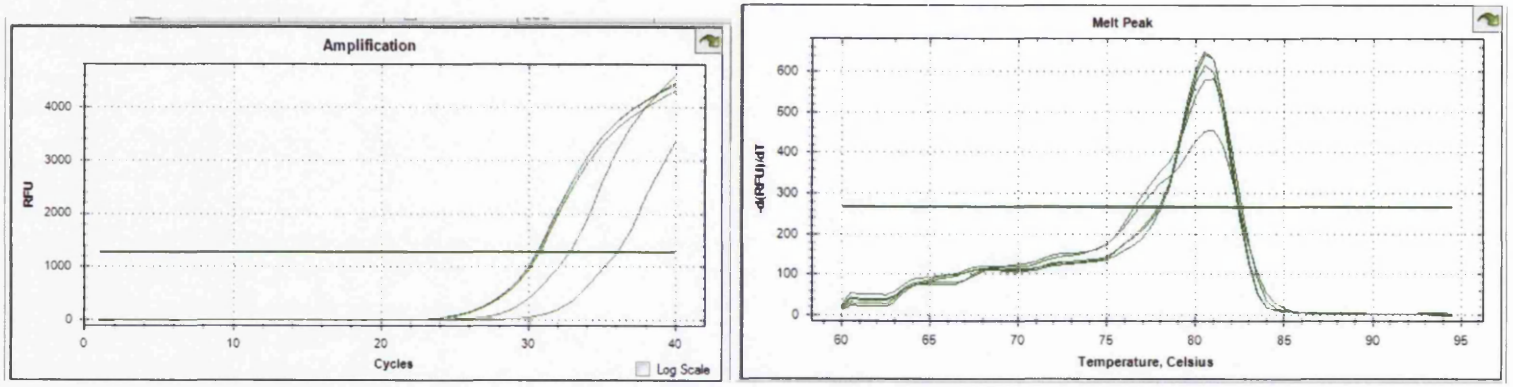

Primer Name	Sequence	Location	Amplicon	Primer length (bp)	Beacon Rating	Ta (°C)	Tm (°C)
OPN 5 F	TCAGCCAAACGCCGACCAAG	5132-5151	192	20	79.1	51.7	83.7
OPN 5 R	CTAGACACCTTTGTTCCAGGAGACC	5299-5323	192	25	70.3	51.7	83.7

Run at 52.3˚C:

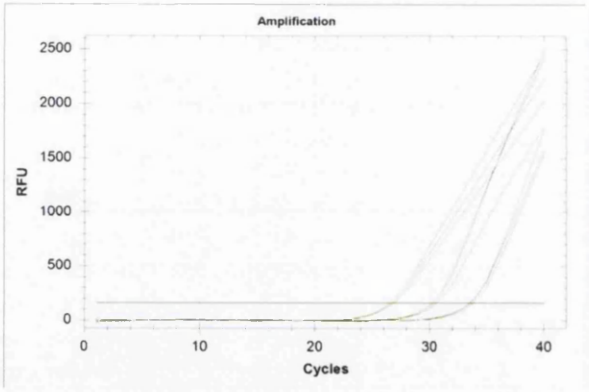

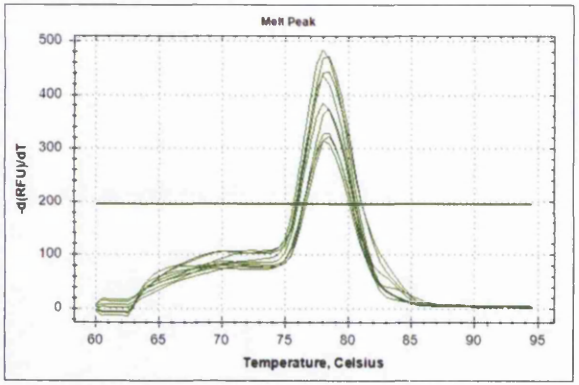

Primer Name	Sequence	Location	Amplicon	Primer length (bp)	Beacon Rating	Ta (°C)	Tm (°C)
OPN 7 F	GGAAACCACCGATGCTAATCAG	5386-5407	205	22	79.5	48.5	80.9
OPN 7 R	AGCAGTGGCATATTCAGAAAGG	5569-5590	205	22	80.4	48.5	80.9

At 49:

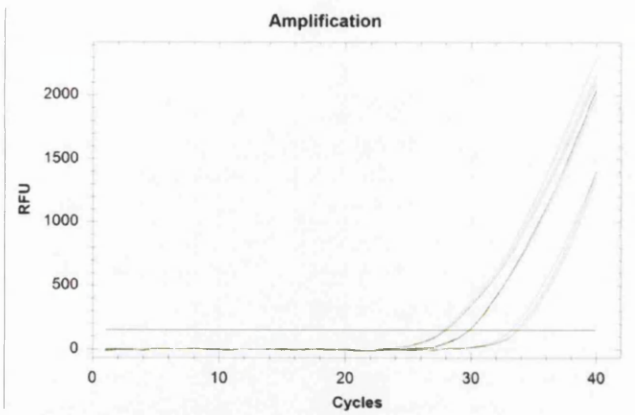

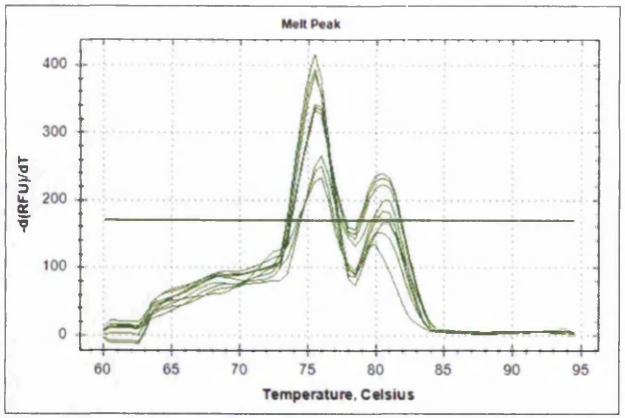

At 60.1:

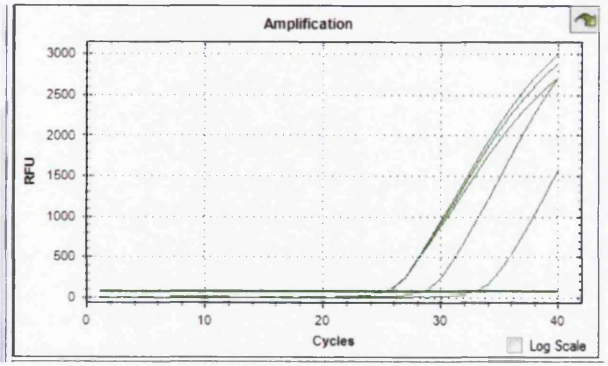

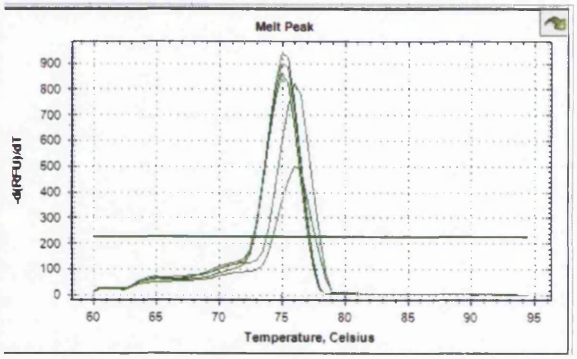

Primer Name	Sequence	Location	Amplicon	Primer length (bp)	Beacon Rating	Ta (°C)	Tm (°C)
OPN 8 F	TGTATGATGAGTTATCGCATGTAAG	6682-6706	243	25	81.5	48.8	81.8
OPN 8 R	ACAAACAGCACACATAGACTTTC	6902-6924	243	23	81	48.8	81.8

Run at 48.8 ˚C:

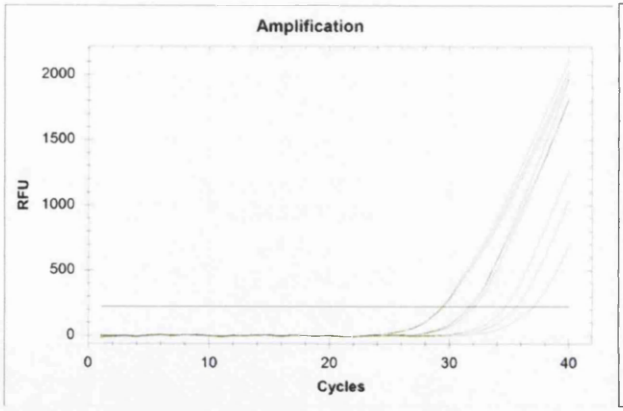

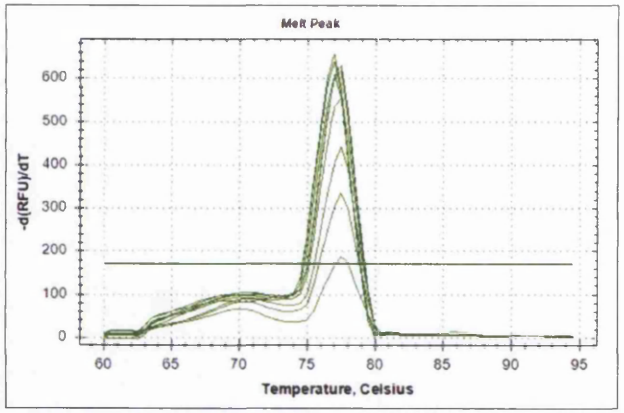

Primer Name	Sequence	Location	Amplicon	Primer length (bp)	Beacon Rating	Ta (°C)	Tm (°C)
OPN 9 F	GCTACTGGGTTGTGCATTC	5166-5175	243	19	68.1	48.5	83
OPN IRF 9 R	TTCTGATTAGCATCGGTGG	5387-5409	243	19	75.3	48.5	83

Run at 48.8˚C:

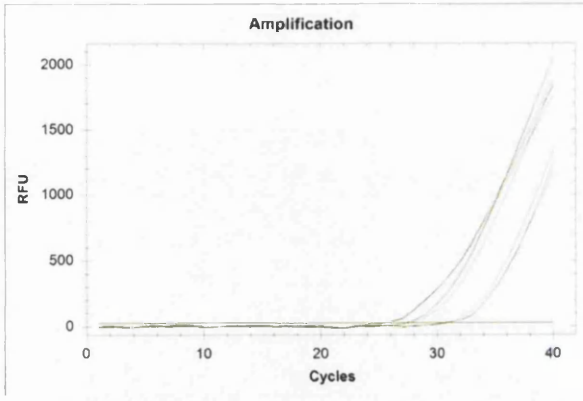

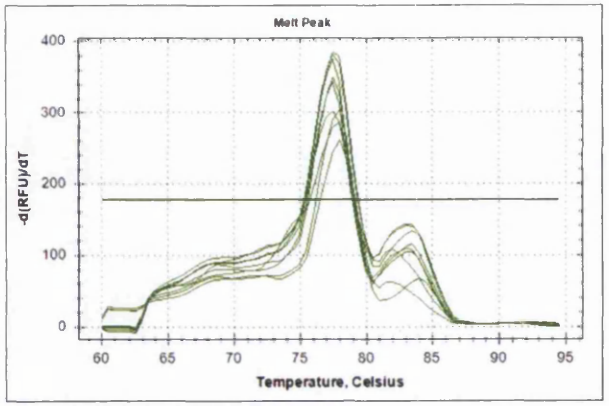

At 60.5˚C:

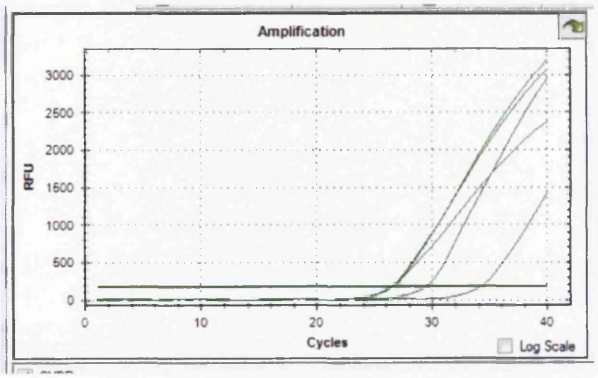

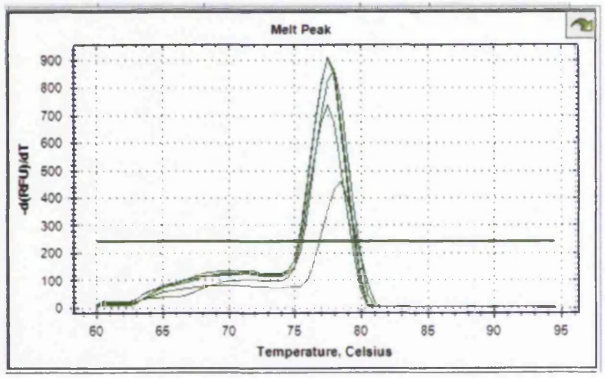

Primer Name	Sequence	Location	Amplicon	Primer length (bp)	Beacon rating	Ta (°C)	Tm (°C)
CD44 2 F	ACACTGGCTTGAACACATGGGTTAG	4593-4617	250	25	72.3	57.7	91.9
CD44 2 R	GCTGGAGAGAGGGCGAGGTC	4823-4842	250	20	77.5	57.7	91.9

Run at 57.1˚C

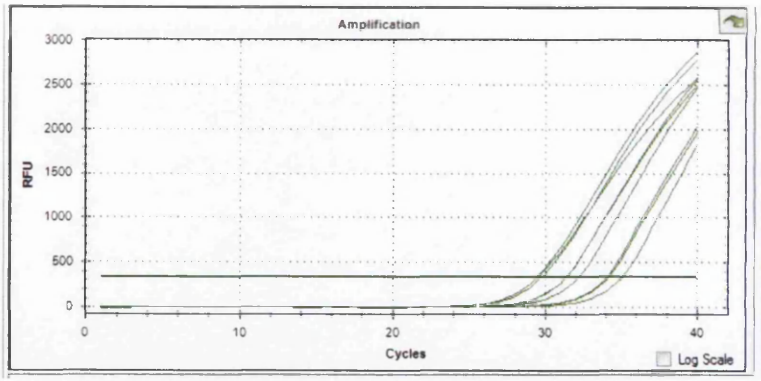

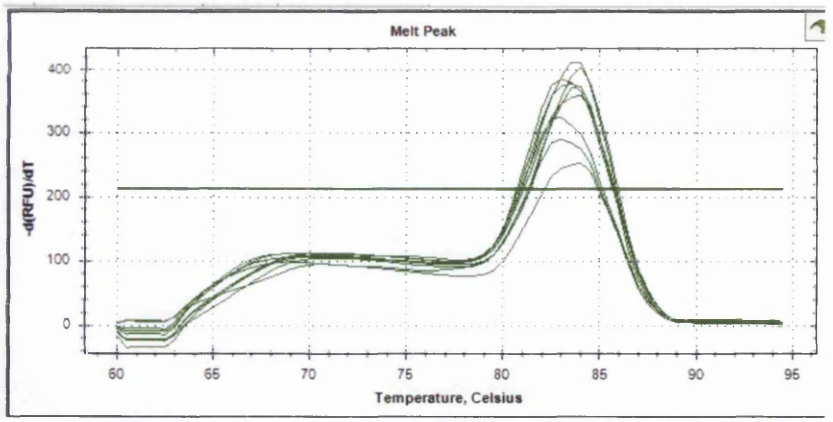

Primer Name	Sequence	Location	Amplicon	Primer length (bp)	Beacon rating	Ta (°C)	Tm (°C)
CD44 3 F	TGGGTGCG GGGTGCTCAG	5532-5541	159	19	71.7	61	95.2
CD44 3 R	TGCTTCCACAGACACATTCTCCAAC	5666-5690	159	25	77.6	61.5	95.2

At 61°C:

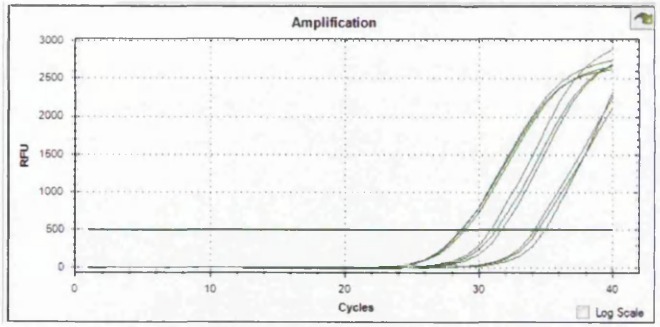

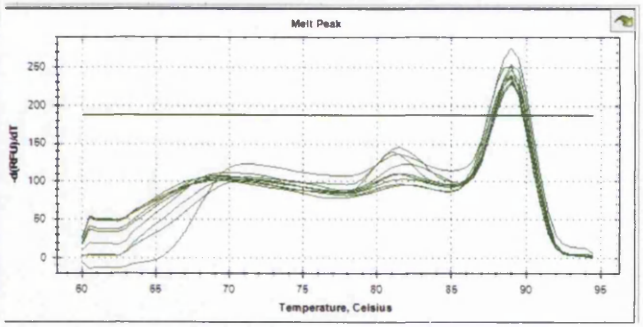

At 59.4:

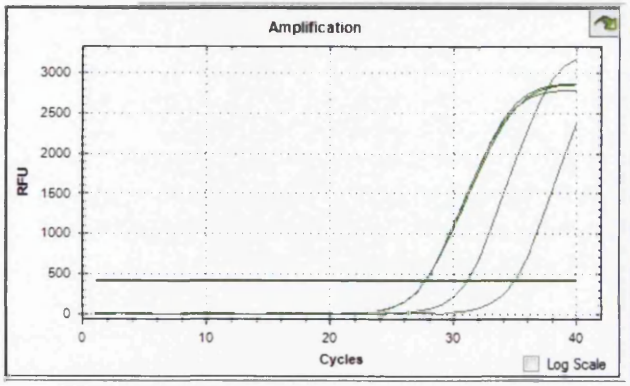

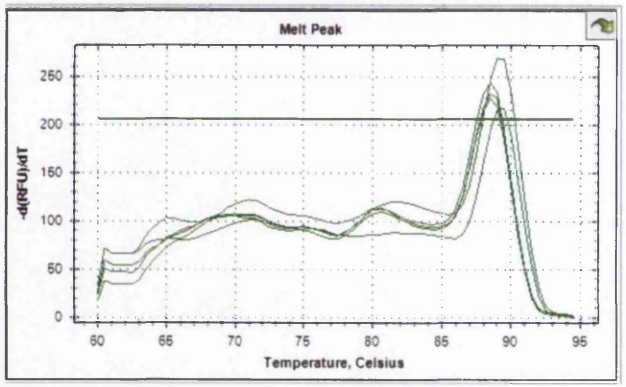

Primer Name	Sequence	Location	Amplicon	Primer length (bp)	Beacon rating	Ta (°C)	Tm (°C)
CD44 4 F	TGTGTCTAGGCAGGGCAGAG	5876-5896	179	20	74.5	56.7	92.2
CD44 4 R	GCTTTGGAACAAGGCTCAGTG	6034-6054	179	21	75.8	56.7	92.2

Run at 60.1:

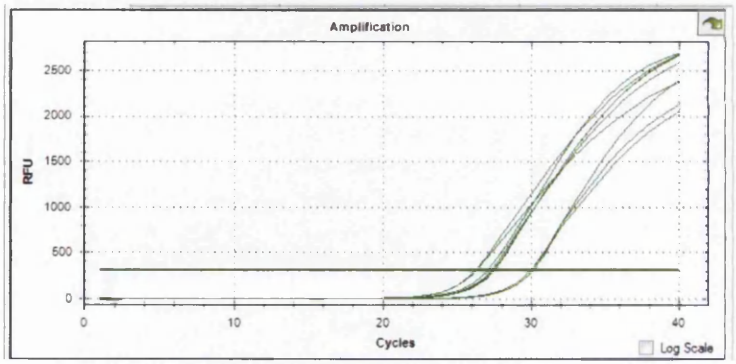

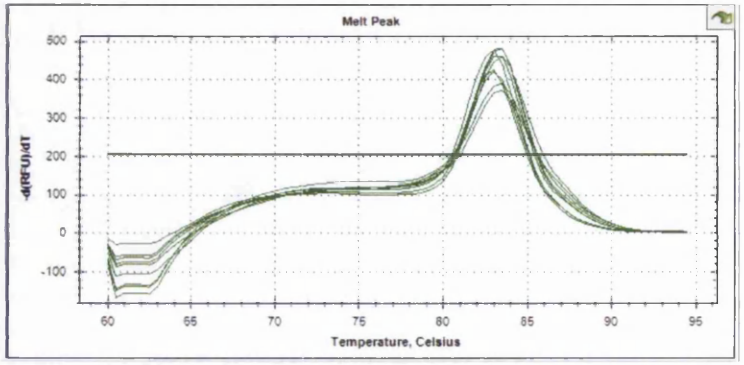

Run at 56:

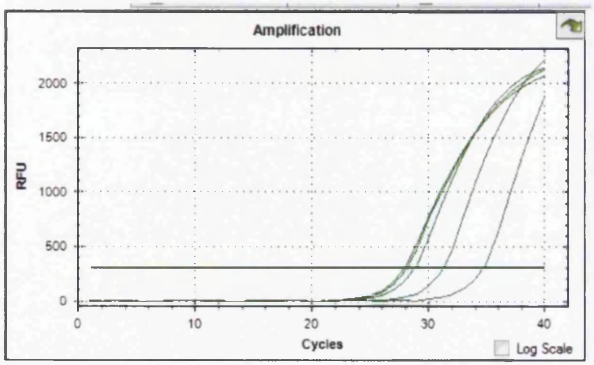

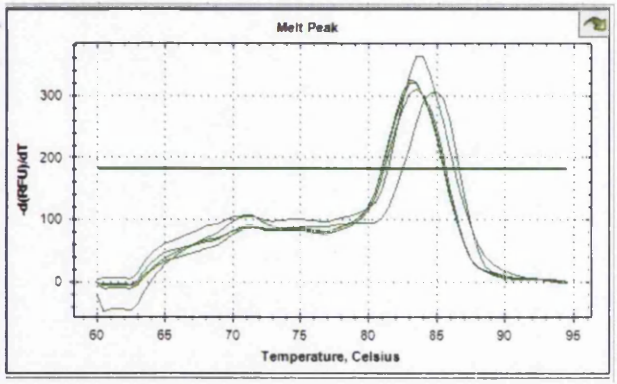

Primer Name	Sequence	Location	Amplicon	Primer length (bp)	Beacon rating	Ta (°C)	Tm (°C)
CD44 6 F	GCCTGGCAGCCTCAGAGCAGAGAG	6264-6287	131	24	65.8	58.3	90.5
CD44 6 R	CGCAGCCCCTCCCCTCCATAGC	6373-6394	131	22	71.7	58.3	90.5

At 58:

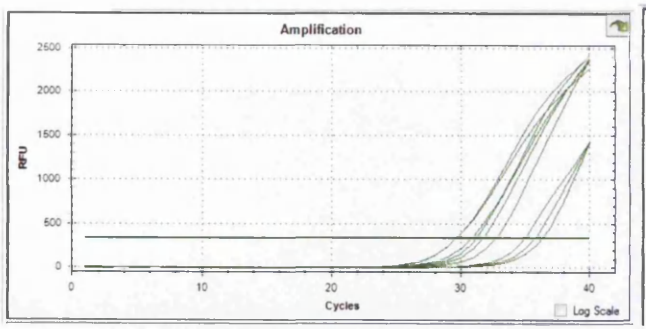

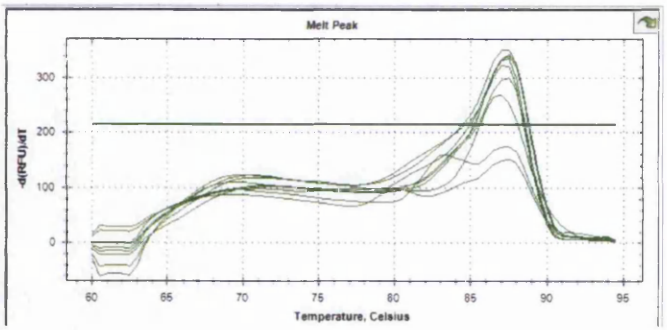

At 55.1:

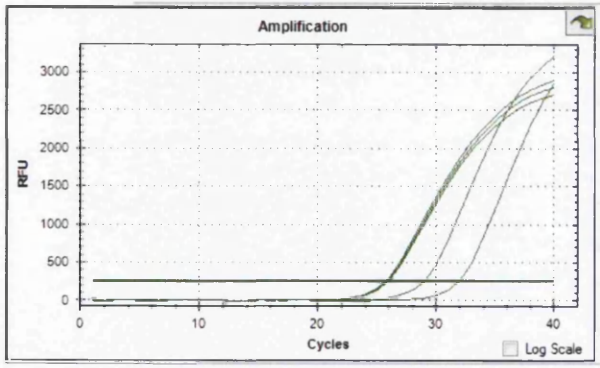

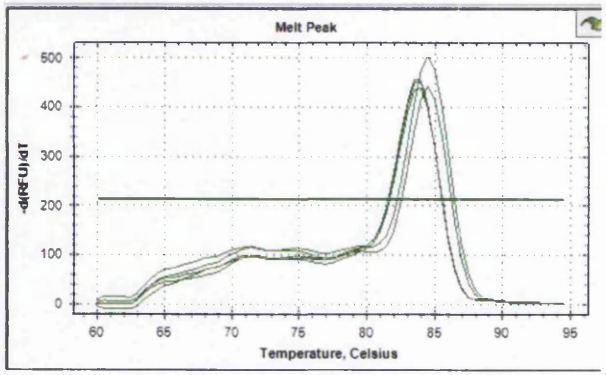

Primer Name	Sequence	Location	Amplicon	Primer length (bp)	Beacon rating	Ta (°C)	Tm (°C)
CD44 7 F	AGGCAAGGTCACACAACTAAGAAGC	3358-3382	241	25	76	54.5	88.3
CD44 7 R	ACCATTCCTAGAGAAGGGAGTCAC	3575-3598	241	24	65.3	54.5	88.3

Run at 54.3˚C:

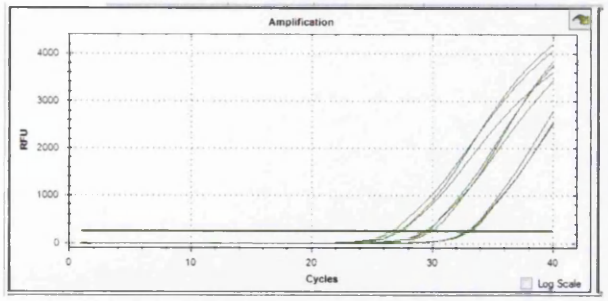

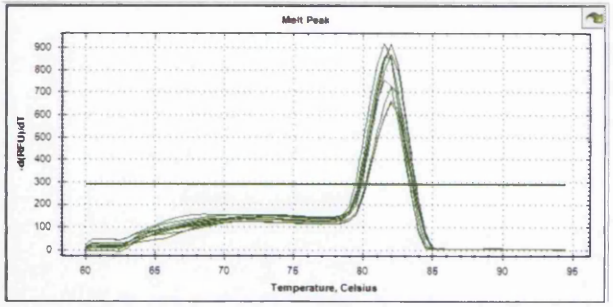

Primer Name	Sequence	Location	Amplicon	Primer length (bp)	Beacon rating	Ta (°C)	Tm (°C)
CD44 9 F	GCACAGTCGTTGTCTGGACT	5813-5833	185	20		58.89	59.5
CD44 9 R	ACCCATTGCCAGCTAGTC	5978-5998	185	20		60.9	

Run at 60˚C:

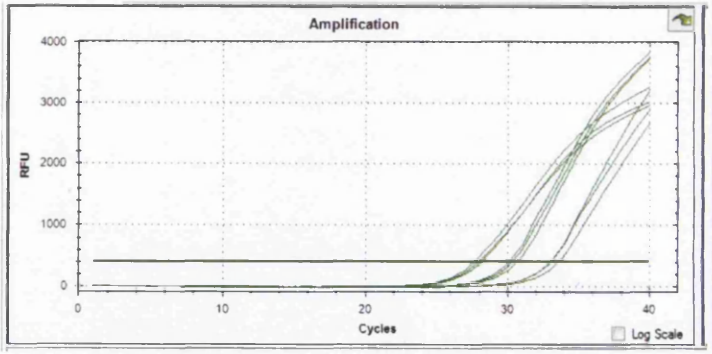

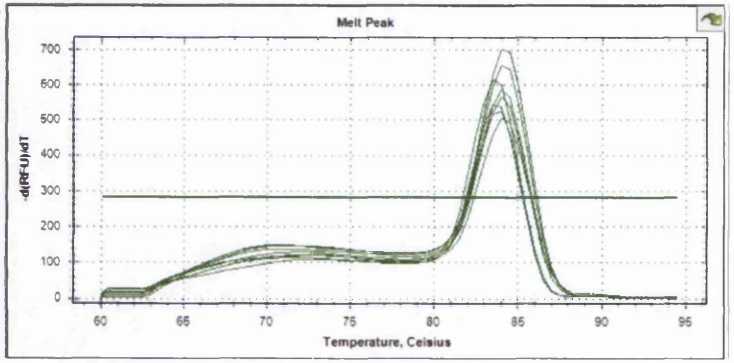

Bibliography

Achache, H. and Revel, A. 2006. Endometrial receptivity markers, the journey to successful embryo implantation. *Human reproduction update* 12(6), pp. 731–46.

Afify, A., Craig, S. and Paulino, A.F.G. 2006. Temporal variation in the distribution of hyaluronic acid, CD44s, and CD44v6 in the human endometrium across the menstrual cycle. *Applied immunohistochemistry molecular morphology AIMM official publication of the Society for Applied Immunohistochemistry* 14(3), pp. 328–333.

Afify, A., Craig, S., Paulino, A.F.G. and Stern, R. 2005. Expression of hyaluronic acid and its receptors, CD44s and CD44v6, in normal, hyperplastic, and neoplastic endometrium. *Annals of diagnostic pathology* 9(6), pp. 312–8.

Afify, A., McNiel, M.A., Braggin, J., Bailey, H. and Paulino, A.F. 2008. Expression of CD44s, CD44v6, and Hyaluronan Across the Spectrum of Normal-hyperplasia-carcinoma in Breast. *Applied Immunohistochemistry & Molecular Morphology* 16(2), pp. 121–127.

Aflatoonian, A. and Mashayekhy, M. 2011. Transvaginal Ultrasonography in Female Infertility Evaluation. *Donald School Journal of Ultrasound in Obstetrics and Gynecology* 5(3), pp. 311–316.

Agnholt, J., Kelsen, J., Schack, L., Hvas, C.L., Dahlerup, J.F. and Sørensen, E.S. 2007. Osteopontin, a protein with cytokine-like properties, is associated with inflammation in Crohn's disease. *Scandinavian journal of immunology* 65(5), pp. 453–60.

Ailane, S., Long, P., Jenner, P. and Rose, S. 2013. Expression of integrin and CD44 receptors recognising osteopontin in the normal and LPS-lesioned rat substantia nigra. *The European journal of neuroscience* (November 2012), pp. 1–9.

Albers, A., Thie, M., Hohn, H. and Denker, D. 1995. Differential expression and localization of integrins and CD44 in the membrane domains of human uterine epithelial cells during the menstrual cycle. *Acta Anatomica* 153(1), pp. 12–19.

Alberti, K.G.M.M., Zimmet, P. and Shaw, J. 2006. Metabolic syndrome--a new world-wide definition. A Consensus Statement from the International Diabetes Federation. *Diabetic medicine : a journal of the British Diabetic Association* 23(5), pp. 469–80. Available at: http://www.ncbi.nlm.nih.gov/pubmed/16681555.

Albitar, L., Pickett, G., Morgan, M., Davies, S. and Leslie, K.K. 2007. Models representing type I and type II human endometrial cancers: Ishikawa H and Hec50co cells. *Gynecologic oncology* 106(1), pp. 52–64.

Alho, A. and Underhill, C. 1989. The Hyaluronate Receptor Is Preferentially Expressed on Proliferating Epithelial Cells. *Cell Biology* 108(April), pp. 1557–1565.

Allison, D.F., Wamsley, J.J., Kumar, M., Li, D., Gray, L.G., Hart, G.W., Jones, D.R. and Mayo, M.W. 2012. Modification of RelA by O-linked N-acetylglucosamine links glucose metabolism to NF-κB acetylation and transcription. *PNAS* 109(42), pp. 16888–16893.

Amato, G., Conte, M., Mazziotti, G., Lalli, E., Vitolo, G., Tucker, A.T., Bellastella, A., Carella, C. and Izzo, A. 2003. Serum and follicular fluid cytokines in polycystic ovary syndrome during stimulated cycles. *Obstetrics and gynecology* 101(6), pp. 1177–82.

American Diabetes Association 2011. Standards of medical care in diabetes--2011. *Diabetes care* 34 Suppl 1, pp. S11–61.

Anthony, F.W., Mukhtar, D.D., Pickett, M.A. and Cameron, I.T. 2003. Progesterone up-regulates WT1 mRNA and protein, and alters the relative expression of WT1 transcripts in cultured endometrial stromal cells. *Journal of the Society for Gynecologic Investigation* 10(8), pp. 509–16.

Apparao, K., Lovely, L.P., Gui, Y., Lininger, R. a and Lessey, B. 2002. Elevated endometrial androgen receptor expression in women with polycystic ovarian syndrome. *Biology of reproduction* 66(2), pp. 297–304.

Apparao, K., Murray, M.J., Fritz, M. a, Meyer, W.R., Chambers, a F., Truong, P.R. and Lessey, B. 2001. Osteopontin and its receptor alphavbeta(3) integrin are coexpressed in the human endometrium during the menstrual cycle but regulated differentially. *The Journal of clinical endocrinology and metabolism* 86(10), pp. 4991–5000.

Asaumi, S., Takemoto, M., Yokote, K., Ridall, A.L., Butler, W.T., Fujimoto, M., Kobayashi, K., Kawamura, H., Take, A., Saito, Y. and Mori, S. 2003. Identification and characterization of high glucose and glucosamine responsive element in the rat osteopontin promoter. *Journal of diabetes and its complications* 17(1), pp. 34–8.

Ashkar, S., Weber, G.F., Panoutsakopoulou, V., Sanchirico, M.E., Jansson, M., Zawaideh, S., Rittling, S.R., Denhardt, D.T., Glimcher, M.J. and Cantor, H. 2000. Eta-1 (osteopontin): an early component of type-1 (cell-mediated) immunity. *Science (New York, N.Y.)* 287(5454), pp. 860–4.

Asselman, M. 2003. Calcium Oxalate Crystal Adherence to Hyaluronan-, Osteopontin-, and CD44-Expressing Injured/Regenerating Tubular Epithelial Cells

in Rat Kidneys. *Journal of the American Society of Nephrology* 14(12), pp. 3155–3166.

Assoian, R. and Klein, E. 2008. Growth control by intracellular tension and extracellular stiffness. *Trends in cell biology* 18(7), pp. 347–352.

Aznaurova, Y.B., Zhumataev, M.B., Roberts, T.K., Aliper, A.M. and Zhavoronkov, A. a 2014. Molecular aspects of development and regulation of endometriosis. *Reproductive biology and endocrinology : RB&E* 12(1), p. 50. Available at: http://www.pubmedcentral.nih.gov/articlerender.fcgi?artid=4067518&tool=pmcentrez&rendertype=abstract [Accessed: 29 July 2014].

Baaten, B.J., Li, C.-R. and Bradley, L.M. 2010. Multifaceted regulation of T cells by CD44. *Communicative & integrative biology* 3(6), pp. 508–12. Available at: http://www.pubmedcentral.nih.gov/articlerender.fcgi?artid=3038050&tool=pmcentrez&rendertype=abstract [Accessed: 29 April 2014].

Barker, M., Boehnlein, L.M., Kovacs, P. and Lindheim, S. 2009. Follicular and luteal phase endometrial thickness and echogenic pattern and pregnancy outcome in oocyte donation cycles. *Journal of assisted reproduction and genetics* 26(5), pp. 243–9.

Bates, R.C., Edwards, N.S., Burns, G.F., Akt, P., Cells, C. and Fisher, D.E. 2001. A CD44 Survival Pathway Triggers Chemoresistance via Lyn Kinase and Phosphoinositide 3-Kinase / Akt in Colon Carcinoma Cells A CD44 Survival Pathway Triggers Chemoresistance via Lyn Kinase and. , pp. 5275–5283.

Batt, R.E. 2011. A History of Endometriosis. 1(1846), pp. 13–39.

Bazer, F.W., Burghardt, R.C., Johnson, G.A., Spencer, T.E. and Wu, G. 2008. Interferons and progesterone for establishment and maintenance of pregnancy : interactions among. 8(3), pp. 179–211.

Bedaiwy, M. a, Falcone, T., Sharma, R.K., Goldberg, J.M., Attaran, M., Nelson, D.R. and Agarwal, A. 2002. Prediction of endometriosis with serum and peritoneal fluid markers: a prospective controlled trial. *Human reproduction (Oxford, England)* 17(2), pp. 426–31.

Beg, A.A., Finco, T.S., Nantermet, P. V and Jr, A.S.B. 1993. Tumor necrosis factor and interleukin-1 lead to phosphorylation and loss of I kappa B alpha : a mechanism for NF-kappa B activation. *Molecular and cellular biology* 13(6), p. 330103310.

Behzad, F., Seif, M.W., Campbell, S. and Aplin, J.D. 1994. Expression of two isoforms of CD44 in human endometrium. *Biology of reproduction* 51(4), pp. 739–47.

Bellahcène, A., Castronovo, V., Ogbureke, K.U.E., Fisher, L.W. and Fedarko, N.S. 2008. Small integrin-binding ligand N-linked glycoproteins (SIBLINGs): multifunctional proteins in cancer. *Nature reviews. Cancer* 8(3), pp. 212–26.

Bidder, M., Shao, J.-S., Charlton-Kachigian, N., Loewy, A.P., Semenkovich, C.F. and Towler, D. a 2002. Osteopontin transcription in aortic vascular smooth muscle cells is controlled by glucose-regulated upstream stimulatory factor and activator protein-1 activities. *The Journal of biological chemistry* 277(46), pp. 44485–96.

Bliss, S.K., Marshall, a J., Zhang, Y. and Denkers, E.Y. 1999. Human polymorphonuclear leukocytes produce IL-12, TNF-alpha, and the chemokines macrophage-inflammatory protein-1 alpha and -1 beta in response to Toxoplasma gondii antigens. *Journal of immunology (Baltimore, Md. : 1950)* 162(12), pp. 7369–75.

Bourdeau, V., Deschênes, J., Métivier, R., Nagai, Y., Nguyen, D., Bretschneider, N., Gannon, F., White, J.H. and Mader, S. 2004. Genome-wide identification of high-affinity estrogen response elements in human and mouse. *Molecular endocrinology (Baltimore, Md.)* 18(6), pp. 1411–27.

Bouwmeester, T., Bauch, A., Ruffner, H., Angrand, P.-O., Bergamini, G., Croughton, K., Cruciat, C., Eberhard, D., Gagneur, J., Ghidelli, S., Hopf, C., Huhse, B., Mangano, R., Michon, A.-M., Schirle, M., Schlegl, J., Schwab, M., Stein, M. a, Bauer, A., Casari, G., Drewes, G., Gavin, A.-C., Jackson, D.B., Joberty, G., Neubauer, G., Rick, J., Kuster, B. and Superti-Furga, G. 2004. A physical and functional map of the human TNF-alpha/NF-kappa B signal transduction pathway. *Nature cell biology* 6(2), pp. 97–105.

Brown, L.F., Berse, B., Van de Water, L., Papadopoulos-Sergiou, A., Perruzzi, C. a, Manseau, E.J., Dvorak, H.F. and Senger, D.R. 1992. Expression and distribution of osteopontin in human tissues: widespread association with luminal epithelial surfaces. *Molecular biology of the cell* 3(10), pp. 1169–80.

Bruemmer, D. and Collins, A. 2003. Angiotensin II–accelerated atherosclerosis and aneurysm formation is attenuated in osteopontin-deficient mice. *Journal of Clinical Investigation* 112(9), pp. 1318–1331.

Bulletti, C., Coccia, M.E., Battistoni, S. and Borini, A. 2010. Endometriosis and infertility. *Journal of assisted reproduction and genetics* 27(8), pp. 441–7.

Burke, S.J., Goff, M.R., Lu, D., Proud, D., Karlstad, M.D. and Collier, J.J. 2013. Synergistic expression of the CXCL10 gene in response to IL-1β and IFN-γ involves NF-κB, phosphorylation of STAT1 at Tyr701, and acetylation of histones H3 and H4. *Journal of immunology (Baltimore, Md. : 1950)* 191(1), pp. 323–36.

Byun, H.-S., Lee, G.-S., Lee, B.-M., Hyun, S.-H., Choi, K.-C. and Jeung, E.-B. 2008. Implantation-related expression of epidermal growth factor family molecules

and their regulation by progesterone in the pregnant rat. *Reproductive sciences (Thousand Oaks, Calif.)* 15(7), pp. 678–89.

Campo, G.M., Avenoso, A., Campo, S., D'Ascola, A., Nastasi, G. and Calatroni, A. 2010. Small hyaluronan oligosaccharides induce inflammation by engaging both toll-like-4 and CD44 receptors in human chondrocytes. *Biochemical pharmacology* 80(4), pp. 480–90.

Carson, D.D., Lagow, E., Thathiah, A., Al-Shami, R., Farach-Carson, M.C., Vernon, M., Yuan, L., Fritz, M. a and Lessey, B. 2002. Changes in gene expression during the early to mid-luteal (receptive phase) transition in human endometrium detected by high-density microarray screening. *Molecular human reproduction* 8(9), pp. 871–9.

Carvalho, R.S., Schaffer, J.L. and Gerstenfeld, L.C. 1998. Osteoblasts induce osteopontin expression in response to attachment on fibronectin: demonstration of a common role for integrin receptors in the signal transduction processes of cell attachment and mechanical stimulation. *Journal of cellular biochemistry* 70(3), pp. 376–90.

Casals, G., Ordi, J., Creus, M., Fábregues, F., Carmona, F., Casamitjana, R. and Balasch, J. 2012. Expression pattern of osteopontin and αvβ3 integrin during the implantation window in infertile patients with early stages of endometriosis. *Human reproduction (Oxford, England)* 0(0), pp. 1–9.

Casals, G., Ordi, J., Creus, M., Fábregues, F., Casamitjana, R., Quinto, L., Campo, E. and Balasch, J. 2008. Osteopontin and αvβ3 integrin expression in the endometrium of infertile and fertile women. *Reproductive BioMedicine Online* 16(6), pp. 808–816.

Cavagna, M. 2003. Biomarkers of Endometrial Receptivity - A Review. *Placenta* 24, pp. S39–S47.

Ceydeli, N., Kaleli, S., Calay, Z. and Tamer, C. 2006. Difference in avb3 integrin expression in endometrial stromal cell in subgroups of women with unexplained infertility §. *European Journal of Obstetrics & Gynecology and Reproductive Biology* 126, pp. 206–211.

Chaen, T., Konno, T., Egashira, M., Bai, R., Nomura, N., Nomura, S., Hirota, Y., Sakurai, T. and Imakawa, K. 2012. Estrogen-dependent uterine secretion of osteopontin activates blastocyst adhesion competence. *PloS one* 7(11), p. e48933.

Check, J.H. 2007. Ovulation disorders: part I anovulation associated with estrogen deficiency. *Clinical and experimental obstetrics & gynecology* 34(1), pp. 5–8. Available at: http://www.ncbi.nlm.nih.gov/pubmed/17447629 [Accessed: 13 July 2014].

Cho, S., Ahn, Y.S., Choi, Y.S., Seo, S.K., Nam, A., Kim, H.Y., Kim, J.-H., Park, K.H., Cho, D.J. and Lee, B.S. 2009. Endometrial osteopontin mRNA expression and plasma osteopontin levels are increased in patients with endometriosis. *American journal of reproductive immunology* 61(4), pp. 286–93.

Christensen, B., Schack, L., Kläning, E. and Sørensen, E.S. 2010. Osteopontin is cleaved at multiple sites close to its integrin-binding motifs in milk and is a novel substrate for plasmin and cathepsin D. *The Journal of biological chemistry* 285(11), pp. 7929–37.

Ciampelli, M., Fulghesu, A.M., Cucinelli, F., Pavone, V., Ronsisvalle, E., Guido, M., Caruso, A. and Lanzone, A. 1999. *Impact of insulin and body mass index on metabolic and endocrine variables in polycystic ovary syndrome.*

Cole, S.W., Hawkley, L.C., Arevalo, J.M., Sung, C.Y., Rose, R.M. and Cacioppo, J.T. 2007. Social regulation of gene expression in human leukocytes. *Genome biology* 8(9), p. R189.

Cornier, E. 1984. The Pipelle: a disposable device for endometrial biopsy. *American journal of obstetrics and gynecology* 148(1), pp. 109–10.

Critchley, H.O.D. 2002. Wild-Type Estrogen Receptor (ERbeta1) and the Splice Variant (ERbetacx/beta2) Are Both Expressed within the Human Endometrium throughout the Normal Menstrual Cycle. *Journal of Clinical Endocrinology & Metabolism* 87(11), pp. 5265–5273.

Darling, T.W.A. and D.A. 1952. Asymptotic Theory of Certain "Goodness of Fit" Criteria Based on Stochastic Processes. *Ann. Math. Statist.* 23(2), pp. 193–212.

Déchaud, H., Maudelonde, T., Daurès, J.P., Rossi, J.F. and Hédon, B. 1998. Evaluation of endometrial inflammation by quantification of macrophages, T lymphocytes, and interleukin-1 and -6 in human endometrium. *Journal of assisted reproduction and genetics* 15(10), pp. 612–8.

Delimpoura, V., Bakakos, P., Tseliou, E., Bessa, V., Hillas, G., Simoes, D.C.M., Papiris, S. and Loukides, S. 2010. Increased levels of osteopontin in sputum supernatant in severe refractory asthma. *Thorax* 65(9), pp. 782–6.

Department of Health 2009. *Regulated Fertility Services : A commissioning aid.*

Desai, B., Ma, T., Zhu, J. and Chellaiah, M. a 2009. Characterization of the expression of variant and standard CD44 in prostate cancer cells: identification of the possible molecular mechanism of CD44/MMP9 complex formation on the cell surface. *Journal of cellular biochemistry* 108(1), pp. 272–84.

Desai, B., Rogers, M.J. and Chellaiah, M. a 2007. Mechanisms of osteopontin and CD44 as metastatic principles in prostate cancer cells. *Molecular cancer* 6, p. 18.

Desai, P. 2007. Cytokines in Obstetricsand Gynaecology. 57(3), pp. 205–209.

Desgrosellier, J.S. and Cheresh, D. a 2010. Integrins in cancer: biological implications and therapeutic opportunities. *Nature reviews. Cancer* 10(1), pp. 9–22.

Dharmaraj, N., Wang, P. and Carson, D.D. 2010. Cytokine and progesterone receptor interplay in the regulation of MUC1 gene expression. *Molecular endocrinology (Baltimore, Md.)* 24(12), pp. 2253–66.

Dhindsa, G., Bhatia, R., Dhindsa, M. and Bhatia, V. 2004. Insulin resistance, insulin sensitization and inflammation in polycystic ovarian syndrome. *Journal of postgraduate medicine* 50(2), pp. 140–4.

Diamanti-Kandarakis, E., Paterakis, T., Alexandraki, K., Piperi, C., Aessopos, A., Katsikis, I., Katsilambros, N., Kreatsas, G. and Panidis, D. 2006. Indices of low-grade chronic inflammation in polycystic ovary syndrome and the beneficial effect of metformin. *Human reproduction (Oxford, England)* 21(6), pp. 1426–31.

Dimitriadis, E., White, C.A., Jones, R.L. and Salamonsen, L.A. 2005. Cytokines, chemokines and growth factors in endometrium related to implantation. *Human reproduction update* 11(6), pp. 613–30.

Dominguez, F., Yáñez-Mó, M., Sanchez-Madrid, F. and Simón, C. 2005. Embryonic implantation and leukocyte transendothelial migration: different processes with similar players? *The FASEB journal : official publication of the Federation of American Societies for Experimental Biology* 19(9), pp. 1056–60.

Dunaif, A., Segal, K.R., Futterweit, W. and Dobrjansky, A. 1989. Profound peripheral insulin resistance, independent of obesity, in polycystic ovary syndrome. *Diabetes* 38(9), pp. 1165–74.

DuQuesnay, R., Wright, C., Aziz, A.A., Stamp, G.W.H., Trew, G.H., Margara, R. a and White, J.O. 2009. Infertile women with isolated polycystic ovaries are deficient in endometrial expression of osteopontin but not alphavbeta3 integrin during the implantation window. *Fertility and sterility* 91(2), pp. 489–99.

El-Tanani, M.K., Campbell, F.C., Kurisetty, V., Jin, D., McCann, M. and Rudland, P.S. 2006. The regulation and role of osteopontin in malignant transformation and cancer. *Cytokine & growth factor reviews* 17(6), pp. 463–74.

Essah, P.A., Wickham, E.P. and Nestler, J.E. 2007. The metabolic syndrome in polycystic ovary syndrome. *Clinical obstetrics and gynecology* 50(1), pp. 205–25.

Fakih, H., Baggett, B., Holtz, G., Tsang, K.Y., Lee, J.C. and Williamson, H.O. 1987. Interleukin-1: a possible role in the infertility associated with endometriosis. *Fertility and sterility* 47(2), pp. 213–7.

Fanta, M. 2013. Is polycystic ovary syndrome, a state of relative estrogen excess, a real risk factor for estrogen-dependant malignancies? *Gynecological endocrinology : the official journal of the International Society of Gynecological Endocrinology* 29(2), pp. 145–7. Available at: http://informahealthcare.com/doi/abs/10.3109/09513590.2012.730575 [Accessed: 13 July 2014].

Fatemi, H.M. and Popovic-Todorovic, B. 2013. Implantation in assisted reproduction: a look at endometrial receptivity. *Reproductive biomedicine online*.

Fazleabas, A.T. and Kim, J.J. 2003. Development. What makes an embryo stick? *Science (New York, N.Y.)* 299(5605), pp. 355–6.

Foster, L., Arkonac, B., Sibinga, N., Shi, C., Perrella, M. and Haber, E. 1998. Regulation of CD44 Gene Expression by the Proinflammatory Cytokine Interleukin-1B in Vascular Smooth Muscle Cells. *Journal of Biological Chemistry* 273(32), pp. 20341–20346.

Franchi, A., Zaret, J., Zhang, X., Bocca, S. and Oehninger, S. 2008. Expression of immunomodulatory genes, their protein products and specific ligands/receptors during the window of implantation in the human endometrium. *Molecular human reproduction* 14(7), pp. 413–21.

Francis, L.W., Lewis, P.D., Wright, C.J. and Conlan, R.S. 2010. Atomic force microscopy comes of age. *Biology of the cell* 102(2), pp. 133–43.

Friedrichs, K., Franke, F., Lisboa, B. and Kãgler, G. 1995. CD44 Isoforms Correlate with Cellular Differentiation but not with Prognosis in Human Breast Cancer CD44 Isoforms Correlate withCellular Differentiation butnotwithPrognosis in HumanBreastCancer. *Cancer research* 55, pp. 5424–5433.

Froment, P. and Touraine, P. 2006. Thiazolidinediones and Fertility in Polycystic Ovary Syndrome (PCOS). *PPAR research* 2006, p. 73986.

Gagnon, C. and Baillargeon, J. 2007. Suitability of recommended limits for fasting glucose tests in women with polycystic ovary syndrome. *Canadian Research Association Journal* 176(7), pp. 933–938.

Geisert, R.D., Ross, J.W., Ashworth, M.D., White, F.J., Johnson, G. a and DeSilva, U. 2006. Maternal recognition of pregnancy signal or endocrine disruptor: the two faces of oestrogen during establishment of pregnancy in the pig. *Society of Reproduction and Fertility supplement* 62, pp. 131–45.

Gelman, A., Hill, J. and Yajima, M. 2012. Why We (Usually) Don't Have to Worry About Multiple Comparisons. *Journal of Research on Educational Effectiveness* 5(2), pp. 189–211.

Giachelli, C.M., Liaw, L., Murry, C.E. and Schwartz, S.M. 1995. Osteopontin Expression in Cardiovascular Diseases. *Annals new york academy of science* 760, pp. 109–26.

Giannelli, G., Bergamini, C., Marinosci, F., Fransvea, E., Quaranta, M., Lupo, L., Schiraldi, O. and Antonaci, S. 2002. Clinical role of MMP-2/TIMP-2 imbalance in hepatocellular carcinoma. *International journal of cancer. Journal international du cancer* 97(4), pp. 425–31.

Giudice, L.C. 1994. Growth factors and growth modulators in human uterine endometrium: their potential relevance to reproductive medicine. *Fertility and sterility* 61(1), pp. 1–17.

Goldman, L. and Ausiello, D. 2008. Menstrual Cycle and Fertility. In: *Cecil Medicine*. 23rd Editi. p. 1814.

Gómez-Ambrosi, J., Catalán, V., Ramírez, B., Rodríguez, A., Colina, I., Silva, C., Rotellar, F., Mugueta, C., Gil, M.J., Cienfuegos, J. a, Salvador, J. and Frühbeck, G. 2007. Plasma osteopontin levels and expression in adipose tissue are increased in obesity. *The Journal of clinical endocrinology and metabolism* 92(9), pp. 3719–27.

Gong, Q., Chipitsyna, G., Gray, C.F., Anandanadesan, R. and Arafat, H. a 2009a. Expression and regulation of osteopontin in type 1 diabetes. *Islets* 1(1), pp. 34–41.

Gong, Q., Chipitsyna, G., Gray, C.F., Anandanadesan, R. and Arafat, H. a 2009b. Expression and regulation of osteopontin in type 1 diabetes. *Islets* 1(1), pp. 34–41.

González, F., Rote, N.S., Minium, J. and Kirwan, J.P. 2006. In vitro evidence that hyperglycemia stimulates tumor necrosis factor-alpha release in obese women with polycystic ovary syndrome. *The Journal of endocrinology* 188(3), pp. 521–9.

Gonzalez, F., Thusu, K., Abdei-rahman, E., Prabhala, A., Tomani, M., Dandona, P., Sciences, B., Diego, I.S. and Hospital, C. 1999. Elevated Serum Levels of Tumor Necrosis Factor Alpha in Normal-Weight Women With Polycystic Ovary Syndrome. *Society* 4(4), pp. 437–441.

Goodison, S., Urquidi, V. and Tarin, D. 1999. CD44 cell adhesion molecules. *Molecular pathology : MP* 52(4), pp. 189–96.

Goshen, R., Ariel, L., Shuster, S., Hochberg, A., Vlodavsky, L., de Groot, N., Ben-Rafael, Z. and Stern, R. 1996. Hyaluronan, CD44 and its variant exons in human trophoblast invasion and placental angiogenesis. *Molecular human reproduction* 2(9), pp. 685–91.

Grassinger, J., Haylock, D.N., Storan, M.J., Haines, G.O., Williams, B., Whitty, G. a, Vinson, A.R., Be, C.L., Li, S., Sørensen, E.S., Tam, P.P.L., Denhardt, D.T., Sheppard, D., Choong, P.F. and Nilsson, S.K. 2009. Thrombin-cleaved osteopontin

regulates hemopoietic stem and progenitor cell functions through interactions with alpha9beta1 and alpha4beta1 integrins. *Blood* 114(1), pp. 49–59.

Gray, P.W. and Goeddel, D. V 1982. Structure of the human immune interferon gene. *Nature* 298(5877), pp. 859–63.

Green, J. and Britten, N. 1998. Qualitative research and evidence based medicine. *BMJ (Clinical research ed.)* 316(7139), pp. 1230–2.

Grzechocinska, B. and Wielgos, M. 2012. Management of infertility in women with endometriosis. *Neuro endocrinology letters* 33(7), pp. 674–9.

Gupta, A., Zhou, C. and Chellaiah, M. 2013. Osteopontin and MMP9: Associations with VEGF Expression/Secretion and Angiogenesis in PC3 Prostate Cancer Cells. *Cancers* 5(2), pp. 617–638.

Halis, G. and Arici, A. 2004. Endometriosis and inflammation in infertility. *Annals of the New York Academy of Sciences* 1034, pp. 300–15.

Hebbard, L., Steffen, A., Zawadzki, V., Fieber, C., Howells, N., Moll, J., Ponta, H., Hofmann, M. and Sleeman, J. 2000. CD44 expression and regulation during mammary gland development and function. *Journal of cell science* 113 (Pt 1, pp. 2619–30.

Heider, K., Dämmrich, J., Skroch-angel, P., Herrlich, P. and Ponta, H. 1993. Differential Expression of CD44 Splice Variants in Intestinal- and Diffuse-Type Human Gastric Carcinomas and Normal Gastric Mucosa Differential Expression of CD44 Splice Variants in Intestinal- and Diffuse-Type Human Gastric Carcinomas and Normal Gastric . , pp. 4197–4203.

Heuck, C.-C., Home, P.D., Reinauer, H. and Kanagasabapathy, A.S. 2002. Laboratory Diagnosis and Monitoring of Diabetes Mellitus. *World health Organisation*, pp. 1–26.

Hinz, M., Lemke, P., Anagnostopoulos, I., Hacker, C., Krappmann, D., Mathas, S., Dorken, B., Zenke, M., Stein, H. and Scheidereit, C. 2002. Nuclear Factor B-dependent Gene Expression Profiling of Hodgkin's Disease Tumor Cells, Pathogenetic Significance, and Link to Constitutive Signal Transducer and Activator of Transcription 5a Activity. *Journal of Experimental Medicine* 196(5), pp. 605–617.

Hnatyszyn, H.J., Liu, M., Hilger, A., Herbert, L., Gomez-Fernandez, C.R., Jorda, M., Thomas, D., Rae, J.M., El-Ashry, D. and Lippman, M.E. 2010. Correlation of GREB1 mRNA with protein expression in breast cancer: validation of a novel GREB1 monoclonal antibody. *Breast cancer research and treatment* 122(2), pp. 371–80.

Hole, a K., Belkhiri, A., Snell, L.S. and Watson, P.H. 1997. CD44 variant expression and estrogen receptor status in breast cancer. *Breast cancer research and treatment* 43(2), pp. 165–73.

Horiuchi, T., Mitoma, H., Harashima, S., Tsukamoto, H. and Shimoda, T. 2010. Transmembrane TNF-alpha: structure, function and interaction with anti-TNF agents. *Rheumatology (Oxford, England)* 49(7), pp. 1215–28. Available at: http://www.pubmedcentral.nih.gov/articlerender.fcgi?artid=2886310&tool=pmcentrez&rendertype=abstract [Accessed: 11 July 2014].

Hsu, C.-C., Chuang, W.-J., Chang, C.-H., Tseng, Y.-L., Peng, H.-C. and Huang, T.-F. 2011. Improvements in endotoxemic syndromes using a disintegrin, rhodostomin, through integrin αvβ3-dependent pathway. *Journal of thrombosis and haemostasis : JTH* 9(3), pp. 593–602. Available at: http://www.ncbi.nlm.nih.gov/pubmed/21143376 [Accessed: 13 July 2014].

Hutás, G., Bajnok, E., Gál, I., Finnegan, A., Glant, T.T. and Mikecz, K. 2008. CD44-specific antibody treatment and CD44 deficiency exert distinct effects on leukocyte recruitment in experimental arthritis. *Blood* 112(13), pp. 4999–5006. Available at: http://www.pubmedcentral.nih.gov/articlerender.fcgi?artid=2597605&tool=pmcentrez&rendertype=abstract [Accessed: 29 April 2014].

Huttenlocher, A. and Horwitz, A.R. 2011. Integrins in cell migration. *Cold Spring Harbor Perspectives in Biology* 3(9), pp. 1–16.

Iczkowski, K. a 2010. Cell adhesion molecule CD44: its functional roles in prostate cancer. *American journal of translational research* 3(1), pp. 1–7.

Igarashi, T.M., Bruner-Tran, K.L., Yeaman, G.R., Lessey, B., Edwards, D.P., Eisenberg, E. and Osteen, K.G. 2005. Reduced expression of progesterone receptor-B in the endometrium of women with endometriosis and in cocultures of endometrial cells exposed to 2,3,7,8-tetrachlorodibenzo-p-dioxin. *Fertility and sterility* 84(1), pp. 67–74.

Illera, M.J., Lorenzo, P.L., Gui, Y., Beyler, S.A., Apparao, K. and Lessey, B. 2003. A Role for avb3 Integrin During Implantation in the Rabbit Model 1. *Developmental Biology* 771, pp. 766–771.

Ingamells, S., Campbell, I.G., Anthony, F.W. and Thomas, E.J. 1996. Endometrial progesterone receptor expression during the human menstrual cycle. *Journal of reproduction and fertility* 106(1), pp. 33–8.

Iwadate, H., Kobayashi, H., Kanno, T., Asano, T., Saito, R., Sato, S., Suzuki, E., Watanabe, H. and Ohira, H. 2013. Plasma osteopontin is correlated with bone resorption markers in rheumatoid arthritis patients. *International journal of rheumatic disease* (Il), pp. 1–7.

Jensterle, M., Janez, A., Mlinar, B., Marc, J., Prezelj, J. and Pfeifer, M. 2008. Impact of metformin and rosiglitazone treatment on glucose transporter 4 mRNA expression in women with polycystic ovary syndrome. *European journal of endocrinology / European Federation of Endocrine Societies* 158(6), pp. 793–801.

Johnson, G. a, Burghardt, R.C., Bazer, F.W. and Spencer, T.E. 2003. Osteopontin: roles in implantation and placentation. *Biology of reproduction* 69(5), pp. 1458–71.

Johnson, G. a, Burghardt, R.C., Spencer, T.E., Newton, G.R., Ott, T.L. and Bazer, F.W. 1999. Ovine osteopontin: II. Osteopontin and alpha(v)beta(3) integrin expression in the uterus and conceptus during the periimplantation period. *Biology of reproduction* 61(4), pp. 892–9.

Johnson, G., Spencer, T.E., Burghardt, R.C., Taylor, K.M., Gray, C. and Bazer, F.W. 2000. Progesterone modulation of osteopontin gene expression in the ovine uterus. *Biology of reproduction* 62(5), pp. 1315–21.

Johnson, P., Maiti, A., Brown, K.L. and Li, R. 2000. A role for the cell adhesion molecule CD44 and sulfation in leukocyte-endothelial cell adhesion during an inflammatory response? *Biochemical pharmacology* 59(5), pp. 455–65.

Johnson, P. and Ruffell, B. 2009. CD44 and its role in inflammation and inflammatory diseases. *Inflammation & allergy drug targets* 8(3), pp. 208–20.

Jones, R.L., Findlay, J.K., Farnworth, P.G., Robertson, D.M., Wallace, E. and Salamonsen, L. a 2006. Activin A and inhibin A differentially regulate human uterine matrix metalloproteinases: potential interactions during decidualization and trophoblast invasion. *Endocrinology* 147(2), pp. 724–32.

Kang, H.S., Liao, G., DeGraff, L.M., Gerrish, K., Bortner, C.D., Garantziotis, S. and Jetten, A.M. 2013. CD44 plays a critical role in regulating diet-induced adipose inflammation, hepatic steatosis, and insulin resistance. Brennan, L. ed. *PloS one* 8(3), pp. 1–15.

Kao, L.C., Tulac, S., Lobo, S., Imani, B., Yang, J.P., Germeyer, A., Osteen, K., Taylor, R.N., Lessey, B. and Giudice, L.C. 2002. Global gene profiling in human endometrium during the window of implantation. *Endocrinology* 143(6), pp. 2119–38.

Kasza, A. 2013. IL-1 and EGF regulate expression of genes important in inflammation and cancer. *Cytokine* 5.

Kawamura, H., Yokote, K., Asaumi, S., Kobayashi, K., Fujimoto, M., Maezawa, Y., Saito, Y. and Mori, S. 2004. High glucose-induced upregulation of osteopontin is mediated via Rho/Rho kinase pathway in cultured rat aortic smooth muscle cells. *Arteriosclerosis, thrombosis, and vascular biology* 24(2), pp. 276–81.

Kelly, C.C., Lyall, H., Petrie, J.R., Gould, G.W., Connell, J.M. and Sattar, N. 2001. Low grade chronic inflammation in women with polycystic ovarian syndrome. *The Journal of clinical endocrinology and metabolism* 86(6), pp. 2453–5.

Khan, J. a, Bellance, C., Guiochon-Mantel, A., Lombès, M. and Loosfelt, H. 2012. Differential regulation of breast cancer-associated genes by progesterone receptor isoforms PRA and PRB in a new bi-inducible breast cancer cell line. *PloS one* 7(9), pp. 1–19.

Kiefer, F.W., Zeyda, M., Gollinger, K., Pfau, B., Neuhofer, A., Weichhart, T., Sa, M.D., Schlederer, M., Kenner, L. and Stulnig, T.M. 2010. Neutralization of Osteopontin Inhibits Obesity-Induced Inflammation and Insulin Resistance. 59(April), pp. 935–946.

Kim, M.K.-H., Min, D.J., Rabin, M. and Licht, J.D. 2011. Functional characterization of Wilms tumor-suppressor WTX and tumor-associated mutants. *Oncogene* 30(7), pp. 832–42. Available at: http://www.ncbi.nlm.nih.gov/pubmed/20956941 [Accessed: 12 July 2011].

King, A.E. and Critchley, H.O.D. 2010. Oestrogen and progesterone regulation of inflammatory processes in the human endometrium. *The Journal of steroid biochemistry and molecular biology* 120(2-3), pp. 116–26.

Knudson, W. and Loeser, R.F. 2002. CD44 and integrin matrix receptors participate in cartilage homeostasis. *Cellular and Molecular Life Sciences (CMLS)* 59(1), pp. 36–44.

Kodama, K., Horikoshi, M., Toda, K., Yamada, S., Hara, K., Irie, J., Sirota, M., Morgan, A. a, Chen, R., Ohtsu, H., Maeda, S., Kadowaki, T. and Butte, A.J. 2012. Expression-based genome-wide association study links the receptor CD44 in adipose tissue with type 2 diabetes. *Proceedings of the National Academy of Sciences of the United States of America* 109(18), pp. 7049–54. Available at: http://www.pubmedcentral.nih.gov/articlerender.fcgi?artid=3344989&tool=pmcentrez&rendertype=abstract [Accessed: 20 July 2014].

Koo, Y.H., Na, Y.J., Ahn, M.Y., Jeon, H.N., Yeom, J.I. and Lee, K.S. 2013. Expression of CD44 in endometrial stromal cells from women with and without endometriosis and its effect on the adherence to peritoneal mesothelial cells. *Obstetrics & Gynecology Science* 56(2), p. 102.

Kruskal, W.H. and Wallis, W.A. 1952. Use of Ranks in One-Criterion Variance Analysis. *Journal of the American Statistical Association* 47(260), pp. 583–621.

Kuramoto, H. 1972. Studies of the growth and cytogenetic properties of human endometrial adenocarcinoma in culture and its development into an established line. *Acta obstetrica et gynaecologica Japonica* 19(1), pp. 47–58.

Kuramoto, H., Nishisda, M., Morisawa, T., M, H., Hata, H., Kato, Y., Ohno, E. and TOMOHIRO, I. 1991. Establishment and Characterization of Human Endometrial Cancer Cell Lines. *Annals of the New York Academy of Sciences* 622(1 The Primate E), pp. 402–421.

Kuramoto, H., Tamura, S. and Notake, Y. 1972. Establishment of a cell line of human endometrial adenocarcinoma in vitro. *American journal of obstetrics and gynecology* 114(8), pp. 1012–9.

Kuzuya, M. and Iguchi, A. 2003. Role of matrix metalloproteinases in vascular remodeling. *Journal of atherosclerosis and thrombosis* 10(5), pp. 275–82.

Kyama, C.M., Debrock, S., Mwenda, J.M. and D'Hooghe, T.M. 2003. Potential involvement of the immune system in the development of endometriosis. *Reproductive biology and endocrinology : RB&E* 1, p. 123.

De La Motte, C. a, Hascall, V.C., Calabro, A., Yen-Lieberman, B. and Strong, S. a 1999. Mononuclear leukocytes preferentially bind via CD44 to hyaluronan on human intestinal mucosal smooth muscle cells after virus infection or treatment with poly(I.C). *The Journal of biological chemistry* 274(43), pp. 30747–55.

Laganà, A.S., Sturlese, E., Retto, G., Sofo, V. and Triolo, O. 2013. Interplay between Misplaced Müllerian-Derived Stem Cells and Peritoneal Immune Dysregulation in the Pathogenesis of Endometriosis. *Obstetrics and gynecology international* 2013, p. 527041. Available at: http://www.pubmedcentral.nih.gov/articlerender.fcgi?artid=3697788&tool=pmcentrez&rendertype=abstract.

Laird, S.M., Tuckerman, E.M. and Cli, T. 1996. The production of tumour necrosis factor a (TNF-a) by human endometrial cells in culture. 11(6), pp. 1318–1323.

Lebovic, D.I., Mueller, M.D. and Taylor, R.N. 2001. Immunobiology of endometriosis. *Fertility and sterility* 75(1), pp. 1–10.

Lecce, G., Meduri, G., Ancelin, M., Bergeron, C. and Perrot-Applanat, M. 2001. Presence of estrogen receptor beta in the human endometrium through the cycle: expression in glandular, stromal, and vascular cells. *The Journal of clinical endocrinology and metabolism* 86(3), pp. 1379–86.

Lee, J.-L., Wang, M.-J., Sudhir, P.-R., Chen, G.-D., Chi, C.-W. and Chen, J.-Y. 2007. Osteopontin promotes integrin activation through outside-in and inside-out mechanisms: OPN-CD44V interaction enhances survival in gastrointestinal cancer cells. *Cancer research* 67(5), pp. 2089–97.

Lee, J.-L., Wang, M.-J., Sudhir, P.-R. and Chen, J.-Y. 2008. CD44 engagement promotes matrix-derived survival through the CD44-SRC-integrin axis in lipid rafts. *Molecular and cellular biology* 28(18), pp. 5710–23. Available at:

http://www.pubmedcentral.nih.gov/articlerender.fcgi?artid=2546932&tool=pmcentrez&rendertype=abstract [Accessed: 29 April 2014].

Legro, R.S., Arslanian, S. a, Ehrmann, D. a, Hoeger, K.M., Murad, M.H., Pasquali, R. and Welt, C.K. 2013. Diagnosis and treatment of polycystic ovary syndrome: an Endocrine Society clinical practice guideline. *The Journal of clinical endocrinology and metabolism* 98(12), pp. 4565–92. Available at: http://www.ncbi.nlm.nih.gov/pubmed/24151290 [Accessed: 12 July 2014].

Legro, R.S., Finegood, D. and Dunaif, A. 1998. A fasting glucose to insulin ratio is a useful measure of insulin sensitivity in women with polycystic ovary syndrome. *The Journal of clinical endocrinology and metabolism* 83(8), pp. 2694–8.

Lessey, B. 2002. Adhesion molecules and implantation. *Journal of reproductive immunology* 55(1-2), pp. 101–12.

Lessey, B. 2003. Two pathways of progesterone action in the human endometrium: implications for implantation and contraception. *Steroids* 68(10-13), pp. 809–815.

Lessey, B. and Arnold, J. 1998. Paracrine signaling in the endometrium: integrins and the establishment of uterine receptivity. *Journal of reproductive immunology* 39(1-2), pp. 105–16.

Lessey, B., Killam, A.P., Metzger, D.A., Haney, A.F., Greene, G.L. and McCarty, K.S. 1988. Immunohistochemical Analysis of Human Uterine Estrogen and Progesterone Receptors Throughout the Menstrual Cycle. *Journal of Clinical Endocrinology & Metabolism* 67(2), pp. 334–340.

Lieberman, M.D. and Cunningham, W. a 2009. Type I and Type II error concerns in fMRI research: re-balancing the scale. *Social cognitive and affective neuroscience* 4(4), pp. 423–8.

Liu, F., Bardhan, K., Yang, D., Thangaraju, M., Ganapathy, V., Waller, J.L., Liles, G.B., Lee, J.R. and Liu, K. 2012. NF-κB directly regulates Fas transcription to modulate Fas-mediated apoptosis and tumor suppression. *The Journal of biological chemistry* 287(30), pp. 25530–40.

Livak, K.J. and Schmittgen, T.D. 2001. Analysis of relative gene expression data using real-time quantitative PCR and the 2(-Delta Delta C(T)) Method. *Methods (San Diego, Calif.)* 25(4), pp. 402–8. Available at: http://www.ncbi.nlm.nih.gov/pubmed/11846609 [Accessed: 23 May 2014].

Lokeshwar, B., Lokeshwar, V. and Block, N. 1995. Expression of CD44 in prostate cancer cells: association with cell proliferation and invasive potential. *Anticancer research* 15(4), pp. 1191–8.

Longcope, C., Abend, S., Braverman, L.E. and Emerson, C.H. 1990. Androstenedione and estrone dynamics in hypothyroid women. *The Journal of clinical endocrinology and metabolism* 70(4), pp. 903–7.

Louderbough, J.M. V, Brown, J. a, Nagle, R.B. and Schroeder, J. a 2011. CD44 Promotes Epithelial Mammary Gland Development and Exhibits Altered Localization during Cancer Progression. *Genes & cancer* 2(8), pp. 771–81.

Lucidi, R.S., Witz, C. a, Chrisco, M., Binkley, P. a, Shain, S. a and Schenken, R.S. 2005. A novel in vitro model of the early endometriotic lesion demonstrates that attachment of endometrial cells to mesothelial cells is dependent on the source of endometrial cells. *Fertility and sterility* 84(1), pp. 16–21.

Lund, S.A., Giachelli, C.M. and Scatena, M. 2009. The role of osteopontin in inflammatory processes. *Journal of cell communication and signaling* 3(3-4), pp. 311–22.

Mackay, C.R., Terpe, H.J., Stauder, R., Marston, W.L., Stark, H. and Günthert, U. 1994. Expression and modulation of CD44 variant isoforms in humans. *The Journal of cell biology* 124(1-2), pp. 71–82.

Makker, A. and Singh, M.M. 2006. Endometrial receptivity: clinical assessment in relation to fertility, infertility, and antifertility. *Medicinal research reviews* 26(6), pp. 699–746.

Makrigiannakis, A., Coukos, G., Mantani, A., Prokopakis, P., Trew, G., Margara, R., Winston, R., White, J., Science, R., Mak, M.A., Man, A. and College, I. 2001. Expression of Wilms' Tumor Suppressor Gene (WT1) in Human Endometrium : Regulation through Decidual Differentiation. *Journal of Clinical Endocrinology & Metabolism* 86(12), pp. 5964–5972.

Makrigiannakis, A., Minas, V., Kalantaridou, S.N., Nikas, G. and Chrousos, G.P. 2006. Hormonal and cytokine regulation of early implantation. *Trends in endocrinology and metabolism: TEM* 17(5), pp. 178–85.

Mann, H.B. and Whitney, D.R. 1947. On a Test of Whether one of Two Random Variables is Stochastically Larger than the Other. *Ann. Math. Statist.* 18(1), pp. 50–60.

Margarit, L., Taylor, A., Roberts, M.H., Hopkins, L., Davies, C., Brenton, a G., Conlan, R.S., Bunkheila, A., Joels, L., White, J.O. and Gonzalez, D. 2010. MUC1 as a discriminator between endometrium from fertile and infertile patients with PCOS and endometriosis. *The Journal of clinical endocrinology and metabolism* 95(12), pp. 5320–9.

Martin, V.T. and Behbehani, M. 2006. Ovarian hormones and migraine headache: understanding mechanisms and pathogenesis--part 2. *Headache* 46(3), pp. 365–86.

Maruyama, T. and Yoshimura, Y. 2012. Stem cell theory for the pathogenesis of endometriosis. *Frontiers in bioscience (Elite edition)* 4, pp. 2854–63.

Mazzali, M., Kipari, T., Ophascharoensuk, V., Wesson, J.A., Johnson, R. and Hughes, J. 2002. Osteopontin--a molecule for all seasons. *QJM* 95(1), pp. 3–13.

Millard, M., Odde, S. and Neamati, N. 2011. Integrin targeted therapeutics. *Theranostics* 1, pp. 154–88.

Montagna, P., Capellino, S., Villaggio, B., Remorgida, V., Ragni, N., Cutolo, M. and Ferrero, S. 2008. Peritoneal fluid macrophages in endometriosis: correlation between the expression of estrogen receptors and inflammation. *Fertility and sterility* 90(1), pp. 156–64. Available at: http://www.ncbi.nlm.nih.gov/pubmed/17548071 [Accessed: 24 June 2014].

Montes, M., Cloutier, A., Sánchez-Hernández, N., Michelle, L., Lemieux, B., Blanchette, M., Hernández-Munain, C., Chabot, B. and Suñé, C. 2012. TCERG1 regulates alternative splicing of the Bcl-x gene by modulating the rate of RNA polymerase II transcription. *Molecular and cellular biology* 32(4), pp. 751–62.

Van Mourik, M.S.M., Macklon, N.S. and Heijnen, C.J. 2009. Embryonic implantation: cytokines, adhesion molecules, and immune cells in establishing an implantation environment. *Journal of leukocyte biology* 85(1), pp. 4–19.

Mueller, M.D., Vigne, J.L., Vaisse, C. and Taylor, R.N. 2000. Glycodelin: a pane in the implantation window. *Seminars in reproductive medicine* 18(3), pp. 289–98.

Nácher, M., Blázquez, A.B., Shao, B., Matesanz, A., Prophete, C., Berin, M.C., Frenette, P.S. and Hidalgo, A. 2011. Physiological contribution of CD44 as a ligand for E-Selectin during inflammatory T-cell recruitment. *The American journal of pathology* 178(5), pp. 2437–46.

Nathan, D.M., Buse, J.B., Davidson, M.B., Ferrannini, E., Holman, R.R., Sherwin, R. and Zinman, B. 2009. Medical management of hyperglycemia in type 2 diabetes: a consensus algorithm for the initiation and adjustment of therapy: a consensus statement of the American Diabetes Association and the European Association for the Study of Diabetes. *Diabetes care* 32(1), pp. 193–203.

Nau, G.J., Liaw, L., Chupp, G.L., Berman, J.S., Hogan, B.L. and Young, R.A. 1999. Attenuated host resistance against Mycobacterium bovis BCG infection in mice lacking osteopontin. *Infection and immunity* 67(8), pp. 4223–30.

NICE 2012. Fertility : assessment and treatment for people with fertility problems (update). (May), pp. 1–75.

Nishida, M., Kasahara, K., Kaneko, M., Iwasaki, H. and Hayashi, K. 1985. Establishment of a new human endometrial adenocarcinoma cell line, Ishikawa cells,

containing estrogen and progesterone receptors. *Nippon Sanka Fujinka Gakkai zasshi* 37(7), pp. 1103–11.

Nomiyama, T., Perez-tilve, D., Ogawa, D., Gizard, F., Zhao, Y., Heywood, E.B., Jones, K.L., Kawamori, R., Cassis, L.A., Tschöp, M.H. and Bruemmer, D. 2007. Osteopontin mediates obesity-induced adipose tissue macrophage infiltration and insulin resistance in mice. 117(10).

Noyes, R.W., Hertig, A.W. and Rock, J. 1950. Dating the Endometrial Biopsy. *Fertility and sterility* 1, pp. 3–25.

O'Brien, E.R., Garvin, M.R., Stewart, D.K., Hinohara, T., Simpson, J.B., Schwartz, S.M. and Giachelli, C.M. 1994. Osteopontin is synthesized by macrophage, smooth muscle, and endothelial cells in primary and restenotic human coronary atherosclerotic plaques. *Arteriosclerosis, Thrombosis, and Vascular Biology* 14(10), pp. 1648–1656.

Old, L.J. 1985. Tumor necrosis factor (TNF). *Science (New York, N.Y.)* 230(4726), pp. 630–2.

Oldberg, a, Franzén, A. and Heinegård, D. 1986. Cloning and sequence analysis of rat bone sialoprotein (osteopontin) cDNA reveals an Arg-Gly-Asp cell-binding sequence. *Proceedings of the National Academy of Sciences of the United States of America* 83(23), pp. 8819–23.

Orian-Rousseau, V., Chen, L., Sleeman, J.P., Herrlich, P. and Ponta, H. 2002. CD44 is required for two consecutive steps in HGF/c-Met signaling. *Genes & development* 16(23), pp. 3074–86.

Pellicer, A., Albert, C., Mercader, A., Bonilla-Musoles, F., Remohí, J. and Simón, C. 1998. The follicular and endocrine environment in women with endometriosis: local and systemic cytokine production. *Fertility and sterility* 70(3), pp. 425–31.

Pellicer, A., Albert, C., Mercader, A., Bonilla-Musoles, F., Remohí, J. and Simón, C. 1999. The pathogenesis of ovarian hyperstimulation syndrome: in vivo studies investigating the role of interleukin-1beta, interleukin-6, and vascular endothelial growth factor. *Fertility and sterility* 71(3), pp. 482–9.

Petz, L.N. 2002. Estrogen Receptor alpha and Activating Protein-1 Mediate Estrogen Responsiveness of the Progesterone Receptor Gene in MCF-7 Breast Cancer Cells. *Endocrinology* 143(12), pp. 4583–4591.

Peyghambari, F., Salehnia, M., Forouzandeh Moghadam, M., Rezazadeh Valujerdi, M. and Hajizadeh, E. 2010. The correlation between the endometrial integrins and osteopontin expression with pinopodes development in ovariectomized mice in response to exogenous steroids hormones. *Iranian biomedical journal* 14(3), pp. 109–19.

Pfaffl, M.W. 2001. A new mathematical model for relative quantification in real-time RT-PCR. *Nucleic acids research* 29(9), p. e45. Available at: http://www.pubmedcentral.nih.gov/articlerender.fcgi?artid=55695&tool=pmcentrez&rendertype=abstract.

Poncelet, C., Cornelis, F., Tepper, M., Sauce, E., Magan, N., Wolf, J.P. and Ziol, M. 2010. Expression of E- and N-cadherin and CD44 in endometrium and hydrosalpinges from infertile women. *Fertility and sterility* 94(7), pp. 2909–12.

Poncelet, C., Leblanc, M., Walker-Combrouze, F., Soriano, D., Feldmann, G., Madelenat, P., Scoazec, J.-Y. and Daraï, E. 2002. Expression of cadherins and CD44 isoforms in human endometrium and peritoneal endometriosis. *Acta obstetricia et gynecologica Scandinavica* 81(3), pp. 195–203.

Ponta, H., Sherman, L. and Herrlich, P.A. 2003. CD44: from adhesion molecules to signalling regulators. *Nature reviews. Molecular cell biology* 4(1), pp. 33–45.

Proctor, M. and Farquhar, C. 2006. Diagnosis and management of dysmenorrhoea. *BMJ (Clinical research ed.)* 332(7550), pp. 1134–8.

Qu, X., Yang, M., Zhang, W., Liang, L., Yang, Y., Zhang, Y., Deng, B., Gao, W., Liu, J., Yang, Q., Kong, B. and Gong, F. 2008. Osteopontin expression in human decidua is associated with decidual natural killer cells recruitment and regulated by progesterone. *In vivo (Athens, Greece)* 22(1), pp. 55–61.

Ransohoff, R.M., Kivisäkk, P. and Kidd, G. 2003. Three or more routes for leukocyte migration into the central nervous system. *Nature reviews. Immunology* 3(7), pp. 569–81.

Renkl, A.C., Wussler, J., Ahrens, T., Thoma, K., Kon, S., Uede, T., Martin, S.F., Simon, J.C. and Weiss, J.M. 2005. Osteopontin functionally activates dendritic cells and induces their differentiation toward a Th1-polarizing phenotype. *Blood* 106(3), pp. 946–55. Available at: http://www.ncbi.nlm.nih.gov/pubmed/15855273 [Accessed: 29 April 2014].

Riesewijk, a. 2003. Gene expression profiling of human endometrial receptivity on days LH+2 versus LH+7 by microarray technology. *Molecular Human Reproduction* 9(5), pp. 253–264.

Ringel, J., Jesnowski, R., Schmidt, C., Köhler, H.J., Rychly, J., Batra, S.K. and Löhr, M. 2001. CD44 in normal human pancreas and pancreatic carcinoma cell lines. *Teratogenesis, carcinogenesis, and mutagenesis* 21(1), pp. 97–106.

Rodrigues, L.R., Teixeira, J. a, Schmitt, F.L., Paulsson, M. and Lindmark-Mänsson, H. 2007. The role of osteopontin in tumor progression and metastasis in breast cancer. *Cancer epidemiology, biomarkers & prevention: a publication of the American Association for Cancer Research, cosponsored by the American Society of*

Preventive Oncology 16(6), pp. 1087–97. Available at: http://www.ncbi.nlm.nih.gov/pubmed/17548669 [Accessed: 30 July 2013].

Rokitansky, C. 1855. *Pathologischen Anatomie*. Wilhelm Braumuller.

Roman, J., Rangasamy, T., Guo, J., Sugunan, S., Meednu, N., Packirisamy, G., Shimoda, L. a, Golding, A., Semenza, G. and Georas, S.N. 2010. T-cell activation under hypoxic conditions enhances IFN-gamma secretion. *American journal of respiratory cell and molecular biology* 42(1), pp. 123–8.

Ruan, X. and Dai, Y. 2009. Study on chronic low-grade inflammation and influential factors of polycystic ovary syndrome. *Medical principles and practice : international journal of the Kuwait University, Health Science Centre* 18(2), pp. 118–22.

Saegusa, M., Hashimura, M. and Okayasu, I. 1998. CD44 expression in normal, hyperplastic, and malignant endometrium. *The Journal of pathology* 184(3), pp. 297–306.

Samant, R.S., Clark, D.W., Fillmore, R. a, Cicek, M., Metge, B.J., Chandramouli, K.H., Chambers, A.F., Casey, G., Welch, D.R. and Shevde, L. a 2007. Breast cancer metastasis suppressor 1 (BRMS1) inhibits osteopontin transcription by abrogating NF-kappaB activation. *Molecular cancer* 6, p. 6.

Samitas, K., Zervas, E., Vittorakis, S., Semitekolou, M., Alissafi, T., Bossios, A., Gogos, H., Economidou, E., Lötvall, J., Xanthou, G., Panoutsakopoulou, V. and Gaga, M. 2011. Osteopontin expression and relation to disease severity in human asthma. *The European respiratory journal* 37(2), pp. 331–41.

Sampson, J. 1927. Peritoneal endometriosis due to the menstrual dissemination of endometrial tissue into the peritoneal cavity. *American Journal Obstetrics Gynecology* 14, p. 422.

Samy, N., Hashim, M., Sayed, M. and Said, M. 2009. Clinical significance of inflammatory markers in polycystic ovary syndrome: their relationship to insulin resistance and body mass index. *Disease Markers* 26(4), pp. 163–170.

Sarapik, A., Velthut, A., Haller-Kikkatalo, K., Faure, G.C., Béné, M.-C., de Carvalho Bittencourt, M., Massin, F., Uibo, R. and Salumets, A. 2012. Follicular proinflammatory cytokines and chemokines as markers of IVF success. *Clinical & developmental immunology* 2012, p. 606459.

Schroder, K., Hertzog, P.J., Ravasi, T. and Hume, D.A. 2004. Interferon-gamma: an overview of signals, mechanisms and functions. *Journal of leukocyte biology* 75(2), pp. 163–89.

Senger, D.R., Wirth, D.F. and Hynes, R.O. 1979. Transformed mammalian cells secrete specific proteins and phosphoproteins. *Cell* 16(4), pp. 885–893.

Shankaranarayanan, P., Mendoza-Parra, M.-A., Walia, M., Wang, L., Li, N., Trindade, L.M. and Gronemeyer, H. 2011. Single-tube linear DNA amplification (LinDA) for robust ChIP-seq. *Nature methods* 8(7), pp. 565–7.

Sharma, P., Kumar, S. and Kundu, G.C. 2010. Transcriptional regulation of human osteopontin promoter by histone deacetylase inhibitor, trichostatin A in cervical cancer cells. *Molecular cancer* 9, p. 178.

Sharpless, J. 2003. Polycystic Ovary Syndrome and the Metabolic Syndrome. *Cinical Diabetes* 21(4), pp. 154–161.

Singh, H. and Aplin, J.D. 2009. Adhesion molecules in endometrial epithelium: tissue integrity and embryo implantation. *Journal of Anatomy* 215(1), pp. 3–13.

Skrzypczak, J., Wirstlein, P., Mikołajczyk, M., Ludwikowski, G. and Zak, T. 2007. TGF superfamily and MMP2, MMP9, TIMP1 genes expression in the endometrium of women with impaired reproduction. *Folia histochemica et cytobiologica / Polish Academy of Sciences, Polish Histochemical and Cytochemical Society* 45 Suppl 1, pp. 5143–8.

Smith, J.H. and Denhardt, D. 1987. Molecular cloning of a tumor promoter-inducible mRNA found in JB6 mouse epidermal cells: induction is stable at high, but not at low, cell densities. *Journal of cellular biochemistry* 34(1), pp. 13–22.

Srichai, M.B. and Zent, R. 2010. Cell-Extracellular Matrix Interactions in Cancer. In: Zent, R. and Pozzi, A. eds. *Cell-Extracellular Matrix Interaction in Cancer*. New York, NY: Springer New York, pp. 19–41.

Stein, I. and Leventhal, N. 1935. Amenorrhea associated with bilateral polycystic ovaries. *American Journal Obstetrics Gynecology*, pp. 29–181.

Steiner, C.A., Janez, A., Jensterle, M., Reisinger, K., Forst, T. and Pfützner, A. 2007. Impact of treatment with rosiglitazone or metformin on biomarkers for insulin resistance and metabolic syndrome in patients with polycystic ovary syndrome. *Journal of diabetes science and technology* 1(2), pp. 211–7.

Stossi, F., Barnett, D.H., Frasor, J., Komm, B., Lyttle, C.R. and Katzenellenbogen, B.S. 2004. Transcriptional profiling of estrogen-regulated gene expression via estrogen receptor (ER) alpha or ERbeta in human osteosarcoma cells: distinct and common target genes for these receptors. *Endocrinology* 145(7), pp. 3473–86.

Sze, L., He, Q., Chen, J., Xu, P., Ling Tsang, L., Yu, S., Wa Chung, Y. and Chang Chan, H. 2010. Interaction between endometrial epithelial cells and blood leucocytes promotes cytokine release and epithelial barrier function in response to Chlamydia trachomatis lipopolysaccharide stimulation. *Cell biology international* 34(9), pp. 951–8.

Tabibzadeh, S. 1991. Human Endometrium: An Active Site of Cytokine Production and Action. *Endocrine Reviews* 12(3), pp. 272–290.

Takemoto, M., Yokote, K., Yamazaki, M., Ridall, a L., Butler, W.T., Matsumoto, T., Tamura, K., Saito, Y. and Mori, S. 2000. Enhanced expression of osteopontin by high glucose. Involvement of osteopontin in diabetic macroangiopathy. *Annals of the New York Academy of Sciences* 902, pp. 357–63.

Taketani, Y., Kuo, T.M. and Mizuno, M. 1992. Comparison of cytokine levels and embryo toxicity in peritoneal fluid in infertile women with untreated or treated endometriosis. *American journal of obstetrics and gynecology* 167(1), pp. 265–70.

Tamada, M., Nagano, O., Tateyama, S., Ohmura, M., Yae, T., Ishimoto, T., Sugihara, E., Onishi, N., Yamamoto, T., Yanagawa, H., Suematsu, M. and Saya, H. 2012. Modulation of glucose metabolism by CD44 contributes to antioxidant status and drug resistance in cancer cells. *Cancer research* 72(6), pp. 1438–48.

Tan, S., Scherag, A., Janssen, O.E., Hahn, S., Lahner, H., Dietz, T., Scherag, S., Grallert, H., Vogel, C.I.G., Kimmig, R., Illig, T., Mann, K., Hebebrand, J. and Hinney, A. 2010. Large effects on body mass index and insulin resistance of fat mass and obesity associated gene (FTO) variants in patients with polycystic ovary syndrome (PCOS). *BMC Medical Genetics* 11, p. 12.

Tanabe, K., Ellis, L. and Saya, H. 1990. Expression of CD44R1 adhesion molecule in colon carcinomas and metastases. *The Lancet* 13, pp. 725–726.

Tei, C., Maruyama, T., Kuji, N., Miyazaki, T., Mikami, M. and Yoshimura, Y. 2003. Reduced expression of alphavbeta3 integrin in the endometrium of unexplained infertility patients with recurrent IVF-ET failures: improvement by danazol treatment. *Journal of assisted reproduction and genetics* 20(1), pp. 13–20.

The Rotterdam ESHRE/ASRM-sponsored PCOS consensus workshop group 2004. Revised 2003 consensus on diagnostic criteria and long-term health risks related to polycystic ovary syndrome (PCOS). *Human Reproduction* 19(1), pp. 41–47.

Treasure T, Bewley S, Bhattacharya S, Brain K, Child T, D.M. 2013. Fertility : assessment and treatment for people with fertility problems. , p. 148.

Trejdosiewicz, L.K., Morton, R., Yang, Y., Banks, R.E., Selby, P.J. and Southgate, J. 1998. INTERLEUKINS 4 AND 13 UPREGULATE EXPRESSION OF CD44 IN HUMAN COLONIC. 10(10), pp. 756–765.

Tsai, S.-W., Liou, H.-M., Lin, C.-J., Kuo, K.-L., Hung, Y.-S., Weng, R.-C. and Hsu, F.-Y. 2012. MG63 osteoblast-like cells exhibit different behavior when grown on electrospun collagen matrix versus electrospun gelatin matrix. Chin, W.-C. ed. *PloS one* 7(2), p. e31200.

Uede, T. 2011. Osteopontin, intrinsic tissue regulator of intractable inflammatory diseases. *Pathology international* 61(5), pp. 265–80.

Van der Voort, R. 1999. Heparan Sulfate-modified CD44 Promotes Hepatocyte Growth Factor/Scatter Factor-induced Signal Transduction through the Receptor Tyrosine Kinase c-Met. *Journal of Biological Chemistry* 274(10), pp. 6499–6506.

Wan, P.-C., Bao, Z.-J., Wu, Y., Yang, L., Hao, Z.-D., Yang, Y.-L., Shi, G.-Q., Liu, Y. and Zeng, S.-M. 2011. αvβ3 Integrin may participate in conceptus attachment by regulating morphologic changes in the endometrium during peri-implantation in ovine. *Reproduction in Domestic Animals* 46(5), pp. 840–7.

Wang, D., Yamamoto, S., Hijiya, N., Benveniste, E.N. and Gladson, C.L. 2000a. Transcriptional regulation of the human osteopontin promoter: functional analysis and DNA-protein interactions. *Oncogene* 19(50), pp. 5801–9. Available at: http://www.ncbi.nlm.nih.gov/pubmed/11126367.

Wang, D., Yamamoto, S., Hijiya, N., Benveniste, E.N. and Gladson, C.L. 2000b. Transcriptional regulation of the human osteopontin promoter: functional analysis and DNA-protein interactions. *Oncogene* 19(50), pp. 5801–9.

Wang, K.X. and Denhardt, D. 2008. Osteopontin : Role in immune regulation and stress responses. *Cytokine & Growth Factor Reviews* 19, pp. 333–345.

Wang, X., Chao, L., Chen, L., Jin, G., Hua, M., Liu, H., Ouyang, A. and Zhang, X. 2010. Primary Breast Carcinoma : Association of Mammographic Calcifi cations with Osteopontin. *Radiology* 254(1), pp. 69–78.

Way, D.L., Grosso, D.S., Davis, J.R., Surwit, E.A. and Christian, C.D. 1983. Characterization of a new human endometrial carcinoma (RL95-2) established in tissue culture. *In vitro* 19(3 Pt 1), pp. 147–58.

Weber, G.F., Zawaideh, S., Hikita, S., Kumar, V. a, Cantor, H. and Ashkar, S. 2002. Phosphorylation-dependent interaction of osteopontin with its receptors regulates macrophage migration and activation. *Journal of leukocyte biology* 72(4), pp. 752–61.

Weerasinghe, D., McHugh, K.P., Ross, F.P., Brown, E.J., Gisler, R.H. and Imhof, B. a 1998. A role for the alphavbeta3 integrin in the transmigration of monocytes. *The Journal of cell biology* 142(2), pp. 595–607. Available at: http://www.pubmedcentral.nih.gov/articlerender.fcgi?artid=2133044&tool=pmcentrez&rendertype=abstract.

Wei, Q., St Clair, J.B., Fu, T., Stratton, P. and Nieman, L.K. 2009. Reduced expression of biomarkers associated with the implantation window in women with endometriosis. *Fertility and sterility* 91(5), pp. 1686–91.

Weiss, G., Goldsmith, L.T., Taylor, R.N., Bellet, D. and Taylor, H.S. 2009. Inflammation in reproductive disorders. *Reproductive sciences (Thousand Oaks, Calif.)* 16(2), pp. 216–29.

Weiss, L., Botero-Anug, A.M., Hand, C., Slavin, S. and Naor, D. 2008. CD44 Gene Vaccination for Insulin-Dependent Diabetes Mellitus in Non-Obese Diabetic Mice [Online].

Willis, C. 2003. Cytokine production by peripheral blood monocytes during the normal human ovulatory menstrual cycle. *Human Reproduction* 18(6), pp. 1173–1178.

Woerner, S.M., Givehchian, M., Dürst, M., Schneider, a, Costa, S., Melsheimer, P., Lacroix, J., Zöller, M. and Doeberitz, M.K. 1995. Expression of CD44 splice variants in normal, dysplastic, and neoplastic cervical epithelium. *Clinical cancer research : an official journal of the American Association for Cancer Research* 1(10), pp. 1125–32. Available at: http://www.ncbi.nlm.nih.gov/pubmed/9815903.

Wolff, M. 2003. Glucose Transporter Proteins (GLUT) in Human Endometrium: Expression, Regulation, and Function throughout the Menstrual Cycle and in Early Pregnancy. *Journal of Clinical Endocrinology & Metabolism* 88(8), pp. 3885–3892.

Wolff, M., Strowitzki, T., Becker, V., Zepf, C., Tabibzadeh, S. and Thaler, C.J. 2001. Endometrial osteopontin, a ligand of beta3-integrin, is maximally expressed around the time of the "implantation window". *Fertility and sterility* 76(4), pp. 775–81.

Wolff, M., Strowitzki, T., Becker, V., Zepf, C., Tabibzadeh, S. and Thaler, C.J. 2001. Endometrial osteopontin, a ligand of β3-integrin, is maximally expressed around the time of the "implantation window." *Fertility and Sterility* 76(4), pp. 775–781.

Xu, L., Ma, X., Wang, Y., Li, X., Qi, Y., Cui, B., Li, X., Ning, G. and Wang, S. 2011. The expression and pathophysiological role of osteopontin in Graves' disease. *The Journal of clinical endocrinology and metabolism* 96(11), pp. E1866–70.

Xu, Q. 2011. The Indian blood group system. *Immunohematology / American Red Cross* 27(3), pp. 89–93.

Yaegashi, N., Fujita, N., Yajima, A. and Nakamura, M. 1995. Menstrual cycle dependent expression of CD44 in normal human endometrium. *Human pathology* 26(8), pp. 862–5.

Yagisawa, T., Ito, F., Osaka, Y., Amano, H., Kobayashi, C. and Toma, H. 2001. The Influence Of Sex Hormones On Renal Osteopontin Expression And Urinary Constituents In Experimental Urolithiasis. *The Journal of Urology* 166(3), pp. 1078–1082.

Yao, Y., Richman, L., Morehouse, C., de los Reyes, M., Higgs, B.W., Boutrin, A., White, B., Coyle, A., Krueger, J., Kiener, P. a and Jallal, B. 2008. Type I interferon: potential therapeutic target for psoriasis? *PloS one* 3(7), p. e2737.

Yen, S. and Jaffe, R. 2009. *Yen and Jaffe's Reproductive Endocrinology*. 6th ed. Strauss, J. and Barbieri, R. eds. Elsevier.

Young, M.F., Kerr, J.M., Termine, J.D., Wewer, U.M., Wang, M.G., McBride, O.W. and Fisher, L.W. 1990. cDNA cloning, mRNA distribution and heterogeneity, chromosomal location, and RFLP analysis of human osteopontin (OPN). *Genomics* 7(4), pp. 491–502.

Yu, W., Woessner, J.F., Mcneish, J.D. and Stamenkovic, I. 2002. CD44 anchors the assembly of matrilysin / MMP-7 with heparin-binding epidermal growth factor precursor and ErbB4 and regulates female reproductive organ remodeling. *Genes & Development* 16, pp. 307–323.

Yu, X.Q., Nikolic-Paterson, D.J., Mu, W., Giachelli, C.M., Atkins, R.C., Johnson, R.J. and Lan, H.Y. 1998. A functional role for osteopontin in experimental crescentic glomerulonephritis in the rat. *Proceedings of the Association of American Physicians* 110(1), pp. 50–64.

Yumoto, K., Ishijima, M., Rittling, S.R., Tsuji, K., Tsuchiya, Y., Kon, S., Nifuji, A., Uede, T., Denhardt, D.T. and Noda, M. 2002. Osteopontin deficiency protects joints against destruction in anti-type II collagen antibody-induced arthritis in mice. *Proceedings of the National Academy of Sciences of the United States of America* 99(7), pp. 4556–61.

Zurick, K.M., Qin, C. and Bernards, M.T. 2013. Mineralization induction effects of osteopontin, bone sialoprotein, and dentin phosphoprotein on a biomimetic collagen substrate. *Journal of biomedical materials research. Part A* 101(6), pp. 1571–81.